ICONAT 2022

# IV. INTERNATIONAL CONFERENCE ON NATURAL SCIENCES AND TECHNOLOGIES

24-26 AUGUST 2022 ANTALYA-TURKEY

www.iconat-2022.com

## CONFERENCE PROGRAMME & PROCEEDINGS BOOK

2022

ISBN: 978-605-73552-2-5

## HONORRARY PRESIDENT OF CONFERENCE

**Prof. Dr. Kamile PERÇİN AKGÜL**
**Antalya AKEV Üniversitesi Rektörü**

## CHAIRMAN OF CONFERENCE

Prof. Dr. Abidin KILIÇ, Eskişehir Technical University

## ORGANIZING COMMITTEE

Prof. Dr. Tuncay Döğeroğlu, Rector, Eskişehir Technical University
Prof. Dr. Gürsoy Arslan, Vice Rector, Eskişehir Technical University
Prof. Dr. Mehmet Nesip Öğün, Rector, University of Mediterranean Karpasia
Doç. Dr. Serdar Yurtsever, Vice Rector, University of Mediterranean Karpasia
Prof. Dr. Valerii Semenets, Rector, Kharkiv National University of Radio Electronics
Prof. Dr. Murad Omarov, Vice Rector, Kharkiv National University of Radio Electronics
Prof. Dr. Saadet Namiq Aliyeva, Rector, Azerbaijan University
Prof. Dr. Yusif Gasimov, Vice Rector, Azerbaijan University
Prof. Dr. Ömer Arıöz, Rector, Toros University
Prof. Dr. Kamile Perçin Akgül, Rector, Antalya AKEV University
Prof. Dr. Zafer Demir, Eskişehir Technical University
Prof. Dr. Abidin KILIÇ, Eskişehir Technical University

## International Scientific Committee

Prof. Dr. Andrii Chukhrai (Ukraine)
Prof. Dr. Arturas Mickus (Lithuania)
Dr. Asif Pashayev (Azerbaijan)
Prof. Dr. Cengiz Türe (Turkey)
Prof. Dr. Dmytro Fedasyuk (Ukraine)
Prof. Dr. Dursun Aydın (Turkey)
Prof. Dr. Ekrem Aydıner (Turkey)
Prof. Dr. Ekrem Gürel (Turkey)
Prof. Dr. Feridun Ay (Turkey)
Prof. Dr. Hakan Dal (Turkey)
Prof. Dr. Hüseyin Sarı (Turkey)
Prof. Dr. Igor Nevlidov (Ukraine)
Prof. Dr. Igor Ruzhentsev (Ukraine)
Prof. Dr. İsmail Sökmen (Turkey)
Prof. Dr. Kadir Aslan (USA)
Prof. Dr. Khanmammadov Agil (Azerbaijan)
Dr. Latifa Agamalieva (Azerbaijan)
Prof. Dr. Marzena S. MIichalowska (Poland)
Prof. Dr. Mehmet Candan (Turkey)
Prof. Dr. Meryem Akbelen (Turkey)
Prof. Dr. Murat Tanışlı (Turkey)
Prof. Dr. Mustafa Hoştut (Turkey)
Prof. Dr. Nihal Kus (Turkey)
Prof. Dr. Oguz Gülseren (Turkey)
Prof. Dr. Oleg Lazarenko (Ukraine)
Prof. Dr. Oleh Avrunin (Ukraine)
Prof. Dr. Oleksandr Lemeshko (Ukraine)
Prof. Dr. Oleksandr Tsopa (Ukraine)
Dr. Rahul M. Mane (India)
Prof. Dr. Rauf Amirov (Turkey)
Prof. Dr. Saliha Ilıcan (Turkey)
Prof. Dr. Sedef Dikmen (Turkey)
Prof. Dr. Sevil Çetinkaya Gürer (Turkey)
Prof. Dr. Svetlana Kashuba (Poland)
Prof. Dr. Tayfun Akın (Turkey
Prof. Dr. Urfat Nuriyev (Turkey)
Prof. Dr. Valentin Filatov (Ukraine)
Prof. Dr. Volodymyr Storozhenko (Ukraine)
Prof. Dr. Yevgenii Bodyansky (Ukraine)
Prof. Dr. Yevgen Nelin (Ukraine)
Prof. Dr. Yuri Machekhin (Ukraine)
Prof. Dr. Yüksel Ergün (Turkey)

ISBN: 978-605-73552-2-5

Official Opening of the ICONAT-2022

24 August 2022 Meeting Salon I – Antalya AKEV University

**Meeting ID: 939 7615 4284**

**Passcode:**

08.00 The Start of Registration Process

09.30 Official Opening of the ICONAT-2022
Welcome by Conference

Prof. Dr. Abidin Kılıç,
Eskisehir Technical University, Türkiye
Chairman of Organization Committee

Prof. Dr. Omarov Murad,
Vice-Rector, NURE, Ukraine

Prof. Dr. Kamile Perçin Akgül,

Rector, Antalya AKEV University, Türkiye

HONORARY PRESIDENT OF CONGRESS

Invited Speaker
Prof. Dr. Orhan Gemikonaklı

Invited Speaker
Prof. Dr. Atilla Aydınlı

Invited Speaker
Prof. Dr. Ali Demirsoy

12.30 **Lunch Break**

19.00 **Conference Dinner**

**POSTER PRESENTATION SEASION: 25.08.2022 Thursday-**10.00-16.00
LAST MEETING: 26. 08 2022

ISBN: 978-605-73552-2-5

**MEETING ZOOM INFORMATION**

Official Opening of the ICONAT-2022 Welcome by Conference

Meeting ID: 957 89853779
Passcode: 869245

| | HALL 1 | HALL 2 | HALL 3 |
|---|---|---|---|
| 24.08.2022 | Meeting ID: 957 89853779<br>Passcode: 869245 | Meeting ID: 935 6107 4404<br>Passcode: 172974 | Meeting ID: 965 3010 3073<br>Passcode: 767483 |
| 25.08.2022 | Meeting ID: 976 52087030<br>Passcode:105450 | Meeting ID: 969 0741 1407<br>Passcode: 820009 | Meeting ID: 921 8237 2810<br>Passcode: 386082 |
| 26.08.2022 | Meeting ID: 940 18206872<br>Passcode: 988620 | Meeting ID: 965 7362 9424<br>Passcode: 181284 | Meeting ID: 944 0915 8643<br>Passcode: 305809 |

ISBN: 978-605-73552-2-5

**24.08.2022 Wednesday-**14.00-15.00

| | **ORAL PRESENTATIONS** | |
|---|---|---|
| | **Chairing Kevser Köklü** | **Hall 1** |
| 01 | Pınar Koç BAKACAK<br>*Türkiye* | Why Graphene for Optical Device Design? |
| 02 | Çağdaş ALLAHVERDI<br>*Türkiye* | Nucleation and Growth Mechanism of Colloidal Chalcogenide Semiconductor Nanoparticles |
| 03 | Sara Jamoudi SBAI<br>*Morocco* | Carbon Footprint of Road project for Sustainable Development - Lessons Learnt from Traffic Management of a Developing Urban Centre |

**24.08.2022 Wednesday-**14.00-15.00

| | **ORAL PRESENTATIONS** | |
|---|---|---|
| | **Chairing Zafer Demir** | **Hall 2** |
| 01 | Mohamad Tareq KHANJI<br>*Türkiye* | The Role of Strategies and Policies for Sustainable Architecture: A New Perspective for Energy-Efficient Buıldings in Turkey |
| 02 | Christy A.A.<br>*Norway* | Dessicant Properties of Natural Bio-polymers studied by NIR spectroscopy |
| 03 | Salem SATI<br>*Libya* | Optimal Cluster Size Using LEACH for Wireless Sensor Networks |

**24.08.2022 Wednesday-**14.00-15.00

| | **ORAL PRESENTATIONS** | |
|---|---|---|
| | **Chairing Elif Öztetik** | **Hall 3** |
| 01 | Saima Kalsoom BABAR<br>*Pakistan* | Comparative Response of Two Wheat Varieties to Basal and Split Potassium Nutrition under Field Conditions of Tandojam Pakistan |
| 02 | Yıldız Uygun CEBECI<br>*Türkiye* | Synthesis and Investigation of Biological Activity of Tryptamine Derivatives Containing Fluoroquinolone and 1,2,4-triazole Ring |
| 03 | Senanur DOKUZ<br>*Türkiye* | Lysogenic Phage Isolation from Methicillin-Resistant S.aureus Clinical Isolates |
| 04 | Giuma Fellah W. ATIA<br>*Libya* | The model for estimating daily atmospheric column-averaged $CO_2$ concentration |

ISBN: 978-605-73552-2-5

**24.08.2022 Wednesday-**15.10-16.10

| | ORAL PRESENTATIONS | |
|---|---|---|
| | **Chairing Zafer Dikmen** | **Hall 1** |
| 01 | Nihal KUŞ<br>*Türkiye* | Molecular Structure, Nbo and Td-Dft Analysis of 4-Methyl-3-Furaldehyde Based On Dft Calculations |
| 02 | Salih Kagan KALYONCU<br>*Türkiye* | All-fiber Linearly Polarized Single-Mode Q-switched Tm +3 Ho 3+ -Doped Pulse Laser at 2.1µm |
| 03 | Hülya Kuru MUTLU<br>*Türkiye* | The Effect of Temperature in Tile Production from Oily Clay And Nil Clay Mixture |
| 04 | Fei Fu<br>Chaina | Pathophysiology of mesangial expansion in diabetic |

**24.08.2022 Wednesday-**15.10-16.10

| | ORAL PRESENTATIONS | |
|---|---|---|
| | **Chairing Zafer Demir** | **Hall 2** |
| 01 | Yosra RAJİ<br>*Morocco* | The development of mosquito-repellent textiles based on local natural products |
| 02 | Berfin ALTUNDAL<br>*Türkiye* | Lactobacillus reuteri ve Streptococcus thermophilus İçeren Fermente Süt Ürününün Üretim Basamakları Teknolojik Özellikleri ve Aroma Profillerinin Belirlenmesi |
| 03 | Serkan SOYMAZ<br>*Türkiye* | Antiproliferative and apoptotic effects of Trachystemon orientalis(L.) G. Don on HCT116, AGS and HepG2 cells |
| 04 | Nurjamal MIRZAOVA<br>*Kyrgyzstan* | Pathways of Future Energy Systems |

**24.08.2022 Wednesday-**15.10-16.10

| | ORAL PRESENTATIONS | |
|---|---|---|
| | **Chairing Elif Öztetik** | **Hall 3** |
| 01 | H. Mehmet GÜZEY<br>*Türkiye* | Nonlinear Interconnected Stormwater Ponds Control Through Neuro Sliding Mode Consensus |
| 02 | Kevser KÖKLÜ<br>*Türkiye* | Mathematical Analysis of the 09 March 2012 Intense and 08 May 2014 Weak Storm |
| 03 | Adnan MAZMANOĞLU<br>*Türkiye* | Principal Component Statistical Analysis on The Relationship Between Violence and Addictıon Applied to Healthcare Professionals |
| 04 | Mark Blend<br>*France* | Energy landscapes for future |

ISBN: 978-605-73552-2-5

**24.08.2022 Wednesday-**16.20-17.20

| | ORAL PRESENTATIONS | |
|---|---|---|
| | **Hülya Kuru Mutlu** | **Hall 1** |
| 01 | S. Nattermann<br>*Germany* | A Study of Transmission Error Modeling |
| 02 | Süleyman DEMIR<br>*Türkiye* | Complex Octonionic Formulation for the Field Equations of Multifluid Plasma |
| 03 | Sedef DIKMEN<br>*Türkiye* | Adsorption of Acid Red By Sepiolite Belongs to Eskişehir (Sivrihisar) Region and It's Surface Active Agents-Modified Forms |
| 04 | Deniz Emre<br>*Türkiye* | Hidrofobik Nanomateryal Olarak Grafen Katkili Polimer Yüzeylerin Üretimi |

**24.08.2022 Wednesday-**16.20-17.20

| | ORAL PRESENTATIONS | |
|---|---|---|
| | **Şadiye Çakmak** | **Hall 2** |
| 01 | Hande HANÇER<br>*Türkiye* | Cloning of Bacteriophage Lytic Protein |
| 02 | Sajjad Shukur ULLAH<br>*Pakistan* | Carbon Footprint of Road project for Sustainable Development - Lessons Learnt from Traffic Management of a Developing Urban Centre |
| 03 | Nehir KAYMAK<br>*Türkiye* | Trophic niches of native and non-native Cyprinid fishes in Karacaören Reservoir |

**24.08.2022 Wednesday-**16.20-17.20

| | ORAL PRESENTATIONS | |
|---|---|---|
| | **Adnan Mazmanoğlu** | **Hall 3** |
| 01 | Baboo ALİ<br>*Türkiye* | Presence Of Insect Species in The Research Field of Sweat Sorghum and Sorghum Sudangrass Hybrid Varieties in Canakkale |
| 02 | SAADOUNI Meriem<br>*Morocco* | Removal of Organic Dyes of Finishing and Dyeing Industrial Units by Transformed Technical Textile Fiber |
| 03 | Fırat ALATÜRK<br>*Türkiye* | Effects of Different Harvesting Practices on The Agronomic Characteristics of Some Sweet Sorghum and Sorghum X Sudangrass Hybrid Varieties |
| 04 | Fırat PALA<br>*Türkiye* | Early Weed Control's Impact On Lentils Yield |

ISBN: 978-605-73552-2-5

**25.08.2022 Thursday-**10.00-11.00

| | ORAL PRESENTATIONS | |
|---|---|---|
| | **Chairing Nihal Kuş** | **Hall 1** |
| 01 | Hülya Kuru MUTLU<br>*Türkiye* | The Effect of Electric and Hoffman Furnace on The Strength of Tiles Produced From Schist Material |
| 02 | El Mehdi ABDEDDINE<br>*Morocco* | Non-Linear Large Longitudinal Amplitude Vibration of Variable Slope of Rods with Different Boundaries Conditions |
| 03 | Zhumadil BAIGUNCHEKOV<br>*Kazakistan* | Direct Kinematics of a 3-Prps Type Parallel Manipulator |
| 04 | Suriati Taumin<br>*Malaysia* | Nolinear waves Equations |

**25.08.2022 Thursday-**10.00-11.00

| | ORAL PRESENTATIONS | |
|---|---|---|
| | **Chairing Süleyman Demir** | **Hall 2** |
| 01 | Burak ŞAHIN<br>*Türkiye* | Effect of Reaction Time on Li doped TiO2 Nanostructures Synthesized by Hydrothermal Method |
| 02 | Şadiye ÇAKMAK<br>*Türkiye* | Gamow-Teller transitions for odd-odd nuclei of zinc isotopes by using pn-QRPA |
| 03 | Hasan Hüseyin IŞIK<br>*Türkiye* | Enhanced Her Process with Ultra-Small Pt 25 Au 75 Alloy Nanoparticles |
| 04 | Zulkifly Pah<br>*Malaysia* | An Investigation of the Effects of Daily Physical Activity |

**25.08.2022 Thursday-**10.00-11.00

| | ORAL PRESENTATIONS | |
|---|---|---|
| | **Chairing Sedef Dikmen** | **Hall 3** |
| 01 | İlknur BALDAN IŞIK<br>*Türkiye* | Investigation of Hydrogen Evolution Reaction With Low-Pt Loading In Ptcu Alloy |
| 02 | Mine FAKILI<br>*Türkiye* | Application Of Biquaternion Algebra To Hydrodynamics |
| 03 | Baghdad Abdulhameed Abdullah AL-BADANI<br>*Yemen* | An Investigation of Molecular Spectroscopy with Geometric Algebra |

ISBN: 978-605-73552-2-5

**25.08.2022 Thursday-**11.10-12.20

| | ORAL PRESENTATIONS | |
|---|---|---|
| | **Chairing Nihal Kuş** | **Hall 1** |
| 01 | Volodymyr CHUMAKOV<br>*Ukraine* | On The Problem of Monopulse UV Sterilization |
| 02 | Volodymyr CHUMAKOV<br>*Ukraine* | On The Simulation of Pulse Signals by Polygonal Functions |
| 03 | Ersin YILMAZ<br>*Türkiye* | Estimation Of Multi-Response Semiparametric Regression Model Based On Kernel Smoother: An Application With Agricultural Data |
| 04 | Mohd ABDULLAH<br>*Malaysia* | The Investigation of Physical Properties of Polyester |

**25.08.2022 Thursday-**11.10-12.20

| | ORAL PRESENTATIONS | |
|---|---|---|
| | **Chairing Süleyman Demir** | **Hall 2** |
| 01 | Omar BATAINEH<br>*Jordan* | Development of an Empirical Model for the Wear Rate of AISI 420 Martensitic Stainless Steel Material Using a Standard Pin-On-Disc Test |
| 02 | Ivan YARMAK<br>*Ukraine* | Using The Colorimetric Method In Certain Technologies |
| 03 | Utku KAYA<br>*Türkiye* | The Effect of Adding Artificial Noise on The Success of A Deep Learning Network |
| 04 | Atef Ali AMARA<br>*Algeria* | Investigation of Relations Between Physical Properties and Electrical Properties |

**25.08.2022 Thursday-**11.10-12.20

| | ORAL PRESENTATIONS | |
|---|---|---|
| | **Chairing Sedef Dikmen** | **Hall 3** |
| 01 | El Mehdi ABDEDDINE<br>*Morocco* | Mechanical Behavior Convergence Of Fdm 3d Printed And Isotropic Parts: Geometrically Nonlinear Effect |
| 02 | Güneş Süheyla KÜRKÇÜOĞLU<br>*Türkiye* | Vibrational Spectroscopic, Thermal Studies and Electrical Properties of Cyanide Complexes with 2-(Hydroxymethyl) Pyridine |
| 03 | Andriy ONISHCHENKO<br>*Ukraine* | Fractal and Multi-Fractal Analyses of The Geomagnetic Field Variations Caused By The Earthquake On January 24, 2020 in Turkey |
| 04 | Nazarov Nora HALIDOVICH<br>*Uzbekistan* | An investigation of balance performance |

ISBN: 978-605-73552-2-5

**25.08.2022 Thursday-**14.00-15.00

| | ORAL PRESENTATIONS | |
|---|---|---|
| | **Chairing Şadiye Çakmak** | **Hall 1** |
| 01 | Zafer DİKMEN<br>*Türkiye* | Öğütülmüş Uçucu Kül ve Çelikhane Cürufunun Cam Seramik Eldesinde Kullanilabilirliğinin Araştırılması |
| 02 | Zeynep DAŞDELEN<br>*Türkiye* | Synthesis of Gold Nanoparticles on Reduced Graphene Oxide-Fumed Silica Hybrid Support to Use As Anode Catalyst in Alcohol Fuel Cells |
| 03 | Karimova Z. TASHEVNA<br>*Uzbekistan* | The Investigation of The Teaching of Physical Education |

**25.08.2022 Thursday-**14.00-15.00

| | ORAL PRESENTATIONS | |
|---|---|---|
| | **Chairing Nazire Burçin Hamutoğlu** | **Hall 2** |
| 01 | Ese AK<br>*Türkiye* | Interpreting Convolutional Neural Netwoks Output With Fuzzy Logic |
| 02 | Omar LAROUK<br>*France* | Evaluation The Information Services of Professional Social Networks |
| 03 | Mohammadjavad RANJBARAN<br>*Iran* | Numerical and experimental investigation on the repair impact of arrow-shaped and hexagonal glass-epoxy composite patches. |
| 04 | Bahlul M. ELKABIR<br>*Libya* | Investigation of the effect of local atomic polarization on magnetic field |

**25.08.2022 Thursday-**14.00-15.00

| | ORAL PRESENTATIONS | |
|---|---|---|
| | **Chairing Utku Kaya** | **Hall 3** |
| 01 | Pınar KAPÇI<br>*Türkiye* | Synthesis of N-Acylbenzotriazolylpyridine-Ruthenium Complex and Investigation Heteregenous Catalytic Hydrogenation Activity in Continious Flow System |
| 02 | Fatih Burak ÖZKANLI<br>*Türkiye* | Comparison of Energy Efficiency Studies of Turkey and Germany |
| 03 | Ömer Faruk GÖRÇÜN<br>*Türkiye* | Evaluation of Cybersecurity Platform Providers for Manufacturing Industries by Using The Codas Approach Based on T2nfn Sets |
| 04 | Fatih Doğan KOCA<br>*Türkiye* | Antioksidant Activity of Tornabea Scutellifera Extract Based Pt Nanoparticles |

**25.08.2022 Thursday-**15.10-16.10

ISBN: 978-605-73552-2-5

| | ORAL PRESENTATIONS | |
|---|---|---|
| | **Chairing Şadiye Çakmak** | **Hall 1** |
| 01 | Adwan YASIN<br>*Palestine* | A New Mechanism For Vanet Attacks Detection |
| 02 | İbrahim UÇAR<br>*Türkiye* | Real-Time Detection Of Rail Defects By Machine Learning |
| 03 | Fatih Doğan Koca<br>*Türkiye* | Antioksidant Activity Of *Tornabea Scutellifera* Extract Based Pt Nanoparticles |

**25.08.2022 Thursday-**15.10-16.10

| | ORAL PRESENTATIONS | |
|---|---|---|
| | **Chairing Nazire Burçin Hamutoğlu** | **Hall 2** |
| 01 | İsmail Cengiz YILMAZ<br>*Türkiye* | An Evaluation on the Gaining of Secondary School Science Concepts in Engineering Education |
| 02 | Mohammadjavad RANJBARAN<br>*Iran* | Investigation of Fracture Prevention Effects of Composite Patches Repair on Cracked Aluminum Plates Experimental and Numerical Study |
| 03 | Seray KEKEÇ<br>*Türkiye* | Syntheses and Structural Analyses of Heteronuclear Hexacyanometalate(Iii) Complexes with 4-(2-Aminoethyl)Pyridine |

**25.08.2022 Thursday-**15.10-16.10

| | ORAL PRESENTATIONS | |
|---|---|---|
| | **Chairing Utku Kaya** | **Hall 3** |
| 01 | Ayberk Salim MAYIL<br>*Türkiye* | Experimental Study of Electrical Heater Working Function For Improving Energy Consumption in A Domestic Oven |
| 02 | Vusala MURADOVA<br>*Ukraine* | Bayesian Regularization of Learning |
| 03 | Müge ŞENGÜL<br>*Türkiye* | Production and Characterization of Phospho-Silicate Glass and Glass-Ceramics |
| 04 | Hüseyin Ali ERKUŞ<br>*Türkiye* | Influence of Al Doping on Some Physical Properties of Spray-Deposited CuO Thin Films |

ISBN: 978-605-73552-2-5

**25.08.2022 Thursday-**16.20-17.30

| | ORAL PRESENTATIONS | |
|---|---|---|
| | **Chairing Şadiye Çakmak** | **Hall 1** |
| 01 | Kagan Han CATAN<br>*Türkiye* | Web Application for Statistical Analysis And Machine Learning Algorithms With R And Python Programming Languages |
| 02 | N. Burcin HAMUTOGLU<br>*Türkiye* | How The Pre-Service Teachers Are Adapted For An Unexpected Situation: Evaluating The Activities Designed for Online Learning Environments |
| 03 | N. Burcin HAMUTOGLU<br>*Türkiye* | A Practice for Quality Assurance in The Design of Blended Learning Environments: Educational Program Goals |
| 04 | Tuba HAS<br>*Türkiye* | The Role of the Media in the Dissemination of Science |

**25.08.2022 Thursday-**16.20-17.30

| | ORAL PRESENTATIONS | |
|---|---|---|
| | **Chairing Utku Kaya** | **Hall 2** |
| 01 | Tugce PEKDOGAN<br>*Türkiye* | A Study on Air Quality Near Solid Waste Treatment Plants Among University Population: Adana Case |
| 02 | Aimen ALSHIREEDAH<br>*Türkiye* | Image Classificaton with an Artificial Intelligence Network Based on Deep Learning |
| 03 | Volkan ARSLAN<br>*Türkiye* | 3D Printed Paving Stones: A Lab-Scale Research |

**25.08.2022 Thursday-**16.20-17.30

| | ORAL PRESENTATIONS | |
|---|---|---|
| | **Chairing Abidin Kılıç** | **Hall 3** |
| 01 | Tunay KARAN<br>*Türkiye* | Biosynthesis of Silver Nanoparticles Using Potato and Their Cytotoxic Effect |
| 02 | Lili ARABULI<br>*Georgia* | Co-Aggregation Of S100a9 Protein With L- Dopa And Cyclen-Based Compounds – Effect On The Amyloid Fibril Self-Assembly |
| 03 | Elif ÖZTETIK<br>*Türkiye* | The Effects of Lead Application on Different Physiological Processes in Some Wheat Varieties |
| 04 | Aysevil SALMAN DURMUŞLAR<br>*Türkiye* | Determination of 1-Propanol Ratio in Water with Two-Dimensional Phononic Crystal |

ISBN: 978-605-73552-2-5

**26.08.2022 Friday-**10.00-11.00

| | **ORAL PRESENTATIONS** | |
|---|---|---|
| | **Chairing Emre Aytuğ Özsoy** | **Hall 1** |
| 01 | Ahmet Murat ERTURAN<br>*Türkiye* | Robot Positioning in Indoor Environments Using A Deep Learning Model |
| 02 | A. K. DARBAN<br>*Iran* | Study of Physo-Chemical Activation Effect on Rare Earth Elements Surface Properties in Concentrated Phosphate Mineral By Planetary Ball Mill |
| 03 | Oğuz Kaan ATAR<br>*Türkiye* | NH Fuse with New Polymer Thermoset Body |

**26.08.2022 Friday-**10.00-11.00

| | **ORAL PRESENTATIONS** | |
|---|---|---|
| | **Chairing Şadiye Çakmak** | **Hall 2** |
| 01 | Muhammad WAQAS<br>*Pakistan* | Prediction of The High Heating Value of Organic Waste and It's Potential Utilization As A Source of Sustainable Bioenergy |
| 02 | Vusala MURADOVA<br>*Ukraine* | Bayesian Regularization of Learning |
| 03 | Fatih Doğan KOCA<br>*Türkiye* | Plant-Based Synthesis of Organic@Inorganic Hybrid Cu Based Nanoflower Using Cucumber Leaf Extract as Organic Component |

**26.08.2022 Friday-**10.00-11.00

| | **ORAL PRESENTATIONS** | |
|---|---|---|
| | **Chairing Özlem Erol** | **Hall 3** |
| 01 | Olga ZAICHENKO<br>*Ukraine* | Derivation of Expression for Photocurrent Density for Non-Destructive Testing of 3d Printing Filament By Means of Teraherz Spectroscopy |
| 02 | İsmail YÜCEL<br>*Türkiye* | Effect of Ca and Ba Atoms on CsPbBr 3 Perovskite Material |
| 03 | Başak KARAKURT ÇEVİK<br>*Türkiye* | The Importance Of Indoor Air Quality Strategies To Reduce The Spread Of Airborne Transmitted Diseases |

ISBN: 978-605-73552-2-5

**26.08.2022 Friday-**11.10-12.10

| | ORAL PRESENTATIONS | |
|---|---|---|
| | **Chairing Utku Kaya** | **Hall 1** |
| 01 | Alparslan GÜZEY<br>*Türkiye* | Optimal Energy Consuming on Spraying an Agricultural Field by Using Multiple UAVs |
| 02 | Nur ULUHAN<br>*Türkiye* | Electromagnetic Energy Conservation By Biquaternions |
| 03 | Seniye KARAKAYA<br>*Türkiye* | Highly transparent Mn-doped ZnO thin films prepared by ultrasonic spray pyrolysis |

**26.08.2022 Friday-**11.10-12.10

| | ORAL PRESENTATIONS | |
|---|---|---|
| | **Chairing Şadiye Çakmak** | **Hall 2** |
| 01 | İlkan KAVLAK<br>*Türkiye* | Applying of The New Generation Plastic Additives to The Kitchen Appliances: Investigation of Structural and Thermostatic Properties of Organometallic Mn (Ii) and Cu (Ii) Streat- Borate Complexes |
| 02 | Salih Kagan KALYONCU<br>*Türkiye* | All-fiber Linearly Polarized Single-Mode Q-switched Tm +3 Ho 3+ -Doped Pulse Laser at 2.1µm |
| 03 | Aygün Işık YILDIZ<br>*Türkiye* | Structural and Electronic Properties of Undoped and Be-Doped Ca 2 $TiO_4$ Ruddlesden Popper Perovskite |

**26.08.2022 Friday-**11.10-12.10

| | ORAL PRESENTATIONS | |
|---|---|---|
| | **Chairing Özlem Erol** | **Hall 3** |
| 01 | Bushra MWAKET<br>*Türkiye* | Sustainable Housing Quality Assessment for Better Housing Development in Syria Post-War |
| 02 | Zeyneb BELHI<br>*Algeria* | Evaluation of Phytochemical Composition and Antimicrobial Properties of Extracts from Two Asteraceae Species Growing Wild in South-West of Algeria |
| 03 | Emre Aytuğ ÖZSOY<br>*Türkiye* | Sustainability Practices in Vocational Education: Green Buildings |

ISBN: 978-605-73552-2-5

**26.08.2022 Friday-**14.00-15.00

| | **ORAL PRESENTATIONS** | |
|---|---|---|
| | **Chairing Emre Aytuğ Özsoy** | **Hall 1** |
| 01 | Igor NEVLİUDOV<br>*Ukraine* | Detection and Identification of Potentially Explosive Objects in Open Area |
| 02 | Hüseyin ATAL<br>*Türkiye* | Phylogenetic analysis of the genus Jasione L. (Campanulaceae) in Turkey based on chloroplast DNA matK and trnL intron sequences |
| 03 | Elif Merve ERTURAN<br>*Türkiye* | The Use of Lidar Technology in Architecture: Plan Typology of Historical Odunpazari Houses |

**26.08.2022 Friday-**14.00-15.00

| | **ORAL PRESENTATIONS** | |
|---|---|---|
| | **Chairing Utku Kaya** | **Hall 2** |
| 01 | Serhii TESLIUK<br>*Ukraine* | Robot Group Interaction Technology Using A Cloud Server |
| 02 | Iryna ZHARIKOVA<br>*Ukraine* | Flexible Printed Structures Quality Models for Mobile Robot Platform |
| 03 | İlhan ÖZKAPLAN<br>*Türkiye* | Implementation of Up-to-Date Cyber Security Requirements to Hydroelectric Power Plant (Hepp) Scada Systems |
| 04 | Iryna ZHARIKOVA<br>*Ukraine* | Flexible Printed Structures Quality Models for Mobile Robot Platform |

**26.08.2022 Friday-**14.00-15.00

| | **ORAL PRESENTATIONS** | |
|---|---|---|
| | **Chairing Abidin Kılıç** | **Hall 3** |
| 01 | Ozlem EROL<br>*Türkiye* | Mineralization of Iron Phosphate on Carbon Nanotube Via Amphiphilic Peptide |
| 02 | Manel ZAOUI<br>*Algeria* | Effect of temperature on molecular interactions in binary mixture containing alkyl ester |
| 03 | Mehmet Semih BİNGÖL<br>*Türkiye* | Investigation of Congo Red Removal With Prepared Fe 2 O 3 Added Chitosan/Glutaraldehyde |
| 04 | Patrick S. CLAIR<br>*USA* | Antagonistic effects of mitochondrial matrix |

ISBN: 978-605-73552-2-5

**25.08.2022 Thursday-**10.00-16.00

| | POSTER PRESENTATIONS | |
|---|---|---|
| | | **Poster Presentation Hall** |
| 01 | Selen KIZILKAYA<br>*Türkiye* | Determination Of Water Quality In Dipsiz- İne (Muğla-Aydin) Stream According To Macrozoobentic Organisms And Physicochemical Methods |
| 02 | M. Amin JALALI<br>*İran* | Feeding experiences modulate prey preferences and olfactory responses of two predatory ladybeetles (Coccinellidae, Coleoptera) |
| 03 | Samira Hamza REGUIG<br>*Algeria* | Organic synthesis of new products in the presence of a catalyst, which may have cytotoxic activity |
| 04 | Aigerim ZHAKIPBEKOVA<br>*Ukraine* | Ganoderma Lucidum As a Promising Source of Biologically Active Substances |
| 05 | Buse Melek CABAS<br>*Türkiye* | Colour Enrichment Process of Malt Extract By Ultrafiltration Technology and Usage for Food Application |
| 06 | Annisyah Nurmitha OKTARINA<br>*Indonesia* | In-Silico Study of Crispr-Cas Single-Guide RNA Construction for Salmonella Phage |
| 07 | Rahmadyfa M. AZZAHRAH<br>*Indonesia* | Microplastic Contamination in Consumed Bivalves in Jember Coastal, Indonesia |
| 08 | Ladiya Husna SARIATI<br>*Indonesia* | First Report on Microplastics and Attached Bacteria in Consumed Shellfish of Jember Coastal, Indonesia. |
| 09 | Sophi SANDRINA<br>*Indonesia* | Histopathology of Rattus Norvegicus After Injected with Spike Protein Epitope-Based Recombinant Protein of Sars-Cov-2 |
| 10 | S. Zeynab HASHIMZADA<br>*Azerbaijan* | Synthesis and Study of Surfactants Basis on Alkylbromides (C 14 , C 18) and Proxylated Derivatives |
| 11 | Ulkar SHIRALIYEVA<br>*Azerbaijan* | Analysis of The Current State of Research on The Thermal Stability of Organic Coolants |
| 12 | Ulkar SHIRALIYEVA<br>*Azerbaijan* | Justification of The Choice of Catalyst for The Oxidation of C3- C4 Aldehydes Into Acids and Their Modification |
| 13 | Tunay KARAN<br>*Türkiye* | Antibacterial Activity Of Silver Nanoparticles From Basciflik Potato |
| 14 | Ibrahim A. SADIQ<br>*Iraq* | On The Classical Ideal Gas in Two Dimensions |
| 15 | Oleksandra YEREMENKO<br>*Ukraine* | Results of An Experimental Study of The Fault-Tolerant Routing Method With The Glbp Protocol |
| 16 | Tuğba DERICI<br>*Türkiye* | Parafin Bazlı Nanoemülsiyon Geliştirilmesi |
| 17 | Ikram JOMAA<br>*Tunisia* | The Coordination Behavior of A New Hybrid Compound Structural Features, Physicochemical Characterization and Theoretical Study |
| 18 | Miluvka STANCHEVA<br>*Bulgaria* | Diopside Ceramic Pigments Obtained By A Sol-Gel Method: Synthesis, Structure and Properties |
| 19 | Tsvetan DIMITROV<br>*Bulgaria* | Synthesis and Characterization of Cr-Doped Diopside Ceramic Pigments |

ISBN: 978-605-73552-2-5

# ABSTRACTS

ISBN: 978-605-73552-2-5

**051-OP**

# MATHEMATICAL ANALYSIS OF THE 09 MARCH 2012 INTENSE AND 08 MAY 2014 WEAK STORM

Kevser KÖKLÜ

Yildiz Technical University, Department of Mathematical Engineering, Davutpasa Campus, İstanbul, Türkiye,
ozkoklu@yildiz.edu.tr, kevserkoklu@gmail.com

**Abstract**

The in-depth investigation of the solar wind parameters (E, v, P, T, N, $B_z$) and the zonal geomagnetic indices (Kp, Dst, AE, ap) is the keyspace weather researches and is in the center of relationship to the sun and earth. The investigations gain meaning by modeling various interplanetary parameters and geomagnetic indices. These models, built on the basis of the correlations between solar wind parameters and zonal geomagnetic indices, and that must strictly obey to physical principles, will not only reveal the properties of geomagnetic activity but also allow estimates of their formations. In a severe storm, which usually has two main phases, solar parameters have enough time to react, but weak storms cannot find this time. They have to yield their reaction in a short time. Since the time scale of weak storms is about half the time scale of intense storms, it is troublesome and important to examine the solar wind parameters/Interplanetary Magnetic Field to evolve and affect to zonal geomagnetic indices. One can find a weak (Dst=-46) on May 08, 2014, and intense (Dst=-145 nT) storm on March 09, 2012, in order to reveal, examine the consistency of discussions and compare models that have proven themselves in previous storms in this study. The author tries to think over all possible correlations between solar wind parameters and zonal geomagnetic indices and tries to obey the cause-effect relationship while creating mathematical models while not ignoring the physical principles. Therefore, the physical principles govern the study. The results visualize with tables and graphs for the understanding of the dynamic structure of the storm. In the paper, comparisons are made between two different storms and the reader is able to comment about it.

**Keywords:** Zonal geomagnetic indices, solar wind parameters, mathematical modeling

**Acknowledgment**

This work has been supported by Yildiz Technical University Scientific Research Projects Coordination Unit under project number FBA-2021-4739

I would like to thank Halil İbrahim ÖZKUL and Ata KÖKLÜ for their help.

ISBN: 978-605-73552-2-5

**052-OP**

# THE ROLE OF STRATEGIES AND POLICIES FOR SUSTAINABLE ARCHITECTURE: A NEW PERSPECTIVE FOR ENERGY-EFFICIENT BUILDINGS IN TURKEY

Mohamad Tareq KHANJI[1] Assoc. Prof. Hatice KALFAOĞLU HATİPOĞLU[2]

[1]Ankara Yıldırım Beyazıt University, Faculty of Natural Sciences, Ankara / Turkey
[2]Ankara Yıldırım Beyazıt University, Faculty of Architecture and Fine Arts , Ankara / Turkey

**Abstract:** Turkey is highly vulnerable to climate change; as part of the southern belt of Mediterranean Europe, the country is already facing observed warming in temperatures and a decrease in precipitation. Passive House criteria is a sustainable building standard which is nearly zero energy building, intended to be implemented by all member states by the European Parliament Resolution of 31 January 2008 until 2011. On 17 November 2009, the European Parliament and Council set 2020 as the deadline for bringing all new buildings to the level of low-energy buildings. This study aims to learn from their policies and experiences how passive designs assist different EU countries providing an intermediate national target to reduce energy consumption. Specifically, it investigates how the Energy Performance of Buildings Directive (EPBD) policies adopted principles of sustainability to all new buildings, implemented them, and the results of applying.

Research has been conducted to draw a perspective on how these experiences can be implemented in Turkey. A review was conducted to identify different EU countries' experiences to achieve energy-efficient buildings and the implementation results. The results showed various applications could be reflected on Turkey to guarantee the energy performance of new buildings.

These results suggest many applications to merge in the Turkish building regulations to achieve energy efficiency of the buildings which maintain CGC commission national goals and mitigate upcoming climate change risks.

***Key Words:*** Architecture, Passive house design, Energy-efficient, Sustainability, Risk mitigation

ISBN: 978-605-73552-2-5

**053-PP**

# DETERMINATION OF WATER QUALITY IN DİPSİZ-ÇİNE (MUĞLA-AYDIN) STREAM ACCORDING TO MACROZOOBENTIC ORGANISMS AND PHYSICOCHEMICAL METHODS

Selen Kızılkaya

Muğla Sıtkı Koçman University, Turkey

This study was carried out between periods of 2015-2016 and 2020 in order to determine water quality changes in Dipsiz-Çine (Muğla-Aydın) Stream according to macrozoobentic organisms and physicochemical methods.

From chosen 6 stations on Dipsiz- Çine Stream water samples were taken and macrozoobentic organisms were collected. In order to determine the physico-chemical properties of water, ammonium nitrogen, nitrite nitrogen, nitrate nitrogen, ortho-phosphate phosphorus, total hardness, sulfate hardness, carbonate hardness, calcium ion and magnesium ion were measured and evaluated. Water temperature, conductivity, pH, dissolved oxygen parameters were measured during the field.

Samples belonging to Mollusca, Annelida and Arthropoda branches were collected from the research area. 88 taxa belonging to the classes Gastropoda, Bivalvia, Oligochaeta, Hirudinea, Arachnida, Crustacea and Insecta were determined. Frequency, dominance, diversity values of macrozoobentic organisms determined at stations and similarities of stations with respect to these organisms were determined and evaluated together with water quality results.

ASPT, BMWP, Belgian Biotic Index, Saprobi Index, Pollution Tolerance Index and Family Biotic Index were used to determine water quality and water quality was determined according to the results obtained.

Physicochemical data were interpreted according to Klee (1991), and 1 st and 3 th stations I-II. in quality class, 2 nd, 5 th and 6 th stations II. in quality class, 4. station II-III. determined to be in the quality class.

According to surface water quality legislation (2012), the water quality classes of the stations are 1 st, 2 nd and 3 th, 4 th, 5 th and 6 th stations are included in I. Class (high quality) water quality class. It has been determined that the stations are included in the II. Class (less polluted) water quality class.

Dipsiz-Çine Stream is included in critically polluted water class according to FBI, slightly polluted water class according to BBI, slightly polluted water class according to SI, slightly polluted water class according to ASPT and moderately polluted water class according to BMWP has been determined.

The values obtained from ASPT, BMWP, Belgian Biotic Index, Saprobi Index, Pollution Tolerance Index and Family Biotic Indexes were examined in a common table and it was observed that there were differences in water quality classes between the indices.

ISBN: 978-605-73552-2-5

**055-OP**

# HOW THE PRE-SERVICE TEACHERS ARE ADAPTED FOR AN UNEXPECTED SITUATION: EVALUATING THE ACTIVITIES DESIGNED FOR ONLINE LEARNING ENVIRONMENTS

Emine Nur UNVEREN BILGIÇ[1,*], Emre CAM[2], Nazire Burcin HAMUTOGLU[3]

[1] Mathematics Education, Education Faculty, Düzce University, Düzce, Turkey
[2] Niksar Vocational School, Tokat Gaziosmanpasa University, Tokat, Turkey
[3] The Centre for Teaching and Learning Excellence, Eskisehir Technical University, Eskisehir, Turkey

## ABSTRACT

21st century skills and competencies which are communication, critical thinking, creativity, problem solving, perseverance, collaboration, information literacy, technology skills and digital literacy required to be adapted in an uncertain situations with. Emergency online learning-teaching environments, which entered our lives with the pandemic in 2019, once again demonstrated the importance of knowing the design of online learning-teaching processes. This has become an important issue that to increase the awareness on the importance of online learning environment dynamics. To increase the readiness of the pre-service teachers it is important to design teaching and learning activities considering the online learning environment dynamics. Accordingly, in case of facing such an unexpected situation (i.e. pandemic, natural disaster, etc.) the pre-service teachers should be switched on/off to adapt to the emergency conditions. Hence, this study aims to investigate how the pre-service teachers are ready for an unexpected situations with the basis of online learning environments dynamics. To do this, the designed teaching and learning activities will be assessed via a rubric developed by researchers. The process will be assessed formatively and the pre-service teachers will be informed about the feedback on their designed materials to develop their adaptability skills for an unexpected situation. Activities designed by pre-service teachers were examined in detail in order to increase the awareness and adaptability skills of pre-service teachers about emergency online applications in the learning environments. For the purpose of the research, it was designed as an internal case study by following the qualitative paradigm. Internal case studies are frequently used by educational researchers to describe a program and to show how effective it is. For this purpose, activities designed by 123 pre-service teachers were used as data. Based on the findings of the research; the necessity of adding a course that will deal with emergency distance education in teacher training programs has been revealed. In addition, the need for the Computer Education and Technologies Department has been underlined once again.

**Keywords:** emergency remote teaching, instructional design, mathematics education, online learning, pre-service teachers

ISBN: 978-605-73552-2-5

**057-PP**

IV. INTERNATIONAL CONFERENCE
ON
NATURAL SCIENCES AND TECHNOLOGIES
ICONAT-2022
24-26 August 2022
Antalya-Turkey

# ORGANIC SYNTHESIS OF NEW PRODUCTS IN THE PRESENCE OF A CATALYST, WHICH MAY HAVE CYTOTOXIC ACTIVITY

**Samira HAMZA REGUIG[a], Ghenia Bentabed-ababsa[a]**

*[a]Laboratory of Applied Organic Synthesis, Faculty of Exact and Applied Sciences, University of Oran 1 Ahmed Benbella, BP 1524 Es-Sénia, Oran 31000, Algeria.*

hr.samira@yahoo.fr, Badri_sofi@yahoo.fr

## INTRODUCTION :

The objective of our work is the synthesis of a family of heterocycles such as tetrahydrofurans and dihydrofurans [1-2]. To access it, we chose *gem*-dicyanoepoxides as dipole and activated alkenes and alkynes as dipolarophiles. The method used is conventional heating in the absence and in the presence of a catalyst such as CuCl.

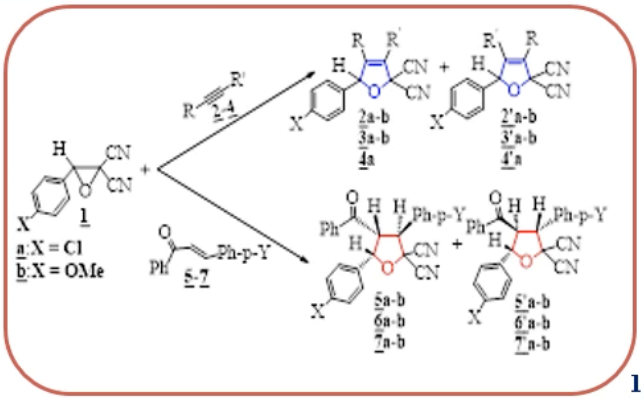


1

ISBN: 978-605-73552-2-5

**058-OP**

# NONLINEAR INTERCONNECTED STORMWATER PONDS CONTROL THROUGH NEURO SLIDING MODE CONSENSUS

H. Mehmet Güzey[1,*]

[1] Electrical-Electronics Engineering Department, Sivas University of Science and Technology, Sivas, Turkey

## ABSTRACT

In this paper, a novel neuro sliding mode consensus controller is designed for interconnected stormwater ponds in the presence of unknown precipitation. In order to minimize the effect of urbanization on the hydrological cycle, studies on stormwater management have been continuing in recent years. In the management of these systems, the requirements of smart cities should be considered as the primary constraint. It is assumed that the maximum water carrying amount of the waterways and the water holding amount of each stormwater pool are known. Besides, it is assumed that the amount of precipitation falling on the city at any given time is not known, and it is assumed that the amount of precipitation is equal in every part of the city at any given time. The amount of angling of the covers of each stormwater pond will directly affect the amount of water in the waterways and other ponds. Therefore, the system to be controlled emerges as an interconnected system. Consensus-based interconnected controller is designed so that the occupancy rate of each stormwater pond and waterway is equal to each other. The advantage of choosing a consensus-based controller, which is a decentralized control approach, is that consensus on occupancy rate can be reached even when some of the sensors cannot provide information. The unknown amount of precipitation falling is estimated through two-layer Neural Networks (NN) in real time. Then, a novel neuro sliding mode interconnected consensus controller (NSICC) is developed. By using Lyapunov stability theorem, it is proven that the NN weight estimation errors and the differences in the occupancy rates of the ponds (consensus errors) are all bounded. It is also stated that these bounds can be lowered depending on the parameters in the control signal. At the end of the article, the simulation results in the MATLAB environment are provided. Simulations illustrate that the innovative control algorithm we developed theoretically works smoothly in the case of uncertain precipitation. It has been observed that chattering is almost absent when the saturation function is used instead of sign function in the control signal. This means increased availability of the control signal in real-time applications.

**Keywords:** Flood mitigation, Real time interconnected control, Neuro sliding mode Control, Consensus.

ISBN: 978-605-73552-2-5

**059-OP**

# NUCLEATION and GROWTH MECHANISM of COLLOIDAL CHALCOGENIDE SEMICONDUCTOR NANOPARTICLES

Çağdaş ALLAHVERDİ[1,*]

[1] Department of Software Engineering, Faculty of Engineering, Toros University, Mersin, Turkey.

## ABSTRACT

A particle whose one of the dimensions is about 100 nm or smaller is called as nanoparticle. Electrical, electronic, magnetic, thermal, and optical properties of nanoparticles are different from their macroscopic bulk counterparts. These new properties being triggered at nanoscale allow nanoparticles to be used at various scientific and technological applications such as water-repellent fabrics, radiographic contrast agents, drug delivery systems, solid-state lighting. It is crucial to synthesize colloidal nanoparticles at a desired composition, size and size distribution with regard to these applications. Understanding of nucleation and growth mechanisms will indicate new ways to be able to produce high quality colloidal nanoparticles. In this study, chalcogenide semiconductor nanoparticles such as cadmium selenide, cadmium telluride and cadmium sulfide have been synthesized in octadecene. Nucleation and diffusion-limited growth of these synthesized semiconductor nanoparticles in high boiling point octadecene solvent have been monitored. Classical and nonclassical nucleation, diffusion-limited growth, Ostwald ripening and oriented attachment are going to be addressed upon these observations.

**Keywords:** Nucleation, Growth, Nanoparticles, Chalcogenide, Octadecene.

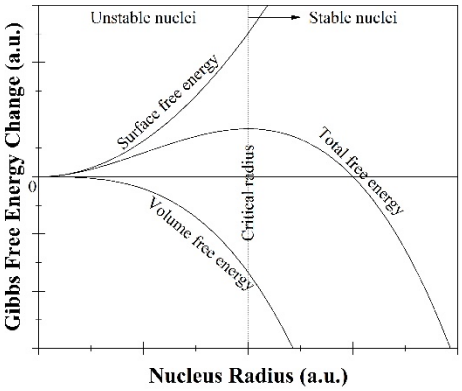


**Figure 1.** Classical nucleation. Stable nuclei form above critical radius which corresponds to maximum point of total Gibbs free energy curve. Stable nuclei can be grown by using diffusion-limited growth.

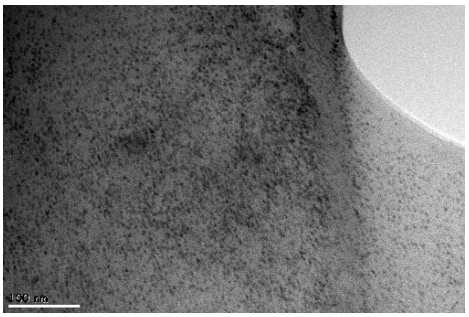

**Figure 2.** TEM photo of nucleated and growth cadmium selenide nanoparticles. Scale bar is 100 nm.

## REFERENCES

[1] Wu KJ, Tse ECM, Shang C, Guo Z. Nucleation and growth in solution synthesis of nanostructures – from fundamentals to advanced applications. Progress in Materials Science 2022; 123: 1-43.

[2] Thanh NTK, Maclean N, Mahiddine S. Mechanisms of nucleation and growth of nanoparticles in solution. Chem Rev 2014; 114: 7610-7630.

ISBN: 978-605-73552-2-5

[3] Whitehead CB, Özkar S, Finke RG. LaMer's 1950 model of particle formation: a review and critical analysis of its classical nucleation and fluctuation theory basis, of competing models and mechanisms for phase-changes and particle formation, and then of its application to silver halide, semiconductor, metal, and metal-oxide nanoparticles. Mater Adv 2021; 2: 186-235.

ISBN: 978-605-73552-2-5

**063-OP**

# COMPARATIVE RESPONSE OF TWO WHEAT VARIETIES TO BASAL AND SPLIT POTASSIUM NUTRITION UNDER FIELD CONDITIONS OF TANDOJAM PAKISTAN

Saima Kalsoom BABAR[1,*], Tarique Ali JATOI[1], Hanife AKÇA[2], Inayatullah RAJPAR[1]

[1] Department of Soil Science, Faculty of Crop Production, Sindh Agriculture University, Tandojam, Pakistan
[2] Department of Soil Science and Plant Nutrition, Faculty of Agriculture, Ankara University, Turkey

## ABSTRACT

Countless research is available on basal application of potassium (K) in relation to yield and quality of wheat (*Triticum aestivum* L.). Conversely, very fewer data is being existent on split application of K fertilizers. With the introduction of high yielding varieties under intensive cropping system with inadequate K fertilization, soil K reservoirs have started depleting which result in yield loss and high economic risk to farmers. Keeping the importance of K fertilization in wheat at right time this field experiment was conducted during 2018-2019 at Southern Wheat Research Station, Agriculture Research Centre, Tandojam, Pakistan. The experiment included 18 plots each had an area of $12m^2$ (4m × 3 m) using two cultivars of wheat, Benazir and Sindhu sown in two-factor Randomized Complete Block Design, with split-plot arrangement (main plot=varieties, sub plots=treatment) with three replications. Three regimes of K fertilization was applied i.e. $T_1$ = No K application, $T_2$ = K application at 50 kg $K_2O$ $ha^{-1}$ at the time of sowing, $T_3$ = K applications in two splits, i.e. 25 kg $K_2O$ $ha^{-1}$ at sowing and 25 kg $K_2O$ $ha^{-1}$ at grain filling stage. The yield components were observed after harvesting the crop. On average, split K application had advantage over basal application. The highest number of tillers (407 $m^2$) per plant, number of grains per spike (47), seed index (43.89), and grain yield (3.93 t $ha^{-1}$) was obtained under split application of K ($p \leq 0.01$). It is suggested to apply K fertilizer in split application to achieve the desired economic yield.

**Keywords:** cereal; fertilization methodology; modern cultivars; yield constraints

ISBN: 978-605-73552-2-5

**065-OP**

# A PRACTICE FOR QUALITY ASSURANCE IN THE DESIGN OF BLENDED LEARNING ENVIRONMENTS: EDUCATIONAL PROGRAM GOALS

Emre CAM, Emine Nur UNVEREN-BILGIC, Nazire Burcin HAMUTOGLU

[1] Niksar Vocational School, Tokat Gaziosmanpasa University, Tokat,
[2] Mathematics Education, Education Faculty, Düzce University, Düzce, Turkey
[3] The Centre for Teaching and Learning Excellence, Eskisehir Technical University, Eskisehir, Turkey

## ABSTRACT

This study provides an infrastructure regarding the necessity of designing activities to be carried out in blended learning environments. In the study, an example of instructional design related to the subject area titled " Mathematics Teacher Training" carried out within the scope of " Teaching Statistics and Probability" in a state university is presented. The educational program goals of mathematics teacher training departments (f=86) in Turkey were examined via qualitative research methods. Regarding the findings on educational program goals, the design of the Teaching Statistics and Probability course was carried out with the basis of blended learning dynamics. In this online activity, the design of instruction consists of the steps of plan, implement, control and take action to ensure quality assurance. It is thought that the related study will provide a framework for providing quality assurance in the effective, efficient and attractive design of activities to be carried out in blended learning environments. In addition, a lesson plan for "Probability and Statistics Teaching", which is an important subject area in the process of training mathematics teachers who are the instructors of the discipline of mathematics, which has a difficult, abstract and cumulative structure, will be brought to the literature in line with the quality assurance system.

**Keywords:** blended learning, mathematics education, probability and statistics teaching, educational program goals, quality assurance.

ISBN: 978-605-73552-2-5

**069-PP**

ISBN: 978-605-73552-2-5

# COLOUR ENRICHMENT PROCESS OF MALT EXTRACT BY ULTRAFILTRATION TECHNOLOGY AND USAGE FOR FOOD APPLICATION

**Buse Melek ÇABAS[1*], Cansu GENCAN[1], Arda SERPEN[1]**

[1]Döhler Gıda, Neighbourhood of Bahçelievler, Ereğliyolu Street, 214/70100, Karaman, Turkey
*Corresponding author: buse.cabas@dohler.com.tr

## ABSTRACT

The colour malt can be an alternative to the artificial colorant (caramel E150), which is widely used in the food industry, it will be an important ingredient for clean label products. This product will appeal to a wide market by using it in confectionery, bakery products, alcoholic and non-alcoholic beverages. In this study, the colour of malt extract was enriched by ultrafiltration technology and dried by spray dryer. Afterward, food application was carried out with the colour malt in powder form. The colour value (EBC; European Brewing Convention units) of the malt extract increased 2.4 times after ultrafiltration process. After the ultrafiltration process, malt extract was evaporated up to 50 °brix. The quality properties of the final product were 53 °Brix, 18.3 NTU, and 18106 EBC. Then, malt extract was dried up to 95% dry matter by spray dryer. The powder form of malt colour matter was obtained and measured as 10.5 °Brix (10 % solution). Then, colour malt powder was used to make cookies and confectionery. Sensory evaluation was carried out for malty cookies. Gumminess increased and chewability decreased as dosage of colour malt matter increase in the cookies. 1.0% dosage of malt colour powder in cookies could be preferred according to taste and colour properties by consumers. Bitterness increased as dosage of colour malt powder increased in cookies. It was determined that colour malt powder was suitable for usage in confectionery in terms of colour. The dosage of powder can be arranged by customer expectations.

**Keywords:** Natural, Colour, Malt, Ultrafiltration, Spray drying, Food Application

## INTRODUCTION

### Malt

Malt is defined as dried barley that has been germinated under controlled conditions. Malt extract are dark-brown liquids or powders that are obtained by the processing of barley malts; used as flavours and not permitted for use solely as a colour additive. It is an alternative to artificial brown colour matter (Wissgott and Bortlik, 1996). The significance of malt extract as an ingredient is its relatively high colour matter, low sweetness, flavour, and nutritional qualities (Anonymous, 2021).

### Basics of Ultrafiltration and Spray Drying Process

The UF technology has higher processing efficiency, better treatment effect, and lower energy consumption than the other traditional technologies. The process can be understood as taking the pressure difference between the two sides of the membrane as the driving force. Under the static pressure, using ultrafiltration membrane as the filter medium, the solvent in the raw material liquid and the small-molecular with smaller pore diameter pass through the ultrafiltration membrane from the high-pressure side to the low-pressure side, while the large molecular are trapped on the high-pressure side (Li et al., 2018). The colour molecules can not pass through the filtration membrane and retain into the retentant phase.

High moisture content in the foodstuff leads to having high water activity which leads the quality loss in food by increasing the enzyme activity and microbial growth. Therefore, reducing moisture content in food by drying technology is always desirable to maintain the quality of food. The quality of spray-dried foods is affected by the process parameters such as inlet temperature, air dry flow rate, feed flow rate, atomizer speed, types of carrier agent of the spray-drying process (Chegni and Ghobadian, 2005; Chegni and Ghobadian, 2007).

The objectives of this study were i) to investigate the applicability of the colour enrichment of malt extract by ultrafiltration technology and to determine the optimum drying condition, ii) to investigate the usable of the colour malt powder in the food application iii) to determine the best dosage for confectionery and cookies.

## MATERIAL & METHODS

### Flow Chart of Colour Malt Powder

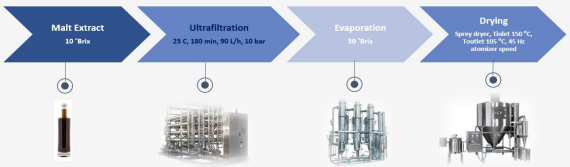


### Methods

**Colour analysis (EBC):** Sample was diluted approx. 1:10. The absorbance was measured at 430 and 700 nm wavelengths by spectrophotometer (Shimadzu, UV-1800, Germany).

$$°EBC = 30.8 \times (A_{430nm} - A_{700nm}) * DF$$

**Total soluble dry matter (TSDM; Brix) & Dry matter (DM; %):** TSDM of sample was measured by refractometer (Atago, Rx-5000α, Japan). DM of sample was measured by moisture analyzer (Sartorius, MA150, Germany).

**Turbidity (NTU):** Turbidity of sample was measured by turbidimeter (Hach, TL2310, USA).

## RESULT & DISCUSSION

- The colour values at 50 brix are expressed in the Figure 1. The colour value of malt extract increased proportionally as the process time increased during the ultrafiltration process (Figure 1). At the end of the process, it was determined that the colour unit of the malt extract increased 2.4 times compared to the pre-process.

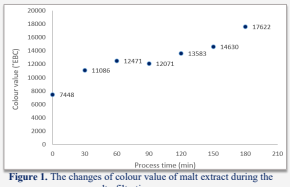


**Figure 1.** The changes of colour value of malt extract during the ultrafiltration process

- After ultrafiltration process, malt extract was evaporated up to 50 brix by the multiple-effect evaporator. The colour value of concentrated malt extract was determined as 18106 °EBC at 50 °Brix (Table 1).

**Table 1.** Quality properties of malt extract before and after process

| | °Brix | NTU | °EBC (@50 °Brix) |
|---|---|---|---|
| Before Process | 10.11 | 1.2 | 7448 |
| After Process | 53.24 | 18.3 | 18106 |

- After colour enrichment process by ultrafiltration system, malt extract was dried from 45% to 95% dry matter by spray dryer. The colour value of malt powder was determined as 37729 °EBC (Table 2).

**Table 2.** Quality properties of malt powder before and after drying process

| | DM% | °Brix | NTU (@1 °Brix) | °EBC |
|---|---|---|---|---|
| Before Process | 45.6 | 53.24 | 18.3 | 18106 |
| After Process | 95.0 | 10.5* | 13.9 | 37729 |

** It was measured in 10 % aqueous solution.*

### Sensory Evaluation


- Sensory evaluation was carried out for malty cookies. Gumminess increased and chewability decreased as dosage of colour malt matter increase in the cookies. 1.0% dosage of colour malt powder in cookies can be preferred according to taste and colour properties by consumers. Bitterness increased as dosage of colour malt powder increased in cookies.

- Colour malt powder was determined to use suitable in confectionery. The dosage of powder can be arranged by customer expectations.

## CONCLUSION.

To sum up, the colour unit of malt extract increased proportionally as the process time increased during the ultrafiltration process. After 180 minutes of processing time, colour value of malt extract was raised up from 8000 EBC to 18000 EBC approximately by ultrafiltration technology, and then colour enriched malt extract was dried to 95% total dry matter by spray dryer. Colour malt powder was determined that it was suitable for using in cookies and confectionery. It was made an inference that 1.0% malt colour powder in cookies was more suitable for consumption in terms of taste and colour properties.

## REFERENCES

**Chegini, G. R., & Ghobadian, B.** (2005). Effect of spray-drying conditions on physical properties of orange juice powder. Drying technology, 23(3), 657-668.
**Chegini, G. R., & Ghobadian, B.** (2007). Spray dryer parameters for fruit juice drying. World Journal of Agricultural Sciences, 3(2), 230-236.
**Li, X., Jiang, L., & Li, H.** (2018). Application of ultrafiltration technology in water treatment. In IOP Conference Series: Earth and Environmental Science (Vol. 186, No. 3, p. 012009). IOP Publishing.
**Wissgott, U., & Bortlik, K.** (1996). Prospects for new natural food colorants. Trends in Food Science & Technology, 7(9), 298-302.

ISBN: 978-605-73552-2-5

**070-OP**

# CO-AGGREGATION OF S100A9 PROTEIN WITH L- DOPA AND CYCLEN-BASED COMPOUNDS – EFFECT ON THE AMYLOID FIBRIL SELF-ASSEMBLY

L. Arabuli[1,2], I. A. Iashchishyn[1], N. V. Romanova[1], G. Musteikyte[3], V. Smirnovas[3], H. Chaudhary[1], Ž. M. Svedruži´c[4], and L. A. Morozova-Roche[1]

[1]Department of Medical Biochemistry and Biophysics, Umeå University, SE-90781 Umeå, Sweden
[2]Department of Natural Sciences, School of Science and Technology, University of Georgia, 0171 Tbilisi, Georgia
[3]Institute of Biotechnology, Life Sciences Center, Vilnius University, LT-10257 Vilnius, Lithuania
[4]Department of Biotechnology, University of Rijeka, HR-51000 Rijeka, Croatia
E-mail: l.arabuli@ug.edu.ge

We studied the effect of cyclic compounds and their conjugates on the amyloid formation of pro-inflammatory S100A9 protein, which was found to be a common denominator in Alzheimer's and Parkinson's disease as well as in traumatic brain injury, which is considered as a pre-cursor state for neurodegenerative ailments [1,2]. Indeed, amyloid formation is commonly associated with neuroinflammation, and pro-inflammatory S100A9 protein acts both as an alarmin, inducing the production of pro-inflammatory cytokines, and as a highly amyloidogenic protein, which self-assembles into amyloids under physiological conditions.

The amyloid cascade is central for the neurodegeneration disease pathology, including Alzheimer's and Parkinson's, and remains the focus of much current research. S100A9 protein drives the amyloid-neuroinflammatory cascade in these diseases. DOPA and cyclen-based compounds were used as amyloid modifiers and inhibitors previously, and DOPA is also used as a precursor of dopamine in Parkinson's treatment. Here, by using fluorescence titration experiments we showed that five selected ligands: DOPA-D-H-DOPA, DOPA-H-H-DOPA, DOPA-D-H, DOPA-cyclen, and H-E-cyclen, bind to S100A9 with apparent Kd in the sub-micromolar range. Ligand docking and molecular dynamic simulation showed (Fig.1) that all compounds bind to S100A9 in more than one binding site and with different ligand mobility and H-bonds involved in each site, which all together is consistent with the apparent binding determined in fluorescence experiments. By using amyloid kinetic analysis, monitored by thioflavin-T fluorescence, and AFM imaging, we found that S100A9 co-aggregation with these compounds does not hinder amyloid formation but leads to morphological changes in the amyloid fibrils, manifested in fibril thickening. Thicker fibrils were not observed upon fibrillation of S100A9 alone and may influence the amyloid tissue propagation and modulate S100A9 amyloid assembly as part of the amyloid-neuroinflammatory cascade in neurodegenerative diseases.

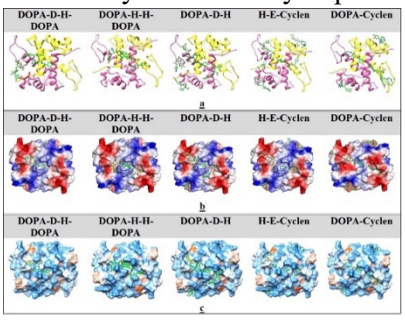


Figure 1. Binding sites on S100A9 homo-dimer for different DOPA and Cyclen-based compounds.

[1] Wang, C.; Klechikov, A.G.; Gharibyan, A.L.; Wärmländer, S.K.T.S.; Jarvet, J.; Zhao, L.; Jia, X.; Narayana, V.K.; Shankar, S.K.; Olofsson, A.; et al. Acta Neuropathol. 2014, 127, 507–522.
[2] Horvath, I.; Iashchishyn, I.A.; Wang, C.; Moskalenko, R.A.; Wärmländer, S.K.T.S.; Wallin, C.; Gräslund, A.; Kovacs, G.G.; Morozova-Roche, L.A. J. Neuroimmun. 2018, 15, 172.

ISBN: 978-605-73552-2-5

**071-OP**

# PRINCIPAL COMPONENT STATISTICAL ANALYSIS ON THE RELATIONSHIP BETWEEN VIOLENCE AND ADDICTION APPLIED TO HEALTHCARE PROFESSIONALS

Adnan MAZMANOĞLU[1,*], Emine Merve KALINLI[2], Nur Selin ÖZEN[1] , Müzeyyen CÖMERT AKSU[3], Seda MAZMANOĞLU ATILMAN[4], İbrahim İNAN[5]

[1] Industrial Engineering Department, Engineering Faculty, Toros University, Mersin, Turkey
[2] Psychology, Faculty of Economics, Administrative and Social Sciences, Toros University, Mersin, Turkey
[3] Toros University, Mersin, Turkey
[4] Department of Pathology, Haydarpaşa Numune Education and Research Hospital, Health Sciences University, İstanbul, Turkey
[5]Çağ University, Mersin, Turkey

## ABSTRACT

The randomness of the fluctuations of social events makes it difficult for us to make a decision about the future, because in every event there is an order that cannot be observed at first glance and one or more factors that cause this event. Violence, especially against physicians in health institutions, includes verbal, behavioral or physical attacks that pose a risk to the health worker, from the patient, patient relatives or another individual. When the international literature is reviewed, the data on the relationship between violence against healthcare workers and psychiatric disorders and addiction are very limited. In order to find the most effective factors of the relationship between these two conditions, a questionnaire was prepared about the relationship between psychiatric disorders and addiction, consisting of 14 questions and 36 variables, and the data sent to the healthcare professionals were analyzed in the SPSS package program. In the survey participated by 259 health workers, it was concluded that 115 of the participants were health workers who were exposed to violence. As a result of the question asked about the psychiatric history of the attacker, the rate of the attackers in the mass according to the answers received from 97 individuals for those with "behavioral disorder", "impulse control disorder", "anxiety disorder", "affective disorder" and those who did not write the type of attacker's psychiatric history. 84.5% was found. When the types of addiction history of the attacker were examined, the results obtained were 8.7% with drug addiction, 4.3% with alcohol addiction, 7% with tabacism, and 1.7% with gambling addiction. People with substance abuse showed aggression at a rate of approximately 22%. Kaiser-Meyer-Olkin Measure of Sampling Adequacy value was found to be 0.539 as a result of the factors on which clusters between addiction and violence were collected in factor analysis tests. This value is suitable for the condition that the sampling criterion is more than 50%. Age, professional year, institution (public-private) and gender are the most loaded correlations, with an average correlation ratio of 78%.year, institution (public-private) and gender are the most loaded correlations, with an average correlation ratio of 78%. This explains 64.915% of the variability in variation of the first four variables. As the first factor, an estimate of approximately 70% correlation was obtained, on average, the type of violence, addiction histories and psychiatric histories, the most effective factor to be considered. In addition, the second factor that should be emphasized is estimated as the factor in which "psychiatric stories" and "addiction stories" are ranked. These results were calculated with the Principal Components Method of Factor Analysis, our statistical estimation method with SPSS. This method selects the factor with the highest variance value in the sample. This factor accounts for the largest portion of the total variance. The method selects the second factor with the lowest correlation in the first factor. This factor has the second highest variance value in the sample. Sorting continues in this way until the last factor is selected. Another important result of our research is the violence perpetrated by substance addicts. It has been estimated that among those with the most common addiction history, 8.7% in general, alcohol addienerji ürection 4.3%, tabacism 7%, and gambling addiction history 1.7%, reaching 21.7% in total.

**Keywords:** Violence, Aggression, Psychiatric History, Addiction History, Factor Analysis

ISBN: 978-605-73552-2-5

**072-OP**

## ROBOT POSITIONING IN INDOOR ENVIRONMENTS USING A DEEP LEARNING MODEL

Ahmet Murat ERTURAN[1,2*], Abdullah YUSEFI[3], Akif DURDU[1], Seyfettin Sinan GÜLTEKİN[1]

[1] Electrical-Electronics Engineering Department, Faculty of Engineering and Natural Sciences, Konya Technical University, Konya, Turkey
[2] Electrical-Electronics Engineering Department, Faculty of Engineering, Erzurum Technical University, Erzurum, Turkey
[3] Computer Engineering Department, Faculty of Engineering and Natural Sciences, Konya Technical University, Konya, Turkey

### ABSTRACT

The issue of positioning in closed environments has become popular in recent years. Positioning a robot in outdoor can be easily accomplished with GPS signals. However, it is very difficult to make an accurate positioning because GPS signals cannot be received in indoor environments. In order to solve this problem, researchers, especially bayes prediction methods; He used methods such as wheel data, image processing, barcode-data matrix marker. In this study, in addition to the methods discussed in the literature, a deep learning model was used and it was aimed to recognize the two traffic signs that the robot encountered during the autonomous movement and position itself. The robot has determined its own position with an average of 88.11% and 88.39% accurately with the proposed mathematical method according to the location of the two traffic signs it knows.
**Keywords:** Indoor Localization, Deep Learning, Simultaneous Localization And Mapping (SLAM), Faster R-CNN.

**074-OP**

## MOLECULAR STRUCTURE, NBO AND TD-DFT ANALYSIS OF 4-METHYL-3-FURALDEHYDE BASED ON DFT CALCULATIONS

Nihal KUŞ
Department of Physics, Science Faculty, Eskisehir Technical University, 26470, Eskisehir, Turkey.

### ABSTRACT

In this study, molecular structure of 4-methyl-3-furaldehyde (4M3F) was analyzed using density functional theory (DFT) with level of B3LYP/6-311G++(d,p). As a result of the scanning of the CCC=O dihedral angle, two conformers (trans and cis) were found at minimum energy and the trans was more stable than the cis at *ca*. 6.4 kJ $mol^{-1}$.

Time dependent DFT (TD-DFT) calculations have been used to calculate the low-energy excited states energies and oscillator strengths. As a result of calculations, it was found that the highest transition probability and most effective oscillator strength were in the $S_0 \rightarrow S_3$ singlet state for both conformers. This excitation energy corresponds to 5.9 eV for the trans conformer, while it is around 5.6 eV for the cis conformer.

The change in electron density in bonding-antibonding orbitals and their interactions as well as stabilization energies E(2) and natural atomic charges were calculated by Natural Bond Orbital (NBO) analysis. Electronic properties were analyzed using HOMO and LUMO energies.
**Keywords:** 4-methyl-3-furaldehyde, Time dependent DFT, Natural Bond Orbital (NBO) analysis

**ACKNOWLEDGMENT**

This work was supported by the Eskisehir Technical University Commission of Research Project under grant no: 22ADP074.

ISBN: 978-605-73552-2-5

**075-PP**

# IN-SILICO STUDY OF CRISPR-Cas SINGLE-GUIDE RNA CONSTRUCTION FOR *Salmonella* PHAGE

Annisyah Nurmitha OKTARINA[1], Erlia NARULITA[1*], Rina B. OPULENCIA[2]

[1]Biology Education Study Program, Faculty of Teacher Training and Education, University of Jember, Jember, Indonesia
[2]Microbiology Division, Institute of Biological Sciences, University of the Philippines Los Baños, Los Baños, Philippines
*erlia.fkip@unej.ac.id

Foodborne disease cases are still highly found nowadays. The majority of foodborne disease cases are caused by *Salmonella*. Bacteriophage therapy is a solution to overcome *Salmonella* infection without induced antibiotics resistance effects. Jumbo phage can be used to overcome the host range limitation of bacteriophages for example in *Salmonella* with various serovars, but the isolation process is difficult and cost consuming. The alternative way to enhance the host range of bacteriophage is using genome editing. In this study, we conducted an in-silico study of single guide RNA (sgRNA) construction as the initial stage of genome editing using the CRISPR-Cas9 system on *Salmonella bacteriophage SSE-121* to broaden its host range. The target gene in this study was a tail fiber protein that plays a role in the process of recognizing and attaching viruses to the bacterial hosts. The research is conducted using bioinformatics tools. The *Salmonella* phage genome was obtained from the NCBI gene bank (NCBI Reference Sequence: NC_027351.1) and the Cas9 protein was obtained from the RCSB PDB Protein Data Bank (PDB ID: 4ZT0). The results of the study were 188 sgRNA candidates using CHOPCHOP website design-based tools (http://chopchop.cbu.uib.no/). Fourteen sgRNAs candidate were selected based on efficiency score, GC content, and self-complementarity. Further selection to obtain the optimum sgRNA was carried out based on molecular docking score. All selected candidates were docked using website docking based tools HNADOCK (http://huanglab.phys.hust.edu.cn/hnadock/) and the top 7 candidate sgRNAs were docked using HDOCK (http://hdock.phys.hust.edu.cn/) with the Cas9 protein. The visualization and bonding stability of final optimum sgRNA and Cas9 protein is calculated using molecular dynamics application. In summary, the in-silico study for sgRNA construction can determine the optimum sgRNA for *Salmonella* phage and its expected to minimize failures and errors during in-vivo experiments.

**Keywords:** Genome editing, CRISPR, molecular docking.

ISBN: 978-605-73552-2-5

**076-OP**

# COMPLEX OCTONIONIC FORMULATION FOR THE FIED EQUATIONS OF MULTIFLUID PLASMA

Süleyman DEMİR[1,*], Murat TANIŞLI[1] , Neslihan ŞAHİN[1]

[1] Department of Physics, Faculty of Science, Eskisehir Technical University, Eskişehir, Turkey

**ABSTRACT**

The resemblance between the basic equations of electrodynamics and fluid dynamics led scientists to reformulate the fluid equations motion in a form similar to a set of Maxwell equations in electromagnetism. On the other hand, in many cases, mechanical forces subjected to the plasma are consistent with a fluid treatment. Using the isomorphism between behaviors of fluids and plasmas, the Maxwell-type field equations of multifluid plasma have been reformulated in terms of complex octonions. The expressions derived in this work are capable of summarizing the well-known equations of plasma in a compact and elegant way.

**Keywords:** Complex Octonion, Multifluid Plasma, Maxwell Equations, Field Equations

**Acknowledgment:** This study is supported by Eskişehir Technical University Scientific Research Projects Commission under the grant no:22ADP136

**REFERENCES**

[1] Thompson R J, Moeller T M, A Maxwell formulation for the equations of a plasma, Phys. Plasmas 2012; 19: 010702.
[2] Thompson R J, Moeller T M, Classical field isomorphism in two-fluid plasmas, Phys. Plasmas 2012; 19: 082116.
[3] Demir S, Tanışlı M, Hyperbolic octonion formulation of the fluid Maxwell equations. J. Korean Phys. Soc. 2016; 68: 616-623.
[4] Tanışlı M, Demir S, Şahin N, Octonic formulations of Maxwell type fluid equations. J. Math. Phys. 2015; 56: 091701.
[5] Demir S, Zeren E, Multifluid plasma equations in terms of hyperbolic octonions, Int. J. Geo. Meth. Mod. Phys. 2018; 15: 1850053.

ISBN: 978-605-73552-2-5

**077-OP**

# A STUDY ON AIR QUALITY NEAR SOLID WASTE TREATMENT PLANTS AMONG UNIVERSITY POPULATION: ADANA CASE

Tugce PEKDOGAN

[1] Department of Architecture, Faculty of Architecture, Adana Alparslan Türkeş Science and Technology University, Adana, Turkey

## ABSTRACT

In the city of Adana, which constitutes the field of this study, rapid urbanization with rapid population growth causes increasing waste consumption. This uneven increase has brought along the problem of urban waste collection and disposal. The fact that the Sofulu solid waste disposal facility in Adana is located within the residential areas causes the health and social life of the city to be negatively affected. Even if measures are taken for sanitary landfills, it is likely to adversely affect public health as they create various sources of air pollutants such as chemicals, odor and volatile organic compounds. The aim of this study; Alparslan Türkeş Science and Technology University, which is located near the Adana Sofulu solid waste disposal facility and hosts many individuals every day, investigates the impact of a solid waste disposal facility on the user with a user-oriented survey. Statistical techniques were used to examine the relationships between residents' responses to the layout of the landfill. The research was carried out among 100 participants, 50 of them were university students, and another 50 were academic and administrative staff working at the university. The difference between these two groups was observed statistically with the cross-classification analysis. In addition, research findings make research on environmental awareness towards solid waste disposal facilities.

**Keywords:** Solid waste landfill, air quality, environmental awareness, survey

ISBN: 978-605-73552-2-5

**078-PP**

# MICROPLASTIC CONTAMINATION IN CONSUMED BIVALVES IN JEMBER COASTAL, INDONESIA

Rahmadyfa Maulida AZZAHRAH1, Selvi ARIYUNITA1, Erlia NARULITA1,*, Andreas NICOLAI2

1 Biology Education, Teacher Training and Education, University of Jember, Jember, Indonesia
2 Energy and Biotechnology, Biotechnology, Food Technology and Chemical Engineering, Flensburg University of Applied
Science, Flensburg, Germany
*erlia.fkip@unej.ac.id

**ABSTRACT**

Bivalvia is a filter feeder animal that could accumulate various kinds of pollutants due to foraging needs, one of which is microplastic. Bivalves have a great concern about microplastic exposure to humans. One of their means is human consumption, which needs to regulate under seafood safety. This study aims to consider human food safety and observe the dangers of ingested microplastic for the organism and humans. The study consists of sample collection, identification, and preparation, microplastic isolation and identification, and data analysis. Samples were collected and identified from the Malikan and Puger coasts of Jember, Indonesia, from December 2021 to April 2022. Sample preparation goes through a destruction process with 30% H2O2 solution under 65oC. The result is filtered using a Whatman paper filter No. 42, remaining the microplastic particles on it. Isolated microplastics were then identified based on their size, shape, color, and polymer type. Identification of the polymer type using FTIR spectroscopy. Data analysis is calculated abundance based on the average particles per individual. The average microplastic abundance is 37,9 particles/ind were found on the Malikan coast from species Perna viridis and 23,5 particles/ind on the Puger coast from species Pilsbryoconcha exilis. Both have the dominant characteristics in sizes of 500 – 1000 µm, the form of fiber, and the color of colored. Most of them are polystyrene types, an aromatic polymer formed from the polymerization of styrene monomers which potentially bring carcinogenic effects. Ingestion of microplastics in organisms could bring physiological effects while it also brings potential toxical effects in humans as the top predator through bioaccumulation and biomagnification.

Keywords: Bivalves, Food safety, Microplastic, Seafood

ISBN: 978-605-73552-2-5

**079-PP**

# First Report on Microplastics and Attached Bacteria in Consumed Shellfish of Jember Coastal, Indonesia

Ladiya Husna SARIATI[1], Selvi ARIYUNITA[1], Erlia NARULITA[1*], Birte NICOLAI[2]

1 Biology Education, Teacher Training and Education, University of Jember, Jember, Indonesia
2 Energy and Biotechnology, Faculty of Biotechnology, Food Technology and Chemical Engineering, Flensburg University of Applied Science, Flensburg, Germany
*erlia.fkip@unej.ac.id

**ABSTRACT**

Food security can be affected by climate variability, eutrophication, ocean acidification, oxygen depletion, conflict, economic recession, pathogens, and pollution. Microplastic can be found in commonly consumed seafood. Microplastics are known as vectors of various pollutants due to their ability to absorb pollutants. Microplastics have a broad and specific surface area; therefore, many microorganisms colonize microplastic surfaces, including bacteria, fungi, algae, and protists. In this study, we identified bacteria attached to the surface of microplastics in bivalves in the coastal area of Jember, Indonesia. Samples were taken from the Malikan coast and the Gethem Mangrove coast. The number of samples collected in the Malikan Coastal and Gatheam Mangrove were two and three samples, respectively. Prior to the isolation of microplastic shellfish torn apart, they were washed with 9% NaCl. The microplastics were isolated under a stereomicroscope and transferred to a sterile general medium. The identification carried out included morphological and biochemical tests based on Cowan and Steel's manual for the identification of medical bacteria. There were five different genera found, namely Alcaligenes, Moraxella, Micrococcus, Neisseria, and Bacillus. Further research to determine the species by molecular approach is needed.

**Keywords:** Microplastics, seafood, identification, bacteria.

ISBN: 978-605-73552-2-5

**080-PP**

# HISTOPATHOLOGY OF *Rattus norvegicus* AFTER INJECTED WITH SPIKE PROTEIN EPITOPE-BASED RECOMBINANT PROTEIN OF SARS-CoV-2

Sophi SANDRINA[1], Erlia NARULITA[1*], Ma. Carmina C. MANUEL[2]

1Biology Education, Faculty of Teacher Training and Education, University of the Jember, Jember, Indonesia
2Institute of Biological Sciences, College of Art and Science, University of the Philippines Los Baños, Los Baños, Philippines
*erlia.fkip@unej.ac.id

**ABSTRACT**
SARS-CoV-2 uses the spike glycoprotein (S) to bind with the Angiotensin-Converting Enzyme 2 (ACE2) receptor in the host. The vital role of S protein makes it a potential target for vaccine development. This study aimed to examine the effect of injected synthetic protein-encoding from the epitope selected of the SARS-CoV-2 sequence of Indonesian to histopathology of lungs, kidney, and liver. Eighteen Wistar rat (*Rattus norvegicus*) were used and divided into three groups which were treated by 0.9% NaCl physiological fluids (P0), 200µg of recombinant protein with adjuvants (P1), and 200µg of recombinant protein without adjuvants (P2). The injection was conducted once every 14 days for 42 days. Wistar rat was terminated on the 43rd day. The level of damage was observed by scoring and analysed using the Kruskal-Wallis method. The results of Kruskal-Wallis analysis revealed that the significance value of lungs, kidney and liver were 0.492, 0.213, 0.063, respectively. These values show no significant effect of spike protein epitope-based recombinant to the histopathology of three organs. However, further tests for development its recombinant protein as vaccine candidates are importantly needed.

**Keywords:** Spike protein, recombinant protein, histopathology, Indonesian.

ISBN: 978-605-73552-2-5

**082-OP**

# THE USE OF LIDAR TECHNOLOGY IN ARCHITECTURE: PLAN TYPOLOGY OF HISTORICAL ODUNPAZARI HOUSES

Elif Merve ERTURAN[1,*], Mine ULUSOY[2]

[1] Department of Architecture, Faculty of Architecture and Design, Konya Technical University, Konya, Turkey
[2] Department of Architecture, Faculty of Architecture and Design, Konya Technical University, Konya, Turkey

## ABSTRACT

With the development of technology, the need for human power has decreased and machines have become able to do almost any job. When examined in the historical process, it is possible to witness that all disciplines have moved forward with technology. Unlike traditional methods, robotic systems can measure distances more easily. The Lidar (Light Detection and Ranging) sensor is one of the sensors that gives fast results thanks to its system that rotates 360 degrees and sends thousands of lasers per second to the surfaces.
Lidar Technology is currently used in archaeology, urban planning, oil and gas exploration, mapping, autonomous cars, forest and underwater research. In the study, which is expected to be one of the pioneering studies to be used in the field of architecture, it is aimed to draw a plan typology in historical Odunpazarı houses.
It is necessary to have detailed knowledge in the use of laser technologies used in the discipline of architecture due to their large dimensions and sensitive structures. Lidar sensor, on the other hand, is a device that is more economical, easier to carry and can measure quickly. It is predicted that the Lidar sensor, which has different models and measurement ranges, will be preferred because it will provide both lower cost and easier accessibility to be applied to the field of architecture by making use of the algorithms used in robotic systems. Obtaining high accuracy at low cost reveals the necessity of using some algorithms. HectorSLAM algorithm was also used as a method in the study.
Although the Odunpazarı houses, which are an important cultural heritage for Eskişehir, are used for touristic purposes today, it is seen that the traditional life continues. There are hundreds of houses that witnessed history and were used by the Seljuks and Ottomans in the region, which was declared as a protected area by the metropolitan municipality. For this reason, examining the houses in order to understand the lifestyle and culture of that period will contribute to the literature. The plans of the traditional houses examined within the scope of the study were obtained by measuring with the Lidar sensor, and some data about the lifestyle of the period were revealed with the photographs and the information provided by the individuals living in the houses.

**Keywords:** Lidar technologies and architecture, Lidar sensor, measurement techniques in architecture, laser and lidar

ISBN: 978-605-73552-2-5

**084-OP**

## INVESTIGATION OF CONGO RED REMOVAL WITH PREPARED $Fe_2O_3$ ADDED CHITOSAN/GLUTARALDEHYDE

Mehmet Semih BİNGÖL [1,*]

[1,*] DAYTAM, Ataturk University, Erzurum, TURKEY

### ABSTRACT

As technology develops and production increases, environmental problems have become serious. Because every production results in waste. Therefore, environmental pollution has reached vital limits for nature and human beings. In this study, the removal of congo red, one of the textile dyes that cause serious problems for the environment, from wastewater was investigated. Adsorption of congo red was achieved with the prepared Fe2O3 added Chitosan/Glutaraldehyde. Parameters such as pH, temperature and time were investigated in adsorption studies. In addition, kinetic, isotherm and thermodynamic studies were carried out in the adsorption study. Accordingly, over 90% adsorption was achieved in the studies carried out. Optimal adsorption was achieved at pH 7, 2 hours, and 25ºC temperature. It was also found to be suitable for Langmuir isotherm and pseudo second order kinetic model.

**Keywords:** Congo Red, Chitosan, Adsorption, $Fe_2O_3$

**085-OP**

## APPLICATION OF BIQUATERNION ALGEBRA TO HYDRODYNAMICS

Mine FAKILI*, Neslihan ŞAHİN

Department of Physics, Faculty of Science, Eskişehir Technical University, Eskişehir, Turkey

### ABSTRACT

In this study, the definitions are given about the frequently used algebras in the theoretical physics. Some properties and applications are given about biquaternions. The applications in theoretical physics are remarkable in terms of the ease of operation in multidimensional space and the definition of equations in these spaces. Furthermore, the equations of quantum hydrodynamics, also called as the Madelung equations, can be thought as alternative formulation to the Schrödinger equation in higher dimensions. Therefore, the Navier-Stokes equation, modified to include quantum potential and fluctuating viscosity for motions of the quantum fluid medium, are tried to be re-written with biquaternion algebra.

**Keywords:** Biquaternion Algebra, Hydrodynamics Equations, Fluids Medium

ISBN: 978-605-73552-2-5

**086-OP**

# ADSORPTION OF ACID RED BY SEPIOLITE BELONGS TO ESKIŞEHIR (SIVRIHISAR) REGION AND ITS SURFACE ACTIVE AGENTS-MODIFIED FORMS

Sedef DİKMEN[1,*], Zafer DİKMEN[1]

[1] Department of Physics, Science Faculty, Eskişehir Technical University, Eskisehir, Turkey

## ABSTRACT

In this research, firstly a natural clay mineral, which is sepiolite, was transformed into Na-sepiolite forms and then Na-sepiolite was modified by hexadecyltrimethylammonium (HDTMA) bromide [CH3(CH2)15N(CH3)3Br]. The characterization studies by using different methods (BET, XRF, XRD, SEM, FT-IR, TG/DTA, immersion heat, and zeta potential measurement) were also carried out to identify the modification of natural sepiolite with HDTMA-Br and its adsorption behavior. Then, the adsorption of hazardous dyestuff, which are present in wastewater or underground water with HDTMA-sepiolite were investigated in batch technique. In this manner, the effects of adsorbent dosage, contact time, and pH were investigated for the adsorption of acid red onto HDTMA-sepiolite. Adsorption kinetics and isotherm parameters were deduced by using experimental data. Pseudo-first-order, pseudo-second-order, and Weber-Morris models and Langmuir and Freundlich isotherms were applied to the experimental data to obtain adsorption kinetics and adsorption equilibrium, respectively. According to this, the adsorption of acid red data fits well with the pseudo-first-order kinetic model (with high correlation coefficients).

**Keywords:** adsorption, dyestuff, sepiolite, surface active agents

ISBN: 978-605-73552-2-5

**087-OP**

# Lysogenic Phage Isolation from Methicillin-Resistant *S.aureus* Clinical Isolates

Senanur DOKUZ[1], Görkem GÜNGÖR[2], Tülin ÖZBEK[3]*

[1] Yıldız Technical University, Faculty of Arts and Sciences, Molecular Biology and Genetics, İstanbul, Turkey.
[2] Yıldız Technical University, Faculty of Arts and Sciences, Molecular Biology and Genetics, İstanbul, Turkey.
[3*] Yıldız Technical University, Faculty of Arts and Sciences, Molecular Biology and Genetics, İstanbul, Turkey.

ozbektulin@gmail.com

## ABSTRACT

Bacterio(phage)s, the most abundant entities on our planet, are driving forces for the development of their pathogenicity and play important roles in bacterial adaptive evolution. Phages can follow lysogenic and lytic life cycles. Lysogenic phages integrate their genomes into the bacterium genome. The phage following the lytic cycle is a virulent phage, after attaching to the host cell, the nucleic acid of the phage enters the cell, hundreds of phage copies are produced in bacteria, and the phage particles are released into the environment by lysing the cell. Integration of lysogenic phages into the genome is a process that can change gene expression in bacteria, bring genes in the cell that provide advantages such as antibiotic resistance, create new phenotypes, and result in virulence factor production of the bacteria. In the presence of stress factors such as temperature change, hydrogen peroxide and mitomycin-C, phage can leave the lysogenic cycle and switch to the lytic cycle.

Methicillin-resistant *Staphylococcus aureus* (MRSA) is one of the strains that are especially important among nosocomial infections, cause many diseases like skin infections, impedigo, endocarditis, osteomyelitis, toxic shock syndrome and have developed antibiotic resistance. In this study, phage filtrates from MRSA clinical strain were obtained by applying mitomycin-C and hydrogen peroxide at different concentrations and changing the incubation temperature of the bacteria. The lytic effect was observed by performing spot tests using *S. aureus* RN4220 and MRSA strains. As a result of sequencing the obtained genome, it is aimed to contribute to the literature by discovery of new phage species, understanding the effects of lysogenic MRSA phages on MRSA strains, understanding the formation process of antibiotic resistance profile, analysis of virulence factors created by the lysogenic genome, and determination of integration regions of prophage.

ISBN: 978-605-73552-2-5

**088-OP**

# Cloning of Bacteriophage Lytic Protein

Hande HANÇER[1], Gül Begüm EREN[2], Tülin ÖZBEK[3*]

[1] Molecular Biology and Genetics, Faculty of Arts and Sciences, Yıldız Technical University, İstanbul, Turkey
[2] Molecular Biology and Genetics, Faculty of Arts and Sciences, Yıldız Technical University, İstanbul, Turkey
[*3] Molecular Biology and Genetics, Faculty of Arts and Sciences, Yıldız Technical University, İstanbul, Turkey
ozbektulin@gmail.com

## ABSTRACT

*Staphylococcus aureus* is extremely pathogenic and seen among the most common causes of hospital-acquired infections, which has been increasing in worldwide. In the antibiotic era, *S. aureus* infections were treated with various antibiotics. However, the very intensive and unconscious use of these antibiotics has resulted in the presence of resistant bacterial strains. Therefore, while leaving antibiotics age behind, scientists have begun to look for new therapeutic approaches to combat antimicrobial resistance. Bacteriophage and bacteriophage-based antimicrobials are seen as an alternative and promising agents for antibiotic resistance.

Bacteriophages are viruses which infect bacteria. They have two life cycles, lytic and lysogenic. Two main phage proteins, endolysin and holin, are used by lytic phages infecting bacteria in the process of lysing the bacteria for the release of virions. Holins localize to the cell membrane with their transmembrane domain (TMD) and trigger hole formation in the host cell membrane during infection, which causes destruction of the membrane proton motive force, resulting in both growth arrest and cell death. In the literature, antibacterial effects of phage lytic proteins on bacteria have been observed when they are expressed recombinantly in the cell and applied exogenously.

In the study, the *TMD* gene obtained from a lytic phage that infects *S. aureus* bacteria was successfully cloned into the expression vector and transformed into *E. coli* Bl21 (DE3). Transformed colonies on selective medium with ampicillin were confirmed by sequence analysis and colony PCR. The aim of this study is to provide the use of this antibacterial product in all areas where have bacterial contamination crisis such as health, food, agriculture, cosmetics are used, and also introduce holin proteins to the literature.

**Keywords:** Bacteriophage, Lytic protein, *Staphylococcus aureus*, Recombinant protein

ISBN: 978-605-73552-2-5

**089-PP**

# ANTIBACTERIAL ACTIVITY OF SILVER NANOPARTICLES FROM BASCIFLIK POTATO

Tunay KARAN[1*], Zafer GONULALAN[2], Yasin Bedrettin KARAN[3]

[1] Department of Genetics, Faculty of Veterinary, Yozgat Bozok University, Yozgat, Turkey
[2]Department of Food Hygiene and Technology, Faculty of Veterinary, Erciyes University, Kayseri,Turkey
[3]Department of Field Crops, Faculty of Agriculture, Tokat Gaziosmanpasa University, Tokat, Turkey

## ABSTRACT

Potato (*Solanum tuberosum* L.) is a significant vegetable and one of the most widely consumed crops. Photochemical investigation revealed that the potatoes had antibacterial, anticancer and antioxidant properties. In this study, Basciflik Potato Genotype (BPG) was used for the synthesis of silver nanoparticles. The BPG was extracted with distilled water. After filtration, the solution was treated with silver nitrate at 50°C to yield silver nanoparticles (AgNPs). The color change indicated the formation of AgNPs. Moreover, the structure AgNPs was elucidated by spectroscopic techniques such as Fourier transform infrared spectroscopy (FTIR), Ultraviolet-visible (UV-Vis), X-ray diffraction (XRD), and Scanning electron microscope (SEM). The characteristic functional groups were presented by FTIR. The signal observed at 3267 $cm^{-1}$ corresponded to the hydroxyl group. The absorption at 430 nm in UV-Vis spectrum showed establishment of AgNPs. The crystalline structure of AgNPs was confirmed by XRD analysis. SEM analysis also revealed the desired product with the average size of 37.31 nm. The antibacterial activity of AgNPs was carried out using *Staphylococcus aerus*, *Salmonella Enteritidis*, *Escherichia coli*, *Listeria monocytogenes* bacteria. The AgNPs have considerable antibacterial activity at Minimum Inhibition Concentration (MIC), 0.5 mg/mL except for *E. coli* which revealed the activity at 0.25 mg/mL.

**Keywords:** *Solanum tuberosum*, silver nanoparticles, antibacterial activity

ISBN: 978-605-73552-2-5

**089-OP**

# BIOSYNTHESIS OF SILVER NANOPARTICLES USING POTATO AND THEIR CYTOTOXIC EFFECT

Tunay KARAN[1*], Yasin Bedrettin KARAN,[2] Busra BOZER[3], Ramazan ERENLER[4]

[1]Department of Genetics, Faculty of Veterinary, Yozgat Bozok University, Yozgat, Turkey
[2]Department of Field Crops, Faculty of Agriculture, Tokat Gaziosmanpasa University, Tokat, Turkey
[3]Scientific Technical Research and Application Center, Hitit University, Corum
[4]Department of Chemistry, Faculty of Arts and Sciences, Tokat Gaziosmanpasa University,Tokat, Türkiye

## ABSTRACT

Potato (*Solanum tuberosum*) was extracted with distilled water and then, they were filtered. The filtrate was treated with $AgNO_3$ to produce the AgNPs. The structure of green synthesized AgNPs was determined by Ultraviolet-visible (UV-Vis), and Fourier transform infrared (FTIR) spectroscopic techniques. The cytotoxic effect of extract and AgNPs was carried out on L929 fibroblast, A-549 (Human lung carcinoma), and DLD-1 (Colon adenocarcinoma) cell lines using MTT [3- (4,5-dimethyl-thiazol-2-yl)-2,5-diphenyl tetrazolium bromide] assay. The solution of extract and AgNPs were prepared at the concentration of 1.0 mg/mL, 0.5 mg/mL, 0.25 mg/mL, 0.125 mg/mL and 0.0625 mg/mL and mixed with the medium. The absorbance values were read in the ELISA 96-well plate at 570 nm to determine cell viability. The viability of (%) A-549 cell lines for AgNPs was found as 30.21 ± 2.94 (1.0 mg/mL), 33.20 ± 1.72 (0,5 mg/mL), 80.98 ± 3.46 (0.25 mg/mL). However, the viability of A-549 cell lines for extract was determined as 10.24 ± 0.80 (1.0 mg/mL), 9.17 ± 0.67 (0.5 mg/mL), 14.29 ± 0.45 (0.25 mg/mL). The viability of DLD-1 cell lines for AgNPs was presented as 14.13 ± 0.930 (1.0 mg/mL), 31.38 ± 1.03 (0.5 mg/mL), 25.77 ± 1.56 (0.25 mg/mL). The viability of DLD-1 cells for extract was 53.37 ± 6.92 (1.0 mg/mL), 13.97 ± 1.56 (0.5 mg/mL), 13.48 ± 0.34 (0.25 mg/mL). The viability of L929 fibroblast for AgNPs was found as 49.26 ± 1.89 (1.0 mg/mL), 63.59 ± 3.12 (0.5 mg/mL), 71.27 ± 2.75 (0.25 mg/mL). Moreover, the viability of L929 fibroblast for extract was 68.95 ± 5.73 (1.0 mg/mL), 84.67 ± 2.20 (0.5 mg/mL), 100.15 ± 4.58 (0.25 mg/mL). Percentages of apoptotic and necrotic cells were obtained by the double staining method. Apoptotic effects for AgNPs on A549 and DLD-1 cell lines were higher than the extract sample. The apoptotic effects of the AgNPs and extract were lower in fibroblast cells compared to cancer cells. While AgNPs showed the toxic effect on A-549 and DLD-1 cancerous cell lines, they did not show a noticeable toxic effect on L929 cells. These results indicated that the AgNPs synthesized from *Solanum tuberosum* and extract have the potential to be used for anticancer agents and further study should be carried out to determine potential usage in the drug development process.

**Keywords:** Potato, cytotoxicity; silver nanoparticles, MTT

ISBN: 978-605-73552-2-5

**090-OP**

# Stable isotope ratio of basal sources and consumers in Karacaören Reservoir

Nehir KAYMAK[1*], Nesrin EMRE[1], F. Banu YALIM[2], Cihan TOSLAK[2], Yılmaz EMRE[1], Şenol AKIN[3]

[1] Biology, Faculty of Science, Akdeniz Üniversity, Antalya, Turkey
[2] Mediterranean Fisheries Research, Production and Training Institute Antalya, Turkey
[3] Biology, Faculty of Science, Bozok Üniversity, Yozgat, Turkey

## ABSTRACT

Stable isotope analysis has become a key technique in determining anthropogenic pressures and land use effects on aquatic systems. Both carbon and nitrogen stable isotopes are sensitive to nutrient enrichment and increased primary productivity, especially $\delta^{15}N$ values. In this study, the isotope ratios of both consumer and basal sources in the Karacaören reservoir were evaluated, and seasonal variation in C and N isotope ratios of organisms was investigated.

We sampled fishes, benthic and pelagic invertebrates, and basal production sources in summer and winter from the reservoir during 2019-2020. We used one-way analysis of variance to test the significance of seasonal differences in $\delta^{13}C$ and $\delta^{15}N$ of basal resources and consumers. Pairwise differences were tested using Tukey's post hoc test. All analyses were conducted using SPSS.

Both $\delta^{13}C$ and $\delta^{15}N$ of macrophyte and detritus were significantly lower in winter than in summer. Seston, invertebrates, and fish samples had similar $\delta^{13}C$ values in both seasons. However, it has been determined that all consumers and seston were much more $^{15}N$-enriched. The Aksu stream flowing into the reservoir carries a very high risk of pollution because of the discharge of sewage into streams. These findings might explain the high $\delta^{15}N$ values of both seston and consumer tissues.

**Keywords:** stable isotope, nitrogen isotope, nutrient load; bioindicators, Karacaören reservoir

ISBN: 978-605-73552-2-5

**091-OP**

# ELECTROMAGNETIC ENERGY CONSERVATION BY BIQUATERNIONS

Nur ULUHAN[1,*], Abidin KILIÇ[2]

[1] Graduate Education iInstitute, Eskisehir Technical University, Eskisehir, Turkiye
[2] Physics Department, Faculty of Science, Eskisehir Technical University, Eskisehir, Turkiye

## ABSTRACT

In this document, after defining biquaternions algebra, Poynting Theorem in this algebra is derived. Because of 8-component biquaternions containing 3-dimensional vector space and 4-dimensional quaternion space, we can examine many physical quantities in biquaternion algebra. Based on this information, the generalized field Maxwell equations and Gauge transformations is showed in non-comutative but associative biquaternion algebra in homogenous media. Then, Noether and Poynting Theorem is introduced in terms of biquaternionic differential operator equation and used for deriving equations in electromagnetic energy conservation. In conclusion, it is seen that these biquaternionic equations can be derived from generalized 3-dimensional vector space in literature before.

**Keywords:** Quaternions, Biquaternions, Maxwell Equations, Poynting Theorem

ISBN: 978-605-73552-2-5

**093-OP**

# PRESENCE OF INSECT SPECIES IN THE RESEARCH FIELD OF SWEAT SORGHUM AND SORGHUM SUDANGRASS HYBRID VARIETIES IN CANAKKALE

Baboo ALİ[1,*], Fırat ALATÜRK[2]

[1] Department of Field Crops, Faculty of Agriculture, Canakkale Onsekiz Mart University, Canakkale, 17100, Turkey

## ABSTRACT

Sorghum belongs to the grass family, Gramineae. Sorghum is one of the most important fodder crops. This crop is mainly cultivated on shallow and heavy clay soils. Sorghum is attacked by different species of insects every year from its sowing till harvesting. Most important insect species of sorghum are recorded as sorghum shoot fly, sorghum midge, field earwigs, sorghum stem borer, green bugs, aphids and thrips. Sorghum also faces problem, and a decrease in terms of quality and yield every year in its growing regions, generally in Turkey and particularly in Canakkale. For the purpose to make sure the presence of different species of insects in sorghum field in Canakkale province of Turkey, a research was conducted in sorghum sowing season in the years 2000-2001 by sowing four sub varieties of two main sorghum varieties, namely sweat sorghum (M81-E and Topper-76) and sorghum sudangrass hybrid (Nutrima and Nutri honey). In this research, the insect pest population has been determined on the bases of crop harvesting in terms of maintaining different harvesting heights of sorghum crop such as 30 cm, 60 cm, 90 cm, 120 cm and 150 cm along with a control treatment (physical stage). According to the overall results of our research study, a total of 994 harmful insects were recorded in the 1st year (2000), while 2777 harmful insects were observed during the 2nd year (2001) of our study. Consequently, the larval and adult stages of sorghum shoot fly (*Atherigona soccata*) were present prominently in all parcels harvested with different level of heights. Moreover, M81-E and Topper-76 sub varieties of sweat sorghum were affected more and caused damage by *A. soccata* because of their broad leaf sheaths, thick stems and high value of nutrient contents as compared to Nutrima and Nutri honey sub varieties of sorghum sudangrass hybrid.

**Keywords:** Sorghum varieties, fodder crop, harvesting height, insect population

ISBN: 978-605-73552-2-5

**094-OP**

# 3D PRINTED PAVING STONES: A LAB-SCALE RESEARCH

**Volkan ARSLAN [1,*], Hüseyin Zekeriya DOĞAN**

[1,2] Department of Civil Engineering, Faculty of Engineering, Zonguldak Bulent Ecevit University, Zonguldak, Turkey

## ABSTRACT

Technological developments in the world lead to changes in the construction sector as well as in many other sectors. Three-dimensional (3D) printer technology also stands out as a new production method that has become popular in the construction industry. The use of 3D printers in the construction industry is a fairly new practice. It is estimated that the use of such printers will increase in the coming years.

In the construction industry, the main methods for producing with 3D printers are (i) additive manufacturing method, (ii) contour work, (iii) concrete printing and (iv) D-shaped process. In addition to the production methods, the materials to be used in this process also play an important role in the production quality. Today, concrete mixtures consist cement, steel, fiberglass or other construction wastes are already in use in the construction industry. Moreover, glass-filled resins, various plastics, clay, and ceramic materials are also utilized in order to create concrete mixture.

The main objective of this study is to produce concrete paving stones with 3D printers. It is also aimed to design a 3D printer to achieve this goal. Although there are 3D printer models used in current applications, it is also possible to design 3D printers according to the needs. Within the scope of the study, a 3D printer that can be used to produce the paving stone and the mixtures to be used for production will be designed. Thus, as a result of the study, a new method in cobblestone production will be developed and a 3D printer that can be redesigned to be used in the production of different building materials will be obtained.

**Keywords:** 3D printer, construction technology, construction industry

ISBN: 978-605-73552-2-5

**095-OP**

## AN INVESTIGATION OF MOLECULAR SPECTROSCOPY WITH GEOMETRIC ALGEBRA

Baghdad Abdulhameed Abdullah AL-BADANI[1,*], Abidin KILIÇ[2]

Physics Department, Faculty of Science, Eskişehir Technical University, Eskişehir, Turkey

**ABSTRACT**

In this study Geometric Algebra was used to create a general and practical method for obtaining the operators of the kinetic energy of the molecular vibration-rotation of polyatomic molecules. On the other hand, these polyatomic molecules' precise intrinsic kinetic energy operators include a metric tensor. The elements of this metric tensor were expressed as the mass-weighted sum of measuring vector inner product vectors compatible with the molecule's nucleus. Whereas, the vibrational and rotational measuring vectors that appear in the metric tensor for any geometrically defined coordinates of the shape and frames of the body were easily determined using geometric algebra. The current method (geometric algebra) generates molecular vibration-rotation kinetic energy operators that are in perfect agreement with earlier studies.

In the last of this study, we took the Lagrangian Formulation where the component of kinetic energy was expressed in the form of generalized velocities. We found the relation between the covariant metric tensor and contravariant metric tensor by means of geometric products.

**Keywords:** Geometric Algebra, Operator of the kinetic energy, Covariant metric tensor, Rotational measuring vectors, Vibrational measuring vectors

**096-OP**

## THE EFFECTS of LEAD APPLICATION on DIFFERENT PHYSIOLOGICAL PROCESSES in SOME WHEAT VARIETIES

Betülnur ÖZEL, Elif ÖZTETİK*

Department of Biology, Science Faculty, Eskisehir Technical University, Eskişehir, Türkiye

**ABSTRACT**

Heavy metals are among the most dangerous pollutants due to their high toxicity and significant amounts of them released into the environment as a result of natural and anthropogenic processes. The accumulation of these non-biodegradable elements in the soil has a negative effect on plants, and their transfer through the food web endangers human health. Lead (Pb) ranks second among the dangerous heavy metals. Accumulation of Pb in plant tissues has a negative effect on a number of physiological processes, such as seed germination, root and shoot elongation, mineral nutrient uptake, chlorophyll biosynthesis and enzymatic reactions. Photosynthesis is a fundamental event in the energy production of plants, where the chlorophyll pigment is responsible for this. The phenomenon of photosynthesis is one of the most sensitive processes to heavy metal stress. Exposure to Pb damages the structure of chloroplasts in the plant, causing a decrease in the level of photosynthetic pigments. In this study, the effect of lead chloride ($PbCl_2$) exposure on different physiological processes has been investigated in two wheat varieties (*Triticum aestivum* cv. Bezostaya ve Yunus). $PbCl_2$ has been applied to plants in the growth stage in 4 different concentrations: 150 µM, 300 µM, 1.5 mM and 3.0 mM. Germination rates, root-shoot lengths and chlorophyll amount of plants were calculated after heavy metal exposures. According to the results obtained, it was concluded that $PbCl_2$ exposure triggers oxidative stress in the wheat plant, since all the measured parameters are critically reduced.

**Keywords:** Chlorophyll contents, Heavy metal (Pb), Oxidative stress, Wheat.

ISBN: 978-605-73552-2-5

**097-OP**

# JUSTIFICATION OF THE CHOICE OF CATALYST FOR THE OXIDATION OF C3- C4 ALDEHYDES INTO ACIDS AND THEIR MODIFICATION

Elmira HUSEYNOVA, Ulkar SHIRALIYEVA, Nasiba IMANOVA, Ziba BAGIROVA, Kamala ISMAYILOVA, Saida NADJAFOVA

Scientific Research Institute "Geotechnological Problems of Oil, Gas and Chemistry", ASOİU, Baku, Azerbaijan

## ABSTRACT

The catalysts used to oxidize unsaturated aldehydes into the corresponding acids are complex oxide systems. The main component of such oxide systems is molybdenum. Molybdenum itself, without additives, is not used as an independent catalyst. The most widespread use as an additive is phosphorus, which markedly increases the stability of the molybdenum catalyst.

Significantly improve the properties of the catalyst named the presence of vanadium as well, an important role played by such elements as copper, antimony, tungsten, iron, tellurium, and bismuth. The presence of these elements brings the yield of acrylic acid to an average of 95% and methacrylic acid up to 68%.The use of heteropolyacids as oxidation catalysts is advantageous because they possess a particular set of properties necessary for processes in catalysis. The use of heteropolyacids as oxidation catalysts is beneficial because they contain a special set of required properties for processes in catalysis. High thermal stability in the solid-state uses heterogeneous catalysts in oxidation reactions with a wide temperature range. An essential role in the effective use of phosphormolybdenum heteropoly acids is played by their preparation methods, which involve the synthesis based on ammonium salts of phosphorus and molybdenum and on phosphormolybdenum acid. Each series of experiments is represented by samples of catalysts with a wide range. A characteristic point in the formation of the desired catalytic system is the activation of the catalyst. For polycomponent systems, it is difficult to assess the contribution of each introduced component or modify the additive that affects the activity and selectivity of the catalyst. The formation of a two-phase system of zinc molybdate and the ammonium salt of the heteropoly acid appears to be the decisive condition for increasing the activity of the multi-component catalyst when zinc is introduced into its composition. One should pay attention to the number of water molecules in the heteropolyanion sphere and in the channels between them. The catalyst of the proposed composition provides a high yield of the target product.

**Keywords***:* heteropoly acid, acrolein, methacrolein, oxidation, thermal stability.

ISBN: 978-605-73552-2-5

**098-OP**

# The development of mosquito-repellent textiles based on local natural products

Yosra RAJİ[12], Souad ZYADE[2], Omar CHERKAOUİ[1]

[1] Laboratory for Research on Textile Materials (REMTEX), Higher School of Textile and Clothing industries (Esith),Casablanca,Morocco.
[2] Genie Laboratory of Materials for Environment and Valorization (GeMEV), Aïn Chock Faculty of Sciences, Hassan II University, Casablanca, Morocco.

## ABSTRACT

Mosquito-borne diseases are one of the major threats to human health. The long-term use of synthetic repellents has made mosquitoes resistant to these products, leading to the search for new methods of mosquito control. In nature, many aromatic plants (lemongrass, peppermint, thyme, eucalyptus, rosemary and lavender) secrete insect repellent molecules that have a repulsive effect on mosquitoes, which we can benefit from by extracting their essential oils. In this study, the leaves of each plant were hydrodistilled for 3 hours using a modified Clevenger apparatus. The yield obtained was approximately 2-3% for each plant. The technique used to apply the essential oils to the textile is the coating process, we chose to apply a foam to have more free volume which facilitates the release of the active principle (essential oil). The coating foam is made up of a polyurethane polymer and additives that complete the composition of the coating resins (1% essential oil, 2% ammonia, 3% cross-linking agent, 1% foam stabiliser and 1% thickener). As the density of the polyurethane increases, the liquid polyurethane is expelled from the generator tube, the fabric to be coated is passed horizontally between two offset rollers, the coating material flows between the cylinder and the roller. The colorimetric study by Data-color justified the release of the active principle of the essential oils by the degradation of the colour of the treated fabric day after day, then the cage test also confirmed the repellent property against mosquitoes by registering a repulsion rate of about 78%, and finally the washing test showed the good resistance of the coated fabric after 20 washing tests . It can be concluded that the developed repellent fabrics can be a safe, environmentally friendly and effective alternative to chemical repellents for protection against mosquito bites.

**Keywords:** Mosquito ,Coating, Cage test

ISBN: 978-605-73552-2-5

**099-OP**

# ANALYSIS OF THE CURRENT STATE OF RESEARCH ON THE THERMAL STABILITY OF ORGANIC COOLANTS.

Zarifa MAMMADOVA, Elmira HUSEYNOVA, Ulkar SHIRALIYEVA, Aida RZAYEVA, Nurana MARDANOVA, Kamala ISMAYILOVA

Scientific Research Institute "Geotechnological Problems of Oil, Gas and Chemistry", ASOİU, Baku, Azerbaijan

## ABSTRACT

The need to select compositions that work for a long time without causing corrosion, decomposition, and withstanding high-temperature regimes, leads to the search for new thermal power plants. Fulfilling these conditions is possible using single-component and multi-component coolants containing molecules of the most diverse form. The stability of the coolant is enhanced by the presence of halogen-containing hydrocarbons.

Using stable carbon compounds is possible by carefully studying the connection of atoms to the basic lattice. Among the halogenated hydrocarbons, the bond strength increases from iodine, bromine, and chlorine to fluorine. In terms of stability, fluorine-containing aromatic compounds are the most acceptable. Qualitative analysis methods are based on evaluating the thermal stability of substances by color changes and the formation of deposits on the heating surface. It was found that the main factor in selecting the working body is the rate of thermal decomposition. The research conditions also play a crucial role in evaluating the thermal stability of the substance.

**Keywords***:* coolants, thermal resistance, halogen hydrocarbons, corrosion resistance, heating surface.

ISBN: 978-605-73552-2-5

**101-PP**

# ON THE PROBLEM OF MONOPULSE UV STERILIZATION

Volodymyr CHUMAKOV[1], Oksana KHARCHENKO[2], Vasiliy MURAVEİNYC[3]

[1] Department of Design and Operation of Electronics Devices, Faculty of Aautomation and Computer Technologies, Kharkiv National University of Radio Electronics, Kharkiv, Ukraine
[2] Department of Media Engineering and Information Madioelectronic Systems, Faculty of Information Radio Technologies and Technical Information Security, Kharkiv National University of Radio Electronics, Kharkiv, Ukraine
[3] limited Liability Company «Triix», Chernihiv, Ukraine

**ABSTRACT**

The results of experimental investigations of the effect of ultra-high power pulsed ultraviolet radiation (UV) on pathogens and viruses are presented. It is shown that with a powerful pulsed effect, the shock mechanism of the destruction of pathogenic microflora and viruses is realized. The models of sterilization efficiency depending on the UV radiation dose are considered. It is shown that with the traditional technology of UV sterilization by low-intensity irradiation sources, a cumulative sterilization mechanism is manifested, in which the speed of destruction of irradiated objects depends on their number. The main disadvantage of such exposure is the presence of residual bacterial and/or viral population, which is the cause of clinical infection. In addition, achieving a high level of sterilization requires a lot of energy and time.

With pulsed exposure, a regularity of the impact mechanism is manifested, which consists in the fact that the integral dose of radiation necessary to achieve the sterilization effect decreases with increasing exposure power. Thus, by increasing the pulse power of the UV source, it was possible to increase the efficiency of sterilization and significantly reduce the processing time. For the first time, the effect of complete 100% destruction of pathogens and viruses as a result of exposure to a single pulse of microsecond duration has been realized experimentally.

The structure of a pulsed source of UV radiation providing a power of about 3.6 MW in the bactericide band 200 - 420 nm is considered. The technique of experimental researches is developed as well. The prospects for the construction of highly efficient emitters of pulsed UV radiation and the fundamentals of monopulse sterilization technology are discussed.

**Keywords**: UV sterilization, pathogens, viruses, pulse mechanism

ISBN: 978-605-73552-2-5

**102-PP**

# ON THE SIMULATION OF PULSE SIGNALS BY POLYGONAL FUNCTIONS

Volodymyr CHUMAKOV[1], Vitalii ROMANCHUK[1], Oksana KHARCHENKO[2]

[1] Department of Design and Operation of Electronics Devices, Faculty of Aautomation and Computer Technologies, Kharkiv National University of Radio Electronics, Kharkiv, Ukraine
[2] Department of Media Engineering and Information Madioelectronic Systems, Faculty of Information Radio Technologies and Technical Information Security, Kharkiv National University of Radio Electronics, Kharkiv, Ukraine

## ABSTRACT

The results of studies on the application of the Lapaz transform to the analysis of the process of passing pulse signals through linear inertial circuits are presented. It is shown that the majority of pulse signals can be described by piecewise analytic functions. So, in particular, for modeling video pulses in information systems, as well as for describing the envelope of radio pulses in radio engineering systems, polygonal functions can be used. The representation of pulses in the form of a polygonal function is shown to make it possible to significantly simplify the calculation of the image according to Laplace, and, consequently, the calculation of the signal spectrum.

The calculation of the spectral density of pulses described by polygonal functions shows that the width of the spectrum in such a model is due to a discontinuity at the junction points of individual sections of the function. So, if the limits of the function on the left and on the right at the junction point do not coincide, then the spectral density decreases with frequency according to law $\omega^{-1}$. In the case when the limits at the indicated points coincide, the decrease in spectral density with frequency occurs according to the law of a quadratic hyperbola.

It is shown that the calculation of the pulse spectrum using the Laplace transform expands the possibilities of using computer simulation, since in the libraries of most software products the Laplace transform covers a wider range of functions than the Fourier transform.

**Keywords**: spectral density, Laplace transform, pojygonal function

ISBN: 978-605-73552-2-5

**103-OP**

# ESTIMATION OF MULTI-RESPONSE SEMIPARAMETRIC REGRESSION MODEL BASED ON KERNEL SMOOTHER: AN APPLICATION WITH AGRICULTURAL DATA

Dursun AYDIN[1] Ersin YILMAZ[1*]

[1] Department of Statistics, Faculty of Science, Mugla Sitki Kocman University, Mugla, Turkey

## ABSTRACT

A multi-response semiparametric regression model differs from the classical semiparametric model by involving the multiple response variables. Accordingly, parametric, and nonparametric components affect the responses individually. Another difference of multi-response model is an existence of a correlation between the response variables. This case brings a need of a symmetric weight matrix. To estimate the introduced model, this paper considers a kernel smoothing method which works based on Nadaraya-Watson estimator. Accordingly, estimators of multi-response semiparametric model are obtained based on penalized weighted least squares technique. Finite-sample properties of the estimators are provided. To show the behaviors of the mentioned estimators, agricultural data obtained from Turkey is analyzed and results are presented.

**Keywords:** Multi-response regression, kernel smoothing, semiparametric model, agricultural data, penalized weighted least squares.

ISBN: 978-605-73552-2-5

**105-OP**

# EFFECTS OF DIFFERENT HARVESTING PRACTICES ON THE AGRONOMIC CHARACTERISTICS OF SOME SWEET SORGHUM AND SORGHUM x SUDANGRASS HYBRID VARIETIES

Fırat ALATÜRK[1,*], Ahmet GÖKKUŞ[1], Harun BAYTEKİN[1], Baboo ALİ[1]

[1] Department of Field Crops, Faculty of Agriculture, Canakkale Onsekiz Mart University, Canakkale, TURKEY

## ABSTRACT

This research has been carried out to determine the variations in certain agronomic features of sweet sorghum (Topper-76 and M81-E) and sorghum x sudangrass hybrid varieties (Nutrima and Nutri Honey) depending on different harvesting practices. This research was conducted in Research and Experimental Area of the Canakkale Onsekiz Mart University, Faculty of Agriculture located at Dardanos, Çanakkale Province in 2020. This study has been established according to randomized complete block design using 4 replications. In the experiment, main plots were consisted of sorghum varieties while the sub plots were formed as different harvesting heights (30, 60, 90, 120, 150 cm and physiological stage). In the study, plants were harvested on a height of 10 cm when they reached their specific harvesting maturity. Later, the plant height, fresh hay yield, dry hay yield, ratio of dry matter and ratio of leaf, stalk and panicle have been determined from the harvested plant samples. According to the results of this study, fresh hay yield, dry hay yield, ratio of dry matter, ratio of stalk and panicle were increased correlatedly with plant growth, but there was a decline in leaf ratio. The highest plant heights were recorded as 131.6 cm and 130.9 cm in Nutri Honey and M81-E varieties, while the highest fresh and dry hay yields were determined in M81-E variety of sweet sorghum. There was non-significant change between varieties in terms of leaf and stalk ratios, but the highest stalk ratio (8.73%) has been observed in Nutri Honey variety. In conclusion, in terms of the investigated characteristics, the Nutri Honey variety of sorghum x sudangrass and M81-E variety of sweet sorghum are recommended as summer roughage crops under similar ecological conditions.

**Keywords:** Sorghum x sudangrass, Sweet sorghum, Hay yield, Leaf ratio, Nutri Honey, M81-E.

**Note:** This is study has been taken as a part from TUBITAK-1001 Project No. 120-O-527.

ISBN: 978-605-73552-2-5

**106-OP**

# WEB APPLICATION FOR STATISTICAL ANALYSIS AND MACHINE LEARNING ALGORITHMS WITH R AND PYTHON PROGRAMMING LANGUAGES

Kagan Han CATAN[1] Betül KAN-KILINÇ

[1]Department of Statistics, Faculty of Science, Eskisehir Technical University, Eskisehir, 26470 Turkey

## ABSTRACT

Machine learning algorithms are powerful tools used extensively to facilitate decision-making, especially when the response variable is dependent on many numerical or categorical variables. In this project, by creating a web page, the user can upload a custom dataset, can present the descriptive statistics with selected choices and the dependent variable can be predicted with a machine learning algorithm chosen by the user. The hyper-parameters can be optimized. An interface presents the results in summary (prediction values, confusion matrix, accuracy, etc.).

An interactive user interface is developed by utilizing the Shiny library provided by the R programming language to develop an interactive web application, and machine learning functions using Python are included in this interface, where machine learning algorithms can be used on the datasets uploaded by the user. Also, necessary statistics and plots and the algorithm that determines the best result by using multiple machine learning algorithms can be obtained.

The project aims to be a simple practice for people who are new to the field of statistics and machine learning via a web application.

**Keywords:** Machine Learning; Statistics; Data Science; Web Application

ISBN: 978-605-73552-2-5

**110-OP**

## EXPERIMENTAL STUDY OF ELECTRICAL HEATER WORKING FUNCTION FOR IMPROVING ENERGY CONSUMPTION IN A DOMESTIC OVEN

Ayberk Salim MAYIL[1, *], Can UGURELLİ[1], Ayben CENGİZ[2], Burak GÜZELTEPE[2]

[1] Haier Europe, Candy- Hoover Group, Research and Development Center, Eskişehir, Türkiye-amayil@hoover.com.tr
[1] Haier Europe, Candy- Hoover Group, Research and Development Center, Eskişehir, Türkiye- cugurelli@hoover.com.tr
[2] Haier Europe, Candy- Hoover Group, Research and Development Center, Eskişehir, Türkiye-acengiz@hoover.com.tr
[2]Haier Europe, Candy- Hoover Group, Research and Development Center, Eskişehir, Türkiye- bguzeltepe@hoover.com.tr

### ABSTRACT

There is a big demand from the customer and regulatory side for higher efficiency products to save electricity consumption and decrease the carbon footprint. Manufacturers and designers must check new improvements to afford such an important request. New improvements related with the energy efficiency cause the new competitive between manufacturers about fast cooking, multi cooking, well designed esthetics etc. During the studies, it needs to high number test to ensure the international regulatory standards. In this study, different heater functions are examined to decrease energy consumption of the oven during standard energy test as an experimentally. 3 versions of the heater working cycles are studied and it shows what is the effect of these function on energy consumption.

**Keywords:** Household Oven, Energy improvements, Experimental methods.

**112-PP**

## USING THE COLORIMETRIC METHOD IN CERTAIN TECHNOLOGIES

Iurii KHOROSHAILO [1], Ivan YARMAK[1], Anna SOVA[2] , Aleksandr MENYAJLO[1], Ihor KLIUCHNYK[1], Eduard CHERNYAKOV[1]

[1] Department of Design and Operation of Electronic Devices, Faculty Of Automa-Tıcs And Computerızed Technologıes, Kharkiv National University of Radio Electronics, Kharkiv, Ukraine
[2] Department of Higher Mathematics, Faculty Of Informatıon And Analytıcal Technologıes And Management, Kharkiv National University of Radio Electronics, Kharkiv, Ukraine

### ABSTRACT

A device is proposed for measuring color characteristics, which, using a measuring transducer, assigns to each radiation three signals proportional to color coordinates. Existing devices have many drawbacks, among them low speed, due to the use of inert elements, which makes it impossible to measure rapidly changing light fluxes. In this device, the authors tried to minimize the shortcomings. Also in this article, a mathematical model of the device is proposed. Attention is paid to the psychophysiological perception of color.

**Keywords:** measurement, device, color, photodiodes, microcontroller, mathematical model, psychophysiology of vision.

ISBN: 978-605-73552-2-5

**113-OP**

# SYNTHESES AND STRUCTURAL ANALYSES OF HETERONUCLEAR HEXACYANOMETALATE(III) COMPLEXES WITH 4-(2-AMINOETHYL)PYRIDINE

Seray KEKEÇ[1], Güneş Süheyla KÜRKÇÜOĞLU[1,*]

[1] Department of Physics, Faculty of Arts and Sciences, Eskişehir Osmangazi University, Eskişehir, Türkiye

## ABSTRACT

The cyanide complexes of transition metals with 4-(2-aminoethyl)pyridine (4aepy), (NH4)[Cd(μ-4aepy)2Fe(μ-CN)2(CN)4]n(1) and (NH4)[Cd(μ-4aepy)2Co(μ-CN)2(CN)4]n(2) (4aepy= 4-(2-aminoethyl)pyridine), were synthesized. The structures of the complexes are determined by vibrational (FT-IR and Raman) spectroscopy, thermal and element analyses techniques. The FT-IR and Raman spectra of the complexes were reported in the range of 4000-225 cm-1 and supported with thermal and element analyses results. The structural properties of the complexes were obtained by considering characteristic bands belonging to ligands from the FT-IR and Raman spectra. Additionally, FT-IR and Raman spectra of the complexes were observed two different ν(CN) absorption bands which act as bridge and terminal. The spectral data show that the characteristic bands of 4aepy were shifted to lower and high frequencies. These shifts arise due to bounding metal and coupling of metal-ligand vibrational modes. Thermal behaviors of the complexes are investigated between the temperature ranges of 30-1000 °C in static air atmosphere.

Keywords: Hexacyanoferrate(III) complex; Hexacyanocobaltate(III) complex; 4-(2-aminoethyl)pyridine complex; Coordination polymer.

ISBN: 978-605-73552-2-5

**113A-OP**

# COMPARATIVE RESPONSE OF TWO WHEAT VARIETIES TO BASAL AND SPLIT POTASSIUM NUTRITION UNDER FIELD CONDITIONS OF TANDOJAM PAKISTAN

Saima Kalsoom BABAR[1,*], Tarique Ali JATOI[1], Hanife AKÇA[2], Inayatullah RAJPAR[1]

[1] Department of Soil Science, Faculty of Crop Production, Sindh Agriculture University, Tandojam, Pakistan
[2] Department of Soil Science and Plant Nutrition, Faculty of Agriculture, Ankara University, Turkey

## ABSTRACT

Countless research is available on basal application of potassium (K) in relation to yield and quality of wheat (*Triticum aestivum* L.). Conversely, very fewer data is being existent on split application of K fertilizers. With the introduction of high yielding varieties under intensive cropping system with inadequate K fertilization, soil K reservoirs have started depleting which result in yield loss and high economic risk to farmers. Keeping the importance of K fertilization in wheat at right time this field experiment was conducted during 2018-2019 at Southern Wheat Research Station, Agriculture Research Centre, Tandojam, Pakistan. The experiment included 18 plots each had an area of $12m^2$ (4m × 3 m) using two cultivars of wheat, Benazir and Sindhu sown in two-factor Randomized Complete Block Design, with split-plot arrangement (main plot=varieties, sub plots=treatment) with three replications. Three regimes of K fertilization was applied i.e. $T_1$ = No K application, $T_2$ = K application at 50 kg $K_2O$ $ha^{-1}$ at the time of sowing, $T_3$ = K applications in two splits, i.e. 25 kg $K_2O$ $ha^{-1}$ at sowing and 25 kg $K_2O$ $ha^{-1}$ at grain filling stage. The yield components were observed after harvesting the crop. On average, split K application had advantage over basal application. The highest number of tillers (407 $m^2$) per plant, number of grains per spike (47), seed index (43.89), and grain yield (3.93 t $ha^{-1}$) was obtained under split application of K ($p \leq 0.01$). It is suggested to apply K fertilizer in split application to achieve the desired economic yield.

**Keywords:** cereal; fertilization methodology; modern cultivars; yield constraints

ISBN: 978-605-73552-2-5

**115-OP**

## Antiproliferative and apoptotic effects of *Trachystemon orientalis(L.) G. Don* on HCT116, AGS and HepG2 cells

Serkan SOYMAZ[1], Görkem DULGER[1*]

[1] Department of Medical Biology, Faculty of Medicine, Duzce University, Duzce, Turkey

**ABSTRACT**

In this study, the effectiveness of *Trachystemon orientalis (L.) G. Don* on gastrointestinal system cancer cells was investigated. Our results showed that increasing doses of the extract of this plant significantly reduced cell viability in HCT116 colon cancer, AGS gastric cancer and HepG2 hepatocellular carcinoma cell lines. While cell viability decreased in a dose-dependent manner in 24 h dose , cell proliferation inhibition increased in 48 h dose application in a time and dose-dependent manner. It was observed that the plant extract increased caspase activation at varying rates in all three cell lines. Caspase-3, 8 and 9 activation was observed in AGS cell line as a result of extract application, while Caspase-3 and 9 activation was significantly increased in HCT116 and HepG2 cell lines. Our study is important in that it contains important results for the transition to further in vivo studies with this plant extract.

**Keywords:** Anticancer, Apoptosis, *Trachystemon orienta/is(L.) G. Don*.

**116-OP**

## EVALUATION OF CYBERSECURITY PLATFORM PROVIDERS FOR MANUFACTURING INDUSTRIES BY USING THE CODAS APPROACH BASED ON T2NFN SETS

Ömer Faruk GÖRÇÜN[1,*], Hande KÜÇÜKÖNDER[2]

[1] Business Management, Faculty of Economics, Administration, and Social Sciences, Kadir Has University, Turkey
[2] Numerical Methods, Faculty of Economics and Administration, Bartın University, Turkey

**ABSTRACT**

Nowadays, the digital transformation concept is the first agenda item of the manufacturing industry. Many companies know it is necessary instead of a choice to survive a highly competitive business environment. Hence, practitioners in various industries try to switch all business activities from physical to digital environments. However, it causes many threats and problems concerning confidential business information and data. Furthermore, companies may remain vulnerable encounter these cyber threats. Therefore, digital transformation strategies may not reach success without using robust and reliable cybersecurity systems. Moreover, limited papers deal with cybersecurity systems by applying a mathematical model or decision support system that can handle complicated uncertainties in the relevant literature. It may make it challenging to select an appropriate cybersecurity system for practitioners in the manufacturing industry, as decision-makers are deprived methodological frame that can help select the best system. The current paper aims to fill two severe gaps in the literature by keeping the industry's requirements in mind. First, it proposes a robust and practical frame to solve decision-making problems. Secondly, it presents up-to-date criteria identified by performing comprehensive fieldwork with highly experienced experts with extensive knowledge of cybersecurity systems. Finally, a comprehensive sensitivity analysis performed to test the validity of the proposed model approves the validity, robustness, and practicality of the proposed approach.

**Keywords:** Cybersecurity, T2NFNs, the CODAS, system selection

ISBN: 978-605-73552-2-5

**117-OP**

## THE EFFECT OF ELECTRIC AND HOFFMAN FURNACE ON THE STRENGTH OF TILES PRODUCED FROM SCHIST MATERIAL

Hülya KURU MUTLU

[1] Opticianry Program, Vocational School of Health Services, Osmangazi University, Eskisehir, Turkey

**ABSTRACT**

In the study, the effects of electric and Hoffman furnaces on the strength of the tiles produced from the schist material obtained from the Rızapaşa district of Bilecik province were investigated. Small rectangular tablet tiles were obtained from the schist material, which was kept at a humidity level of 16.73 by the humidifier, by the vacuum press device. The physical measurements of the samples, such as height, width, and weight, were taken. The tablet tiles were dried in an electric oven at 80°C. Afterward, the reference sample was fired in an electric oven at 950°C and the other tablet tile was fired in a Hoffman oven at 950°C. The tensile values were calculated by taking the physical measurement values of the samples after drying and firing. The strength value of the sample fired with an electric oven in the produced tiles is 156.15 kg/cm$^2$ and has a higher value than the sample fired with a Hoffman oven. The water absorption values in both samples are in the same order and have a value of 14.9%. The two tablet tiles produced in the Hatipoglu Gunes Tile and Brick Industry Inc. factory meet the minimum strength value of 120kg/cm$^2$ in TS EN 1304 (2016) quality standards.
**Keywords:** Schist, industrial product, furnace, tile

**118-OP**

## An Evaluation on the Gaining of Secondary School Science Concepts in Engineering Education

İsmail Cengiz YILMAZ[1,*] Hamdi TEKİN[1,*]

[1] Civil Engineering, Engineering and Architecture, Istanbul Arel University, İstanbul, Turkey

**ABSTRACT**

Engineering education is enriched with more technical concepts than ever before, especially due to the technological development and big data increase in recent years. In order for these new technical concepts to be more qualified to the students, the basic science concepts should be better understood by the students. The concentration in STEM education, which has become increasingly popular in recent years, also points to the importance of this situation. For this reason, understanding, applying and evaluating this importance, especially at the secondary school level, which can be considered as the starting point of science education, is an issue that deserves attention. Within the scope of this study, an evaluation was made by establishing a relationship between the concepts of science education given in secondary schools in Turkey and in the world and engineering education. Evaluation results and various suggestions are presented within the scope of this study.

**Keywords:** Engineering Education, Science Education, STEM

ISBN: 978-605-73552-2-5

**119-OP**

## Investigation of Fracture Prevention Effects of Composite Patches Repair on Cracked Aluminum Plates Experimental and Numerical Study

Mohammadjavad RANJBARAN

*Graduate student (Islamic Azad University of Hamedan, Department of Mechanical Engineering, Mussivand, Hamedan, Iran)*
*E-mail: mohammadjavadranjbaran@yahoo.com*

**ABSTRACT**

Nowadays, composite materials are extensively applicable in various aspects including automotive, marine and most importantly aeronautical engineering because of their excellent characteristics. Innovative maintenance using materials with extraordinary features has led to contributing of composites with the goal of extending their lives services. Glass-epoxy composites are lifesaver, inexpensive and highly practical for repairing the damaged components of aeronautical structures. The present study has employed composite patching technique to repair 50 centrally cracked rectangular aluminum plates subjected uniaxial tensile loading experiment. The 600 KN Santam testing machine used for performing tensile tests. Then, the force-displacement linear graph for each sample was plotted and monitored by its user's software. Next, the Abaqus finite element software simulated the same testing conditions on developed 3D- models using XFEM method. Finally, the numerical and experimental results indicated 0.0266 error percentage between the real and simulated tensile loading tests. In addition, specimens repaired by composite patches whose glass fibers orientations angles are 0,90 proved to have the best optimum performance while those that were repaired by patches with fiber orientations angle -45, +45 had the maximum displacement extension before failure.

**Key Words:** glass-epoxy composite patching, crack, extended finite element method, aluminum alloy 7075, uniaxial tensile test.

**120-OP**

## THE EFFECT OF ADDING ARTIFICIAL NOISE ON THE SUCCESS OF A DEEP LEARNING NETWORK

Utku KAYA

Vocational School of Transportation, Eskişehir Technical University Eskisehir, Turkey

**ABSTRACT**

Image preprocessing methods have a significant impact on increasing the success of the deep learning network. For deep learning networks to be successful, a large amount of data is needed. Obtaining these datasets is a challenging task that requires effort and observation. Therefore, the researchers aim to increase the success of the deep learning network by modifying the existing images and making it more prepared for new test images. In this way, they artificially increase the number of images in the data sets by using methods such as modifications to the color bands, adding noise, and histogram equalization. In this study, the change in success rates of the network will be investigated in detail by adding different noise types to the data set used to train the deep learning network.

ISBN: 978-605-73552-2-5

**121-OP**

# NON-LINEAR LARGE LONGITUDINAL AMPLITUDE VIBRATION OF VARIABLE SLOPE OF RODS WITH DIFFERENT BOUNDARIES CONDITIONS

El Mehdi ABDEDDINE[1,*], Abdelfattah MAJID[1], Khalid ZARBANE[2], Zitouni BEIDOURI[2]

[1] Laboratory of Advanced Research in Industrial and Logistic Engineering (LARILE), National Higher School of Electricity and Mechanics, Hassan II University of Casablanca, Casablanca, Morocco
[2] Laboratory of Advanced Research in Industrial and Logistic Engineering (LARILE), Higher School of Technology, Hassan II University of Casablanca, Casablanca, Morocco

## ABSTRACT

The present study aims to investigate the linear and non-linear longitudinal free vibration of uniform and non-uniform rods with different boundary conditions and determine the effect of the section variation on the maximum amplitude. The rods with a variable cross section are often used as framings of unique buildings. The formulation of these structures is based on Lagrange equations and the harmonic balance method in order to obtain the non-linear algebraic equations. Therefore, the method adopted is consisting of discretizes the problem by using the energy term of linear and non-linear rigidity and mass tensors. The non-linear frequency corresponding to the first, second, and third non-linear mode shapes of Clamped-Free and clamped-clamped uniform and non-uniform rods are obtained via the linearized approach. This latter method leads to reduce calculation time, contrary to iterative methods. Longitudinal vibrations have a huge impact on mechanical structures as cited in the literature. In the same way, to understand their dynamic behavior, we need to demine the effect of all the characteristics on the structure. For this purpose, the convergence of the solution obtained is studied, and the frequency amplitude dependence is exhibited for the first, second, and for the third mode shape. Also, the range of the vibration amplitude under resonance should be considered in the design process. The results have shown that the maximum amplitude gets higher in the case of uniform rods compared to the case of non-uniform rods and these latter depend on the slop variation in different mode shapes.
**Keywords**: Non-Linear Longitudinal Vibration; Lagrange equations; Harmonic Balance Method; Linearized Approach.

ISBN: 978-605-73552-2-5

**122-OP**

# MECHANICAL BEHAVIOR CONVERGENCE OF FDM 3D PRINTED AND ISOTROPIC PARTS: GEOMETRICALLY NONLINEAR EFFECT

Abdelfattah MAJID[1*], El Mehdi ABDEDDINE[1], Zitouni BEIDOURI[2], Khalid ZARBANE[2]

[1] Laboratory of Advanced Research in Industrial and Logistic Engineering (LARILE), National Higher School of Electricity and Mechanics, Hassan II University of Casablanca, Casablanca, Morocco
[2] Laboratory of Advanced Research in Industrial and Logistic Engineering (LARILE), Higher School of Technology, Hassan II University of Casablanca, Casablanca, Morocco

## ABSTRACT

The objective of this paper is to examine the convergence of nonlinear dynamic behavior on thin rectangular FDM 3D printed and isotropic fully free plates. Firstly, the isotropic plates were numerically investigated via Lagrange equations and the harmonic balanced method (HBM) in an effort to highlight the effect of the geometrically nonlinear on these latter structures. The nonlinear dynamic response was obtained by using a semi-analytical approach, focusing on the dependance between the displacement amplitudes and frequencies, mode shape, and the associated bending stress of the fundamental mode shape. Secondly, the obtained findings (mode shape and backbone curves associated to the first mode shape) were compared with those presented numerically and experimentally by Alijani et al. (2013). Furthermore, the experimental backbone curve achieved in the case of FDM plate was compared with the one predicted in case of isotropic plate in order to exhibit and to interpret the convergence of both solutions.

Regarding the investigation performed on the isotropic plate, the first mode shape was illustrated by various parameters. The results obtained for linear frequencies were in a good agreement with the literature studies for various plate's ratios. Actually, the first mode shape had the same shape that was found in the literature. Also, the dependance was examined with amplitude displacement. The backbone curves were investigated for 6 and 9 degrees of freedom (dof). Therefore, good convergence was shown for 9 dof which perfectly matched with those reported by Alijani et al. (2013). Concerning the experimental test made on the FDM plate, the response displacement and frequency were measured and plotted. Furthermore, to emphasis the convergence of the nonlinear behavior of the FDM and the isotropic plate, the numerical and experimental were compared.

Ultimately, the observed mode shape of the FDM plate, was similar to the isotropic plates, and both structures have a hardening type of resonance.

**Keywords:** 3D manufacturing, Nonlinear vibration analysis, Geometrically nonlinear, Fully free rectangular parts,

ISBN: 978-605-73552-2-5

**123-OP**

## A NEW MECHANISM FOR VANET ATTACKS DETECTION

Prof. Adwan Yasin

Arab American University-Palestine
adwan.yasin@aaup.edu

### ABSTRACT

In order to improve vehicle and road safety, traffic control and accident avoidance. a new promising technology which is called Vehicle Ad Hock Network (VANET) has been adopted. This technology provides a lot of benefits and comfort as well as convenience to both drivers and passengers. The major concerns in VANET are availability, Privacy and data integrity that should be achieved to protect this type of network from malicious attacks. One of the most dangerous and severe threats in VANET is a Sybil attack, in this attack the intruder maliciously produces a lot of false identities to spread false messages that lead to system safety-related services interruption or disruption. In this paper we provide a comprehensive review of many researches and publications related to this type of attack as well as many Sybil attack prevention and detection techniques in VANET. A new mechanism of sybil attack detection has been proposed, which based on the information collected by the road side units in VANET which corresponds to the mobility pattern similarities. The employment of unsupervised machine learning methods such as k-means clustering, and statistical significance testing, the sybil attack nodes will be quickly detected.
Keywords—VANET, Sybil attacks, Security, K-means Clustering, Sybil Attack Detection

**124-OP**

## REAL-TIME DETECTION OF RAIL DEFECTS BY MACHINE LEARNING

İbrahim UÇAR[1,*], Utku KAYA[2]

[1] Rail Transport Engineering Master with Thesis, Eskişehir Technical University, Eskisehir, Turkey
[2] Vocational School of Transportation, Eskişehir Technical University, Eskisehir, Turkey

### ABSTRACT

In this study, real-time detection of defects that may occur in rail components will be investigated with machine learning algorithms. This research aims to detect the faults that will occur in the railway components early and to prevent accidents and losses in advance. The study was carried out by detecting the faults of basic parts such as rail fractures, lack of fastener, lack of rail fixing clamp, and lack of screws. Multiple images will be used in our application for training machine learning algorithms. Defective or non-defective images will be classified by a deep learning network. In other words, our deep learning network will detect incoming test images contactless and in real-time. In our study, appropriate methods and success metrics are given and the results are explained comparatively.

**Keywords:** Machine learning, Deep learning, Railway, Rail components

ISBN: 978-605-73552-2-5

**127-OP**

# SYNTHESIS OF N-ACYLBENZOTRIAZOLYLPYRIDINE-RUTHENIUM COMPLEX AND INVESTIGATION HETEREGENOUS CATALYTIC HYDROGENATION ACTIVITY IN CONTINIOUS FLOW SYSTEM

Pınar KAPÇI[1], Halenur ÖZER[1], Filiz YILMAZ[1*], Deniz HÜR[1]

[1] Chemistry Department, Faculty of Science, Eskişehir Technical University, Eskişehir, Türkiye

## ABSTRACT

It is known that synthetic organic chemistry reactions have great application area in industry. Especially, since the flow chemistry provides safer conditions, great advantages can be obtained by applying it to green chemistry. Compared to batch chemistry, it is very advantageous in that it provides the opportunity to work at lower concentrations, allows quick and easy adjustment of such as temperature and pressure parameters. At the same time, flow chemistry gains importance with the reusability of catalysts and the possibility of working with hazardous chemicals quite safely. In this study, a ruthenium catalyst was obtained after synthesis and characterization of (1H-benzo[d][1,2,3]triazole-1-yl)(pyridine-2-yl)methanone, PyrCOBt, ligand designed for use in continuous flow systems. In order to examine the effect of the synthesized catalyst on heterogeneous catalytic hydrogenation, its catalytic activity on hydrogenation of cyclohexene, 1-octene, and styrene were investigated by continuous flow heterogeneous hydrogenations.

**Keywords:** Continuous flow systems, Heterogeneous catalytic hydrogenation, Ruthenium catalyst

ISBN: 978-605-73552-2-5

**128-OP**

# COMPARISON OF ENERGY EFFICIENCY STUDIES OF TURKEY AND GERMANY

Fatih Burak ÖZKANLI[1], Prof. Dr. Zafer DEMİR[2]

[1] Department of Advanced Technologies, Graduate School of Science, Eskişehir Technical University, Eskişehir, Turkey
2 Department of Electricity and Energy, Porsuk Vocational School, Eskişehir Technical University, Eskişehir, Turkey

## ABSTRACT

Where energy is used is as important as obtaining it from a source. It has been demonstrated by the studies that significant savings will be achieved with the regulations to be made in the use of energy. With the concept of energy efficiency, countries attach importance to efficiency studies and adopt various policies to reduce energy waste. Turkey's energy efficiency studies, which started with Turkey's Regulation on Energy Efficiency in Industry, which started in 1995, became more frequent with the 2000s, and with the Energy Efficiency Law enacted in 2007, some obligations and sanctions were introduced in order to ensure energy efficiency. Especially in the European Union harmonization process, legal arrangements have been made for the directives published by the European Union (EU). With the Energy Conservation Law (EnEG) enacted in 1976, Germany took the first step in this sense by giving the government the authority to enact laws in the field of energy efficiency. Then, with the EnEV regulation, standards on energy efficiency were determined and legal regulations were made for citizens to comply. Germany has published new updates over the years in order to comply with the directives and programs published by the European Union. In this study, an overview of the energy efficiency policies determined by Turkey and Germany from the past to the present will be made, and the progress made by the two countries on energy efficiency will be compared. The significant impact of EU Directives on energy efficiency laws will be examined. A comparison will be made about the differences in the laws enacted within the framework of the policies determined by Turkey and Germany. Different reference values in laws and regulations published for energy efficiency in buildings will be compared. The effects of the renewable and emission-free energy target determined by Germany against the domestic energy target determined by Turkey on energy efficiency studies will be examined.

**Keywords**: Energy efficiency, Energy efficiency law, Building energy certificate, Energy efficiency policy

ISBN: 978-605-73552-2-5

**129-OP**

# EFFECT OF REACTION TIME ON LI DOPED TIO2 NANOSTRUCTURES SYNTHESIZED BY HYDROTHERMAL METHOD

Burak ŞAHİN[1*] , Sibel MORKOÇ KARADENİZ[1]

[1]Department of Physics , Graduate School of Natural and Applied Sciences, University of Erzincan Binali Yıldırım, Erzincan, Türkiye
[2]Department of Physics , Faculty of Arts and Science, University of Erzincan Binali Yıldırım, Erzincan, Türkiye
sahinbur4k@gmail.com

## ABSTRACT

In this study, lithium doped titanium dioxide nanostructures were synthesized in acidic solution with different reaction times at constant temperature using hydrothermal synthesis method. Structural, morphological and optical analyzes of the obtained lithium-doped titanium dioxide nanorods were performed using X-Ray Diffraction (XRD), Scanning Electron Microscopy (SEM) and UV-Vis Spectroscopy methods, respectively. As a results it was studied to understand the effect of reaction time on lithium doping TiO2 nanorods. Different morphologies and homogeneous structures were observed at different reaction times, the XRD peaks were examined that, it was observed that the intensity of peaks belong to (110) and (101) rutile phase crystal plane increased with the increasing reaction time. SEM images of the samples showed that structures with different morphologies were obtained at different reaction times and homogeneous nanorods which have smallest diameter, were obtained at 8h. According to UV-Vis measurement results are examined, it is seen that the absorption increased and the transmittance decreased with the increasing reaction time. Keywords: Nanorods, TiO2, Hydrothermal

ISBN: 978-605-73552-2-5

**130-OP**

## SYNTHESIS AND STUDY OF SURFACTANTS BASIS ON ALKYLBROMIDES ($C_{14}$, $C_{18}$) AND PROXYLATED DERIVATIVES

Gulnara AHMADOVA[1], Ravan RAHIMOV[1], S.Zeynab HASHIMZADA[1], Ulviyya YOLCHUYEVA[1], Hasan MAHMUDOV[1]

[1]Institute of Petrochemical Processesof the Azerbaijan National Academy of Sciences,Baku, Azerbaijan
zeynab.hashimzada@gmail.com

### ABSTRACT

A series of cationic gemini surfactants, N,N'-bis(2-hydroxypropyl)ethylenediammonium dibromides and N,N,N',N'-tetrakis(2-hydroxypropyl)ethylenediammonium dibromides synthesid interaction alkylbromdes with propoxylated ethylenediamine [1]. Specific electrical conductivities and surface tensions of the aqueous solutions of these cationic gemini surfactants were determined [2]. Antibacterial properties of the synthesized cationic surfactants against sulfate-reducing bacteria (SRB) were studied.
**Keywords:** Gemini surfactants, alkylbromides, propylene oxide, surface tension, electrical conductivity.

**131-OP**

## Numerical and Experimental Investigation on the Repair Impact of Arrow-shaped and Hexagonal Glass-epoxy Composite Patches

Mohammadjavad RANJBARAN[1] Seyed Masoud HOSSEINI[2]

[1]Graduate student (Islamic Azad University of Hamedan, Department of Mechanical Engineering, Hamedan, Iran)
E-mail: mohammadjavadranjbaran@yahoo.com

[2]Undergraduate student (Islamic Azad University of Hamedan, Department of Mechanical Engineering, Hamedan, Iran)
E-mail: masoud.hosseini1372@gmail.com

### ABSTRACT

Composites as materials with superior characteristics have proved their effectiveness in maintaining of damaged components, especially in aeronautical applications. Within the current research, the arrow-shaped and hexagon glass-epoxy composite patches with fibers orientations angles of 0,90 and -45,45 are employed with the aim of repairing the cracked aluminum alloy 7075 specimens. Total number of 28 one-sided repaired aluminum samples with 30 mm of crack length situated within the center, are prepared to undergo uniaxial tensile loading using the 600 KN santam testing machine. Additionally, to the experimental tests, the Abaqus software is employed so on simulate the testing conditions numerically with XFEM (Extended finite element method) technique. Findings indicate that the arrow-shaped composite patches have higher efficiency of repair and sturdiness compared to ones with hexagonal geometry. Also, by decrease in measurements of the repair patch geometry, the upper tensile load is handled. Specimens repaired with glass-epoxy composites fibers orientation angle of -45,45 degree are extended more, but can withstand lower tensile loading.

Key Words: glass-epoxy composite, Arrow-shaped, Hexagon patch, crack, extended finite element method, aluminum alloy 7075, uniaxial tensile test,

ISBN: 978-605-73552-2-5

**132-OP**

## NH FUSE WITH NEW POLYMER THERMOSET BODY

Oğuz Kaan ATAR[1,*], Mutlu BEKTAŞ[1], Tuba BUĞDAYCI AVŞAR[1]

[1] Research and Development,Yeşilırmak Electricity Distribution Co.,Samsun,Türkiye

### ABSTRACT

Blade type fuses are in the family of fusible wire fuses, like plug fuses. The main principle of operation of these fuses is the heat effect of electric current. It consists of a short circuit for a short period of time. In this paper, a comparison of the new generation NH blade fuse with polymer thermoset body produced by BMC (Bulk Molding Compound) injection and the currently used porcelain blade fuse is compared.

**Keywords:** Blade type fuses; BMC(Bulk Molding Compound); steatite porcelain fuses; short circuit current; NH Fuses; Polymer thermoset.

**135-OP**

## SYNTHESIS AND STUDY OF SURFACTANTS BASIS ON ALKYLBROMIDES ($C_{14}$, $C_{18}$) AND PROXYLATED DERIVATIVES

Gulnara AHMADOVA[1], Ravan RAHIMOV[1], S.Zeynab HASHIMZADA[1], Ulviyya YOLCHUYEVA[1], Hasan MAHMUDOV[1]

[1]Institute of Petrochemical Processesof the Azerbaijan National Academy of Sciences,Baku, Azerbaijan
zeynab.hashimzada@gmail.com

### ABSTRACT

A series of cationic gemini surfactants, N,N'-bis(2-hydroxypropyl)ethylenediammonium dibromides and N,N,N',N'-tetrakis(2-hydroxypropyl)ethylenediammonium dibromides synthesid interaction alkylbromdes with propoxylated ethylenediamine [1]. Specific electrical conductivities and surface tensions of the aqueous solutions of these cationic gemini surfactants were determined [2]. Antibacterial properties of the synthesized cationic surfactants against sulfate-reducing bacteria (SRB) were studied.

**Keywords:** Gemini surfactants, alkylbromides, propylene oxide, surface tension, electrical conductivity

ISBN: 978-605-73552-2-5

**136-OP**

# ENHANCED HER PROCESS WITH ULTRA-SMALL $Pt_{25}Au_{75}$ ALLOY NANOPARTICLES

Hasan Hüseyin IŞIK*, İlknur BALDAN IŞIK, Dogan KAYA, Faruk KARADAĞ, Ahmet EKİCİBİL

Department of Physics, Science and Art Faculty, Çukurova University, Adana, Turkey

## ABSTRACT

Increasing world energy demand urging cost-effective and environmental-friendly alternatives to fossil fuels. Since hydrogen gas can be used as a "clean" energy source for fuel cells by splitting water through the hydrogen evolution reaction (HER), it is one of the most studied reactions in electrocatalysis. Although Pt is the most preferred catalyst due to enhanced catalytic properties, alloying Pt with Au increased on catalytic activities compared to pure Pt and Au catalyst. Herein, we investigated the structural and catalytic properties of low Pt-loaded PtAu nanoparticle (NP) which was synthesized by modified polyol method. The structural properties of PtAu NPs were determined using X-ray diffraction and Rietveld refinement analyses, and the crystal structure of $Pt_{25}Au_{75}$ NP exhibited face-centered cubic formation with two crystalline phases; $Pt_{25}Au_{75}$ and Au with a space group of $Fm\bar{3}m$ . The average particle size was found to be 7.17 nm by analyzing scanning electron microscopy images. The cyclic voltammetry (CV) measurements were performed for the HER process between -0.5 V and -1 V vs. Ag/AgCl at different scanning rates of 5, 10, 20, 50, 75, and 100 mV $s^{-1}$ in 1 M KOH solution at room temperature. We observed a distinct Pt-H formation and Pt-H oxidation regions between -0.1 V and -0.7 V. We also performed CV measurements up to 500 cycles with a scan rate of 50 mV $s^{-1}$ and the performance of $Pt_{25}Au_{75}$ catalyst became stable after the $50^{th}$ cycle up to the $500^{th}$ cycle. We observed that the current value increases as the scanning rate increases. Linear sweep voltammetry measurement was operated by comprehensive the potential between 0 and -1.5 V with a scan rate of 25 mV $s^{-1}$. The onset potential was found to be -1.085 V at 10 mA $cm^{-2}$ and the maximum current at -1.5 V was measured as -44.47 mA $cm^{-2}$.

**Keywords:** Pt-Au nanoparticles, Modified polyol method, Structural analysis, Hydrogen evolution reaction.

**Acknowledgements**
We would like to thank the Research Fund of Çukurova University (FBA-2021-13479 and FBA-2020-13260) for financial support of this research.

ISBN: 978-605-73552-2-5

**137-OP**

# INVESTIGATION OF HYDROGEN EVOLUTION REACTION WITH LOW-Pt LOADING IN PtCu ALLOY

İlknur BALDAN IŞIK*, Hasan Hüseyin IŞIK, Doğan KAYA, Ahmet EKİCİBİL, Faruk KARADAĞ

Department of Physics, Science and Art Faculty, Çukurova University, Adana, Turkey

## ABSTRACT

The hydrogen evolution reaction (HER) is one of the most studied electrochemical processes in water electrolysis. Therefore, the development of Pt-based electrocatalysts with improved activity and stability is important for HER electrocatalysts in fuel cells. In this work, we synthesized bimetallic PtCu NPs with modified polyol method. The crystal structure of PtCu NPs was investigated by using X-ray diffraction and Rietveld refinement analyses which revealed that the crystal structure of PtCu NPs was a face-centered cubic structure with a space group of $Fm\bar{3}m$. The morphology of PtCu NPs was characterized by scanning electron microscopy and observed as monodisperse and spherical NPs with an average particle size of 13.5 nm. The chemical composition of the alloy is found to be $Pt_{13}Cu_{87}$ using energy dispersive spectroscopy. In addition, the electrocatalytic activities of PtCu NPs were examined for HER catalysis in 1 M KOH alkaline solution. The cyclic voltammetry (CV) measurement was performed with a scan rate of 100 mV $s^{-1}$ between -1.2 V and 1.2 V. The current density was measured as -27.2 mA $cm^{-2}$ at -910.5 mV for HER. Moreover, CV measurements were also investigated with different scan rates within the potential range of -0.5 –1.2 V. Increasing scan rate increased the current density. In addition, the durability of Pt-Cu bimetallic NPs was tested by performing continuous 500 CV cycles between -1.0 V and -0.5 V with a scan rate of 100 mV $s^{-1}$. We observed that CV curves started to overlap after the $100^{th}$ cycle and become stable up to 500 cycles. Linear sweep voltammetry measurement was operated the potential between 0 and -1.5 V with a scan rate of 25 mV $s^{-1}$. The onsetpotential for HER process was found to be -1.006 V at 10 mA $cm^{-2}$. The maximum HER activity was also recorded as -158.8 mA $cm^{-2}$ at -1.5 V.

**Keywords:** Pt-Cu nanoparticles, structural analysis, Hydrogen evolution reaction.

**Acknowledgements**
We would like to thank the Research Fund of Çukurova University (FBA-2021-13479) for financial support of this research.

ISBN: 978-605-73552-2-5

**140-OP**

# FRACTAL AND MULTI-FRACTAL ANALYSES OF THE GEOMAGNETIC FIELD VARIATIONS CAUSED BY THE EARTHQUAKE ON JANUARY 24, 2020 IN TURKEY

Andriy ONISHCHENKO[1,*], Leonid CHERNOGOR[2], Oleg LAZORENKO[3]

[1] Physics Department, Faculty of Automatics and Computerized Technologies,
Kharkiv National University of Radioelectronics, Kharkiv, Ukraine
[2] Space Radiophysics Department, School of Radiophysics, Biomedical Electronics and Computer Systems,
V. N. Karazin Kharkiv National University, Kharkiv, Ukraine
[3] General Physics Department, School of Physics, V. N. Karazin Kharkiv National University, Kharkiv, Ukraine

## ABSTRACT

Fractal and multi-fractal properties of the Earth's magnetic field time variations caused by the earthquake took place on January 24, 2020 in Turkey were investigated. Using the Dynamical Fractal Analysis method proposed by the authors for both (D and H) horizontal components of geomagnetic field, the time dependences for the Hurst fractal dimension were obtained. With usage of the Wavelet Transform Module Maxima method and the Multi-Fractal Detrended Fluctuation Analysis method, the set of traditional and original multi-fractal numerical characteristics was estimated. Combining the fractal and multi-fractal analyses results with ones for the time-frequency structure, obtained the Continuous Wavelet Transform application, the set of disturbances caused by the earthquake was discovered. For these disturbances, all needed time-frequency, fractal and multifractal characteristics were estimated. The disturbances were shown to be fractal ultra-wideband processes with complex, non-stationary multi-fractal structure. Two promising candidates for the role of earthquake harbingers were revealed. One possible earthquake harbinger in both horizontal components of the geomagnetic field time variations seems to be detected. This harbinger was shown to be registered 25.5 hours before the earthquake event. Being be found in time variations of the multi-fractal characteristics only for both horizontal components of the geomagnetic field, another possible earthquake harbinger took place 0.5 hours before the earthquake event. The so-called transition of the multi-fractal process to the mono-fractal mode was detected. For both harbingers, the time-frequency, fractal and multifractal characteristics were estimated.

**Keywords:** Fractal Ultra-Wideband Process, Fractal Analysis, Multi-Fractal Analysis, Geomagnetic Field Time Variations, Earthquake.

ISBN: 978-605-73552-2-5

**141-OP**

# LACTOBACILLUS REUTERI VE STREPTOCOCCUS THERMOPHILUS İÇEREN FERMENTE SÜT ÜRÜNÜNÜN ÜRETIM BASAMAKLARI TEKNOLOJIK ÖZELLIKLERI VE AROMA PROFILLERININ BELIRLENMESI

Hakan TAVŞANLI[1], Berfin ALTUNDAL[2]

[1]Veteriner Fakültesi, Veteriner Halk Sağlığı Anabilim Dalı, Balıkesir Üniversitesi, Balıkesir, Türkiye
[2] Sağlık Bilimleri Enstitüsü, Balıkesir Üniversitesi, Balıkesir, Türkiye

## ÖZET

Probiyotikler, patojen mikroorganizmaları inhibe edip, konakçının mikrobiyotasını iyileştirerek ve kendi metabolik faaliyetlerini de devam ettirerek konakçının bağışıklık sistemini güçlendiren ve insan sağlığını olumlu yönde etkilen faydalı mikroorganizmalardır. Bu probiyotik bakterilerden biri olan *L. reuteri* oksijenle sınırlı atmosferlerde gelişmesi, insan ve hayvanların bağırsak duvarında kolonize olması ile bağırsak duvarında fiziksel, biyokimyasal ve immünolojik bariyer oluşturmaktadır. Oluşan bu bariyer antijenlerin ve toksinlerin bağırsak duvarından emilmesini engellemek gibi önemli bir fonksiyona sahiptir. Aynı zamanda insan bağırsaklarında bulunan tek heterofermentatif tür olan *L. reuteri* süt ortamında gelişememektedir. Bu anlamda çalışmamızda, insan mikrobiyatası için oldukça önemli olan bu bakterinin fermente süt ürünleri ile alınabilmesi için *S. thermophilus'un* sinerjik etkisinden yararlanılarak süt ortamında gelişmesi sağlanmıştır. Sonuç olarak 100 ml süte $10^3$ kob/ml düzeyinde inokule edilen *L. reuteri* ve *S. thermophilus*' un 12 ve 24. saat inkubasyon sonrası pH, SH, aw, KM, yağ, protein ve Laktik asit bakteri sayıları tespit edilmiştir. Kazeinin izolelektirik noktası olan pH 4,6 değerine 42 °C de 12 saatte ulaşmıştır. 12 saat inkübasyon ve +4 °C de 24 saat soğultulmasının ardından her iki laktik asit bakteri sayısı $10^9$ kob/gr düzeyinde tespit edilmiştir. 12 ve 24. saatte pH, SH, aw, kurumadde (%), yağ ve protein değerleri sırasıyla 4.47, 4.7, 0.982, 88.53, 3.6, 4.03; 4.36, 2.4, 0.987, 89.34, 3.6, 4.03 olarak tespit edilmiştir.

Sonuç olarak *L. reuteri* süt ortamında *S. thermophilu'un* sinerjik etkisiyle birlikte Türk Gıda Kodeksi Probiyotik kabul edilme değeri olan $10^9$ kob/gr değerine 12. saatte ulaşmıştır. Elde edilen fermente süt ürünü ile insanların probiyotik özelliği oldukça önemli olan *L. reuteri*' ye doğal yollar ile ulaşması sağlanalabilir.

**Keywords:** Probiyotik, *L. reuteri*, S. *thermophilus*

ISBN: 978-605-73552-2-5

**142-OP**

# ÖĞÜTÜLMÜŞ UÇUCU KÜL VE ÇELİKHANE CÜRUFUNUN CAM SERAMİK ELDESİNDE KULLANILABİLİRLİĞİNİN ARAŞTIRILMASI

Serkan KESKİNBAŞ[1], Zafer DİKMEN[2], Sedef DİKMEN[2]

[1]Fizik Öğretmeni, Hüseyin Erçelebi Anadolu Lisesi, Eskişehir, TÜRKİYE

[2]Fizik Bölümü, Fen Fakültesi , Eskişehir Teknik Üniversitesi, Eskişehir, TÜRKİYE

## ÖZET

Bu çalışmada, Çayırhan (Ankara) Termik Santrali'nden temin edilen uçucu kül (UK) ve yardımcı malzeme olarak da Erdemir Demir Çelik Fabrikası A.Ş.'den temin edilen bazik oksijen fırını (BOF) cürufu atıklarının farklı oranlardaki karışımlarının 4, 8, 12 ve 16 saat süreyle gezegen tipi bilyeli bir değirmende öğütme işlemlerinin sinterlenme davranışına etkisi araştırılmıştır. Çalışmanın ilk aşamasında, öğütme işleminin atık malzeme üzerinde mineralojik ve mikroyapısal olarak etkilerini görme amacıyla Parçacık Boyut Dağılımı (PSD), X-ışını Kırınım Analizi (XRD) ve Taramalı Elektron Mikroskopu (SEM) analizleri gerçekleştirilmiştir. Taramalı elektron mikroskopu (SEM) görüntülerinden parçacıkların 8 saatlik öğütme süresinden sonra topaklanma eğilimi göstermeye başladığı görüldü. Uçucu külün medyan tane çapı D(50) 12 saatlik öğütme işlemi sonunda 16,8 µm'den 1,21 µm'ye düşmüştür.

Çalışmanın ikinci aşamasında ise, öğütme süresi, karışım oranları ve sıcaklık parametrelerine bağlı olarak optimum sinterleme koşullarını belirlemek amacıyla, öncelikle UK ile BOF cürufunun farklı oranlarda karışımları 2, 4, 8, 12 ve 16 saat süreyle yaş olarak öğütüldü. Öğütme işleminden sonra, herhangi bir katkı maddesi, bağlayıcı vb. kullanmadan silindirik formda preslenerek 950°C, 1000°C, 1050°C ve 1100°C olmak üzere dört farklı sıcaklıkta sinterlenerek mekanik, mineralojik ve mikroyapısal özellikleri belirlenmiştir. Basınç dayanım testleri sonucunda mukavemet değerleri 4,56 ila 83,95 MPa aralığın da değişim gösterdiği sonucuna varıldı. 2/3 oranında UK ile 1/3 oranında BOF cürufu karışımının 8 saat öğütülmesi ve 1050ºC'de sinterlenmesi sonucunda en yüksek mukavemet değeri elde edildi.

**Anahtar Sözcükler:** Çelikhane cürufu, Uçucu kül, Sinterleme, Mekanik özellikler, XRD, SEM

ISBN: 978-605-73552-2-5

**143-OP**

# ANALYSIS OF C–H···O INTERACTION BETWEEN ANION AND CATION OF 1,3-DIMETHYLIMIDAZOLIUM METHYLSULPHATE USING NATURAL BOND ORBITAL METHOD

Nihal KUŞ

Department of Physics, Science Faculty, Eskisehir Technical University, 26470, Eskisehir, Turkey.

## ABSTRACT

Since the usage areas and importance of ionic liquids have increased a lot today, it is clear that it is necessary to study on it. In this study, geometry optimizations, charge density and natural bond orbital (NBO) analysis of 1,3-dimethylimidazolium and methylsulphate (DIMIM-MS) ionic liquid in cation and anion form were carried out at the Becke, 3-parameter, Lee, Yang-Parr (B3LYP) version with 6-311++G(2d,2p) basis set. Stabilization energies due to the C–H···O weak hydrogen bonds orbital interactions are calculated from the second-order perturbation approach using Fock matrix equation. Donor-acceptor interactions and hybridization for the C–H···O interaction between anion and cation orbital interactions of DIMIM-MS were analyzed and orbital electron density schemes were plotted. HOMO-LUMO, Mulliken charges and NBO charges were calculated and interpreted using DFT-B3LYP/6-311++G(2d,2p) method.

**Keywords:** Ionic liquid, orbital interaction, stabilization energy, 1,3-dimethylimidazolium methylsulphate, NBO.

**ACKNOWLEDGMENT**
This work was supported by the Eskisehir Technical University Commission of Research Project under grant no: 19ADP130.

ISBN: 978-605-73552-2-5

**144-OP**

# SYNTHESIS OF GOLD NANOPARTICLES ON REDUCED GRAPHENE OXIDE-FUMED SILICA HYBRID SUPPORT TO USE AS ANODE CATALYST IN ALCOHOL FUEL CELLS

Zeynep DAŞDELEN[1]*and Ali ÖZCAN[1]

[1] Department of Chemistry, Faculty of Science, Eskisehir Technical University, Eskisehir, Türkiye

## ABSTRACT

In this study, the use of fumed silica-reduced graphene oxide (FS-rGO) hybrid material as a support for gold nanoparticles and the activity of this catalyst (Au@FS-rGO) as an anode catalyst in sorbitol fuel cells were investigated. In order to compare the efficiency of hybrid catalyst support, Au catalysts were synthesized using fumed silica (Au@FS) and reduced graphene oxide (Au@rGO) support with similar method and their efficiency in sorbitol oxidation were compared. Cyclic voltammetry and chronoamperometry were used for the electrochemical characterization of the prepared catalysts, TEM, SEM, XRD, Raman, ICP-MS and EDX were used for the structural characterization.

As a result of the ICP-MS analysis, the amount of Au in the catalysts was found to be 32.8%, 32.5% and 32.0% for Au@FS-rGO, Au@FS and Au@rGO, respectively. When the results of the TEM analysis were examined, the average particle size of the catalysts were measured as 7.05 nm (Au@FS-rGO), 1.51 nm (Au@FS) and 5.90 nm (Au@rGO). The presence of reduced graphene oxide, fumed silica and Au nanoparticles in the catalysts are proven by XRD analysis, and it was observed that graphene oxide is transformed into reduced graphene oxide by Raman analysis.

Cyclic voltammograms of Au@FS, Au@rGO and Au@FS-rGO were obtained in a 0.5 M KOH solution in the absence and presence of sorbitol to evaluate the activities of the nanocomposites. A well-defined peak corresponding to the oxidation of sorbitol was observed in the presence of sorbitol. The current densities of Au@rGO, Au@FS and Au@FS-rGO were measured as 17.68 mA mg-Au, 54.2 mA mg-Au and 64.7 mA mg-Au in 0.5M KOH containing 0.5M sorbitol. The activity of Au@FS-rGO towards sorbitol electrooxidation was 3.66 and 1.19 times higher than that of Au@rGO and Au@FS, respectively, indicating the synergistic effect of FS and rGO.

**Keywords:** Sorbitol Fuel Cell, Gold Nanoparticles, Hybrid Material, Graphene Oxide, Fumed Silica.

ISBN: 978-605-73552-2-5

**147-OP**

# BAYESIAN REGULARIZATION OF LEARNING

Murad Omarov [1] , Vusala Muradova [2]

[1] Department of Computer-integrated technologies, automation and mechatronics, Kharkov National University of Radio
Electronics, Kharkov, Ukraine
[2] Department of Natural Sciences, Kharkov National University of Radio Electronics, Kharkov, Ukraine
Email of corresponding author: viusalia.muradova@nure.ua

**ABSTRACT**

**The subject of research** in the article is the Bayesian approach based on the first principles of the probability theory is the most consistent paradigm of statistical learning. From practical perspective Bayesian learning offers intrinsic regularization procedure providing a viable alternative to traditional cross-validation technique. **Objective:** Machine learning aims to identify patterns in empirical data. In contrast to mathematical modeling, which studies the consequences of known laws, machine learning seeks to recreate the causes by observing the consequences generated by them are empirical data training, so thus, it belongs to the class of inverse problems and, in the general case, is a poorly defined or ill-posed problem. These tasks are different special sensitivity of some solutions to data and finding stable solutions implies a regularization procedure, which is a restriction of the class of feasible solutions. **The following tasks are solved in the article:** Bayesian regularization, the subject of this review, is an alternative technique for optimizing model complexity. It is not based on an estimate of the expected error, but on the choice of the most plausible model supported by the available data. This approach has a number of advantages. First, it proceeds from the first principles of probability theory and statistical learning theory, which guarantee a reduction in generalization error. Secondly, it implies an assessment of variations in the model parameters and, accordingly, an assessment of the accuracy of one's predictions. Thirdly, the problem posed in this way can in some cases of practical importance be solved with a minimum number of additional simplifying assumptions. And finally, as a consequence, last but not least: Bayesian regularization can be built directly into learning algorithms. Moreover, such regularized algorithms no longer imply a validation stage, uniformly using all available data both to select the optimal complexity of the model and to configure its parameters.

**Keywords:** Bayesian regularization, Bayesian learning, machine learning, mathematical modeling.

ISBN: 978-605-73552-2-5

149-OP

# DERIVATION OF EXPRESSION FOR PHOTOCURRENT DENSITY FOR NON-DESTRUCTIVE TESTING OF 3D PRINTING FILAMENT BY MEANS OF TERAHERZ SPECTROSCOPY

Iurii KHOROSHAILO[1], Nataliia ZAICHENKO[2], Olga ZAICHENKO[1*]

[1] Department of Design and Operation of Electronic Devices, Faculty of Automatics and Computerized Technolohies, Kharkiv National University of Radioelectronics, Kharkiv, Ukraine
[2] Department of Microelectronics, Electronic Devices and Appliances, Faculty of Electronic and Biomedical Engineering, Kharkiv National University of Radioelectronics, Kharkiv, Ukraine

## ABSTRACT

The subject of this report is a derivation of expression for photocurrent density in teraherz spectroscopy. Terahertz spectrometry is a means of non-destructive testing, including 3D printed detail testing, which belongs to the interest area of the report authors. 3D printing or additive manufacturing is the construction of a three-dimensional object from a CAD model. It can be done in a variety of processes in which material is deposited, joined or solidified under computer control, with material being added layer by layer. The cause of 3D printing defects and low printing quality problems are weak infill, gaps in thin walls, inconsistent extrusion, layer separation and splitting, bed drop and other issues which make some of 3D printing parts unqualified and unsafe to employ. The ability to affect internal layers without affecting the exterior could lead to the production of malicious defective parts without an alert. It is necessary to test 3D printed detail and 3D filament on every stage of processing preferable by non destructive methods. The analytical review of literature sources showed the perspectives for improving the accuracy of measurements due to a set of improvements in models of terahertz spectrometers. The mathematical model of the photocurrent is a convolution integral of the current density and laser radiation pulse irradiating the surface of the semiconductor antenna. The expression under the integral sign has such arguments as optic pulse duration, currier life time, momentum relaxation time . Then it is calculated to obtain the result of integration as two terms, each of them is product of exponent and complementary error function with the same arguments: optic pulse duration, currier life time, momentum relaxation time. The calculation includes such steps as integration variable change. The verification in Maple software shows coincidence with analytical calculation results and way for further photocurrent density expression upgrade.

**Keywords:** teraherz spectrometry, formula derivation, antenna, photocurrent density, recombination time, uncertainty analysis

ISBN: 978-605-73552-2-5

**150A-OP**

# PLANT-BASED SYNTHESIS OF ORGANIC@INORGANIC HYBRID CU BASED NANOFLOWER USING CUCUMBER LEAF EXTRACT AS ORGANIC COMPONENT

Fatih Doğan KOCA[1,*], Tuğçe ERDEM[2]

[1] Department of Aquatic Animals Science, Faculty of Veterinary Medicine, Erciyes University, Kayseri, Turkeyy
[2] Instıtute of Health, Erciyes University, Kayseri, Turkey Country

## ABSTRACT

For the synthesis of organic@inorganic hybrid nanoflowers, metal ions are used as inorganic components and expensive biomolecules such as enzymes, proteins and DNA are used as organic components. While there are many studies on the use of bioextracts such as various plants, algae, fungi and lichens in the synthesis of nanoparticles, the synthesis of nanoflowers is quite limited. For the first time in this study, cucumber leaves used for synthesis of organic@inorganic hybrid nanoflowers. PBS buffers (pH 3-11) at different pH were used for the synthesis of nanoflowers. Optimum synthesis was observed as a result of 3 days reaction of 1 ml cucumber extract and $8x10^{-4}$ M $Cu^{+2}$ in 50 ml PBS buffer in pH 7.4 medium. Nanoflower and nanopetal structures were revealed by FE-SEM analysis, and the presence of Cu in the skeletal structure was revealed by EDX analysis. The formation scheme of nanoflowers is briefly explained by (i) nucleation, where phosphate crystals form in PBS buffer, (ii) petal growth, and (iii) nanoflower formation termination phase. As a result, it is recommended to synthesize plant extracts and nanoflowers cheaply and easily instead of expensive biomolecules such as enzymes, DNA and protein, and to evaluate the potential of the synthesized nanoflowers in industrial applications such as catalytic and sensory.

**Keywords:** Nanoflowers, cucumber, characterization

*This study was supported by Erciyes University Scientific Research Projects unit with the code TYL-2022-11865 and was produced from Tuğçe Erdem's master's thesis.

ISBN: 978-605-73552-2-5

**150B-OP**

## ANTIOKSIDANT ACTIVITY OF *Tornabea scutellifera* EXTRACT BASED Pt NANOPARTICLES

Haydar Matz MUHY[1,2,*], Fatih Doğan KOCA[3], Mehmet Gökhan HALICI[4]

[1] Institute of Science, Erciyes University, Kayseri, Turkey
[2] Ministry of Oil, Oil Products Distribution Company, Central Dpt. of Environment and Health, Bagdat, Iraq
[3] Department of Aquatic Animals and Diseased, Faculty of Veterinary Medicine, Erciyes University, Kayseri, Turkey
[4] Department of Biology, Science Faculty, Erciyes University, Kayseri, Turkey

### ABSTRACT

First time in this study *Tornabea scutellifera* extract were used for synthesis of Platinium nanoparticles (Pt NPs). The DPPH scavenging activity of *T. scutellifera*-based Pt NPs was determined and its usability as antioxidant activity was evaluated. With characterization tests, it was observed that Pt NPs were in spherical structure and had an average diameter of 68 nm. Functional groups that play a role in the synthesis were determined by FT-IR analysis with the peaks determined at 1623 $cm^{-1}$, 1146 $cm^{-1}$, 1042 $cm^{-1}$ and 987 $cm^{-1}$. Elemental structure (presence of Pt) was revealed by EDX analysis. It was determined that T. scutellifera-BASED Pt NPs exhibited anti-oxidant activity against DPPH (184.06 µg/ml, $R^2$=0.8727). It is thought that the study can be used in nanotechnology-related multidisciplinary studies.

**Keywords:** *T. scutellifera*, Pt Nanoparticles, Antioxidant activity

*This research was derived from the first author's PhD Thesis.

**151-PP**

## ON THE CLASSICAL IDEAL GAS IN TWO DIMENSIONS 3

Ibrahim A. SADIQ[1*], Noor M. YASEEN[2], Wisam MOHAMMED[3]

[1,2,3] Department of Physics, College of Science, Al-Nahrain University, Baghdad, Iraq.
ibrahim.sadiq@nahrainuniv.edu.iq

### ABSTRACT

The kinetic theory of gases is revisited for an ideal classical gas geometrically confined in two dimensions, i.e. two-8 dimensional gas (2D gas). In this revision, the equation of state for the 2D gas is determined as well as some of its 9 thermodynamic quantities. The thermodynamic quantities are like the internal energy, the heat capacities, and distribution 10 functions of molecular speeds and molecular velocities as well as some of the characteristic velocities and the speed of sound. 11 The work shows that the distribution functions of the molecular velocities are unchanged due to the reduction in the size of 12 the spatial dimension but all other revisited quantities are changed. The most remarkable results in the 2D gas are those 13 concern the gas temperature and the speed of sound (compressional waves). The same mean square velocity of the molecules 14 gives a higher temperature in the 2D gas than it gives in the same gas enclosed by a surface, i.e. three-dimensional gas (3D 15 gas). The other remark is that sound waves in the 2D gas can last longer and travel further than sound waves in the same gas 16 enclosed by a surface (3D gas) at the same temperature. 17

**Keywords:** ideal gas in two dimensions, equation of state, distribution molecular velocities, speed of sound, temperature.

ISBN: 978-605-73552-2-5

**152-PP**

# RESULTS OF AN EXPERIMENTAL STUDY OF THE FAULT-TOLERANT ROUTING METHOD WITH THE GLBP PROTOCOL

Oleksandr LEMESHKO[1,*], Oleksandra YEREMENKO[1], Anastasia KRUGLOVA[1], Anna ZHURAVLYOVA[1], Valentyn LEMESHKO[1], Mykhailo PERSIKOV[1]

[1] V.V. Popovskyy Department of Infocommunication Engineering, Faculty of Infocommunications, Kharkiv National University of Radio Electronics, Kharkiv, Ukraine

## ABSTRACT

This work proposes the results of an experimental study of a fault-tolerant routing method in an infocommunication network. The method implements proactive and reactive protection of the default gateway to provide a high level of network fault tolerance. Therefore, method is based on solving an optimization problem related to calculating primary and backup routes and determining the order of balancing the load incoming to edge routers from access networks. If one of the routers creating the virtual default gateway fails, the method changes the load balancing order between the functional border routers. Causes of failure can include overloading, low equipment reliability, hardware and software router failures, and violation of their network security level (compromise). The method considers the flow-based nature of network traffic, and the optimality criterion of routing solutions under Traffic Engineering is a minimum upper bound of network link utilization. To evaluate the effectiveness of the solutions, they were implemented on Cisco equipment. In the lab experiment, the Gateway Load Balancing Protocol functionality was used. Based on this fault-tolerant routing protocol, it is possible to set weighting coefficients administratively, the value of which affects the order of load balancing on the border routers. During the experiment, the weighting coefficients were adjusted not heuristically but according to the calculations obtained by the studied fault-tolerant routing method. The results of the study confirmed the effectiveness of the proposed solution. Ensuring optimal load balancing between border routers compared to the solution based on multipath routing, but without access layer balancing, improved network performance by 25.45% and reduced the upper bound of network link utilization by an average of 63.77 %. Lowering the utilization upper bound positively affects the quantitative values of the main Quality of Service indicators – the average end-to-end delay, jitter, and packet loss probability.

**Keywords:** network, routing, fault-tolerance, method, experiment

ISBN: 978-605-73552-2-5

**153-OP**

# EFFECT OF Ca AND Ba ATOMS ON $CsPbBr_3$ PEROVSKITE MATERIAL

İsmail YÜCEL[1*], Aygün IŞIK YILDIZ[2]

[1] Independent Scholar, Isparta, Turkey
2 Electronics and Automation Department, Technical Sciences Vocational School, Isparta University of Applied Sciences, Isparta, Turkey

## ABSTRACT

In this study, the structural and electronic properties of Ca and Ba doped $CsPbBr_3$ perovskite material have been investigated using FP-LAPW method within the DFT as implemented in WIEN2k code. The structural properties have been analyzed from optimizing bond length and ground state energy of the system. Perdew-Burke-Enzerhof (PBE) generalized gradient approximation (PBE-GGA) is treated in order to find structural parameters such as lattice parameter and bulk modulus. Tran-Blaha modification of the Beckee-Johnson potential (mBJ) has been treated in the self-consistent cycle (SCF) in order to improve band gap energy and electronic structure calculations. The $CsPbBr_3$ have a cubic crystal structure whose space group is Pm-3m (221). The unit cell of $CsPbBr_3$ consists of five atoms which are one Cs atom, one Pb atom and three Br atoms. In this study, we used a 2x2x1 supercell to doped Ca and Ba atoms. One of the Pb atoms is located at the (0.25, 0.25, 0.50) point. While forming the Ca and Ba doped crystal structures the Pb atom at (0.25, 0.25, 0.50) point has been removed and Ca-Ba atoms have been added respectively. The 2x2x1 supercell formed are $Cs_4Pb_4Br_{12}$, $Cs_4Pb_3CaBr_{12}$ and $Cs_4Pb_3BaBr_{12}$, respectively. First of all, the all-crystal structure has been optimized and calculated lattice parameters for $Cs_4Pb_4Br_{12}$, $Cs_4Pb_3CaBr_{12}$ and $Cs_4Pb_3BaBr_{12}$, respectively. The calculated values of lattice parameter are 6.0025 Å, 5.9601 Å and 6.0939 Å for $Cs_4Pb_4Br_{12}$, $Cs_4Pb_3CaBr_{12}$ and $Cs_4Pb_3BaBr_{12}$. The calculated band gap energy of undoped $CsPbBr_3$ is 2.36 eV. This result is in a good agreement with other theoretical and experimental results. Structural and electronic properties have been revealed for all compounds.

**Keywords:** $CsPbBr_3$, WIEN2k, DFT, Electronic properties.

ISBN: 978-605-73552-2-5

**154-OP**

# THE IMPORTANCE OF INDOOR AIR QUALITY STRATEGIES TO REDUCE THE SPREAD OF AIRBORNE TRANSMITTED DISEASES

Başak KARAKURT ÇEVİK

Energy Systems Engineering, Faculty of Engineering, Yalova University, Yalova, Turkey

## ABSTRACT

An average person inhales about 11.000 liters of air daily, and most people spend a substantial amount of their time indoors. The World Health Organization estimates that 3.8 million people die prematurely from indoor air pollution each year. Therefore, it is very important to pay adequate attention to strategies that enhance indoor air quality. For the last couple of years, indoor air quality has become even more crucial with mounting evidence that the main transmission route of coronavirus is airborne. Viruses are a subcategory of bioaerosols that can float in the air for a certain time and travel long distances depending on their size. If a virus is airborne, one can be infected by inhaling droplets or aerosols exhaled by an infected person. There are certain indoor air quality strategies that can be implemented to decrease the chance of contracting an airborne virus in indoor environments such as schools, workplaces, and homes. These strategies include establishing adequate ventilation, upgrading HVAC systems with proper filters, reconfiguring workplaces, monitoring carbon dioxide levels in indoor environments, and taking necessary actions based on the measurements and using commercial air cleaners or using do-it-yourself air cleaners. This study aims to provide a comprehensive analysis of indoor air quality strategies with a focus on the control of airborne transmission of diseases in indoor environments. However, it is also important to note that these strategies can result in improved cognitive function, improved overall health such as reduced asthma, allergy, and respiratory symptoms, reduced sick days, and increased work efficiency.

**Keywords:** Indoor air quality, bioaerosol, airborne transmission

ISBN: 978-605-73552-2-5

**155-OP**

# DEVELOPMENT OF PARAFFINE-BASED NANOEMULSION

Tuğba Derici

Mercan Chemistry, Denizli-Türkiye

## ABSTRACT

An emulsion is defined as a heterogeneous system of two immiscible liquid phases "oil" and "water". The dispersed phase is dispersed in a dispersion medium called the continuous phase. Emulsions consisting of two immiscible liquid phases are obtained homogeneously with the help of mechanical force and surfactant. Paraffin emulsions are made by homogeneously mixing together paraffin's special emulsifying agent and various additives (of the target sector) that are suitable for use with water. They can be either anionic, nonionic, or cationic. Paraffin emulsions are widely used in the concrete, plaster, fiberglass/rock wool, paper, and lumber industry. They are ease of use, liquid at room temperature, slippery, water resistant, and inflammable. According to IUPAC, emulsions consisting of water, oil and surfactants that have a particle diameter of approximately 1-100 nm and are thermodynamically stable are called nanoemulsions. In this study, it is aimed to increase the performance of our emulsions, which are used as water repellent agents, by bringing the particle size from the micro level to the nano level. In our nano emulsion, the surface area of our product is increased, thereby increasing its penetration potential into wood fibers. With this increase in penetrating capacity, the water-repellent property of wood fibers and, accordingly, their quality has increased. Thus, while the production cost of forest products is reduced, its performance is increased. With our nanoemulsion, which has a surface area increased by 300%, there has been a significant increase in export potential by providing sectoral efficiency not only in the country but also abroad.

**Key Words:** Paraffin, emulsion, nanoemulsion, forest industries, water-repellent, surface area, particle size

**References**

[1] Bernard, P. B. 1998. Modern aspects of emulsion science. The Royal Society of chemistry, pp.1-2.

[2] Li, C., Mei, Z., Liu, Q., Wang, J., Xu, J. and Sun, D., 2010. Formation and properties of paraffin wax submicron emulsions prepared by the emulsion inversion point method. Colloids and Surfaces A: Physicochemical and Engineering Aspects, 356(1-3), pp.71-77.

[3] Kale, S.N. and Deore, S.L., 2017. Emulsion micro emulsion and nano emulsion: a review. Systematic Reviews in Pharmacy, 8(1), p.39.

[4] Hielscher Ultrasound Technology. 2019. Ultrasonic Homogenizer. Erişim Tarihi: 27.10. 2019. https://www.hielscher.com/homogenize_01.htm

[5] Xuemei, H. and Hao, Y., 2013. Fabrication of polystyrene/detonation nanographite composite microspheres with the core/shell structure via pickering emulsion polymerization. Journal of Nanomaterials, 2013.

ISBN: 978-605-73552-2-5

**157-OP**

# OPTIMAL ENERGY CONSUMING ON SPRAYING AN AGRICULTURAL FIELD BY USING MULTIPLE UAVs

Alparslan GÜZEY[1,2]

[1] Econometrics Department, Faculty of Economics and Administrative Sciences, Istanbul University, Istanbul, Türkiye
[2] Technology Transfer Office, Istanbul Kültür University, Istanbul, Türkiye

## ABSTRACT

Recently, agricultural areas are decreasing day by day in the face of the constantly increasing population. As a result, it is inevitable that existing production techniques are made much more efficient. In this study, starting from this point, it was aimed to spray the spraying areas of the pre-determined targets in the agricultural land of autonomous unmanned aerial vehicles in communication with each other with time minimization. For this purpose, two scenarios were compared on how to use the drones in the stations placed in all four corners of the field in the most effective way. In the first scenario, the field is divided into four equal parts in a classical way. In the second scenario, the field was divided into 2–4 regions by using the k-means method according to the areas to be sprayed. The route that the drone will use in spraying has been analyzed using the segmental method developed for the traveling salesman problem. For calculations, Julia programming language was used. Each scenario has been examined 100 times for different number of spraying sites. In light of the results obtained, it was found that the k-means method improved the flight time by an average of 19% compared to classical segmentation. In addition, with the developed method, unnecessary flight times of drones were prevented, and their useful lives were extended by finding which stations should be used the least in different situations.

**Keywords:** Energy Optimization, Agriculture, UAVs, Sensors, Robotic

ISBN: 978-605-73552-2-5

**158-OP**

# APPLYING OF THE NEW GENERATION PLASTIC ADDITIVES TO THE KITCHEN APPLIANCES: INVESTIGATION OF STRUCTURAL AND THERMOSTATIC PROPERTIES OF ORGANOMETALLIC MN (II) AND CU (II) STREAT- BORATE COMPLEXES

Dr. İlkan KAVLAK

Br Dizayn Mobilya İnşaat ve Isıtma ve Soğutma Sistemleri A.Ş., Industrial Design Centre, Eskişehir Industrial Area, Str 14 / 2Odunpazarı / Eskişehir, Turkey.

## ABSTRACT

In this study, two new organometallic stearate complexes are described in Mn(C18H35O2)2. (B4O7) (1) and Cu(C18H35O2)2. (B4O7) (2) have been synthesized as plastic additive materials. Thermostatic behaviors of the complexes have been analyzed with described methodology at the ISO 182-2 standard. Additionally, the structural properties of the synthesized complexes were investigated by elemental analysis, powder XRD, and vibrational (FT-IR and Raman) spectroscopic techniques. The Thermostatic analyses show that synthesized complexes act as a strong HCI scavenger during plastic decomposition. If the plastic dough is composed of strong HCl scavenger agents. The heating resistance capacity will be increased. According to the thermostatic analysis results, The synthesized complexes have been added to the PVC rough as plastic additives. Then, Plasticized complexes were injected into the plastic mold. The obtained plastic materials have been used in domestic built-in hobs as thermal insulator gaskets at the burner pools. The thermally insulated behaviors of the new generation plastic additives have been observed in Elimko 32T channel probes digital thermometers and analyzed with described methodology at the TS EN 30-1-1+A3:2014 standard. The results are shown that both complexes behaved as thermal dampers on the surface of kitchen appliances. The thermal decay of the plastic doughs is following 1>2.

Acknowledgement: I am highly thankful to the Eskişehir Osmangazi University, Scientific research Unit (Project No. 2017-1588).

Additionally, thank to Prof. Dr. Güneş Süheyla Kürkçüoğlu due to provide laboratory facilities for synthesis and obtaining spectroscopic data.

Keywords: PVC, plastic additives, thermal damper, organometallic complex, EN ISI 182-2, Dehydrocholorination, HCl scavengers, EN 30-1-1+A3:2014, built-in hobs.

ISBN: 978-605-73552-2-5

**159-OP**

# All-fiber Linearly Polarized Single-Mode Q-switched $Tm^{+3}Ho^{3+}$-Doped Pulse Laser at 2.1µm

Salih Kagan KALYONCU[1, *]

[1] Electro-Optics and Laser Systems Department, TUBITAK BILGEM, Kocaeli, TURKEY

## ABSTRACT

Pulsed fiber lasers emitting at ~2 µm with possessing lesser atmospheric scattering-distortion and reduced thermal blooming, facilitates eye-safe lidar systems, range finders, free-space optical communication or countermeasures by nonlinear optical generation of mid- infrared radiation via optical parametric oscillation (OPO). For all these applications, nanosecond pulses with high peak and average output powers are required. Thanks to the advances in commercially available semiconductor laser diodes (LD) emitting at ~790 nm, multi-clad fiber technology, high quantum efficiency due to cross-relaxation and growing availability of 2 µm fiber components, Thulium ($Tm^{3+}$) doped laser and amplifier systems can be designed in all-fiber format, which provides excellent stability, robustness and reliability. Even though $Tm^{3+}$ doped fiber lasers have broad gain spectrum at 1.8-2.1 µm, to achieve emission at the far end of spectrum (> 2.05 µm), Holmium ($Ho^{3+}$) doped systems such as $Ho^{3+}$ doped fiber lasers and Ho-YAG solid state systems pumped with TDFLs are mostly favored. However, instead of bulky solid state systems, fiber lasers constitute a more practical, reliable and efficient sources with high beam quality.

Experimentally, we have demonstrated an all-fiber linearly polarized single-mode Q-switched fiber laser at 2.1 µm. With the latest developments in doped fiber technology, we employed $Tm^{3+}$-$Ho^{3+}$ co-doped PM DCF (6/130um) as a gain medium which enables broader gain spectrum up to 2.1 µm and direct cladding pumping at 790nm. To produce stable Q-switched pulses, on the other hand, we utilized a fast optical switch (FOS) based on novel opto-ceramic materials. Compared to frequently used acousto-optic modulators (AOM) with high RF power, high insertion loss (~10dB at 2 µm) and slow response (>100ns), FOS enables ultra-fast and reliable switching (<50ns) with ultra-low insertion loss (<1dB at 2 µm). We achieved ~265 µJ near-diffraction-limited pulses at 2089.3 nm with ~0.3 nm linewidth and ~100ns pulse width at 20kHz.

**Keywords:** Mid-IR Lasers, Tm-Ho co-doped fibers, Q-switching.

ISBN: 978-605-73552-2-5

**161-OP**

# STRUCTURAL AND ELECTRONIC PROPERTIES OF UNDOPED AND Be-DOPED $Ca_2TiO_4$ RUDDLESDEN POPPER PEROVSKITE

Aygün IŞIK YILDIZ[1,*], İsmail YÜCEL[2]

[1] Electronics and Automation Department, Technical Sciences Vocational School, Isparta University of Applied Sciences, Isparta, Turkey
[2] Independent Scholar, Isparta, Turkey

## ABSTRACT

$Ca_2TiO_4$ is an interesting Ruddlesden Popper Perovskite due to its characteristics of using as the cutting-edge design of optoelectronic devices. The unit cell consists of 14 atoms which are four Ca atoms, two Ti atoms and eight O atoms, respectively. Because of this, its general chemical formula is $Ca_4Ti_2O_8$. Ruddlesden Popper Perovskites are widely used as optoelectronic applications as solar cells, photodetectors, light emitting devices (LEDs). In this study, the structural and electronic properties undoped, one Be and two Be-doped $Ca_2TiO_4$ defective compound (identified in text as $Ca_3Ti_2O_8Be_1$ and $Ca_2Ti_2O_8Be_2$, respectively) are studied using The Full Potential Augmented Plane Wave Method (FP-LAPW) within The Density Functional Theory (DFT). Firstly, the calculations have been made for undoped $Ca_2TiO_4$ perovskite. The calculations show that, the a and c lattice parameter of undoped $Ca_2TiO_4$ is found 3.8558 Å and 11.9860 Å, respectively. In addition, the band length of Ti-O for undoped $Ca_2TiO_4$ is calculated as 1.9251 Å. The band gap energy of undoped $Ca_2TiO_4$ has calculated as 1.76 eV. This calculation indicates that undoped $Ca_2TiO_4$ displays semiconductor properties. In the second part of this study, lattice parameters, band gap energies, total and partial density of states of Be-doped perovskite materials are calculated. The change in band gap energy have been investigated. Be-doped perovskite materials have exhibited indirect band gap properties because the top of the valance band is at M point and the bottom of the conduction band is at Γ symmetry point. This study is the first step of our future studies about $Ca_2TiO_4$ perovskite.

**Keywords:** $Ca_2TiO_4$, Perovskite, DFT, WIEN2K, Electronic properties

ISBN: 978-605-73552-2-5

**162-OP**

## INFLUENCE OF Al DOPING ON SOME PHYSICAL PROPERTIES OF SPRAY-DEPOSITED CuO THIN FILMS

Hüseyin Ali ERKUŞ[1,*], Evren TURAN[2], Metin KUL[2]

[1] Institution of Graduate Schools, Eskişehir Technical University, Eskişehir, Türkiye
[2] Department of Physics, Faculty of Science, Eskişehir Technical University, Eskişehir, Türkiye

### ABSTRACT

Pure copper oxides (CuO) and Al doped CuO nanostructures with different concentrations (1%, 3%, 5%, 7% and 9% measured as volume percentage) were deposited on glass substrate by ultrasonic spray pyrolysis technique. The solutions were sprayed onto substrate heated at 400 °C to obtain the films. The effect of the concentration of Al doping on the structural, morphological, optical and electrical properties of the CuO nanostructures was studied. X-ray diffraction patterns revealed that all samples exhibit polycrystalline nature corresponding to monoclinic phase with preferred orientations along the (-111) and (111) planes. The crystallite size, lattice parameters, strain and dislocation density of the samples vary with the Al concentrations. The surface morphology of the pure and Al doped CuO nanoparticles were studied by FESEM analysis. The optical band gap of the pure CuO and CuO:Al films were determined from absorption spectra. The samples have exhibited direct transition with the band gap values lying between 1.48 eV and 1.61 eV. The electrical properties of the samples constructed planar structure have been measured in dark at room temperature by applying the voltage between 1 and 100 V. The room temperature resistivity, conductivity, and carrier concentration values of the samples were calculated from I–V measurements. A minimum resistivity of $3.77 \times 10^2$ Ω cm was achieved for 5 % Ag doped film and its optical band gap was 1.60 eV.

**Keywords:** Nanoparticles; CuO; Al doping; Spray pyrolysis

**164-PP**

## ROBOT GROUP INTERACTION TECHNOLOGY USING A CLOUD SERVER

Igor NEVLIUDOV[1], Shakhin OMAROV[1], Serhii TESLIUK[1],
Serhii NOVOSELOV[1], Oksana SYCHOVA[1]

[1]Department of Computer-Integrated Technologies, Automation and Mechatronics, Faculty of Automatics and Computerized Technologies, Kharkiv National University of Radio Electronics, Kharkiv, Ukraine

### ABSTRACT

This paper presents the technology of interaction of a group of robots using a cloud server. The cloud server is designed to collect information from sensors of robotic equipment and use it to build a map of the workspace for the movement of mobile robots and paving the way. The proposed technology can be combined with the robot control system. The paper gives an example of a constructed map using the sensors of a mobile robot. The method of constructing a map of the space based on the data of odometry and methods for updating previously obtained information is considered. The development of a structural diagram of the cloud storage for the construction of the map of the area was carried out. The structure of the data collection server and the algorithm of the mobile platform in the interaction with the cloud server is proposed.

**Keywords:** Lidar, ROS, odometry, cloud server.

ISBN: 978-605-73552-2-5

**165-PP**

# SUSTAINABLE HOUSING QUALITY ASSESSMENT FOR BETTER HOUSING DEVELOPMENT IN SYRIA POST-WAR

Bushra MWAKET[1,*], Assoc. Prof. Dr. Hatice KALFAOĞLU HATİPOĞLU [2]

[1] Department of Post-Disaster and Post-War Reconstruction and Rehabilitation, Graduate School of Natural and Applied Sciences Institute, AYBU University, ANKARA, TURKEY
[2] Architecture Faculty, AYBU University, ANKARA, TURKEY

## ABSTRACT

During the last decade, Syria witnessed a fierce war, causing major damage. Cities were destroyed, homes were demolished, fuel resources became rare, and the system was completely disrupted. While people are suffering and facing difficulties and challenges, the physical environment around them has also been badly affected. This paper contributes to providing knowledge about the problems experienced by the inhabitants in their accommodations and gives some recommendations that are likely to eliminate these problems, and emphasizes the need for appropriate development strategies to ensure the provision of sustainable and quality housing in Syria.

The purpose of the research is to assess the quality of residential buildings in Syria and find out the gaps, in aspects of design and construction, according to the world's contemporary norms. The assessment findings are meant to give good comprehension of the prospective enhancements in order to achieve better reconstruction.

This study depends on the deductive methodology introduced by the Sustainable Housing Quality tool, and analyzes the Syrian built environment. The results focus on listing enhancements that can be developed to lead residential buildings towards efficient environments which consider sustainability in post-war Syria.

**Keywords:** Sustainable Housing Quality, Syria Post-war.

ISBN: 978-605-73552-2-5

**167-OP**

# FLEXIBLE PRINTED STRUCTURES QUALITY MODELS FOR MOBILE ROBOT PLATFORM

Iryna ZHARIKOVA[1], Viktoriia NEVLİUDOVA[1], Olena CHALA[1]

[1] Department of Computer-Integrated Technologies, Automation and Mechatronics, Faculty of Automatics and Computerized Technologies, Kharkiv National University of Radioelectronics, Kharkiv, Ukraine

## ABSTRACT

The flexible printed structures (FPS) using is an actual trend for the development of highly reliable radio electronic devices with a high density of printed circuit elements layout. Such structures include elements of flexible electronics, flexible electronic components, printed circuits and interconnection elements. Particularly useful is the use of FPS for portable telecommunication devices, for terrestrial and satellite communication systems, military, household and medical equipment, as well as for MEMS devices design.

The replacement of rigid hardware components of mobile robot platform (MRP) with flexible ones to improve their quality, functionality, reliability and reduce weight-size parameters, manufacturing labor intensity, cost, as well as the development of tooling based on flexible structures, are currently relevant.

The main factors influencing on quality of the FPS for MRP are analyzed. Requirements for the FPS bases materials characteristics are considered. Models of mechanical, electrical and electromagnetic processes in electronic devices based on FPS are proposed. The developed models allow to predicate FPS quality level for use in the MRP design.

To automate the FPS design on the basis of the proposed models, the software "Flexible PCB Designer" was developed, with the use of which it is possible to determine many design, technological and electrical FPS parameters, in particular, the minimum allowable FPS bending radius; position of the FPS neutral line; allowable voltage drop in the printed conductor; parasitic capacitance of two parallel conductors; FPS self-capacitance and loss power; FPS interlayer capacitance; resistance of the printed conductor and others.

**Keywords:** mobile robot platform, flexible printed structures; quality model, design, production technology.

ISBN: 978-605-73552-2-5

**169-OP**

# PHYLOGENETIC ANALYSIS OF THE GENUS *JASIONE* L. (CAMPANULACEAE) IN TURKEY BASED ON CHLOROPLAST DNA MATK AND TRNL INTRON SEQUENCES

Hüseyin Atal[1], Özlem Çetin[2], Özal Güner[3], Zeki Aytaç[4]

[1]Graduate School of Natural and Applied Sciences, Selçuk University, Konya, Turkey

[2]Department of Biotechnology, Faculty of Science, Selçuk University, Konya, Turkey

Harran District Directore of National Education, Harran, Şanlıurfa, Turkey

[4]Department of Biology, Faculty of Science, Gazi University, Ankara, Turkey

The genus *Jasione* is represented by about 20 species in the world. *Jasione supina* Sieber ex. Spreng. subsp. *supina*, *Jasione supina* subsp. *akmanii* Damboldt, *Jasione supina* subsp. *tmolea* (Stoj.) Damboldt, *Jasione supina* subsp. *pontica* (Boiss.) Damboldt, *J. heldreichii* Boiss. & Orph., *J. idea* Stoj., *J. montana* L. subsp. *montana* are distributed in Turkey. The aim of the study was to understand phylogenetic relationships between *Jasione* taxa distributed in Turkey and to determine which region (matK and trnL intron) was more powerful to understand evolutionary relationships among *Jasione* species.

DNA extractions were performed using the DNeasy Plant Mini Kit (QIAGEN), following manufacturer's instructions. trnL5'-trnL3' intron and matK regions were amplified using universal primers. Alignment of the ITS sequence has been done with Bioedit software and then aligned using ClustalX with the default parameters. Then PAUP* 4.0a152 have been used to construct the phylogenetic tree. *Campanula* L., *Asyneuma* Griseb. & Schenk, *Petkovia* Stef., *Legousia* Durande and *Michauxia* L. have been used as outgroups.

Among the examined species, the length of the trnL intron ranges from 530 to 550 base pairs and matK ranges from 890 to 910 base pairs. Accumulated mutations (indel, transition, transversion) in the trnL intron and matK region were examined in detail. Some *Jasione* taxa have identical or only 1-2 base pairs differences in trnL-F sequences. For this reason the phylogenetics trees of trnL-F are not well resolved and fall on a polytomy.

ISBN: 978-605-73552-2-5

**170-OP**

# DETERMINATION OF 1-PROPANOL RATIO IN WATER WITH TWO-DIMENSIONAL PHONONIC CRYSTAL

Aysevil SALMAN DURMUŞLAR [1],*

[1] Naval Architecture and Marine Engineering Programme, Faculty of Engineering, Piri Reis University, 34940 Istanbul, Turkey

## ABSTRACT

An ultrasonic liquid sensor design is introduced to precisely detect the 1-propanol ratios in a binary mixture with water. Design is composed of water cylinders in a mercury host medium that are aligned as a square array in two dimensional phononic crystal. Linear defect waveguide is formed at the center of phononic crystal by changing the core radius of water cylinders. The samples are filled through the linear waveguide. Band structure and transmission calculations are realized through the finite element method. The optimum parameters of cylinders are decided by obtaining wide range band gap and then comparatively narrow defect mode around the center of gap. The radius of water cylinder is 7 mm and core radius is 1.5 mm, while the lattice constant is 15 mm. To achieve narrow defect mode the supercell structure is compressed on both sides of supercell about 4.5 mm. The band gap frequencies of structure lie between 31.714 kHz and 60.791 kHz. The frequency of defect mode ranges from 47.845 kHz to 50.794 kHz when filled with water. The frequency of defect mode changes with varying 1-propanol ratios inside the water. The obvious frequency shift in the band structure calculations and discrete narrow transmission peaks while the varying proponal-1 ratio into the water serves the proposed design can be used as a liquid sensor.

Keywords: Phononic crystal, liquid sensor, 1-propanol

ISBN: 978-605-73552-2-5

171-OP

# MINERALIZATION OF IRON PHOSPHATE ON CARBON NANOTUBE VIA AMPHIPHILIC PEPTIDE

Ozlem EROL[1,*], Mustafa O. GULER[2]

[1]Chemistry Department, Science Faculty, Gazi University, 06560 Ankara, Türkiye
[2]Pritzker School of Molecular Engineering, The University of Chicago, Chicago, IL 60637, USA

## ABSTRACT

Amorphous iron phosphate has received increasing attention as cathode material for rechargeable lithium-ion batteries due to its being stable, safe, cheap, and having slightly higher theoretical capacity. Due to its possessing poor ionic and electronic conductivity, its practical specific capacity value is lower than the theoretical one [1]. To improve the electrochemical performance of iron phosphate, incorporation of highly conductive carbon additives can be applied [2]. Surface modification is required to increase the interfacial interaction and contact sites between two different materials for improved overall performance. Due to its amphiphilic characteristics, peptide amphiphile (PA) molecules are good candidate for surface modification. Diverse functional groups can be appended to the PA structure for specific purposes.

In this study, short peptide amphiphile (PA) was designed and synthesized for stabilizing and non-covalent surface modification of multiwall-carbon nanotube (MWCNT) and further mineralization of iron phosphate on the MWCNT surface. In the molecular design of the PA, pyrenebutyryl-PPPEK-phosphonoacetyl-Am, pyrene moiety was used to increase the interaction between MWCNT and PA as a hydrophobic side, while phosphonoacetyl residue was substituted to the periphery of the peptide to provide direct nucleation site and growth of iron phosphate after addition of iron(III) ions. The pyrenebutyryl-PPPEK-phosphonoacetyl-Am was synthesized via solid-phase peptide synthesize method and characterized via LC-MS. The MWCNTs were first modified non-covalently with pyrenebutyryl-PPPEK-phosphonoacetyl-Am. Then, phosphonated-MWCNTs were redispersed in water and iron(III) chloride solution was added at 4°C for the iron phosphate mineralization on MWCNT. After centrifugation, the residue was redispersed and iron(III) chloride and sodium phosphate solutions were added and centrifuged subsequently. TEM analysis revealed that iron phosphate particles adhered successfully and homogeneously to MWCNTs owing to PA molecules (Figure 1). SEM-EDX analysis indicated the presence of Fe and P atoms on MWCNTs. To produce high-performance battery materials, designed PA can be used to produce more advanced battery materials in the future.

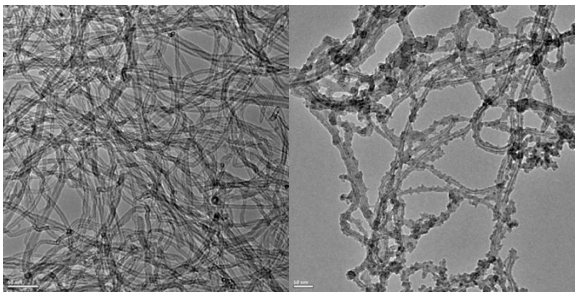

(a) (b)

Figure 1. TEM image of (a) MWCNT and (b) Iron phosphate/MWCNT

**Keywords:** Peptide amphiphile, surface modification, carbon nanotube, iron phosphate, batteries.

**References:**

[1] Wang, Z., Lu, Y., ACS Omega, 2019, 4, 14790−99.
[2] Dou, H., Niea, P., MacFarlane, D.R., J. Mater. Chem. A, 2014, 2, 19536−41.

ISBN: 978-605-73552-2-5

**172-OP**

# EFFECT OF TEMPERATURE ON MOLECULAR INTERACTIONS IN BINARY MIXTURE CONTAINING ALKYL ESTER

Manel ZAOUI – DJELLOUL DAOUADJI[1,*], Tarak MEKHELFI[2]

[1] VPRS Laboratory, Department of chemistry, Faculty of Mathematics and Matter Sciences, University of KASDI Merbah, Ouargla, Algeria
[2] VPRS Laboratory, Department of chemistry, Faculty of Mathematics and Matter Sciences, University of KASDI Merbah, Ouargla, Algeria

## ABSTRACT

Liquid mixture is formed by associating at least two solvent molecules with one another, this result in a significant effect on the intermolecular interactions because of changes in free volume, energy and molecular orientations leading to corresponding variations in the thermodynamic properties. The nature and magnitude of these variations are related to the polarity, size and shape of molecules involved in the liquid mixture. The study of thermodynamic properties such as excess molar volume, deviation in viscosity, excess free energy of activation of viscous flow, deviation in refractive index, etc. of binary liquid mixtures is useful in understanding the nature and strength of molecular interactions between the component molecules that depends on a number of factors including the molecular structure, temperature, and solvent among others.
We report here useful experimental data on density $\rho$, viscosity $\eta$ and refractive index $n_D$, for the mixture of alkyl ester with 2-alkohol in the temperature interval of 293.15-313.15 K for the liquid region and under atmospheric pressure for the whole composition range. The aim of this work is to get a better understanding of the nature of molecular orientation processes. These data have been used to calculate the excess properties, excess molar volume ($V^E$), deviation in viscosity ($\Delta\eta$), excess Gibb's free energy of activation for viscous flow ($\Delta G^{*E}$) and deviation in refractive index ($\Delta n_D$). The Redlich-Kister polynomial equation has been employed to correlate the excess properties.

**Keywords:** Density, dynamic viscosity, refractive index, excess properties, Redlich-Kister equation.

ISBN: 978-605-73552-2-5

**173-OP**

# HİDROFOBİK NANOMATERYAL OLARAK GRAFEN KATKILI POLİMER YÜZEYLERİN ÜRETİMİ

Deniz EMRE[1], İbrahim Fırat BALKAYA[2], Nevin ATALAY GENGEÇ[3,*], Numan AKDOĞAN[4], R. Zerrin YARBAY ŞAHİN[5]

[1] Kimya Mühendisliği, Fen Bilimleri Enstitüsü, Bilecik Şeyh Edebali Üniversitesi, Bilecik, Türkiye
[2] Makine Mühendisliği, Fen Bilimleri Enstitüsü, Bilecik Şeyh Edebali Üniversitesi, Bilecik, Türkiye
[3] Kimya Mühendisliği, Mühendislik Fakültesi, Bilecik Şeyh Edebali Üniversitesi, Bilecik, Türkiye
[4] Fizik, Gebze Teknik Üniversitesi, Kocaeli, Türkiye
[5] Kimya Mühendisliği, Bilecik Şeyh Edebali Üniversitesi, Bilecik, Türkiye

Grafen, %98 optik geçirgenlik, yüksek termal iletkenlik ve yüksek Young modülü gibi üstün birçok özelliklerinden dolayı sensörler, enerji dönüşümü, depolama cihazları, güneş pilleri ve güçlendirilmiş kompozitler vb. birçok farklı uygulama alanlarına sahiptir. Bu çalışmada farklı hidrofobluk ve pürüzlülük derecesinde polisitiren/Grafit Oksit (PS/GrO) ve PS/Gr kompozit yüzeyler daldırarak kaplama yöntemiyle hazırlanmış, kaygan yüzey özelliği göstermeyen yüzeylere yağ emdirilerek kaygan yüzey (SLIP) elde etme ve kendini yenileme potansiyelleri incelenmiştir. Çalışma 4 adımda gerçekleştirilmiştir: i) GrO/PS yüzeylerin sentezi: 50 mg/mL konsantrasyonlu THF ortamında hazırlanmış PS çözeltisine farklı bileşimlerde (%1-10) GrO powder ilavesi sonrasında elde edilen PS/GrO dispersiyonlarının daldırarak kaplama yöntemi ile cam lameller üzerine kaplanması ii) ilk aşamada hazırlanan PS/GrO dispersiyonlarına bulanma noktası öncesine kadar EtOH ilavesi ile hidrofobluk ve pürüzlülük dereceleri farklı PS/GrO yüzeylerin üretimi iii) birinci ve ikinci aşamada üretilen yüzeylerin Hidroiyodik asit/Asetik asit (HI/Ac) karşımında 1 gün 40 ºC'de bekletilmesi ile indirgenmesi sonucunda Gr/PS yüzeylerin elde edilmesi ve iv) indirgenen yüzeylerin silikon yağı ile yağlanması sonucunda SLIP yüzeylerin üretimi. Çalışmada hazırlanan dispersiyonların yapısal ve kimyasal özelliklerinin belirlenmesi için FTIR ve XRD analizleri, yüzey morfolojilerinin belirlenmesi için optik mikroskop ve SEM görüntüleri, yüzey hidrofobluk derecelerinin belirlenmesi için Temas açısı ölçümleri gerçekleştirilmiştir. Bu incelemeler sonucunda farklı hidrofobluk, pürüzlülük ve kayganlık derecesinde grafit oksit katkılı PS yüzeyler elde edilmiştir. Sonuç olarak EtOH ilavesinin PS/GrO yüzeylerinin pürüzlülük ve hidrofobluk derecesinin kontrolü için kritik olduğu, yüzeylerin kontrollü pattern şeklinde pürüzlülük oluşumuna neden olduğu belirlenmiştir. Yüzeylerin grafene indirgenmesi sonucunda beklendiği üzere temas açılarının arttığı ancak grafen nono-powderların sürekli olarak yüzeyde dağılmamasından kaynaklı iletkenliklerinde değişim olmadığı belirlenmiştir. GrO/PS ve Gr/PS yüzeylerinin yağlanmadan önce kaygan değilken, yağlama sonrasında kaygan yüzeylerin elde edildiği ve kaygan yüzeylere çizik atıldığında yüzeyin kendini onardığı belirlenmiştir.

Anahtar Kelimeler: Grafen(Gr), Grafen Oksit(GrO), Polistiren (PS), SLIP Yüzey

ISBN: 978-605-73552-2-5

**174-PP**

# DIOPSIDE CERAMIC PIGMENTS OBTAINED BY A SOL-GEL METHOD: SYNTHESIS, STRUCTURE AND PROPERTIES

Miluvka STANCHEVA[1], Rositsa TITORENKOVA[2], Tsvetan DIMITROV[1,*], Tsvetalina IBREVA[1]

[1]University of Ruse "Angel Kanchev", Branch Razgrad, Bulgaria
[2] Institute of Mineralogy and Crystallography "Acad. I. Kostov", Bulgarian Academy of Sciences, Sofia

## ABSTRACT

The sol-gel method is used for the synthesis of diopside ($CaMgSi_2O_6$) ceramic pigments doped with cobalt, iron, nickel and manganese ions. Pure grade raw materials such as TEOS - $Si(OC_2H_5)_4$ and nitrates of $Ca^{2+}$, $Mg^{2+}$, $Co^{2+}$, $Fe^{2+}$, $Ni^{2+}$ and $Mn^{2+}$ have been used for the synthesis. The aim of this study was to obtain isomorphic substituted diopside based ceramic pigments.
Series of ceramic pigments in the system $CaO.MgO.MeO.2SiO_2$ (Me= $Co^{2+}$, $Fe^{2+}$, $Ni^{2+}$, $Mn^{2+}$) were synthesized via sol-gel method and sintering at 800, 900, 1000, 1100 and 1200°C. The resulting ceramic pigments were studied by powder X-ray diffraction, infrared spectroscopy, electron microscopy, electron paramagnetic resonance.
The ceramics obtained by sol-gel method mainly contain diopside, which crystallizes even at 800°C. Small amounts of additional phases depend on the type of metal ion and the sintering temperature. The effect of the metal ions, their concentration and the sintering temperature on the phase composition and the formation of additional phases, on the diopside structure, and on the color of the obtained ceramics was investigated. The color of the ceramics is determined and presented with color coordinates. The best pigments have been added to white faience glaze and tested as a pigment for sanitary ceramics.

**Keywords:** pigments, ceramic, diopside, sol-gel, color

**Acknowledgements:** The financial support of this work by the Bulgarian Ministry of Education and Science, National Research Fund under the contract number KP-06-H47/10 - 2020 is gratefully acknowledged.

ISBN: 978-605-73552-2-5

**175-PP**

# SYNTHESIS AND CHARACTERIZATION OF Cr-DOPED DIOPSIDE CERAMIC PIGMENTS

Tsvetan DIMITROV[1,*], Yana Tzvetanova[2], Rositsa TITORENKOVA[2]

[1] University of Ruse "Angel Kanchev", Branch Razgrad, Bulgaria
[2] Institute of Mineralogy and Crystallography "Acad. I. Kostov", Bulgarian Academy of Sciences, Sofia, Bulgaria

## ABSTRACT

Ceramic pigments are inorganic substances consisting of crystalline ceramic matrix and a chromophore element that provides the color. These ceramic materials should exhibit certain properties such as thermal stability, insolubility in the glazes, high resistance to chemical and physical agents, high color intensity, cover ability, light stability and have to be acceptable to the production technology.
Diopside ($CaMgSi_2O_6$) is a widespread colorless mineral of pyroxene group. The color of the most natural and synthetic minerals is associated with the presence of transitional metals incorporated in the crystal structure, which have unfilled d- or f-electron orbital determining the electronic transition under the action of light energy.
A series of ceramic pigments in the system $CaO.Cr_2O_3.MgO.2SiO_2$ was synthesized via solid-state high temperature sintering at 1000, 1100 and 1200°C. The resulting ceramic pigments were examined by powder X-ray diffraction, infrared spectroscopy, electron microscopy, electron paramagnetic resonance. The color characteristics were measured spectrophotometrically.
It was found that under the synthesis conditions multiphase ceramic pigments were obtained which contain diopside, wollastonite, Mg – chromite, cristobalite, tridimite and periclase in various proportion.
The synthesized ceramic pigments are gray, gray-green and green in color, depending on the content of Cr additive, temperature of furnace and phase composition. Synthesized pigments can be used for staining of ceramic glazes.

**Keywords:** pigments, ceramic, diopside, mineral composition, colorimetric indices.

**Acknowledgements:** The financial support of this work by the Bulgarian Ministry of Education and Science, National Research Fund under the contract number KP-06-H47/10 - 2020 is gratefully acknowledged.

ISBN: 978-605-73552-2-5

**177-OP**

# SUSTAINABILITY PRACTICES IN VOCATIONAL EDUCATION: GREEN BUILDINGS

Emre Aytuğ ÖZSOY[1, *]

[1] Building Inspection Program, Porsuk Vocational School, Eskisehir Technical University, Eskisehir, TURKEY

## ABSTRACT

The construction sector has a critical importance in terms of increasing the competitiveness of Turkey and making the development sustainable. According to the Sustainable Development Report, the construction sector in Turkey is a sector with a high multiplier effect.

In addition to the added value created, the employment opportunities provided with its sub-sectors caused the sector to be one of the locomotives of the economy. However, approximately 35% of the total sectoral energy consumption in Turkey belongs to buildings. In addition, buildings affect the environment in terms of water consumption, solid waste generation and land use. On the other hand, the construction sector also contains opportunities that can reduce the pressures on the environment in terms of resource use and pollution created due to both the inputs (cement, iron-steel, land, etc.) and outputs (buildings, roads, power plants, etc.).

Environmentally friendly, green buildings constitute an important area of opportunity in the transition to green growth, especially energy efficiency and use of renewable energy. For this reason, the professional skills of construction technicians or building inspection technicians and their training are of great importance in the construction of green buildings. In this study, the training and positive-negative aspects of the building inspection technicians who will work in green jobs in vocational education were examined and solutions were suggested.

**Keywords:** Green Buildings, Vocational Education, Sustainability, Building Inspection.

ISBN: 978-605-73552-2-5

179-OP

# FLEXIBLE PRINTED STRUCTURES QUALITY MODELS FOR MOBILE ROBOT PLATFORM

Iryna ZHARIKOVA[1], Viktoriia NEVLİUDOVA[1], Olena CHALA[1]

[1] Department of Computer-Integrated Technologies, Automation and Mechatronics, Faculty of Automatics and Computerized Technologies, Kharkiv National University of Radioelectronics, Kharkiv, Ukraine

## ABSTRACT

The flexible printed structures (FPS) using is an actual trend for the development of highly reliable radio electronic devices with a high density of printed circuit elements layout. Such structures include elements of flexible electronics, flexible electronic components, printed circuits and interconnection elements. Particularly useful is the use of FPS for portable telecommunication devices, for terrestrial and satellite communication systems, military, household and medical equipment, as well as for MEMS devices design.

The replacement of rigid hardware components of mobile robot platform (MRP) with flexible ones to improve their quality, functionality, reliability and reduce weight-size parameters, manufacturing labor intensity, cost, as well as the development of tooling based on flexible structures, are currently relevant.

The main factors influencing on quality of the FPS for MRP are analyzed. Requirements for the FPS bases materials characteristics are considered. Models of mechanical, electrical and electromagnetic processes in electronic devices based on FPS are proposed. The developed models allow to predicate FPS quality level for use in the MRP design.

To automate the FPS design on the basis of the proposed models, the software "Flexible PCB Designer" was developed, with the use of which it is possible to determine many design, technological and electrical FPS parameters, in particular, the minimum allowable FPS bending radius; position of the FPS neutral line; allowable voltage drop in the printed conductor; parasitic capacitance of two parallel conductors; FPS self-capacitance and loss power; FPS interlayer capacitance; resistance of the printed conductor and others.

**Keywords:** mobile robot platform, flexible printed structures; quality model, design, production technology.

ISBN: 978-605-73552-2-5

**180-OP**

# DETECTION AND IDENTIFICATION OF POTENTIALLY EXPLOSIVE OBJECTS IN OPEN AREA

Igor NEVLİUDOV[1] , Murad Omarov[2] , Ivan PAKHNYTS[1] ,
Sofiia KHRUSTALOVA[1] , Kirill KHRUSTALEV[1] , Olena CHALA[1]

[1] Department of Computer-Integrated Technologies, Automation and Mechatronics, Faculty of Automatics and Computerized
Technologies, Kharkiv National University of Radioelectronics, Kharkiv, Ukraine
[2] Vice-Rector on International Cooperation, Kharkiv National University of Radio Electronics, Kharkiv, Ukraine

## ABSTRACT

The subject of this research is the methods, means and systems for detecting potentially dangerous military objects in open terrain. The purpose of the study is to develop a system for the detection and identification of potentially explosive military objects using an unmanned aerial vehicle (drone), which includes a system for detecting an explosive object using a metal detector with the technology of adjusting the flight height and the detection method using a thermal imager. To achieve the goal, the following tasks were solved: a review and analysis of modern methods and systems for the detection and identification of potentially explosive military objects was carried out, the classification of identifiable explosive objects was determined, system components were selected, a structural diagram and an algorithm of the software control tool were developed system of identification of potentially explosive objects in an open area, a software tool for detection and identification of potentially explosive objects in an open area was created. The following methods are used in the work: the mathematical method of constructing cartographic grids, the method of recording infrared radiation, the method of eddy currents, methods and means of data collection and processing. The following results were obtained: the components of the system were selected, the structure, diagram and algorithm of the software tool for the identification of potentially explosive objects in the open area were developed, and the corresponding software was created. Conclusions: the application of the proposed system makes it possible to increase the accuracy of finding or the absence of a potentially explosive object in a certain area due to the use of two methods of detecting potentially explosive objects at once, and provides the opportunity to identify a sufficiently wide range of objects. The developed system is safe, as it is controlled by an operator who is at a safe distance, allows you to get special maps with terrain markings with information about the possible presence of potentially explosive objects in certain areas of the terrain and, in general, maps of metal detector and thermal imager signals

Keywords: explosive object; mine; drone; thermal imager; metal detector.

ISBN: 978-605-73552-2-5

**181-OP**

# BİLİMİN YAYGINLAŞTIRILMASINDA MEDYANIN ROLÜ

Tuba HAS*

* Basın Yayın, İletişim Bilimleri, Anadolu Üniversitesi, Eskişehir, Türkiye

## ÖZET

Orta Çağ'ın skolastik yapılanmasından doğan Aydınlanma felsefesi ile beraber bilimsel bilginin toplumun her alanında egemen bir ideoloji haline geldiğini söylememiz yanlış olmayacaktır. Farklı bir ifade ile Aydınlanma felsefesini, Ortaçağ'ın karanlığından sıyrılıp, aklın artık bir ideolojinin muhafızı olmaktansa kendisinin bizzat kullanılmaya başlandığı dönem olarak da nitelendirilebilir.

Bununla beraber dünya üzerindeki değişimler ve yaşanan teknolojik gelişmeler ışığında bilimsel ve teknik alandaki ilerlemeler bilimin sunumunu da kendisi kadar önemli bir noktaya getirmiştir. Bu bağlamda medya içeriklerinde yer alan bilim haberlerinde de doğru orantıda artış yaşanması doğal olarak karşımıza çıkmaktadır.

Bu açıdan bakıldığında, kabaca bilim insanları, politikacılar, medya ve halkla bilimsel bilginin alışverişi ve paylaşımı olarak tanımlanan bilim iletişimi, giderek daha önemli bir konu haline gelmeye başlamıştır. Bu bağlamda çalışmada bilim iletişimini ve kitle iletişim mecralarındaki sunumlarının irdelenmeye çalışılmış olup bilim haberciliği, bilim iletişimi ve medyada bilim haberlerinin doğru yorumlanması ihtiyacı ışığında bu konuyla ilgili teorik ve vaka çalışmaları ile çeşitli başlıklar altında sunulmuştur.

**Anahtar Kelimeler:** Bilim, Bilim İletişimi, Medya, Kitle İletişim, Bilim Haberciliği

* thas.anadolu.edu.tr, Orcid: 0000-0001-6132-5261

ISBN: 978-605-73552-2-5

**ICONAT 2022**

# PROCEEDINGS
# OF
# ICONAT 2022

ISBN: 978-605-73552-2-5

## CONTENTS

ISBN: 978-605-73552-2-5

# MATHEMATICAL ANALYSIS OF THE 09 MARCH 2012 INTENSE AND 08 MAY 2014 WEAK STORM

Kevser Koklu

Yildiz Technical University, Department of Mathematical Engineering, Davutpasa Campus, İstanbul, 34220, Turkey,
ozkoklu@yildiz.edu.tr, kevserkoklu@gmail.com

**Abstract**
The sun is an inherent source that continually creates energy with its active system. The in-depth investigation of the solar wind parameters (E, v, P, T, N, $B_z$) and the zonal geomagnetic indices (Kp, Dst, AE, ap) is the key space for weather research and is in the center of relationship to the sun and earth. The investigations gain meaning by modeling various interplanetary parameters and geomagnetic indices. These models, built on the basis of the correlations between solar wind parameters and zonal geomagnetic indices, and that must strictly obey physical principles, will not only reveal the properties of geomagnetic activity but also allow estimates of their formations. In a severe storm, which usually has two main phases, solar parameters have enough time to react, but weak storms cannot find this time. They have to yield their reaction in a short time. Since the time scale of weak storms is about half the time scale of intense storms, it is troublesome and important to examine the solar wind parameters/Interplanetary Magnetic fields to evolve and affect zonal geomagnetic indices. One can find a weak (Dst=-46) on May 08, 2014, and an intense (Dst=-145 nT) storm on March 09, 2012, in order to reveal, examine the consistency of discussions and compare models that have proven themselves in previous storms in this study. The author tries to think over all possible correlations between solar wind parameters and zonal geomagnetic indices and obey the cause-effect relationship while creating mathematical models while not ignoring the physical principles. Therefore, the physical principles govern the study. The results visualize with tables and graphs for the understanding of the dynamic structure of the storm. In the paper, comparisons are made between two different storms and the reader is able to comment on them.

**Keywords:** Zonal geomagnetic indices, solar wind parameters, mathematical modeling

## 1 Introduction

The complex effect of the sun on the earth which is known since ancient times contributes to understanding the solar-earth relationship by examining and modeling data from the sun (Hanslmeier 2007). Underneath this complex effect, there is a dynamic structure (Gonzales et al. 1994; Stern 1996; Saba et al. 1997; Gonzales et al. 1999) in which each variable has its own set of adjustments. Non-Functional variables have no place in events that happened in the universe. Among the existing variables in the dynamic structures, the order of magnitude is in the order of importance. While large variables determine the future of the event, small ones can control the larger ones. If large ones are not tightly controlled by the small variables, the result will be chaos. To understand the behavior of dynamic structures, the correlation between the variables should be analyzed well by obeying the physical principles. The established models based on the analysis of the relationship are going to facilitate the prediction of future events. A geomagnetic storm with the dynamics of the cause-and-effect relationship usually consists of three stages: it starts suddenly, continues with the main phase and ends with recovery (Akasofu 1964; Burton et al. 1975).

Well-posedness identification of repeated natural phenomena, such as geomagnetic storms, can help to reveal some unknown properties of their dynamics. A geomagnetic storm, also called a magnetic storm or storm, is a typical phenomenon covering all magnetosphere from Earth's surface to magnetotail, which lasts for 1-3 days. In a geomagnetic storm, the cause-effect connection and the causality principle (Eroglu 2011; Eroglu 2012a; 2012b; 2018; 2019) are physically restrictive. The solar wind plasma parameters of the phenomenon; the electric field (E), the flow velocity (v), the solar wind dynamic pressure (P), the temperature (T), the proton density (N), and the magnetic field ($B_z$) are the "causes". Kp, ap, Dst, and AE, the zonal geomagnetic indices of the storm, are the "effects". Dst (Disturbance Storm Time) is a geomagnetic index that confirms the magnitude of the geomagnetic storms that cover the earth. It is the average of the horizontal component of the geomagnetic field obtained from stations in different geographical regions of the world. Kp (planetary index) is obtained by a weighted average of K indexes in 13 sub-auroral observations. A

ISBN: 978-605-73552-2-5

linear index obtained from ap, Kp. The AE index is a snapshot general index as a measure of changes in global Auroral Electrojet activity as defined by Davis and Sugiura (1966). If one is trying to unclose scholarly consequence about geomagnetic storms, he should show the correlation between zonal geomagnetic indices and solar wind parameters. This relationship must be fit to the physical essentials. The zonal geomagnetic indicators have been used since former times (Mayaud 1980; Fu et al. 2010a; 2010b). The storm that begins with to the magnetosphere effect (Ngwira et al. 2018) of large solar plasma clouds (coronal mass ejection (CME)) at an average speed of 800 km/s, leaves its site to describe the magnetic action indicators determining the reaction of the geomagnetic storm. Zonal geomagnetic indices are magnetic indicators of a geomagnetic storm (Hanslmeier 2007, Mayaud 1980, Kamide et al. 1998). In this study, hourly measurements of AE and Kp indices are used.

Solar wind parameters and zonal geomagnetic indices are the main elements of the dynamic structure of the storm. This plasma-dense dynamic medium has energy-charged particles that flow out at high speeds from the sun (Parker 1958). Such an intense dynamic structure causes rapid changes in the magnetic field of the sun's plasma-intensive environment. The CME cloud swallows the earth's magnetosphere. Meanwhile, the $B_z$ component of the B magnetic field of CME cloud is negatively charged to the southward. Geomagnetic disturbances occur with magnetic reconnection (Lin and Forbes 2000; Fu et al. 2017) between this component and the earth's magnetic field. The CME causes direct solar wind parameters to change and then the storm process begins (Gonzalez et al. 1999; Kamide et al. 1998). Today, the models among zonal geomagnetic indicators and solar wind parameters are still in use. Various models (Burton et al. 1975; Maruyama 1982; Zhao et al. 2011; Adebesin et al. 2012; Adebesin et al. 2013; Zuo et al. 2015) between parameters and indices are frequently used to understand the storm. These applications are also modeling for the weather forecast (Rathore et al. 2014; 2015). Binary linear models may have hardship in discussing the relationship among variables. However, the introducing of these models is substantial (Eroglu 2018; 2019; Koklu 2020). Weak correlation should lead authors to look for nonlinear models.

In order to discuss the dynamic structure of the storm, it is necessary to establish models by looking at the relationships between the variables and to keep the consistency of these correlations. The mathematical models can guide researchers about data and their relationships whichever in the science area (Eroglu, 2018; 2020; 2021; Koklu, 2020; 2021; 2022). In addition, they may yield clues about the behavior of the variables under different terms (Eroglu et al. 2012b; Celebi et al. 2014; Isik et al. 2014; Eroglu 2018; 2019; 2021). While the storm of May 08, 2014, is one of the weakest storms of the 24$^{th}$ solar cycle, the storm of March 09, 2012, is the first severe storm at the beginning of the same cycle. Therefore, the paper focuses on these weak and intense geomagnetic storms (Sato and Kuwano. 2015; Ngwira et al. 2018; Singh et al. 2018; Habarulema et al. 2018).

In this study, the models established with the deterministic and pragmatic approach of Eroglu (2018, 2019) for geomagnetic storms are discussed for a weak phenomenon for the first time. In addition to this weak event, the March intense storm also offers to opportunity the reader a serious comparison. In all of the analyzes, two storms are handled separately but are exhibited together. The value of minimum-maximum, averages and standard deviations of ten different variables are introduced and the strength of the binary correlations is presented. Hierarchical structures are expressed by cluster analysis, and models and percentages of events are explained. After checking the homogeneity of the distribution of the data and discussing the clusters, linear models with the cause-effect relationship are proposed. Finally, the result section is reached with the visualized variables and nonlinear models (Eroglu, 2018; 2019; Inyurt, 2019; Koklu 2020). The formulated models are exact dependent on the stochastic processes.

## 2. Data

IDL-Based data is utilized from Space Physics Environment Data Analysis Software (SPEDAS) (http://themis.igpp.ucla.edu/software.shtml). OMNI-2 Solar Wind and IMF parameter data are used hourly. Also, the AE and Dst indices are engaged from the World Data Center for Geomagnetism Kyoto by using SPEDAS. Kp, ap are taken from NGDC by using SPEDAS with CDA Web Data Chooser (space physics public data). Geomagnetic classification (Loewe and Prölss 1997) is in the below Table 1.

ISBN: 978-605-73552-2-5

**Table 1.** Geomagnetic storm Dst index

| CLASS | NUMBER | % | DST RANGE (NT) |
|---|---|---|---|
| WEAK | 482 | 44 | -30 - -50 |
| MODERATE | 346 | 32 | -50 - -100 |
| STRONG (I.E., INTENSE) | 206 | 19 | -100 - -200 |
| SEVERE (VERY-INTENSE) | 45 | 4 | -200 - -350 |
| GREAT | 6 | 1 | < -350 |

The representative storms at the weak (Dst=-46 nT) and strong level (Dst=-145 nT) dated 2014 May 08 and 2012 March 09 has been investigated, respectively. Figure 1 shows the OMNI data set from 00:00 UT on 06 May 2014 to 00:00 UT on 10 May 2014 and 00 UT 2012.03.07 to 00 UT 2012.03.11. The interval covers the storm's main phase, two days before and two days after the storm (120 hours).

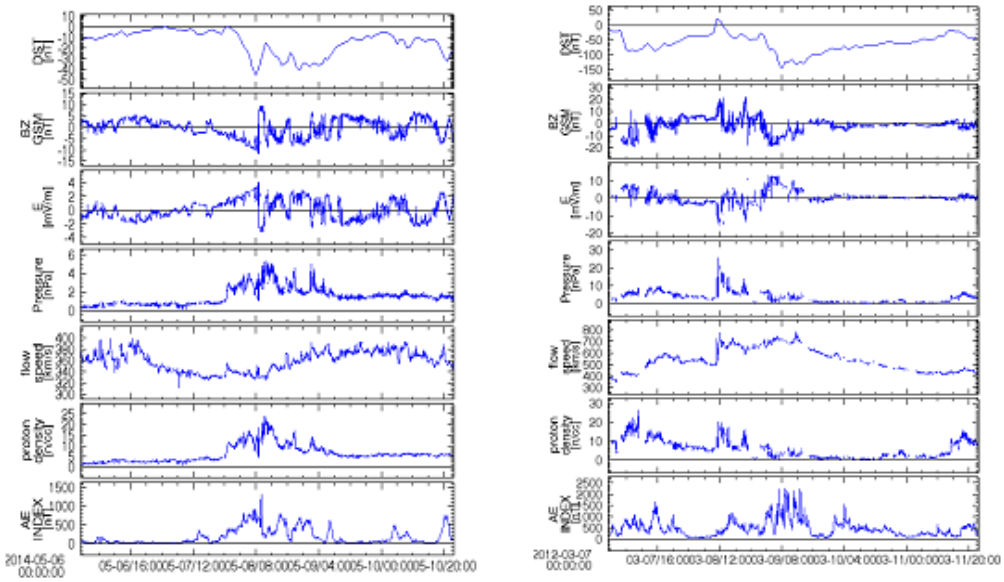


**Figure 1.** From top the bottom parameters shown in Dst index, $B_z$ magnetic field (nT), E electric field (mV/m), solar wind dynamic pressure P (nPa), flow speed v (km/s), proton density N ($cm^3$), and auroral electrojet AE (nT) index for 2014 May 06-10 and 2012 March 07-11, respectively (from NASA NSSDC OMNI data set).

ISBN: 978-605-73552-2-5

The characteristic of the phenomenon at the weak level (Dst=-46 nT) on 08 May 2014 have been investigated. In Figure 1 has been demonstrated the OMNI data set from 00:00 UT on 06 May 2014 to 00:00 UT on 10 May 2014. The plot interval includes the storm day (2014 May 08), two days before and two days after the storm (120 hours). The May storm started on May 08th with CME at 06:00 UT, May 08. The gradually decreasing magnetic field component ($B_z$) reaches the negative peak value -9.2 nT at 07:00 UT. Meanwhile, as the plasma flow speed (v) catches 329 km/s its maximum value, the electric field (E) reaches 3.03 mV/m it's maximum value and the geomagnetic auroral electrojet index (AE) raises to its maximum value of 767 nT. Finally, Dst hits its peak value of -46 nT at 08:00 UT.

Figure 1 can be shortly detailed as follows. On 06.05.2014 at 07:00 UT when the $B_z$ component is at its minimum (-9.2 nT), the Dst index dwindled to -39 nT, the electric field E attains to its maximum value of 3.03 mV/m. Meantime, plasma flow speed v its minimum value becomes 329 km/s, the AE index catches its peak value 767 nT. Within a few hours, the Dst index indicates its minimum value -46 nT, ap index hits its maximum value 39 nT, proton density N reaches its peak value of 21.5 1/cm3.

On 09.05.2014 at 11:00 UT when the $B_z$ component is maximum (6 nT), the electric field E catches -2.25 mV/m, proton density N takes 6.3 1/cm3, AE index diminishes to 69 nT and ap index decreases to 4 nT. As this comes to cross Dst index reaches -10 nT.

The components of Figure 1 can be briefly described as follows. On 2012.03.09 at 08.00 (UT) when Dst is minimum (-145 nT), the $B_z$ component rises to -10.6 nT, the electric field E catches to 7.56 mV/m by decreasing. Meanwhile, the ap index reaches its maximum value 207 nT by increasing, proton density N is 3.2 cm-3, plasma flow speed v one of the maximum values becomes 713 km/s, AE index gets 1109 nT. An hour after the storm peaks, the AE index at 09.00 (UT) takes its own maximum value of 1785 nT.

On 2012.03.09 at 05.00 (UT) when the $B_z$ component is minimum (-16.5 nT), the Dst index endures to diminution towards the minimum, the electric field E takes its maximum value of 11.71 mV/m and plasma beta β takes its minimum value of 0.06.

On 2012.03.08 at 20.00 (UT) when the $B_z$ component is maximum (16.5 nT), the electric field E catches to its minimum value -10.13 mV/m, the ap index continues to increase. Dst index, $B_z$ component 9 hours before reaching maximum (at 11.00 UT) takes the maximum value, continues to decrease to the minimum.

When the Dst index reaches its maximum value (22 nT) in 2012.03.08 at 11.00 (UT), $B_z$ component reaches a value close to maximum, such as 14.1 nT, the electric field E takes a value close to the minimum value of -9.88 mV/m and plasma flow speed v increases to 701 km/s value.

## 3. Mathematical Modeling

The Test of KMO and Bartlett in Table 2 helps to understand the suitability of variables for factor analysis. The closeness of the result to one (1) indicates normally distributed data. As shown in Table 2, the variables of these storms are suitable for factor analysis.

**Table 2.** KMO and Bartlett's Test

| | | 08.05 Weak | 09.03 Intense |
|---|---|---|---|
| Kaiser-Meyer-Olkin Measure of Sampling Adequacy. | | **.731** | **.665** |
| Bartlett's Test of Sphericity | Approx. Chi-Square | 2144.413 | 1500.574 |
| | Df | 45 | 45 |
| | Sig. | .000 | .000 |

ISBN: 978-605-73552-2-5

Variables cluster is displayed in Figure 2 hierarchically.

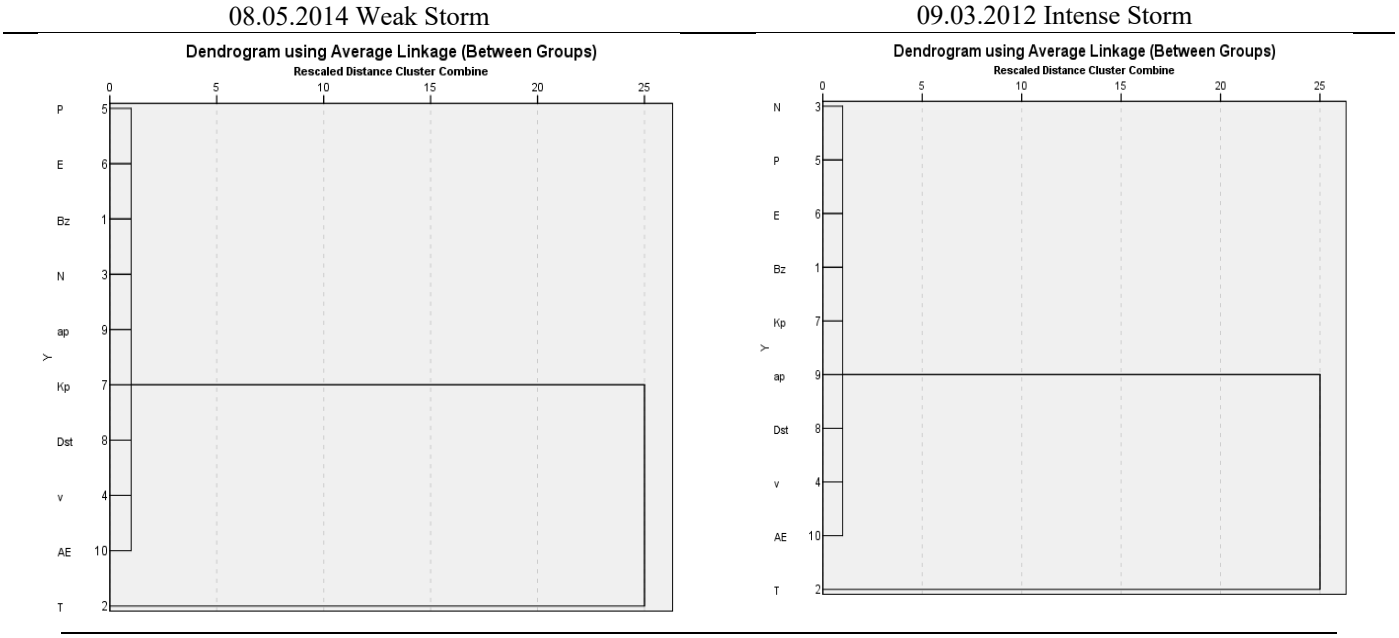


**Figure 2.** Dendrogram of hierarchical cluster analysis.

Principal Component Analysis aid to separate data into subgroups. The maximum eigenvalues that allow the discussion of the events from these subgroups are clustered.

Trying to catch an overview with the general linear models will aid to better understand the storm form. In Table 3, 4, 5, linear models of Dst, ap and AE indices generate by solar wind parameters. The regression coefficients of the models resulting from the analysis describe the significance of the relationships.

**Table 3.** Anova (Analysis of variance)

| | 08.05.2014 Weak Storm | | | | | 09.03.2012 Intense Storm | | | | |
|---|---|---|---|---|---|---|---|---|---|---|
| Model | Sum of Squares | Df | Mean Square | F | Sig. | Sum of Squares | df | Mean Square | F | Sig. |
| Regression | 9970.000 | 3 | 3323.333 | 65.667 | .000 | 56344.589 | 3 | 18781.530 | 36.283 | .000 |
| Residual | 5870.667 | 116 | 50.609 | | | 60046.403 | 116 | 517.641 | | |
| Total | 15840.667 | 119 | | | | 116390.992 | 119 | | | |

Table 4 shows the linear models of Dst.

$$\text{Dst}=(4.501)-(4.597)\text{P}+(1.123)B_z+(0.001)\text{T}, \text{(Weak storm)}$$

$$\text{Dst}=(20.469)-(3.339)\text{E}-(0.159)\text{v}+(0.0005)\text{T}, \text{(Intense storm)}$$

where multiple determination coefficient R is 0.793 and 0.696, respectively.

ISBN: 978-605-73552-2-5

**Table 4.** Regression coefficients

| 08.05.2014 Weak Storm | | | | | | 09.03.2012 Intense Storm | | | | | |
|---|---|---|---|---|---|---|---|---|---|---|---|
| Model | Unstandardized Coefficients | | Standardized Coefficients | t | Sig. | Model | Unstandardized Coefficients | | Standardized Coefficients | t | Sig. |
| | B | Std. Error | Beta | | | | B | Std. Error | Beta | | |
| (Constant) | 4.501 | 1.639 | | 2.747 | .007 | (Constant) | 20.469 | 12.083 | | 1.694 | .039 |
| P(nPa) | -4.597 | 0.835 | -.364 | -5.503 | .000 | E(mV/m) | -3.339 | .677 | -.350 | -4.933 | .000 |
| $B_z$(nT) | 1.123 | .217 | .345 | -5.171 | .000 | v(km/s) | -.159 | .023 | -.516 | -6.793 | .000 |
| T(K) | .001 | .000 | -.529 | 8.629 | .000 | T(K) | $5.02x10^{-5}$ | .000 | .417 | 5.320 | .000 |

Table 5 indicates that the model is significant, while Table 6 shows that the ap index is:

$$ap = -(0.352) + (1.801)E + (1.231)N, \text{ (Weak storm)}$$

$$ap = -(79.823) + (7.299)E + (0.206)v, \text{ (Intense storm)}$$

where multiple determination coefficient R is 0.766 and 0.787, respectively.

**Table 5.** Anova (Analysis of variance)

| 08.05.2014 Weak Storm | | | | | | 09.03.2012 Intense Storm | | | | |
|---|---|---|---|---|---|---|---|---|---|---|
| Model | Sum of Squares | df | Mean Square | F | Sig. | Sum of Squares | df | Mean Square | F | Sig. |
| Regression | 4898.758 | 2 | 2449.379 | 83.198 | .000 | 130851.875 | 2 | 65425.938 | 95.001 | .000 |
| Residual | 3444.542 | 117 | 29.441 | | | 80576.050 | 117 | 688.684 | | |
| Total | 8343.300 | 119 | | | | 211427.925 | 119 | | | |

**Table 6.** Regression coefficients

| 08.05.2014 Weak Storm | | | | | 09.03.2012 Intense Storm | | | | |
|---|---|---|---|---|---|---|---|---|---|
| Model | Unstandardized | Standardized Coefficients | t | Sig. | Model | Unstandardized | Standardized Coefficients | t | Sig. |

ISBN: 978-605-73552-2-5

| | Coefficients | | | | | | Coefficients | | | | |
|---|---|---|---|---|---|---|---|---|---|---|---|
| | B | Std. Error | Beta | | | | B | Std. Error | Beta | | |
| (Constant) | -.352 | .981 | | -.359 | .007 | (Constant) | -79.823 | 13.057 | | -6.114 | .000 |
| E(mV/m) | 1.801 | .441 | .272 | 4.086 | .000 | E(mV/m) | 7.299 | .736 | .568 | 9.911 | .000 |
| N(1/cm$^3$) | 1.231 | .136 | .604 | 9.068 | .000 | v(km/s) | .206 | .024 | .498 | 8.685 | .000 |

Table 7 shows that the model is significant, while Table 8 shows that the AE index is:

$$AE = (58.028) - (33.471)B_z + (18.990)N, \text{ (Weak storm)}$$

$$AE = -(381.820) + (55.840)E + (1.479)v, \text{ (Intense)}$$

where multiple determination coefficient R is 0.816 and 0.740, respectively.

**Table 7.** Anova (Analysis of variance)

| | 08.05.2014 Weak Storm | | | | | 09.03.2012 Intense Storm | | | | |
|---|---|---|---|---|---|---|---|---|---|---|
| Model | Sum of Squares | df | Mean Square | F | Sig. | Sum of Squares | df | Mean Square | F | Sig. |
| Regression | 3399775.034 | 2 | 1699887.517 | 116.999 | .000 | 7247973.552 | 2 | 3623986.776 | 70.940 | .000 |
| Residual | 1699904.558 | 117 | 14529.099 | | | 5977008.814 | 117 | 51085.545 | | |
| Total | 5099679.592 | 119 | | | | 13224982.37 | 119 | | | |

**Table 8.** Regression coefficients

| | 08.05.2014 Weak Storm | | | | | 09.03.2012 Intense Storm | | | | |
|---|---|---|---|---|---|---|---|---|---|---|
| Model | Unstandardized Coefficients | | Standardized Coefficients | t | Sig. | Model | Unstandardized Coefficients | | Standardized Coefficients | t | Sig. |
| | B | Std. Error | Beta | | | | B | Std. Error | Beta | | |
| (Constant) | 58.028 | 21.751 | | 2.668 | .009 | (Constant) | -381.820 | 112.453 | | -3.395 | .001 |
| $B_z$(nT) | -33.471 | 3.510 | -.572 | -9.536 | .000 | E(mV/m) | 55.840 | 6.343 | .549 | 8.803 | .000 |
| N(1/cm$^3$) | 18.990 | 3.026 | .377 | 6.275 | .000 | v(km/s) | 1.479 | .205 | .451 | 7.230 | .000 |

ISBN: 978-605-73552-2-5

For many years, $B_z$-Dst linear relationship has been an important part of the researchers' discussions (Gilmour et al. 2002). In addition to these discussions, the author offers the reader to the visualize relationship between the Dst, ap and AE indices and $B_z$ magnetic field. Thus, the linear or nonlinear correlation will be understood more clearly. Figures 3a and 3b visualize the physical scattering of zonal geomagnetic indices (Dst, ap, AE) according to solar wind parameters (just $B_z$). In this paper, the solar wind propagation time from bow shock to Earth doesn't take into account when they use Dst, ap and AE data from ground stations. Figures 3a and 3b help for the visualizing of the scattering of solar wind parameters.

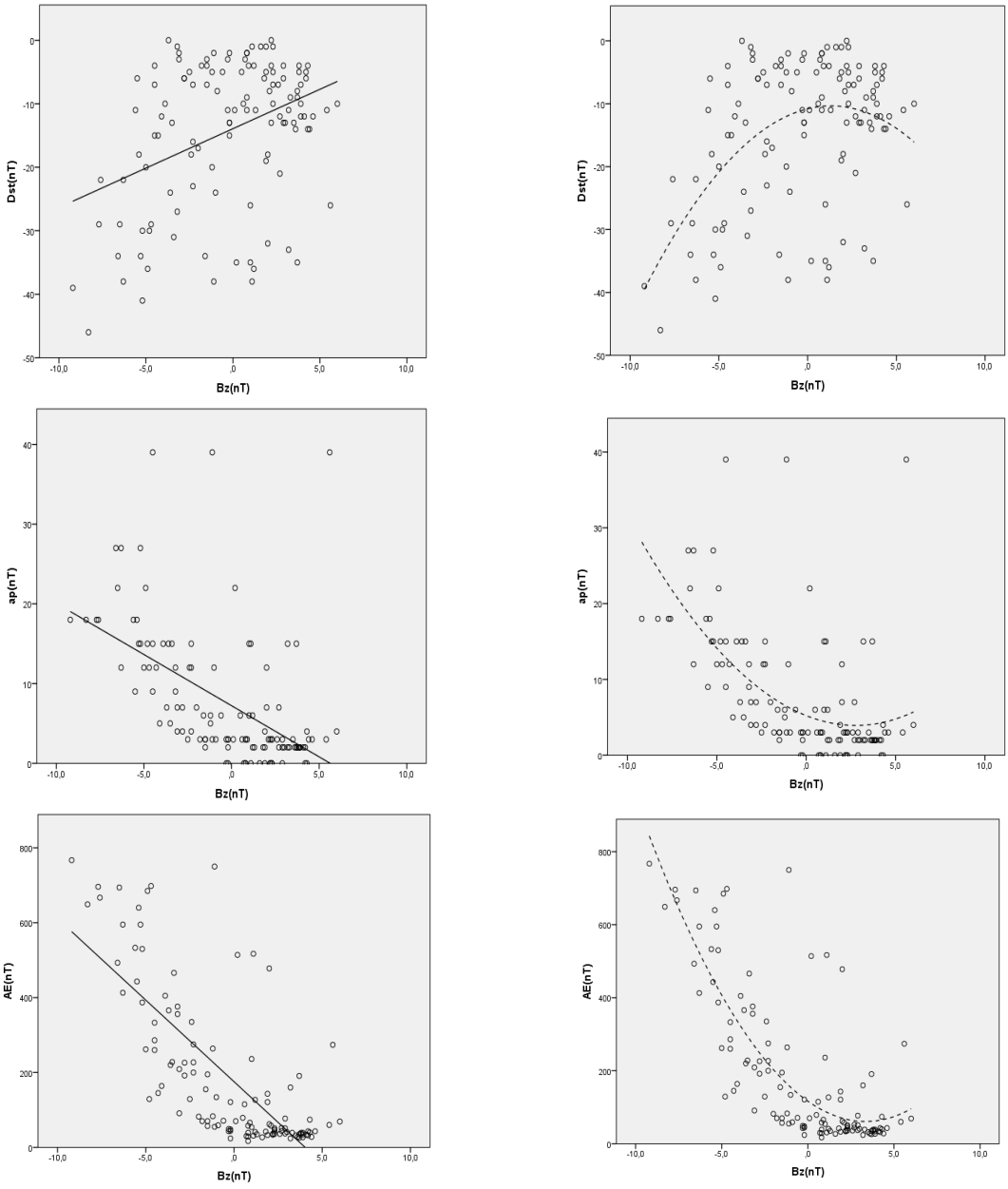


**Figure 3a.** Linear and quadratic relation of Dst-ap-AE and $B_z$ (Weak storm).

ISBN: 978-605-73552-2-5

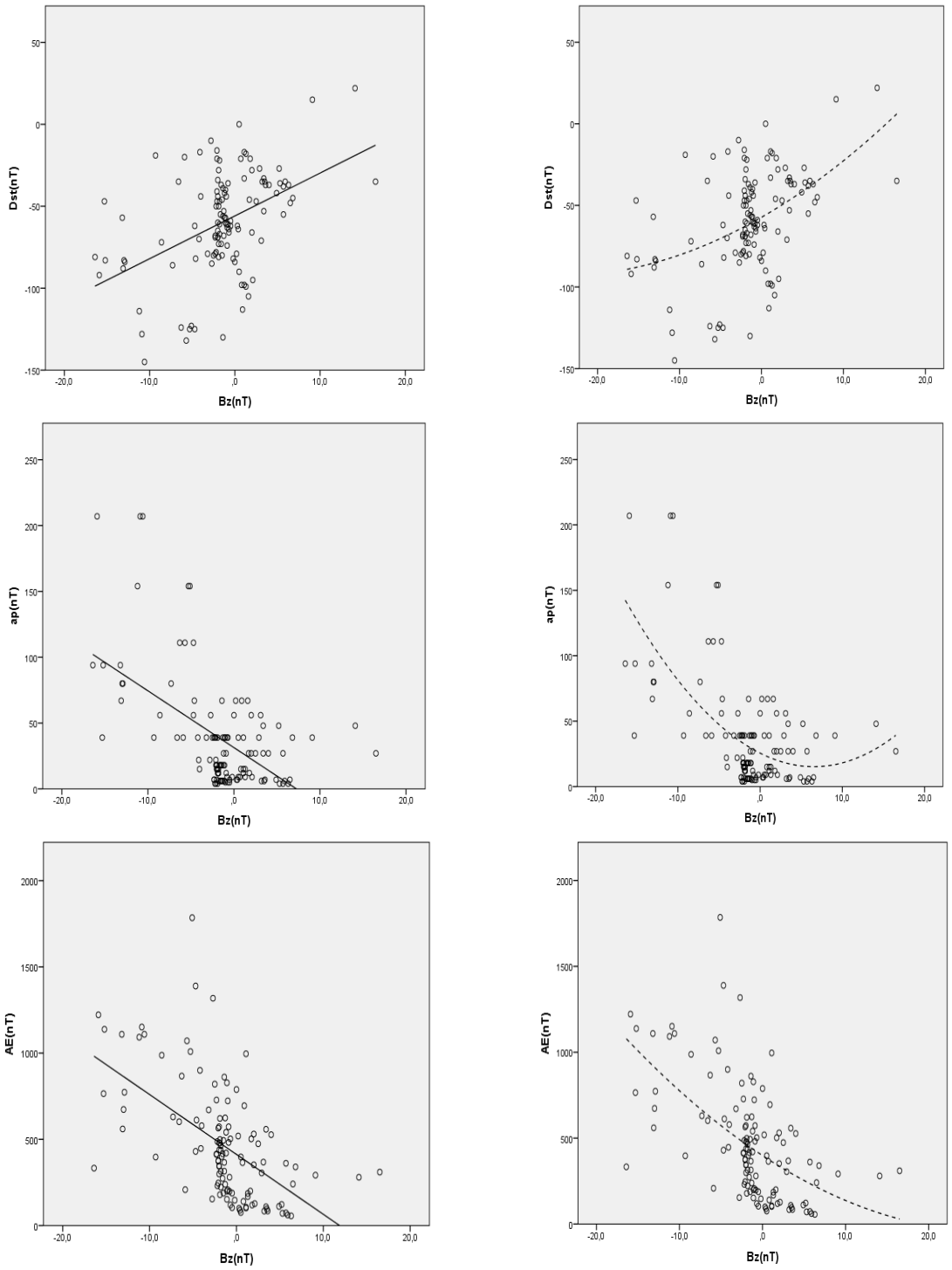


**Figure 3b.** Linear and quadratic relation of Dst-ap-AE and $B_z$ (Intense storm)

ISBN: 978-605-73552-2-5

Physically, the magnetospheric activity is nonlinearly proportional to the proton density (N) and plasma flow speed (v), is linearly proportional to the interplanetary magnetic field (IMF) (Temerin and Li, 2006; Agopyan, 2010). Changes in solar wind pressure and CME cause nonlinear behavior, fluctuations, and changes in the density of particles. Directing the $B_z$ component of the magnetic field to the south for a period causes pressure in the Dst to lead in a negative direction. This negative direction is the messenger of a storm. Dynamic pressure (P) and proton density (N) propagate linearly due to fluctuations in the magnetic field, while the ap index propagates logarithmically.

## 4. Conclusion

Geomagnetic storms are dynamic events, directly affecting the magnetosphere of our earth. Because of their dynamic structures, they need the investigation of each variable separately. Relations between the variables of the storm are remarkable because they cannot be simulated in the laboratory. Any models that can be established under the guidance of these correlations may help to illuminate the unknowns of the sun. The study focuses on the 2014 May weak and 2012 March strong storm. Since the weak geomagnetic storm on May 08, 2014, is one of the weakest storms in the 24th solar cycle and the intense storm of March 09, 2012, is the first severe storm at the beginning of the same solar cycle, the author meticulously analyzes them and compares the data. The models designed in accordance with the physical principles in the analysis reveal the mutual effects between solar wind parameters and zonal geomagnetic indices. Some possible binary or multiple relationships and models are presented to the reader even if not statistically significant. The linear axis presented by the rotation matrix and the linear models of the Dst, ap, AE indices shaped by solar wind parameters, aid to-read events more clearly, while nonlinear models including solar wind pressure and proton density provide an idea of the dynamic nature of the different plasmatic structures. In order for the models to be consistent, it is necessary to valid for other storms. The last nonlinear model among flow pressure (P), ap and proton density (N) explains the storms with 97% (weak) and 68% (intense) accuracy. All results are in the 95% confidence interval. Graphs and tables have visualized the correlation between zonal geomagnetic indices and solar wind parameters, as well as their interactions with each other.

## Availability of data and materials

I thank the NASA CDA Web for OMNI Database (http://themis.igpp.ucla.edu/software.shtml) and Kyoto World Data Center for providing AE index and Dst index. I acknowledge the usage of the ap and Kp index from the National Geophysical Data Center. The Dst index and AE data were provided by the World Data Center for Geomagnetism at Kyoto University.

## Acknowledgment

This work has been supported by Yildiz Technical University Scientific Research Projects Coordination Unit under project number FBA-2021-4739

I would like to thank Halil İbrahim ÖZKUL, Ata KÖKLÜ and Mevlüde CANLICA for their help.

## References

Adebesin BO, Ikubanni SO & Kayode JS (2012) Solar Wind Dynamic Pressure Dependency on the Plasma Flow Speed and Imf $B_z$ During Different Geomagnetic Activities. WJYR, 2(3), 43.

Adebesin BO, Ikubanni SO, Kayode JS & Adekoya BJ (2013) Variability of Solar Wind Dynamic Pressure with Solar Wind Parameters During Intense and Severe Storms. The African Review of Physics, 8, 119-128.

Agopyan H (2010) Istanbul iyonoküresinde ölçülen şiddetli manyetik fırtına etkilerine göre jeofizikten bir örnek. Tubav Bilim Dergisi, 3, 315 (in Turkish).

Akasofu SI, (1964) A source of the energy for geomagnetic storms and auroras. Planet, Space Sci., 12, 801.

Burton RK, Mcpherron RL & Russell CT (1975) An Empirical Relationship between Interplanetary Conditions and Dst. Journal of Geophysical Research, 80, 4204-4214. http://dx.doi.org/10.1029/JA080i031p04204

Davis TN and Sigiura M (1966) Auroral electrojet index, AE and its universal time variations. J. Geophys. Res., 71,785-801.

Eroglu E (2011) Dalga Kılavuzları Boyunca Geçici Sinyallerin Transferi (Transferring of The Transient Signals Along Waveguides). Ph.D. Dissertation, Gebze Institute of Technology.

Eroglu E, Aksoy S, Tretyakov OA (2012) Surplus of energy for time-domain waveguide modes. Energy Educ. Sci. Tech., 29, 495.

Eroglu E, Ak N, Koklu K, Ozdemir Z, Celik N, Eren N (2012) Special functions in transferring of energy; a special case: “Airy function”. Energy Educ. Sci. Tech, 30, 719.

Eroglu E (2018) Mathematical modeling of the moderate storm on 28 February 2008. Newast, 60, 33, https://doi.org/10.1016/j.newast.2017.10.002

Eroglu E (2019) Modeling the super storm in the 24th solar cycle. Earth Planets Spaces, 71(26), 1-12 https://doi.org/10.1186/s40623-019-1002-1

Eroglu E (2021) Analysis of the first four moderate geomagnetic storms of the year 2015. Arab J Geosci, 14, 2538. https://doi.org/10.1007/s12517-021-08816-3

Fu HS, Tu J, Song P, Cao JB, Reinisch BW & Yang B (2010) The nightside-to-dayside evolution of the inner magnetosphere: Imager for Magnetopause-to-Aurora Global Exploration Radio Plasma Imager observations. J. Geophys. Res., 115, A04213, doi:10.1029/2009JA014668

Fu HS, Tu J, Cao JB, Song P, Reinisch BW, Gallagher DL, Yang B (2010) IMAGE and DMSP observations of a density trough inside the plasmasphere. Journal of Geophysical Research Atmospheres, 115, A07227, DOI:10.1029/2009JA015104

Fu HS, Vaivads A, Khotyaintsev YV, André M, Cao JB, Olshevsky V, Eastwood JP and Retinò A (2017) Intermittent energy dissipation by turbulent reconnection. Geophys. Res. Lett., 44(1), 37-43. doi:10.1002/2016GL071787

Gonzales WD, Joselyn JA, Kamide Y, Kroehl HW, Rostoker G, Tsurutani BT, Vasyliunas VM (1994) What is a geomagnetic storm?. J. Geophys. Res., 99, 5771, https://doi.org/10.1029/93JA02867

Gonzales WD, Tsurutani BT & Gonzalez ALC (1999) Interplanetary origin of geomagnetic storms. Space Sci. Rev., 88, 529-562.

Habarulema JB, Dubazane MB, Katamzi-Joseph ZT, Yizengaw E, Moldwin MB & Uwamahoro JC (2018) Long-term estimation of diurnal vertical E × B drift velocities using C/NOFS and ground-based magnetometer observations. J Geophys Res Space Phys., doi:10.1029/2018ja025685

Hampton D (2018) A Study of intense local dB/dt variations during two geomagnetic storms. Sp. Weather, 16, 676, https://doi.org/10.1029/2018SW00191

Hanslmeier A (2007) The Sun and Space Weather. Astrophysics and Space Science, 2nd eds., (Springer e-book).

Inyurt S (2019) Modeling and comparison of two geomagnetic storms. Advance in Space Research, https://doi.org/10.1016/j.asr.2019.11.004 (in press).

Kamide Y, Yokoyama N, Gonzalez W, Tsurutani BT, Daglis IA, Brekke A, Masuda S (1998) Two-step development of geomagnetic storms. Journal of Geophysical Research Space Physics, 103, A4, 6917-6921, https://doi.org/10.1029/97JA03337

Koklu K, "Using Artificial Neural Networks for Comparison of the 09 March 2012 Intense and 08 May 2014 Weak Storms" Advances in Space Research, July 2022 https://doi.org/10.1016/j.asr.2022.07.067

Koklu K "Mathematical Analysis of the 08 May 2014 Weak Storm" Mathematical Problems in Engineering, vol. 2021, Article ID 9948745, 16 September 2021 https://doi.org/10.1155/2021/9948745

Koklu K "Mathematical Analysis of the 09 March 2012 Intense Storm" Advances in Space Research, Volume 66, Issue 4, pages 932-941, 30 April 2020, https://doi.org/10.1016/j.asr.2020.04.053

Lin J and Forbes TG (2000) Effects of reconnection on the coronal mass ejection process. J. Geophys. Res., 105(A2), 2375-2392. doi:10.1029/1999JA900477

Loewe CA & Prölss GW (1997) Classification and mean behavior of magnetic storms. J. Geophys. Res., 102, 14209, doi:10.1029/96JA04020

Mayaud PN (1980) Derivation, Meaning and Use of Geomagnetic Indices. AGU Geophysical Monograph Series, DOI:10.1029/GM022

Ngwira CM, Sibeck D, Marcos VDS, Georgiou M, Weygand JM, Nishimura Y, Hampton D (2018) A Study of intense local dB/dt variations during two geomagnetic storms. Sp. Weather, 16, 676, https://doi.org/10.1029/2018SW00191

Parker EN (1958) Dynamics of the Interplanetary Gas and Magnetic Fields. Astrophysical Journal, 128, 664-676.

Rathore BS, Gupta DC & Parashar KK (2014) Relation between Solar Wind Parameter and Geomagnetic Storm Condition during Cycle-23. International Journal of Geosciences, 5, 1602-1608 http://dx.doi.org/10.4236/ijg.2014.513131

Rathore BS, Gupta DC & Kaushik SC (2015) RAA, 15, 85 (doi:10.1088/1674–4527/15/1/009).

Saba FMM, Gonzalez WD & Gonzalez ALC (1997) Relationships between the AE, ap and Dst indices near solar minimum (1974) and at solar maximum (1979). Ann. Geophysicae 15(10), 1265-1270, https://doi.org/10.1007/s00585-997-1265-x

Sato M and Kuwano R (2015) Influence of location of subsurface structures on development of underground cavities induced by internal erosion, Soils and Foundations. 55, 4, 829-840, https://doi.org/10.1016/j.sandf.2015.06.014

Singh SB, Patel K, Singh AK (2018) Effect of geomagnetic storms on VHF scintillations observed at low latitude. J. Astrophys. Astr., 39(3). doi:10.1007/s12036-018-9529-2

Stern DP (1996) A brief history of magnetospheric physics during the space age. Reviews of Geophysics, 34, 1.

ISBN: 978-605-73552-2-5

Temerin M and Li X (2006) Dst model for 1995–2002. J Geophys Res, 111(A4), doi:10.1029/2005ja011257
Zhao D, Huang Z, Umino N, Hasegawa A, Kanamori H (2011) Structural heterogeneity in the megathrust zone and mechanism of the 2011 Tohoku-oki earthquake (Mw 9.0). Geophysical Research Letters, 38, 17, https://doi.org/10.1029/2011GL048408

ISBN: 978-605-73552-2-5

# ROBOT POSITIONING IN INDOOR ENVIRONMENTS USING A DEEP LEARNING MODEL

**Ahmet Murat ERTURAN[1,2*], Abdullah YUSEFI[3], Akif DURDU[1], Seyfettin Sinan GÜLTEKİN[1]**

[1] Electrical-Electronics Engineering Department, Faculty of Engineering and Natural Sciences, Konya Technical University, Konya, Turkey
[2] Electrical-Electronics Engineering Department, Faculty of Engineering, Erzurum Technical University, Erzurum, Turkey
[3] Computer Engineering Department, Faculty of Engineering and Natural Sciences, Konya Technical University, Konya, Turkey

## ABSTRACT

The issue of positioning in closed environments has become popular in recent years. Positioning a robot in outdoor can be easily accomplished with GPS signals. However, it is very difficult to make an accurate positioning because GPS signals cannot be received in indoor environments. In order to solve this problem, researchers, especially bayes prediction methods; He used methods such as wheel data, image processing, barcode-data matrix marker. In this study, in addition to the methods discussed in the literature, a deep learning model was used and it was aimed to recognize the two traffic signs that the robot encountered during the autonomous movement and position itself. The robot has determined its own position with an average of 88.11% and 88.39% accurately with the proposed mathematical method according to the location of the two traffic signs it knows.
**Keywords:** Indoor Localization, Deep Learning, Simultaneous Localization and Mapping (SLAM), Faster R-CNN.

## 1. INTRODUCTION

Autonomous movements of robots have been a popular topic in recent years. The positioning of robots in open areas is carried out with high accuracy via GPS sensors. However, since GPS signals cannot be received in closed environments, different methods have to be used for correct positioning. Simultaneously Localization and Mapping (SLAM) is a method based on predicting the location while creating a map in an environment. This method has made the position prediction using the state prediction filters used to predict the next situation, called the stochastic map [1]. In a study that was carried out for the first time by addressing the mapping and positioning issues, robot position estimation was made using the Extended Kalman Filter (EKF) [2]. Then, using the Kalman Filter and EKF together, more accurate location estimates were made [3]. KF and GKF are methods that are based on Bayes-based Gauss distribution and are frequently used in many areas, obtaining accurate estimation results. However, since they are based on Gauss, they need a linear system and linearization brings additional time-processing load. This disadvantage has pushed the researchers into the Particle Filters used in nonlinear systems [4]. FastSLAM algorithm was introduced for the first time as an algorithm based on Particle Filter and Rao-Blacwellization method was used [5]. However, in this method, each particle used particle filters, which carried a separate map of the medium, and so the number of particles increased. Increased particle count was reduced in one study using a method that accurately predicted samples, and the risk of particle depletion was relatively eliminated [6]. Adaptive Monte Carlo Localization (AMCL) method, which is the most suitable method with the studies done over time, was used and autonomous movement of the robot was created by creating the environment map [7].

Robots detect physical elders from the environment using various sensors. In most proposed positioning methods, an odometry sensor is used to measure the number of turns and angle of wheel. With the help of this sensor, the robot estimates how far it travels in the environment and in which directions it turns. However, there are two important problems here. First, if the robot is stuck on an obstacle or slides on a soft surface, the wheel turns empty. Because this is a blind count, even if the robot does not move, it thinks that it takes a distance because the wheel turns. The second problem is sensor data is not linear. Therefore, in KF and GKF methods, linearization should be done first. This requires additional time and processing load costs. PF-based Rao-Blackwellization method gives successful results in small maps. However, due to the increasing number of particles in large maps, it also has an effect on increasing the workload cost. In this article, a deep learning based positioning method is proposed for robot positioning in closed environments. Due to the mentioned problems, the determination of the position of the robot was carried out according to two traffic signs by using a camera, not by a blind count. Firstly, the map of the environment was created using the Gmapping algorithm. Two traffic signs were then placed in two known locations on the map. These traffic signs are trained with a

ISBN: 978-605-73552-2-5

deep learning model Faster R-CNN and have been successfully recognized by the robot. The robot receives the information of the position it recognizes and determines its position using a triangulation method. Experimental results are compared with the positioning results obtained with the classical PF based AMCL algorithm. The proposed method has been shown to give accurate results in 88.11% and 88.39%

## 2. Material and Method

### 2.1. Simultateous Localization and Mapping (SLAM)

The problem of Simultaneous Positioning and Mapping (SLAM) is that the robot creates a map of an unknown environment and also determines its position in this environment [8]. There are two main issues here. First, the map of the environment will be created, and secondly, the location of the robot will be determined in this map. It is also important for the robot to provide a partially autonomous movement. Depending on the map and the environment, the robot can be moved autonomously from one location to another. It shows the importance of SLAM algorithms for sending the robot autonomously from the starting position to a targeted point thanks to a path planning algorithm. In experimental studies, SLAM was applied using LIDAR and odometry sensor. LIDAR distance sensor creates the map by determining the distance of the objects around it thanks to the laser beams of the point cloud it emits.,

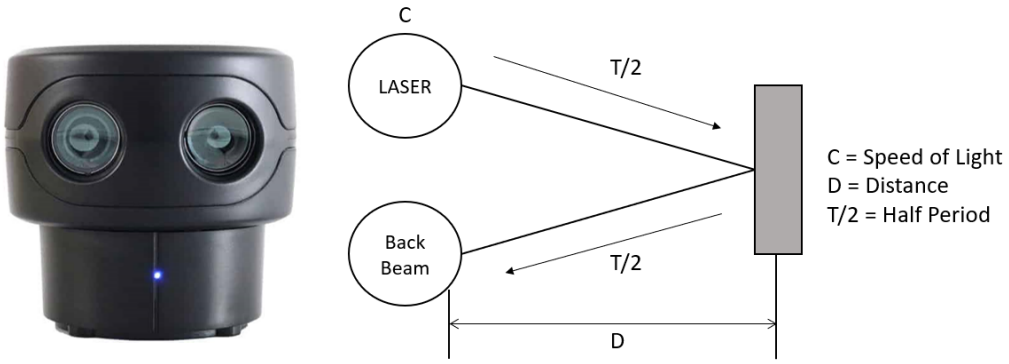


**Figure 1.** LIDAR and its working mechanism

LIDAR sensor is shown in Figure 1. In Equation (1), mathematical calculation of the distance of LIDAR from the object is given.

$$D = \frac{C.T}{2} \tag{1}$$

Here D is the distance of LIDAR to the object, the speed of light C, and T / 2 is the period of the laser beam to exit the LIDAR and hit the object and return again.

Another sensor used is wheel counter encoders. These generate the odometry data and count the distance the robot travels in the environment with dead-reckoning. [9]. The cavities on the wheel shown in Figure 2 create an optical pulse with varying light and dark. This optical pulse number determines the robot position by calculating the wheel radius and certain geometric parameters.

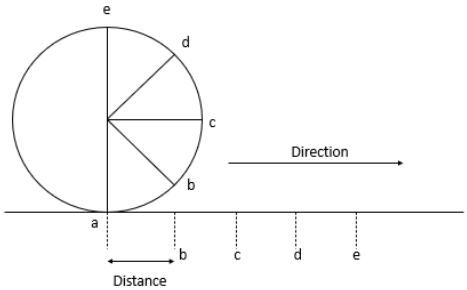


**Figure 2.** Odometry information is provided with the distance traveled by the wheel.

ISBN: 978-605-73552-2-5

### 2.2. Gmapping Method

This approach uses a particle filter that carries a separate map of the environment of each particle [6]. Rao-Blackwellized is a SLAM algorithm based on particle filter. It can be done using distance sensor and odometry sensor. As the robot travels around, it creates the map of the environment by making samples with pointers, and gains the knowledge of how far it has been in the environment with the odometry sensor. Each particle; It is the sum of the robot's previous position example and the previous position example known on the map. The main idea of the Rao-Blackwellized particle filter for SLAM; Given their observations $z_{1:t}$ and the robot's odometry measurements $u_{0:t}$, a $p(x_{1:t} \mid z_{1:t}, u_{0:t})$ to estimate and calculate a precedent value using Equation (2) on the premise $x_{1:t}$ map and trajectories [6].

Using Gmapping probabilistic distribution methods, they create a spreading sample according to the robot's last observation region. Thus, uncertain situations are eliminated and a correct map is created. With Rao-Blackwellized used in this method, resampling is done in every update. Thus, the set of samples representing the robot trajectory and the map is updated. Sampling, assignment by importance weight, resampling according to results and map estimation corresponding to each particle observation are made, respectively. Odometry data is needed with the Rao-Blackwellized particle filter. It was seen that more accurate mapping was done with this method. Because low weight particles have disappeared and high prediction particles have been updated instead, increasing the accuracy of the prediction.

The Gmapping method offers a selective stimulating technique for the resampling of particles. Good fragments of trajectories and maps need to be used carefully for resampling steps. In a study, the resampling step with the proposed approach was used in the Gmapping algorithm [10]. With this approach, particles having significant weight value among the particles are taken into account. In Equation (3), $Ne_{ff}$ indicates how well the particle weighs in the precursor orbit. $\widetilde{\omega}^{(i)}$ is the normalized weight of particle i. A resampling step is performed whenever the particle number of $Ne_{ff}$ falls below half of the N/2 number. Thus, a more accurate map is created while the risk of particle depletion decreases.

$$Ne_{ff} = \frac{1}{\sum_{i=1}^{N} \left(\widetilde{\omega}^{(i)}\right)^2} \tag{3}$$

### 2.3. Deep Learning

Artificial Neural Networks have been developed based on the neurons in the human nervous system. Various methods have been developed, such as Machine Learning and Deep Learning. In machine learning, the raw data of the image should be subjected to a pretreatment and feature extraction should be applied. Deep learning is to eliminate old feature extraction problems [11]. There are many deep learning models. With the Faster R-CNN network that has been introduced in recent years, the location of the object has been made by using the properties removed from the convolutional layer of CNN instead of the region suggestion network. The deep learning [12] network on object recognition with Faster R-CNN has proved a successful result. It has achieved successful results, especially in real-time and instantaneous work, such as object tracking and robotic object recognition. However, the development efforts of this network, which still has deficiencies, continue today.

In the proposed method, the robot positioning in the indoor environment is realized by recognizing two traffic signs. Faster R-CNN model was trained to recognize these traffic signs. A total of 1798 images in 6 different classes were used in the database. 360 of these images were used in the test and 1438 were used in education. A view of the traffic signs used in Figure 3 is given.

The training was carried out with the Nvidia GeForce 1050 Ti GPU. As a result, an accurate recognition of 90% and 95% was achieved in an image taken during simultaneous robot movement and is shown in Figure 4.

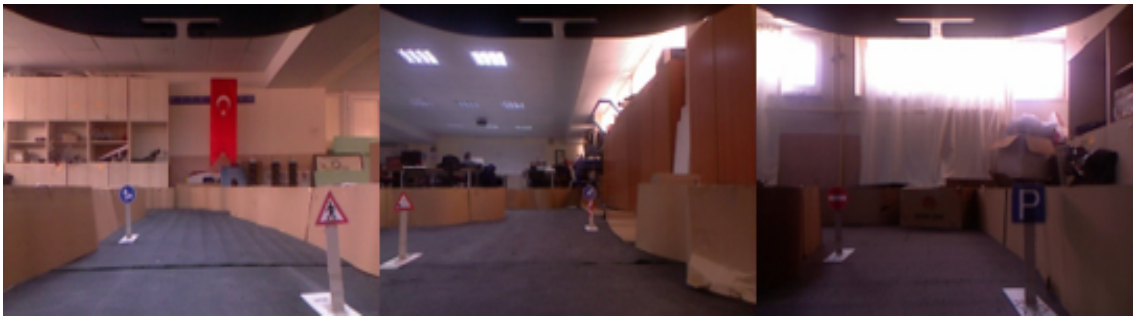

**Figure 3.** Images of the data set used in training from the experimental environment

ISBN: 978-605-73552-2-5


**Figure 4.** Park and right turn signs

### 2.4. Mathematical Method

The boards on the map have been successfully recognized as a result of the trained network. The purpose of this article is to determine the position of the robot relative to these two objects. Let the position of the first plate ($x_1$ , $y_1$), on the map be the position of the second map ($x_2$ , $y_2$) and the robot position (x, y). Traffic sign locations are fixed and information on where they are on the map. However, the robot is constantly in motion and we need to get an instant x, y information. Based on this idea, the coordinate system in Figure 5 was designed. Here, the first plate is considered as a circle with center $M_1(x_1$ , $y_1)$, and the second plate is considered as a circle with center $M_2(x_2$ , $y_2)$. The robot, on the other hand, is at the (x, y) point, which is known and its distance from these $M_1$ and $M_2$ centers.
The boards on the map have been successfully recognized as a result of the trained network. The purpose of this article is to determine the position of the robot relative to these two objects. Let the position of the first plate on the map be the position of the second map and the robot position (x, y). Traffic sign locations are fixed and information on where they are on the map. However, the robot is constantly in motion and we need to get an instant x, y information. Based on this idea, the coordinate system in Figure 5 was designed. Here, the first plate is considered as a centered circle, and the second plate is considered as a centered circle. The robot is at the (x, y) point whose distance from these centers is known and constantly changing.

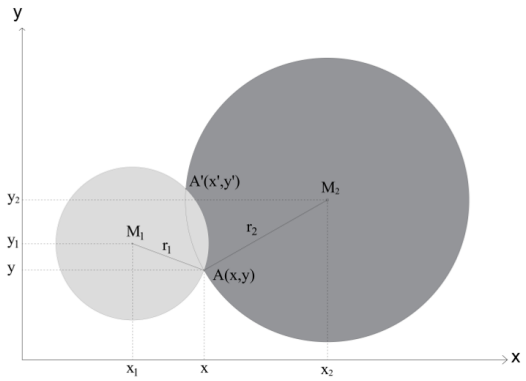


**Figure 5.** Representation of the intersection points of the two circles

Using the intersection point Equation (4, 5, 6) of the two circles, the robot's motion is constantly calculated instantly. Thus, as long as the robot recognizes the two plates and knows their distance from these two plates, the position information is tracked in real time.

$$r_1{}^2 = (x_1 - x)^2 + (y_1 - y)^2 \quad (4)$$

$$r_2{}^2 = (x_2 - x)^2 + (y_2 - y)^2 \quad (5)$$

$$r_1^2 - r_2^2 = x_1^2 - x_2^2 - 2x_1x + 2x_2x + y_1^2 - y_2^2 - 2y_1y + 2y_2y \quad (6)$$

ISBN: 978-605-73552-2-5

## 3. Results and Discussion

### 3.1. Mapping the Research Environment with Simultaneous Positioning and Mapping (SLAM) Method

The experimental environment was created in Konya Technical University RACLAB laboratory as in Figure 6. Later, SLAM was implemented by using Gmapping Algorithm via Robot Operating System.

The map formed as a result of SLAM is given in Figure 7. In addition, the positions of the plates are determined on the created map and the starting and ending points of the robot's autonomous movement are shown.

**Figure 6.** Research environment created in the RACLAB laboratory and the locations of the plates.

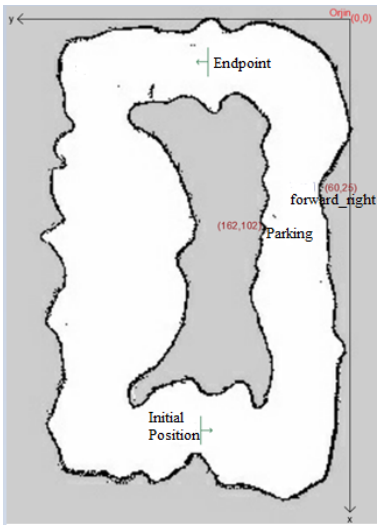


**Figure 7**. Environment map center coordinates and locations of objects.

The position of the parking sign on the robot route according to global_map has been determined as 162 cm on the x axis and 102 cm (162,102) on the y axis. The coordinates with the Forward Right sign were determined as 60 cm on the x axis and 25 cm (60,25) on the y axis.

The Turtlebot 2 robot shown in Figure 8 was used in experimental studies. SLAM was made with the LIDAR sensor in the robot and snapshots were taken with the Kinect camera. Experimental studies were carried out based on three scenarios. In the first scenario, the autonomous movement of the robot from the starting point to the target point is aimed and no loss of odometry data is created during this autonomous movement. Thus, positioning results were obtained with the classical positioning method, MCL method.

In the second and third scenarios, positioning was realized with the proposed method. In the first scenario, the robot successfully reached the end point from the start point. In Figure 9, it is seen that the robot successfully reaches the end

ISBN: 978-605-73552-2-5

point in the RVIZ interface. Therefore, the location was successfully estimated with the MCL method. The robot proceeded on the y axis in an average of 60 cm, as in reality. Thus, in the absence of any wheel slip, the robot made a successful position prediction with the MCL method.

In the next step, it was checked if he made the correct prediction in the method proposed. Firstly, in Figure 10, an image taken from the robot camera showed a correct instant recognition even though there is a distant point to the plates.

**Figure 8.** Turtlebot 2 and Kinect Camera

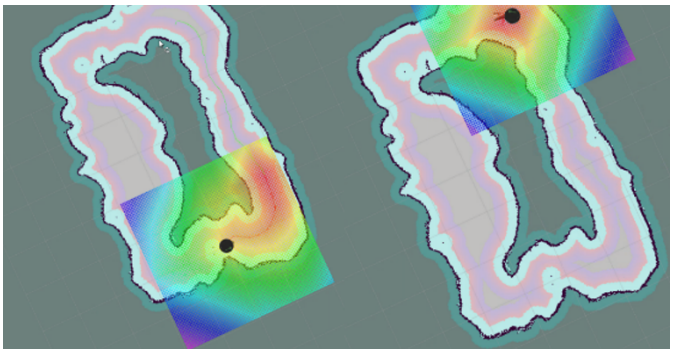

**Figure 9.** In the Rviz environment, the path the robot follows from the starting point to the target point.

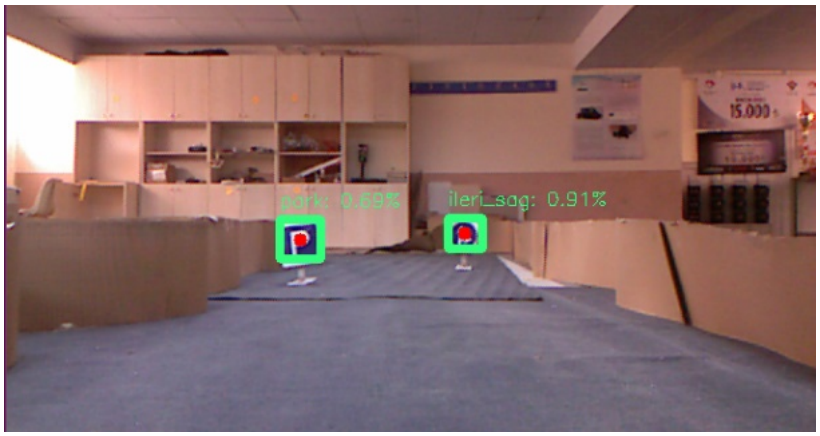


**Figure 10.** Autonomous movement of the robot in case of no data loss

ISBN: 978-605-73552-2-5

The robot determined its position instantly according to the location of the two plates and left it as a red dot on a graph as shown in Figure 11. As can be clearly seen from this graphic, the robot progressed according to two plates and reported its position instantly. With the data received, it proceeded in a line of 56.93 cm on the average y-axis and showed a deviation of 3.07 cm from the correct position. This gives the accuracy rate as 94.8%.

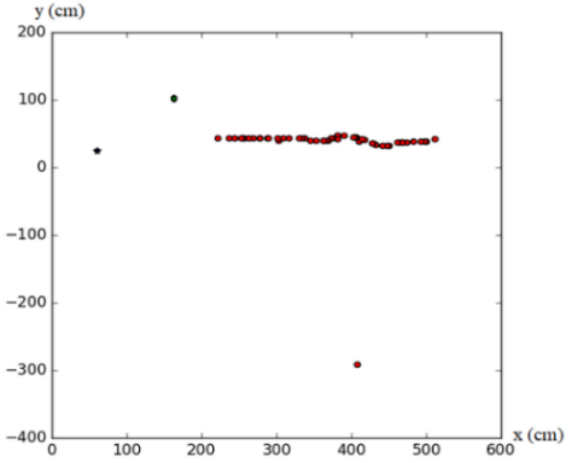


**Figure 11**. The location of the robot with the proposed method. Park plate position (x = 162, y = 102) and Forward Right plate position (x = 60, y = 25).

According to the results obtained, an accuracy of 94.8% was obtained with the method proposed in the first scenario. In conclusion, if there is no odometer data loss or noise, the MCL method gave more accurate results. However, the proposed method has managed to determine the position of the robot with a high accuracy rate.

In the second scenario, this time, the position of the wheel is lost and the location is estimated. After advancing for a while, the robot was removed from its location and placed at 100 cm on the y axis at the level of the plate on the left relative to the robot. As is known, odometry data provides a blind count in the environment. The robot cannot detect this when its position changes and continues to count from the point it knows on the map. Therefore, it misses its position and the false prediction increases cumulatively. Figure 12 shows the RVIZ image taken during the autonomous movement of the robot. As clearly seen, the robot has taken the same path it took in the previous scenario. He also determined his position on the y axis as 60 cm. Therefore, there has been a serious deviation of 40 cm from the actual position.

In the location estimation with the proposed method, the image taken from the camera of the robot is shown in Figure 13. The robot moves in a position close to the plate on the left side according to it. Again, the model successfully recognized both plates.

The robot determined its position instantly according to the location of the two boards and left it as a red dot on a graph as shown in Figure 14. As can be clearly seen from this graphic, the robot has moved closer to the plate located in the position (162,102). Based on the received data, the average progressed in an average of 89.39 cm in the y-axis and showed a deviation of 10.61 cm from the correct position. This gives the accuracy rate as 89.39%.

During the robot's advance in the real position of 100 cm on the y axis, the position estimation was calculated as 89.39 cm on the y axis. The wrong position estimation, which is 60 cm with the MCL method, was obtained with a more accurate result using the proposed method.

The results obtained are shown graphically in Figure 15. Here, the Green line is the 100 cm position on the y axis, which is the real position of the robot. The blue line shows the position estimation with the MCL method. As a result of removing the robot and placing it at another point, the position information was lost and it continued from where it left off and remained at 60 cm on the y axis. The yellow line shows the results obtained with the proposed method. Although the location had some deterioration at the point where it first started, it has managed to predict the real position with high accuracy as it approaches the plates.

It is thought that if there is a better education using more data and class, the deviation that occurs at first will disappear and a much higher accuracy prediction will be achieved.

ISBN: 978-605-73552-2-5

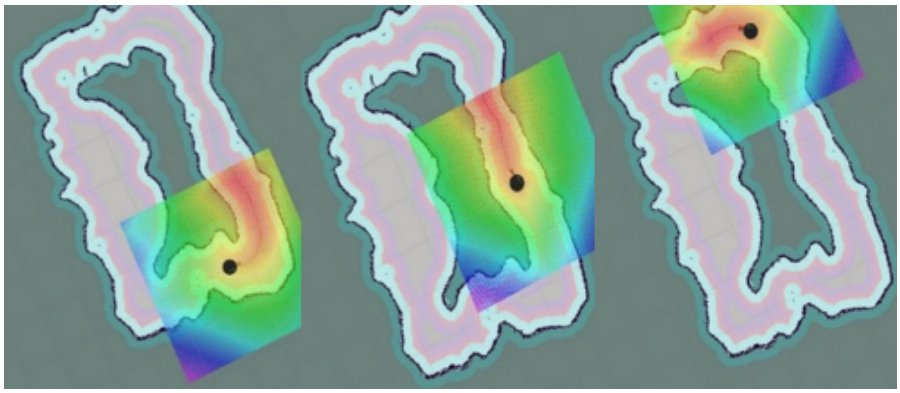

**Figure 12.** Position prediction with MCL during the autonomous movement of the robot from the start point to the target point. The path followed in sequence from the start point to the end point.

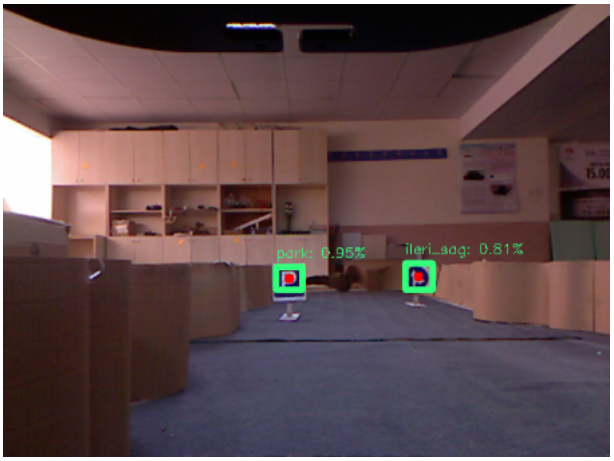


**Figure 13.** According to the traffic signs, the robot moves along the left-hand parking plate

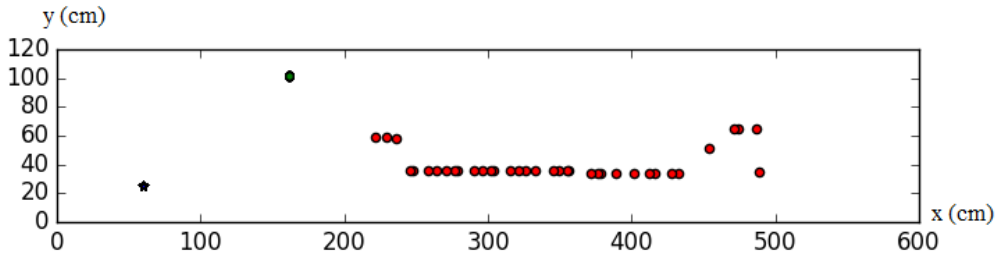


**Figure 14.** Progress of the robot with reference to the parking plate on the left (0-600 cm x axis and 0-120 cm y axis)

ISBN: 978-605-73552-2-5

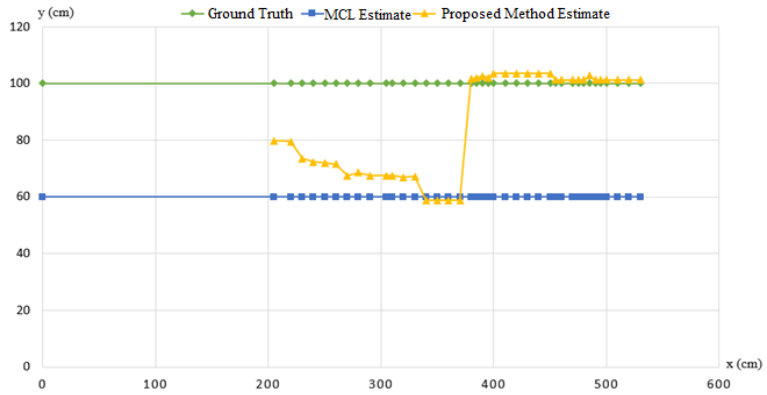


**Figure 15.** The robot's progression at the level of the “Park” traffic sign (real position y axis 100 cm).

Actual position of green line robot, prediction with blue line MCL method, position prediction with yellow line proposed method.

Table 1 shows the actual location, the predicted position with the MCL method, and the predicted location with the proposed method, on the road the robot moves on. While the prediction made with the MCL method obtained 60% accuracy, the proposed method made a successful location prediction with 89.39%.

**Table 1.** MCL method and suggested position prediction method accuracy rates with robot's advance at "Forward_Sigh" plate level

| Coordinates | Y(cm) | X(cm) | Accuracy Rate (%) |
|---|---|---|---|
| Ground Truth | 100 cm | Linear feed from 600 cm to 200 cm | - |
| Monte Carlo Localization Estimate | 60 cm | Linear feed from 600 cm to 200 cm | %60 |
| Proposed Method Estimate | 89,39 cm | Linear feed from 600 cm to 200 cm | %89,39 |

## 4. Conclusion

With the advances in technology, robot use has become widespread in areas such as aviation, space, defense systems integrations and manufacturing industry. In the light of these developments, robotic systems are intended to be self-deciding and autonomously moving systems in the environment, apart from being controlled and command-driven systems. Indoor positioning is important in military applications and works for defense systems. While GPS position can be determined with high accuracy in outdoor environment, different methods are used for positioning because GPS data cannot be obtained in closed environments. Simultaneous Positioning and Mapping (SLAM) problem is the robot's positioning itself in this environment while mapping an unknown environment. SLAM; While it helps positioning the robot in a closed environment, it also gives the robot an autonomous mobility. However, since the robot is positioned in the environment using various estimation methods, incorrect position estimation results can be obtained due to incorrect sensor data. Using the wheel data, the robot mispredicts its position due to odometry data in a situation such as the wheel slipping on a soft surface, the robot is stuck on the obstacle or the robot is missing.

Within the scope of this thesis, the issues of positioning in indoor environments, which are an important problem in defense technologies, and scaling of indoor environments by mapping are discussed. In the first experimental study, it was aimed to position the robot in the environment depending on the location of two objects as a result of the loss of the robot position in the indoor environment. The experimental environment was created and scaled and two objects were placed at known points in the environment. Two objects in the environment were identified by using 1798 data

trained with Faster R-CNN, a Deep Learning model. It is aimed to position the robot using the proposed mathematical method according to two objects that are known and whose positions are known. In the experimental results, first of all, the situation that the robot does not have a wheel loss and the results were compared with the Monte Carlo Localization (MCL) method, which is a classical position estimation method. If there is no data loss, the MCL method has performed an accurate position detection. The proposed method has achieved a successful positioning of 94.8%. In the second scenario, position estimations are examined as a result of the loss of robot wheel data. Due to the blind count in the MCl method, the robot could not detect the lost wheel data and made the position prediction with 60% accuracy. The proposed deep learning based method, on the other hand, has correctly estimated its position at the rate of 89.39% based on the locations of the traffic signs it has recognized and has obtained a good result from MCL.

As a result, MCL is still a method with very good accuracy when the wheel data is not lost. However, in case of loss of wheel data, he made serious erroneous location estimations. The proposed method resolved this error and revealed a successful prediction.

**Acknowledge**
With the contribution of Konya Technical University RACLAB team.

**References**

[1] Smith R, Self M, Cheeseman P. Estimating Uncertain Spatial Relationships in Robotics. Proceedings of the Second Annual Conference on Uncertainty in Artificial Intelligence, University of Pennsylvania, Philadelphia, PA, USA, August 8-10, 1986.

[2] Leonard JJ, Durrant-Whyte H.F. Simultaneous map building and localization for an autonomous mobile robot. Proceedings IROS '91:IEEE/RSJ International Workshop on Intelligent Robots and Systems '91, 2002.

[3] Thrun S, Burgard W, Fox D. A Probabilistic Approach to Concurrent Mapping and Localization for Mobile Robots. Machine Learning and Autonomous Robots (joint issue), 31/5, 1–25, 1998.

[4] Zunino G, Christensen HI. Simultaneous localization and mapping in domestic environments. Multisensor Fusion and Integration for Intelligent Systems, 2001.

[5] Montemerlo M, Thrun S, Koller D, Wgnreit. FastSLAM: A Factored Solution to the Simultaneous Localization and Mapping Problem. Published in AAAI/IAAI 28 July DOI:10.5555/777092.777184, 2002.

[6] Grisetti G, Stachniss C, Burgard W. Improved Techniques for Grid Mapping With Rao-Blackwellized Particle Filters. IEEE Transactions on Robotics Volume: 23, Issue: 1, Feb. 2007.

[7] Zhang T, Chong ZJ, Qin B, Fu JGM, Pendleton S, Ang Jr MH. Sensor fusion for localization, mapping and navigation in an indoor environment. 2014 International Conference on Humanoid, Nanotechnology, Information Technology, Communication and Control, Environment and Management (HNICEM), 2014.

[8] Thrun S. Simultaneous Localization and Mapping. in Robotics and Cognitive Approaches to Spatial Mapping, Berlin, Heidelberg: Springer Berlin Heidelberg, 2008, pp. 13–41. doi: 10.1007/978-3-540-75388-9_3.

[9] Spielmann R, Duchoň F, Kostroš J, Fico T, Balog R. Sensor Module for Mobile Robot. American Journal of Mechanical Engineering, vol. 1, no. 7, pp. 378–383, 2013, doi: 10.12691/ajme-1-7-45.

[10] Murphy K, Russell S. Rao-Blackwellised Particle Filtering for Dynamic Bayesian Networks. in Sequential Monte Carlo Methods in Practice, Springer New York, 2001, pp. 499–515. doi: 10.1007/978-1-4757-3437-9_24.

[11] Lecun Y, Bengio Y, Hinton G. Deep learning. Nature, vol. 521, no. 7553. Nature Publishing Group, pp. 436–444, May 27, 2015. doi: 10.1038/nature14539.

[12] Ren S, He K, Girshick R, Sun J. Faster R-CNN: Towards Real-Time Object Detection with Region Proposal Networks. Jun. 2015, [Online]. Available: http://arxiv.org/abs/1506.01497.

ISBN: 978-605-73552-2-5

# APPLICATION OF BIQUATERNION ALGEBRA TO HYDRODYNAMICS

**Mine FAKILI[1,*], Neslihan ŞAHİN[1]**

[1] Department of Physics, Faculty of Science, Eskişehir Technical University, Eskişehir, Turkey

## ABSTRACT

In this study, the definitions are given about the frequently used algebras in the theoretical physics. Some properties and applications are given about biquaternions. The applications in theoretical physics are remarkable in terms of the ease of operation in multidimensional space and the definition of equations in these spaces. Furthermore, the equations of quantum hydrodynamics, also called as the Madelung equations, can be thought as alternative formulation to the Schrödinger equation in higher dimensions. Therefore, the Navier-Stokes equation, modified to include quantum potential and fluctuating viscosity for motions of the quantum fluid medium, is tried to be re-written with biquaternion algebra.

**Keywords:** Biquaternion Algebra, Hydrodynamics Equations, Fluids Medium

## 1. INTRODUCTION

The mathematical description of the motion of a given macroscopic object in space is given with Newton's second law regarding as an energy conservation equation. In addition, the motion of microscopic objects is described with quantum mechanics [1]. Quantum hydrodynamics is also the topic of the fluid dynamics, currently. Madelung [2] proposed first the hydrodynamical model of quantum mechanics in 1926. Quantum hydrodynamics satisfy the probability density and velocity as the basic physical variables of interest. Quantum mechanics adopts the wave functions as the only variables, and Schrödinger's equation gives the hydrodynamic conservation equations [3]. Besides, quantum fluid dynamics have analogy to conventional fluid mechanics [4]. The quantum potential can be defined to be proportional to the pressure field within the fluid. Bohm also suggested regarding the quantum potential as a force field due to classical potential [5,6].

In the literature, there have been various studies about the application of different algebras in the areas of electromagnetism, magnetohydrodynamics, fluids mechanics, quantum mechanics, hydrodynamic description of vortex plasma [7-10] etc. Especially, quaternions are effective and convenient algebras for many fields in physics. Quaternion algebra makes it possible to describe motions of fluids on a four-dimensional space-time [11]. In this context, the dynamics of quantum fluid can be represented in the biquaternion algebras, also defined as complexified quaternion. In the Madelung fluid, the advective and diffuse velocity are the real and imaginary components of fluid velocity. In the classical diffusive processes, the positive gradient of the quantum potential provides the force causing diffusion [12].

In this study, we intend to use a biquaternion algebra to modified Navier- Stokes equation. The modification Navier-Stokes equation includes the pressure changes and viscous forces causing friction losses. In the study we first described the biquaternion algebra. The general conclusion of this study explains that the quantum hydrodynamics can be represented with biquaternion algebra, and quantum hydrodynamic equations will be studied in more detail with biquaternion algebra in the future. We have written the generalized biquaternionic Navier Stokes Equation with quantum potential and fluctuating viscosity. Finally, remarks and conclusion are given in the last section.

## 2. BIQUATERNION ALGEBRA

Real numbers have 1-component, complex numbers have 2-components, while the plane of the complex numbers is extended to the 4-components space of the quaternions. And then the quaternion algebras are extended to the biquaternion algebras with 8-components. Real numbers are a subset of complex numbers. Thus, complex numbers are a combination of real numbers. Biquaternions, on the other hand, are formed by the combination of the complex numbers. Accordingly, complex numbers must have a subset of quaternions. This result shows that quaternions and biquaternions algebras include both real numbers and complex numbers . Biquaternions are one of the important algebras studied in many areas of physics. Biquaternions are increasingly involved in physical applications in recent years. Recently, some equations in physics have been redefined with biquaternions in the related literature [10, 13,14].

ISBN: 978-605-73552-2-5

When $q_0, q_1, q_2, q_3$ are complex numbers, biquaternion $\mathbb{q}$ is indicated as the follows:

$$\mathbb{q} = q_0\hat{e}_0 + q_1\hat{e}_1 + q_2\hat{e}_2 + q_3\hat{e}_3 \tag{1}$$

where $q_0, q_1, q_2, q_3$ are real numbers and it can be represented as:

$$\begin{aligned} q_0 &= q_0 + iq_0' \\ q_1 &= q_1 + iq_1' \\ q_2 &= q_2 + iq_2' \\ q_3 &= q_3 + iq_3' \end{aligned} \tag{2}$$

$\hat{e}_0$ is unit element and also $\hat{e}_1, \hat{e}_2$ and $\hat{e}_3$ are the quaternions basis elements orthogonal to each other and it can be expressed as follows:

$$\begin{aligned} \hat{e}_0 &= 1 \\ \hat{e}_1^2 = \hat{e}_2^2 = \hat{e}_3^2 &= \hat{e}_1\hat{e}_2\hat{e}_3 = -1 \\ \hat{e}_1\hat{e}_2 &= -\hat{e}_2\hat{e}_1 = \hat{e}_3 \\ \hat{e}_2\hat{e}_3 &= -\hat{e}_3\hat{e}_2 = \hat{e}_1 \\ \hat{e}_3\hat{e}_1 &= -\hat{e}_1\hat{e}_3 = \hat{e}_2 \end{aligned} \tag{3}$$

The center of the biquaternion algebra is the set of real and complex numbers. As can be seen from the definition of biquaternion, the product of two biquaternions is not commutative. However, the product of two biquaternions is associative.

Biquaternion $\mathbb{q}$ in terms of its scalar $q_0$ and vector $\boldsymbol{q}$ parts can be represented as:

$$\mathbb{q} = q_0 + \boldsymbol{q} \tag{4}$$

Here the scalar component and the vector component of the biquaternion, respectively, are written as:

$$\begin{aligned} q_0 &= q_0\hat{e}_0 \\ \mathbf{q} &= q_1\hat{e}_1 + q_2\hat{e}_2 + q_3\hat{e}_3, \end{aligned} \tag{5}$$

Another useful representation of the biquaternion can be expressed follows as:

$$\mathbb{q} = [q_0, q_1, q_2, q_3] \tag{6}$$

The result of $\mathbb{p}$ and $\mathbb{q}$ biquaternions multiplication is still biquaternion. The multiplication is given by following equations:

$$\mathbb{p}\mathbb{q} = p_0q_0 - \boldsymbol{p}\cdot\boldsymbol{q} + p_0\boldsymbol{q} + q_0\boldsymbol{p} + \boldsymbol{p}\times\boldsymbol{q}. \tag{7}$$

The conjugate of biquaternion $\overline{\mathbb{q}}$ is denoted as:

$$\overline{\mathbb{q}} = q_0\hat{e}_0 - q_1\hat{e}_1 - q_2\hat{e}_2 - q_3\hat{e}_3 = [q_0, -\boldsymbol{q}] \tag{8}$$

The complex conjugate of biquaternion $\mathbb{q}^*$ is denoted as:

$$\mathbb{q}^* = q_0^*\hat{e}_0 + q_1^*\hat{e}_1 + q_2^*\hat{e}_2 + q_3^*\hat{e}_3 \tag{9}$$

And then,

ISBN: 978-605-73552-2-5

$$\begin{aligned} q_0^* &= q_0 - iq_0' \\ q_1^* &= q_1 - iq_1' \\ q_2^* &= q_2 - iq_2' \\ q_3^* &= q_3 - iq_3' \end{aligned} \tag{10}$$

The conjugate of the biquaternions multiplication, $\mathbb{p}$ and $\mathbb{q}$, is given by the following equation

$$\overline{\mathbb{pq}} = \overline{\mathbb{qp}} \tag{11}$$

while the complex conjugate of the biquaternions multiplication [5] is

$$(\mathbb{pq})^* = \mathbb{q}^*\mathbb{p}^*. \tag{12}$$

## 3. THE GENERALIZED BIQUATERNIONIC NAVIER-STOKES EQUATION WITH QUANTUM POTENTIAL AND FLUCTUATING VISCOSITY

The original Navier-Stokes equation includes momentum changes affecting the unit mass in the fluid, pressure changes and viscous forces causing friction losses. The fluid motion of the non-relativistic quantum space is tried to be rewritten with biquaternion algebra. The original Navier-Stokes equation to include quantum potential and fluctuating viscosity was tried to be redefined with biquaternion algebra. The modified Navier- Stokes equation can be written as follows [15]:

$$\rho_m \left(\frac{\partial v}{\partial t} + (v \cdot \nabla)v\right) = F(r,t) - \rho_m \nabla\left(\frac{\mathrm{P}}{\rho_m}\right) + \mu(t)\nabla^2 v \tag{13}$$

$\rho_m = m/\Delta V$ is the mass density per unit volume $\Delta V$. $F(r,t)$ is the external force distributed in the volume. The last two terms give the modification of Navier-Stokes equation. Here P and $\mu(t)$ are the pressure and dynamic viscosity coefficients, respectively.

Biquaternionic velocity $\mathbb{v}$ is dependent on space and time and has irrotational $\mathbf{v}$ and solenoidal $i\mathbf{v}'$ vector functions, respectively related to the vortex-free and vortex-motion in fluid medium. We can introduce the biquaternionic velocity $\mathbb{v}$ as:

$$\mathbb{v} = [0, \mathrm{v}_1 + i\mathrm{v}_1', \mathrm{v}_2 + i\mathrm{v}_2', \mathrm{v}_3 + i\mathrm{v}_3'] \tag{14}$$

The scalar component of biquaternionic velocity is zero. The vector components can be defined in $\boldsymbol{v} = \mathbf{v} + i\mathbf{v}'$ and provide the following equations [15, 16]:

$$\begin{aligned} \nabla \cdot \mathbf{v} &= \chi\,, \\ \nabla \times \mathbf{v} &= 0\,, \\ \nabla \cdot i\mathbf{v}' &= 0\,, \\ \nabla \times i\mathbf{v}' &= i\boldsymbol{\omega}\,. \end{aligned} \tag{15}$$

Here, $\boldsymbol{\omega}$ is named as the vorticity. The operator $\nabla$ is expressed:

$$\nabla = \{0, \partial_x, \partial_y, \partial_z\}\,. \tag{16}$$

Biquaternionic multiplication $\nabla\mathbb{v}$ can be defined as the following equation:

$$\nabla\mathbb{v} = -\chi + i\,\boldsymbol{\omega}\,. \tag{17}$$

ISBN: 978-605-73552-2-5

Also using the action is defined as $\mathbf{v} = \frac{\nabla S}{m}$, the scalar function $S$ can be in $\mathrm{v}_1$, $\mathrm{v}_2$ and $\mathrm{v}_3$ in detail

$$\mathbb{v} = \left[0, \frac{\partial_x S}{m} + i\mathrm{v}_1', \frac{\partial_y S}{m} + i\mathrm{v}_2', \frac{\partial_z S}{m} + i\mathrm{v}_3'\right]. \tag{18}$$

The biquaternionic generalized momentum $\mathbb{P}$ can be written follows:

$$\mathbb{P} = m[0, \mathrm{v}_1 + i\mathrm{v}_1', \mathrm{v}_2 + i\mathrm{v}_2', \mathrm{v}_3 + i\mathrm{v}_3'] \tag{19}$$

and then

$$\mathbb{P} = \left[0, \partial_x S + im\mathrm{v}_1', \partial_y S + im\mathrm{v}_2', \partial_z S + im\mathrm{v}_3'\right]. \tag{20}$$

The biquaternionic convective derivative □ can be expressed as

$$\square = \left[\frac{\partial}{\partial t} + \boldsymbol{v}\cdot\nabla, 0, 0, 0\right]. \tag{21}$$

We present the terms $\boldsymbol{v}\cdot\nabla$ and □ as follows:

$$\boldsymbol{v}\cdot\nabla = (\mathrm{v}_1 + i\mathrm{v}_1')\partial_x + (\mathrm{v}_2 + i\mathrm{v}_2')\partial_y + (\mathrm{v}_3 + i\mathrm{v}_3')\partial_z \tag{22}$$

and

$$\square = \left\{\frac{\partial}{\partial t} + (\mathrm{v}_1 + i\mathrm{v}_1')\partial_x + (\mathrm{v}_2 + i\mathrm{v}_2')\partial_y + (\mathrm{v}_3 + i\mathrm{v}_3')\partial_z, 0, 0, 0\right\} \tag{23}$$

If the expression $\boldsymbol{v}\cdot\nabla$ is used in equation (23), the biquaternionic force $\mathbb{F}$ can derived as following equation:

$$\begin{aligned}\mathbb{F} = \mathrm{m}\square\mathbb{v} = m\frac{\partial}{\partial t}\{(\mathrm{v}_1 + i\mathrm{v}_1')e_1 + (\mathrm{v}_2 + i\mathrm{v}_2')e_2 + (\mathrm{v}_3 + i\mathrm{v}_3')e_3\} + m(\mathrm{v}_1\partial_x)\mathrm{v}_1 e_1 + m(\mathrm{v}_2\partial_y)\mathrm{v}_2 e_2 + \\ m(\mathrm{v}_3\partial_z)\mathrm{v}_3 e_3 - m(\mathrm{v}_1'\partial_x)\mathrm{v}_1' e_1 - m(\mathrm{v}_2'\partial_y)\mathrm{v}_2' e_2 - m(\mathrm{v}_3'\partial_z)\mathrm{v}_3' e_3 + im(\mathrm{v}_1\partial_x)\mathrm{v}_1' e_1 + \\ im(\mathrm{v}_2\partial_y)\mathrm{v}_2' e_2 + im(\mathrm{v}_3\partial_z)\mathrm{v}_3' e_3 + im(\mathrm{v}_1'\partial_x)\mathrm{v}_1 e_1 + im(\mathrm{v}_2'\partial_y)\mathrm{v}_2 e_2 + im(\mathrm{v}_3'\partial_z)\mathrm{v}_3 e_3 + \\ m[(\mathrm{v}_1\partial_x)\mathrm{v}_2 - (\mathrm{v}_1'\partial_x)\mathrm{v}_2']e_2 + i[(\mathrm{v}_1\partial_x)\mathrm{v}_2' + (\mathrm{v}_1'\partial_x)\mathrm{v}_2]e_2 + [(\mathrm{v}_1\partial_x)\mathrm{v}_3 - (\mathrm{v}_1'\partial_x)\mathrm{u}_3]e_3 + \\ i[(\mathrm{v}_1\partial_x)\mathrm{v}_3' + (\mathrm{v}_1'\partial_x)\mathrm{v}_3]e_3 + \left[(\mathrm{v}_2\partial_y)\mathrm{v}_1 - (\mathrm{v}_2'\partial_y)\mathrm{v}_1'\right]e_1 + i\left[(\mathrm{v}_2\partial_y)\mathrm{v}_1' + (\mathrm{v}_2'\partial_y)\mathrm{v}_1\right]e_1 + \\ \left[(\mathrm{v}_2\partial_y)\mathrm{v}_3 - (\mathrm{v}_2'\partial_y)\mathrm{u}_3\right]e_3 + i\left[(\mathrm{v}_2\partial_y)\mathrm{u}_3 + (\mathrm{v}_2'\partial_y)\mathrm{v}_3\right]e_3 + [(\mathrm{v}_3\partial_z)\mathrm{v}_1 - (\mathrm{v}_3'\partial_z)\mathrm{v}_1']e_1 + \\ i[(\mathrm{v}_3\partial_z)\mathrm{v}_1' + (\mathrm{v}_3'\partial_z)\mathrm{v}_1]e_1 + [(\mathrm{v}_3\partial_z)\mathrm{v}_3 - (\mathrm{v}_3'\partial_z)\mathrm{u}_2]e_2 + i[(\mathrm{v}_3\partial_z)\mathrm{v}_2' + (\mathrm{v}_3'\partial_z)\mathrm{v}_2]e_2\end{aligned} \tag{24}$$

Equation (24) can be arranged as

$$\mathbb{F} = m\frac{\partial \mathbf{v}}{\partial t} + im(\mathbf{v}\cdot\nabla)\mathbf{v}' + im(\mathbf{v}'\cdot\nabla)\mathbf{v} + im\frac{\partial \mathbf{v}'}{\partial t} + m(\mathbf{v}\cdot\nabla)\mathbf{v} - m(\mathbf{v}'\cdot\nabla)\mathbf{v}'. \tag{25}$$

Here biquaternionic velocity is

$$\frac{\nabla\mathbb{v}^2}{2} = \frac{\nabla(\mathbf{v}+i\mathbf{v}')^2}{2} = -(\mathbf{v}'\cdot\nabla)\mathbf{v}' - \mathbf{v}'\times(\nabla\times\mathbf{v}') + (\mathbf{v}\cdot\nabla)\mathbf{v} + i(\mathbf{v}\cdot\nabla)\mathbf{v}' + i(\mathbf{v}'\cdot\nabla)\mathbf{v} + i\mathbf{v}\times(\nabla\times\mathbf{v}') \tag{26}$$

and

$$\frac{\nabla(\mathbf{v}+i\mathbf{v}')^2}{2} + \mathbf{v}'\times(\nabla\times\mathbf{v}') - i\mathbf{v}\times(\nabla\times\mathbf{v}') = -(\mathbf{v}'\cdot\nabla)\mathbf{v}' + (\mathbf{v}\cdot\nabla)\mathbf{v} + i(\mathbf{v}\cdot\nabla)\mathbf{v}' + i(\mathbf{v}'\cdot\nabla)\mathbf{v}. \tag{27}$$

Here $\nabla\times\mathbf{v}' = \boldsymbol{\omega}$.

ISBN: 978-605-73552-2-5

The biquaternionic expression of $\boldsymbol{\omega}$ is $\mathcal{w}$. Biquaternionic velocity and vorticity are substituted in the equation 27, and rearranged

$$\frac{\nabla \mathbb{v}^2}{2} - i\mathbb{v}\mathcal{w} = (\mathrm{v}\cdot\nabla)\mathrm{v} - (\mathrm{v}'\cdot\nabla)\mathrm{v}' + i(\mathrm{v}\cdot\nabla)\mathrm{v}' + i(\mathrm{v}'\cdot\nabla)\mathrm{v}. \tag{28}$$

When the expression is used in force,

$$\mathbb{F} = m\frac{\partial \mathrm{v}}{\partial t} + im\frac{\partial \mathrm{v}'}{\partial t} + m\frac{\nabla \mathbb{v}^2}{2} - im\mathbb{v}\mathcal{w} \tag{29}$$

The biquaternionic force $\mathbb{F}$ can also be written in terms of the biquaternionic potential $\mathbb{V}$:

$$\mathbb{F} = -\nabla\,\mathbb{V} \tag{30}$$

The biquaternionic potential $\mathbb{V}$ includes the quantum potential $Q$, the kinetic viscosity coefficient $v(t)$ and the other potential $U$ , arising due to external force, and can be defined as

$$\mathbb{F} = -\nabla\,(Q + U + v(t)\nabla^2\,\mathbb{v}) \tag{31}$$

and then if the force expression is substituted in terms of velocity the force,

$$m\frac{\partial \mathrm{v}}{\partial t} + im\frac{\partial \mathrm{v}'}{\partial t} + m\frac{\nabla \mathbb{v}^2}{2} - im\mathbb{v}\mathcal{w} = -\nabla\,(Q + U - v(t)\nabla\,\mathbb{v}). \tag{32}$$

If irrotational vector function of the velocity is $\mathrm{v} = \frac{\nabla \mathrm{S}}{m}$,

$$\nabla\left(\frac{\partial \mathrm{S}}{\partial t} - \frac{1}{2m}(\nabla \mathrm{S})^2 + \frac{m}{2}\mathrm{v}'^2 + Q + U - v(t)\nabla^2 S\right) = -im\frac{\partial}{\partial t}\mathrm{v}' + im\mathbb{v}\mathcal{w} + imv(t)\nabla^2\mathrm{v}' + i\nabla\left(\mathrm{v}'\frac{\nabla \mathrm{S}}{m}\right) \tag{33}$$

$$\nabla\left(\frac{\partial \mathrm{S}}{\partial t} - \frac{1}{2m}(\nabla \mathrm{S})^2 + \frac{m}{2}\mathrm{v}'^2 + Q + U - v(t)\nabla^2 S\right) + i\left(m\frac{\partial}{\partial t}\mathrm{v}' - m\mathbb{v}\mathcal{w} - mv(t)\nabla^2\mathrm{v}' - \nabla\left(\mathrm{v}'\frac{\nabla \mathrm{S}}{m}\right)\right) = 0 \tag{34}$$

$$\frac{\partial \mathrm{S}}{\partial t} - \frac{1}{2m}(\nabla \mathrm{S})^2 + \frac{m}{2}\mathrm{v}'^2 = -Q - U + v(t)\nabla^2 S \tag{35}$$

$$\frac{\partial}{\partial t}\mathrm{v}' - \mathbb{v}\mathcal{w} = +v(t)\nabla^2\mathrm{v}' + \nabla\left(\mathrm{v}'\frac{\nabla \mathrm{S}}{m}\right) \tag{36}$$

## 4. CONCLUSIONS

The quantum potential is different from the classical potential and related to the change in the density. Therefore, the fluid's equation of motion must include the quantum potential. In this study the Navier-Stokes equation, modified to include quantum potential and fluctuating viscosity for motions of the quantum fluid medium, is tried to be represented with biquaternion algebra. It was shown that the biquaternionic expression is re-derived with relation between biquaternionic force and potential, including the quantum potential, the kinetic viscosity coefficient and the other potential. Biquaternions algebras used in this study have extended to complex number system. Biquaternions are useful and effective mathematical structure for representing quantum hydrodynamics and their research areas. It is obvious that will be useful algebra for the defining quantum hydrodynamics as one of the new research fields in fluid dynamics, therefore the biquaternionic wavefunction will be tried to represented.

ISBN: 978-605-73552-2-5

## REFERENCES

[1] Arbab A.I. Dynamics of a moving quantum charged particle. Optik 2021, 233: 166550.

[2] Madelung E. Z. Quanten theorie in hydrodynamischer Form Physik 1926, 40: 322.

[3] Sengupta S. Evolution and dynamics of quantum fluids. Quantum Hydrodynamics 2021.

[4] Lin C T, Kuo J K, Yen T H. Quantum fluid dynamics and quantum computational fluid dynamics. Journal of Computational and Theoretical Nanoscience 2009, 6: 1090–1108.

[5] Córdoba P. Fernández de, Isidro J M, Molina J V. Schroedinger vs. Navier–Stokes. Entropy 2016, 18, 34.

[6] Bohm D. A Suggested interpretation of the quantum theory in terms of "hidden" variables. I. Phys. Rev. 1952, 85.

[7] Mironov Victor L, Mironov Sergey V. Sedeonic equations of ideal fluid. Journal of Mathematical Physics 2017, 58: 083101.

[8] Mironov Victor L. Self-consistent hydrodynamic two-fluid model of vortex plasma. Phys. Fluids 2021, 33: 037116.

[9] Rawat S, Negi O.P.S. Quaternionic Formulation of Supersymmetric Quantum Mechanics. Int J Theor Phys 2009 48: 305–314.

[10] Demir S, Tanışlı M, Şahin N, Kansu M.E. Biquaternionic reformulation of multifluid plasma equations. Chinese Journal of Physics 2017 55: 1329–1339.

[11] Sbitnev Valeriy I. Quaternion algebra on 4D superfluid quantum space-time: can dark matter be a manifestation of the superfluid ether? Universe. 2021; 7, 32.

[12] Heifetz E, Tsekov R, Cohen E, Nussinov Z. On entropy production in the Madelung fluid and the role of Bohm's potential in classical diffusion. Found Phys, 2016; 46, 815–824.

[13] Tanışlı M, Demir S. Biquaternionic description of the Schrödinger equation. Mathematical and Computational Applications 2012; 2: 176-181.

[14] Özgür G. Bikuaternionların Alternatif Cebirlerinin Karşılaştırılması ve Bikuaternionik Dirac Denklemi Master Thesis Anadolu University Institute of Science and Technology 2002.

[15] Sbitnev Valeriy I. Hydrodynamics of superfluid quantum space: de Broglie interpretation of the quantum mechanics. Quantum Stud.: Math. Found. 2018; 5:257–271.

[16] Muralidhar K. Theory of stochastic Schrödinger equation in complex vector space. Foundations of Physics 2017; 47, 532–552.

ISBN: 978-605-73552-2-5

# LYSOGENIC PHAGE ISOLATION FROM METHICILLIN-RESISTANT *S. aureus* CLINICAL ISOLATES

**Senanur DOKUZ[1,*], Görkem GÜNGÖR[1], Tülin ÖZBEK[1*]**

[1] Yıldız Technical University, Faculty of Arts and Sciences, Molecular Biology and Genetics, İstanbul, Turkey.

*** Assoc. Prof. Dr. Tülin ÖZBEK, ozbektulin@gmail.com, 05052364004**

## ABSTRACT

Bacterio(phage)s, the most abundant entities on our planet, are driving forces for the development of their pathogenicity and play important roles in bacterial adaptive evolution. Phages can follow lysogenic and lytic life cycles. Lysogenic phages integrate their genomes into the bacterium genome. The phage following the lytic cycle is a virulent phage, after attaching to the host cell, the nucleic acid of the phage enters the cell, hundreds of phage copies are produced in bacteria, and the phage particles are released into the environment by lysing the cell. Integration of lysogenic phages into the genome is a process that can change gene expression in bacteria, bring genes in the cell that provide advantages such as antibiotic resistance, create new phenotypes, and result in virulence factor production of the bacteria. In the presence of stress factors such as temperature change, hydrogen peroxide and mitomycin-C, phage can leave the lysogenic cycle and switch to the lytic cycle.

Methicillin-resistant Staphylococcus aureus (MRSA) is one of the strains that are especially important among nosocomial infections, cause many diseases like skin infections, impetigo, endocarditis, osteomyelitis, toxic shock syndrome and have developed antibiotic resistance. In this study, phage filtrates from MRSA clinical strain were obtained by applying mitomycin-C and hydrogen peroxide at different concentrations and changing the incubation temperature of the bacteria. The lytic effect was observed by performing spot tests using S. aureus RN4220 and MRSA strains. As a result of sequencing the obtained genome, it is aimed to contribute to the literature by discovery of new phage species, understanding the effects of lysogenic MRSA phages on MRSA strains, understanding the formation process of antibiotic resistance profile, analysis of virulence factors created by the lysogenic genome, and determination of integration regions of prophage.

**Keywords:** Bacteriophage, *S. aureus*, MRSA, mitomycin-C, lysogenic phages

## 1. INTRODUCTION

Antibiotics have been used for the treatment of bacterial diseases as effective medicines since their discovery. The resistance development of pathogens to many antibiotics and the inability of new antibiotic discovery or synthetic production to keep up with the resistance development rate of pathogens has become the most important problem for the treatment of infectious diseases [1]. Analyzing the mechanism of the antibiotic resistance profile, which is the result of unconscious and incorrect of antibiotics, is very important to overcome this resistance. Among the 6179 sequenced microbial genomes, 84% have at least one antibiotic resistance gene, including mostly non-pathogenic bacteria in soils and mud as well as humans and animals. According to the study in the "World health statistics 2022" report published by WHO, the global average of "Proportion of bloodstream infections due methicillin resistant Staphylococcus aureus" in 194 countries is 36%. Antibiotic resistance genes are carried by horizontal gene transfer. Understanding the mechanism of gene transfer and the conditions of spread among pathogens is very important for the treatment of infectious agents, especially common among humans and difficult to treat [2,3]. Bacteriophages that follow the lysogenic life cycle are called prophages after they integrate into the genome of their host. They are like vehicles that increase the virulence and survival of their hosts, carry genes that make their hosts resistant to antibiotics, and contribute to increased genetic diversity in bacteria. Methicillin-resistant *Staphylococcus aureus* (MRSA), which causes life-threatening and dangerous infections with a high rate of transmission, appears to be sensitive to anti-MRSA antibiotics in vitro (according to CLSI standards), but does not respond to treatment at in vivo studies. The antibiotic resistance profile of MRSA, which has resistance to penicillin-like beta-lactam antibiotics, is mostly dependent on phage(s) integrated in its genome, and understanding the integration mechanism and its effects is one of the important goals worldwide. Prophages, which exist between 1 and 4 in the genomes of all MRSA clinical isolates, can be induced by UV light, chemicals such as hydrogen peroxide, antibiotics such as mitomycin-C, environmental stresses such as temperature or pH changes. They can cause their separation from the bacterial genome and transition to the lytic cycle [5]. The elucidation, characterization and genomic studies of the structures of phage particles formed by the induction of prophages integrated into the genome of their hosts will provide answers to many existing questions and problems. By identifying the antibiotic resistance genes and virulence factor genes they carry in their genomes, it is possible to

ISBN: 978-605-73552-2-5

understand the mechanism of infectious diseases caused by their hosts, the pathogenicity of their hosts, to reduce their spread and to develop treatment strategies [6]. Integration sites and integration mechanisms of prophages into the genome can be elucidated. The functions of unknown gene regions can be understood using both sequencing and function-based metagenomic approaches. The uncertainty of environmental factors that support or prevent lysogeny can be eliminated and controlled [7]. It may lead to the identification of phage particles that can play a role in the phage therapy approach, which is an alternative and powerful treatment approach against infectious agents, whose value has been re-understood due to the increase in antibiotic resistance today [8]. The discovery of unidentified phage(s) may contribute to the literature. Identification of the phage genome by genomic annotation can create important and valuable application areas such as i) its use as a natural carrier vector due to its ability to integrate into the genome of its host [9], ii) the use of the endolysin protein of the phage for antimicrobial purposes [10], iii) designing the receptor binding protein as a therapeutic agent that enables it to specifically target its host, iv) the use of capsid proteins as vaccine antigens due to their specific three-dimensional structure [11], v) enabling its use as a modulator of mammalian immune responses [12].

In the present study, the culturing of the clinical isolate MRSA strain, the induction of prophage/prophages integrated into the bacterial genome with MMC and hydrogen peroxide, the extraction and detection of the prophage from the genome by lytic cycling were carried out. A study was carried out that will lead to further studies in understanding the antibiotic resistance and pathogenicity of the MRSA strain and prophage relationship, analyzing the mechanism of integration of the detected prophage into the genome, bringing the previously undefined prophage and the performed methodology to the literature, and identifying the prophage/prophages obtained by genomic annotation

## 2. MATERIALS AND METHODS

### 2.1. Bacterial Strains and Culture Conditions

Clinically isolated MRSA and *S. aureus* RN4220 strains were stored in Luria-Bertani (LB) broth medium containing 15% glycerol at -80 °C. Bacteria were inoculated on LB agar medium and cultured at 37 °C overnight. Colonies grown on LB agar were stored at 4 °C to be used in studies.

### 2.2. Mitomycin-C Preparation

1 mg of MMC was weighed and then taken up in 1 mL of 10% methanol and dissolved using vortex. It was diluted with sterile water at 1, 3 and ug/mL concentrations to be used in the study.

### 2.3. Prophage Induction

#### 2.3.1. Induction with Hydrogen Peroxide

MRSA were grown in LB broth medium at 37 °C overnight in LB broth medium shaking speed of 180 rpm for the induction experiment. 100 µl of the overnight cultures were transferred to 10 mL of fresh LB broth mediums and incubated 37 °C with shaking at 180 rpm. When the $0D_{600}$ value of the cultures reached 0.5-0.6, hydrogen peroxide (Sigma Aldrich) induction started. 0.5, 1, 1.5 µl of hydrogen peroxide were added to the cultures, respectively. One set of culture was incubated at 37 ºC and the other at 44 ºC for 4 hours with shaking at 180 rpm [13,14].

#### 2.3.2. Induction with MMC

MRSA were grown in LB broth medium at 37 °C overnight in LB broth medium shaking speed of 180 rpm for the induction experiment. 100 µl of the overnight cultures were transferred to 10 mL of fresh LB broth mediums and incubated 37 °C with shaking at 180 rpm. When the $0D_{600}$ value of the cultures reached 0.5-0.6, MMC (Sigma Aldrich) induction started. 1, 3, 5 µg/mL of MMC were added to the cultures, respectively. One set of culture was incubated at 37 ºC for 30 min and the other at 44 ºC for 4 h with shaking at 180 rpm [14,15].

### 2.4. Obtaining Phage Filtrates

At the end of the induction and incubation carried out under the specified conditions, the cells were precipitated by centrifugation at 5000 x g for 3 min. After centrifugation, the supernatant was filtered into a clean falcon tube using a sterile 0.22 µm filter (Aisimo Syringe Filter) and phage filtrate was obtained.

### 2.5 Spot Assay

A single colony was taken from the petri dish of *S. aureus* RN4220 strain stocked at 4 ºC and incubated overnight in 3 mL of LB medium. After incubation, the culture was diluted to $OD_{600}$=0.2 ($10^8$ cfu/mL cells). 100 µl of the prepared $10^8$ cfu/mL cell culture was dropped onto the BHI agar (Merck Millipore) petri dishes. Cells were spread using swabs

ISBN: 978-605-73552-2-5

to cover the entire agar surface. After pre-incubation at 37 ºC for 1 h, 10 µl of phage filtrates were taken and dropped onto *S. aureus* RN4220. Petri dishes were incubated at 37 ºC overnight [16].

## 3. RESULTS

The spot test of the phage filtrates obtained as a result of the determined hydrogen peroxide and MMC concentrations, temperatures and incubation times of the cultures was performed.

### 3.1. Induction with Hydrogen Peroxide

Hydrogen peroxide induction was carried out with three different concentrations and two different temperature conditions. 0.5, 1 and 1.5 µl of hydrogen peroxide were added to the cultures and the cultures were incubated for 4 h at 37 ºC and 44 ºC. Figure 1 shows the zones of the spot test after incubation of the determined concentrations of hydrogen peroxide at 37 ºC for 4 h, and Figure 2 shows the zones of the spot test after the incubation of the determined concentrations of hydrogen peroxide at 44 ºC for 4 h.

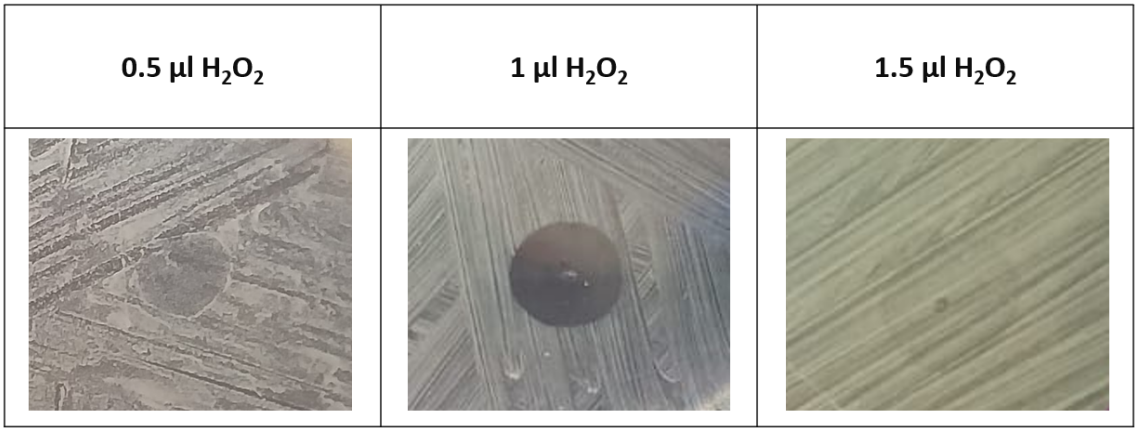


**Figure 1.** Spot test with phage filtrates obtained after 4 h incubation at 37 ºC with determined hydrogen peroxide concentrations

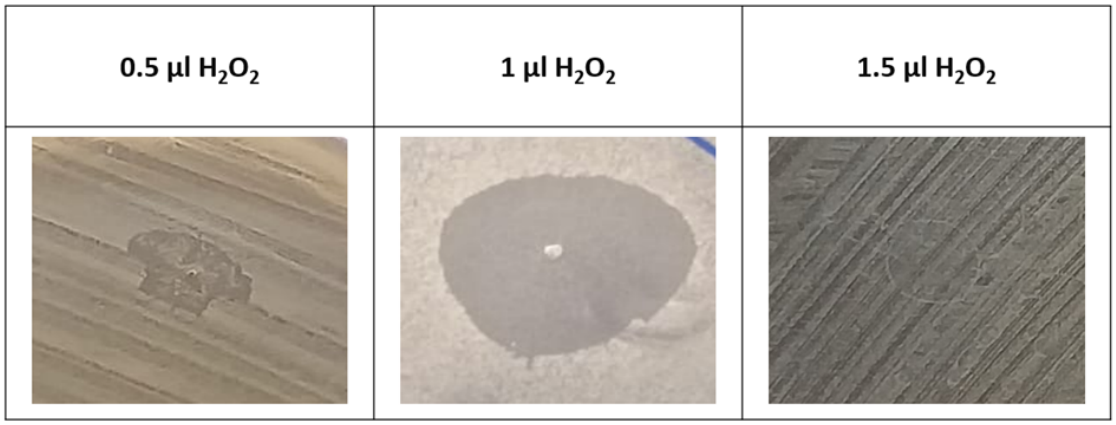


**Figure 2.** Spot test with phage filtrates obtained after 4 h incubation at 44 ºC with determined hydrogen peroxide concentrations

### 3.2. Induction with MMC

MMC induction was carried out with three different concentrations and two different incubation times. 1, 3 and 5 µg/mL of MMC were added to the cultures and the cultures were incubated at 37 ºC for 30 min and 4 h. Table 3 shows the zones of the spot test after incubation of the determined concentrations of MMC at 37 ºC for 30 min, and Table 4 shows the zones of the spot test after the incubation of the determined concentrations of MMC at 37 ºC for 4 h.

ISBN: 978-605-73552-2-5

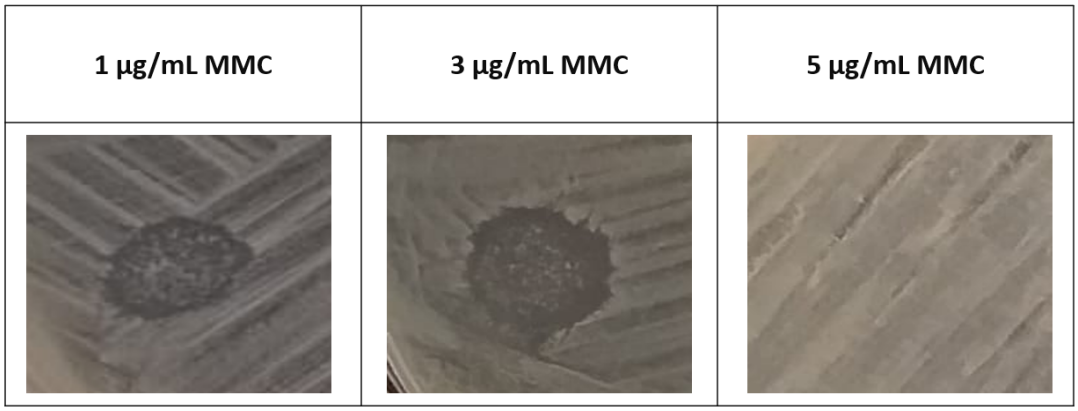


**Figure 3.** Spot test with phage filtrates obtained after 30 min incubation at 37 °C with determined MMC concentrations

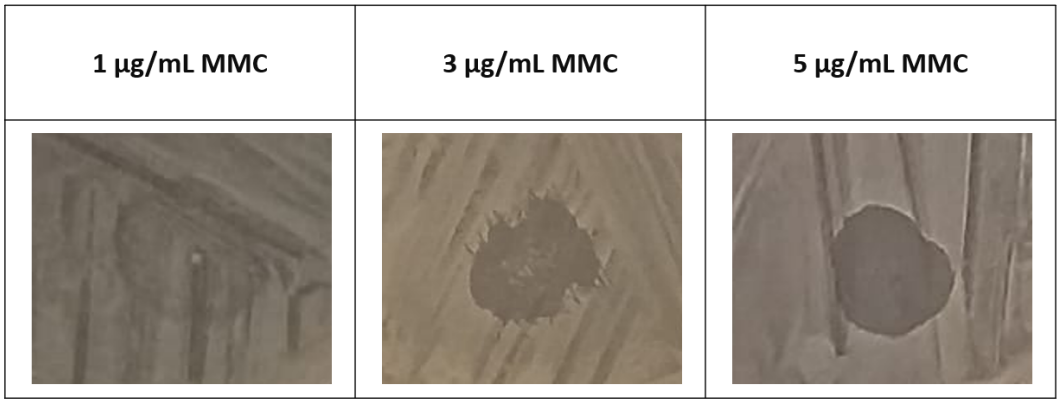


**Figure 4.** Spot test with phage filtrates obtained after 4 h incubation at 37 °C with determined MMC concentrations

## DISCUSSION

In order for the prophage regions, which are integrated into the genome of the MRSA strain, to pass into the lytic life cycle, the bacterial culture was induced with certain concentrations of hydrogen peroxide and MMC and incubated at certain temperatures and times.

Spot testing was performed using *S. aureus* RN4220 strain with phage filtrates obtained from MRSA cultures incubated for 4h at 37 ºC and 44 ºC after induction with 0.5, 1 and 1.5 ul hydrogen peroxide. When the results were evaluated, the phage/phages induced and obtained with 1 µl of hydrogen peroxide under two different temperature conditions gave a clean zone that appears to have high lysis ability. In the application of 1.5 ul hydrogen peroxide, since it is a very faint image, it is seen that a clean zone is not formed and bacteria are not lysed. The phage filtrate obtained from cultures induced with 0.5 µl hydrogen peroxide after incubation at two different temperatures appeared to produce a clearer zone of bacteria than the phage filtrate obtained from cultures induced with 1 µl hydrogen peroxide, but clearer than the phage filtrate obtained from cultures induced with 1.5 µl hydrogen peroxide. (Table1-2) [16,17].

Spot testing was performed using *S. aureus RN4220* strain with phage filtrates obtained from MRSA cultures incubated for 30 min and 4 h at 37ºC after induction with 1, 3 and 5 µg/mL MMC. In cultures incubated for 30 min at 37ºC, phage filtrates obtained after induction of 1 and 3 µg/mL MMC formed a turbid zone, but phage filtrate obtained after induction of 5 µg/mL MMC did not. Therefore, the ability of phage filtrates from cultures induced with 1 and 3 µg/mL MMC to lyse bacteria is higher than that of phage filtrate obtained from culture induced with 5 µg/mL MMC. In cultures incubated for 4 h at 37ºC, the zone formed by the phage filtrate obtained after induction of 3 and 5 ug/mL MMC was found to be cleaner compared to the zone formed by the phage filtrate obtained after induction of 1 ug/mL MMC. Therefore, the ability of phage filtrates from cultures induced with 3 and 5 µg/mL MMC to lyse bacteria is higher than that of phage filtrate obtained from culture induced with 1 µg/mL MMC. (Table 3-4) [16,17]. With the results of the study, it was shown that the MRSA strain we used contains prophage regions as stated in the literature, and that by inducing these regions under certain stress conditions, different densities, lysing rate and perhaps different phages can be obtained.

ISBN: 978-605-73552-2-5

As in the study of Filipiak et al., 2020 when *Escherichia coli* was induced with MMC at different concentrations and then incubated at different times, it was observed that the prophage regions were released from the genome and lysis plaques were better formed over time. In our study, however, it was determined that the duration did not have a curative effect on lysis [18]. In the study of Los et al., 2010 prophage regions were induced with hydrogen peroxide and phage plaques were obtained, but different incubation temperatures were not tried as in our study. In our study, we also aimed to contribute to the literature by experimenting with different incubation temperatures [19].

## CONCLUSION

Antibiotic resistance genes, which play a major role in the pathogenesis of bacteria, are an increasing and unavoidable problem in the world. The antibiotic resistance phenotype formed by this gene region carried by the bacterium can be provided by prophages embedded in its genome. The elucidation and characterization of their structures and genomes is of great importance because of the value of phage and phage subunits in the fields of health and biotechnology. The study will especially lead to the understanding of the antibiotic resistance mechanism of the bacteria, the analysis of the virulence factors produced by the bacterium and playing a major role in its pathogenicity, the discovery of the new phage type(s), the clarification of the integration of the phage into the genome, to give the way for its use in phage therapy, and understanding the bacteria-phage interaction. In our study, clinical isolate MRSA culture was induced with hydrogen peroxide and MMC at certain concentrations, followed by incubation at different temperatures and times, in order to obtain prophages embedded in its genome (Figure 5).

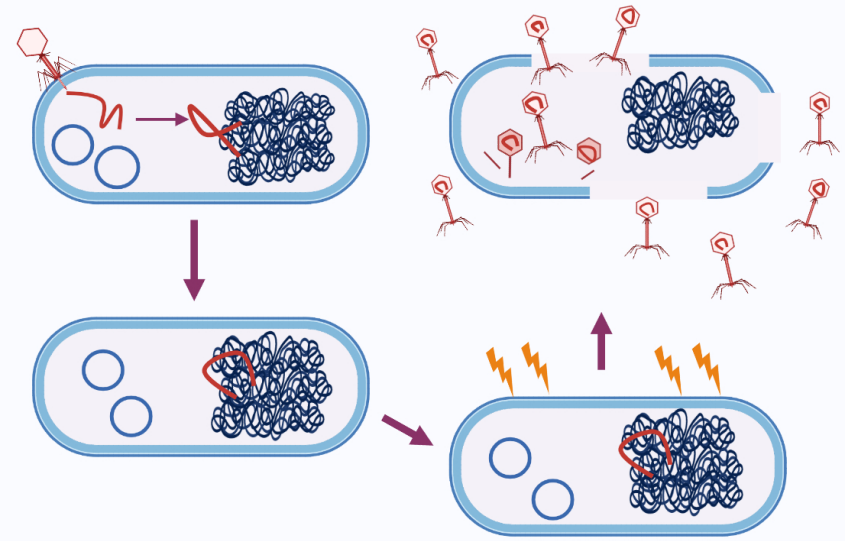

**Figure 5.** Integration of phage genome to the bacterial genome and induction of prophage to enter lytic life cycle (created in Biorender.com)

## ACKNOWLEDGEMENTS

This study was supported by the project number 120R016 of The Scientific and Technological Research Council of Turkey.

## REFERENCES

1. Xu L, Gu J, Wang X, et al. Risk of horizontal transfer of intracellular, extracellular, and bacteriophage antibiotic resistance genes during anaerobic digestion of cow manure. *Bıoresource Technol*. 2022;351. doi:10.1016/j.biortech.2022.127007
2. Wang W, Li H, Li M, et al. Molecular Evolution and Genomic Insights into Community-Acquired Methicillin-Resistant Staphylococcus aureus . *Microbiology Spectrum*.
3. Enault F, Briet A, Bouteille L, Roux S, Sullivan MB, Petit MA. Phages rarely encode antibiotic resistance genes: A cautionary tale for virome analyses. *ISME J*. 2017;11(1). doi:10.1038/ismej.2016.90
4. Kondo K, Kawano M, Sugai M. Prophage elements function as reservoir for antibiotic resistance and virulence genes in nosocomial pathogens. *bioRxiv*. Published online 2020.

5. Stanczak-Mrozek KI, Laing KG, Lindsay JA. Resistance gene transfer: Induction of transducing phage by sub-inhibitory concentrations of antimicrobials is not correlated to induction of lytic phage. *J Antimicrob Chemoth*. 2017;72(6). doi:10.1093/jac/dkx056
6. Balcazar JL. Bacteriophages as Vehicles for Antibiotic Resistance Genes in the Environment. *PLoS Pathog*. 2014;10(7). doi:10.1371/journal.ppat.1004219
7. Luque A, Silveira CB. Quantification of Lysogeny Caused by Phage Coinfections in Microbial Communities from Biophysical Principles. *mSystems*. 2020;5(5). doi:10.1128/msystems.00353-20
8. Mann NH. The potential of phages to prevent MRSA infections. *Res Microbiol*. 2008;159(5). doi:10.1016/j.resmic.2008.04.003
9. Chen Y, Yang L, Yang D, et al. Specific Integration of Temperate Phage Decreases the Pathogenicity of Host Bacteria. *Front Cell Infect Mi*. 2020;10. doi:10.3389/fcimb.2020.00014
10. Alaksandr Ž, Sergey G, Maksim P, et al. Efficient matrix-assisted refolding of the recombinant anti-staphylococcal truncated endolysin LysKCA and its structural and enzymatic description. *Protein Expres Purif*. 2020;174. doi:10.1016/j.pep.2020.105683
11. Sun Y, Roznowski AP, Tokuda JM, et al. Structural changes of tailless bacteriophage Φx174 during penetration of bacterial cell walls. *Proc Natl Acad Sci U S A*. 2017;114(52). doi:10.1073/pnas.1716614114
12. Cieślik M, Bagińska N, Jończyk-Matysiak E, Węgrzyn A, Węgrzyn G, Górski A. Temperate bacteriophages—the powerful indirect modulators of eukaryotic cells and immune functions. *Viruses*. 2021;13(6). doi:10.3390/v13061013
13. Łoś JM. Hydrogen peroxide-mediated induction of the Shiga toxinconverting lambdoid prophage ST2-8624 in Escherichia coli O157: H7. *FEMS Immunol Med Mic*. Published online 2010:322-329.
14. Little JW. Lysogeny, Prophage Induction, and Lysogenic Conversion. In: *Phages*. ; 2014. doi:10.1128/9781555816506.ch3
15. Oliveira J, Mahony J, Hanemaaijer L, et al. Detecting Lactococcus lactis prophages by mitomycin C-mediated induction coupled to flow cytometry analysis. *Front Microbiol*. 2017;8(JUL). doi:10.3389/fmicb.2017.01343
16. Synnott AJ, Kuang Y, Kurimoto M, Yamamichi K, Iwano H, Tanji Y. Isolation from sewage influent and characterization of novel Staphylococcus aureus bacteriophages with wide host ranges and potent lytic capabilities. *Appl Envıron Mıcrob*. 2009;75(13). doi:10.1128/AEM.02641-08
17. Oduor JMO, Onkoba N, Maloba F, Nyachieo A. Experimental phage therapy against haematogenous multi-drug resistant Staphylococcus aureus pneumonia in mice. *African Journal of Laboratory Medicine*. 2016;5(1). doi:10.4102/ajlm.v5i1.435
18. Filipiak M, Łoś JM, Łoś M. Efficiency of induction of Shiga-toxin lambdoid prophages in Escherichia coli due to oxidative and antibiotic stress depends on the combination of prophage and the bacterial strain. J Appl Genet. 2020 Feb;61(1):131-140. doi: 10.1007/s13353-019-00525-8.
19. Loś, J. M., Loś, M., Wegrzyn, A., & Wegrzyn, G. (2010). Hydrogen peroxide-mediated induction of the Shiga toxin-converting lambdoid prophage ST2-8624 in Escherichia coli O157:H7. FEMS immunology and medical microbiology, 58(3), 322–329. https://doi.org/10.1111/j.1574-695X.2009.00644.x

ISBN: 978-605-73552-2-5

# CLONING OF BACTERIOPHAGE LYTIC PROTEIN

**Hande HANÇER[1], Gül Begüm EREN[2], Tülin ÖZBEK[3*]**

[1] Molecular Biology and Genetics, Faculty of Arts and Sciences, Yıldız Technical University, İstanbul, Turkey
[2] Molecular Biology and Genetics,Faculty of Arts and Science, Yıldız Technical University, İstanbul, Turkey
[*3] Molecular Biology and Genetics,Faculty of Arts and Science, Yıldız Technical University, İstanbul, Turkey
[*3]Doç. Dr. Tülin ÖZBEK, ozbektulin@gmail.com, 05052364004

## ABSTRACT

*Staphylococcus aureus* is extremely pathogenic and seen among the most common causes of hospital-acquired infections, which has been increasing in worldwide. In the antibiotic era, *S. aureus* infections were treated with various antibiotics. However, the very intensive and unconscious use of these antibiotics has resulted in the presence of resistant bacterial strains. Therefore, while leaving antibiotics age behind, scientists have begun to look for new therapeutic approaches to combat antimicrobial resistance. Bacteriophage and bacteriophage-based antimicrobials are seen as an alternative and promising agents for antibiotic resistance.
Bacteriophages are viruses which infect bacteria. They have two life cycles, lytic and lysogenic. Two main phage proteins, endolysin and holin, are used by lytic phages infecting bacteria in the process of lysing the bacteria for the release of virions. Holins localize to the cell membrane with their transmembrane domain (TMD) and trigger hole formation in the host cell membrane during infection, which causes destruction of the membrane proton motive force, resulting in both growth arrest and cell death. In the literature, antibacterial effects of phage lytic proteins on bacteria have been observed when they are expressed recombinantly in the cell and applied exogenously.
In the study, the *TMD* gene obtained from a lytic phage that infects *S. aureus* bacteria was successfully cloned into the expression vector and transformed into *E. coli* Bl21 (DE3). Transformed colonies on selective medium with ampicillin were confirmed by sequence analysis and colony PCR. The aim of this study is to provide the use of this antibacterial product in all areas where have bacterial contamination crisis such as health, food, agriculture, cosmetics are used, and also introduce holin proteins to the literature.
**Keywords:** Bacteriophage, Lytic protein, *Staphylococcus aureus*, Recombinant protein

## 1. INTRODUCTION

Staphylococci are among the most common causes of hospital-acquired infections, which are increasing in the world and in our country. Some strains of *Staphylococcus aureus* bacteria, which is one of the important staphylococcal pathogen species in the community and hospitals [1], can cause many chronic diseases and death [2][3]. In the 2021 UHESA (National Nosocomial Infections Surveillance Network) report of the Public Health Institution of Turkey, antibiotic-resistant *S. aureus* bacterial strains are in the first place in the distribution of antimicrobial-resistant pathogens in bacteria causing nosocomial infections [4].
*S. aureus* infection has been tried to be treated with various antibiotics, but incorrect and excessive use of antibiotics has caused the bacteria to become resistant to antibiotics [5]. Alternative treatment methods to antibiotics are being developed by scientists, and one of these alternative methods is phage lysines [6]. This method offers an effective and environmentally friendly method to reduce bacterial contamination [7]. Recently, bacteriophages and phage derivatives are seen as promising treatment modalities in bacterial infections [8]. The inherent ability of phages to specifically recognize and infect bacterial hosts; making them ideal antimicrobial candidates for pathogen-specific therapy in food (food decontamination), agriculture (biopreservative), biotechnology (delivery systems, vaccine and drug designs), and medicine (infection therapy, biodiagnosis, drug targeting, disinfectant) [9][10]. The biggest disadvantage of using phages as an alternative method in antibacterial infections is that they can carry genes related to bacterial drug resistance and virulence in their genomes. Thus, the use of phage lytic proteins is seen as a safer and more effective method than phages [7].
Holin and Endolysins, the lytic proteins of phages with a double-stranded DNA genome, are involved in the release of virions, ending their growth cycle and rapidly lysing cells [11][12]. Holins trigger the formation of holes that cause destruction of membrane proton motif force at a genetically programmed time, leading to growth arrest and cell death. Another task is to allow the release of endolysins, which accumulate in the cytosol and cause degradation of the cell wall by cutting the peptidoglycan network in the cell wall [12][13].
The antibacterial effects of phage lytic proteins have been demonstrated in the literature both by recombinant expression of the relevant proteins in the cell and by their exogenous administration.

ISBN: 978-605-73552-2-5

In 2012, Shi et al. reported lytic enzymes obtained from the *SMP* bacteriophage infecting *Streptecoccus suis* were produced recombinantly and it was observed that they antibacterial effect on the bacteria. In the same study, it was observed that Holin protein is an antimicrobial agent and affects *S. aureus* when applied externally [14]. In 2005, Agu et al. reported that Holin was cytotoxic to eukaryotic cells in vitro and could be used as a potential therapeutic in cancer gene therapy [15]. In a study by Fenton et al. in 2010, it was observed that the catalytic domain (CHAPK) of Endolysin obtained from *Bacteriophage K* killed *S. aureus* bacteria in the mouse nasal region [16]. In 2013, Fenton et al. reported that the biofilm formed by the *S. aureus* bacterial colony was completely removed by CHAPK, which is also obtained from *Bacteriophage K*, within 4 hours [17]. It has been shown by Hoopes et al. that PlyC, a lysine against *S. equi* infection, can significantly reduce the *S. equi* load found on equine equipment. However, lysine was found to be 1,000 more active when compared to common disinfectant [18]. In addition, in the study of Li et al., it was observed that the *HH109* phage of *Vibrio alginolyticus* bacteria caused a decrease in absorbance value in the first four hours during the expression of Holin protein, *E. coli Bl21 (DE3)* cell line [19].

In this study, the Transmembrane Region (TMD), one of the effective regions of the lytic protein obtained from the lytic phage infecting *S. aureus* bacteria, was successfully cloned into the expression vector and transformed into *E. coli Bl21 (DE3)*. Transformed colonies formed on selective medium containing ampicillin were confirmed by sequencing analysis and colony PCR. The aim of this study is to provide the use of this antibacterial product in all areas where there is a bacterial contamination crisis such as health, food, agriculture, cosmetics, and also to bring phage lytic proteins to the literature.

## 2. MATERİAL AND METOD

### 2.1 Phage Development by the Double Layer Agar Method

Serial dilutions of 10-1-10-7 bacteriophage lysate in Brain Heart Infusion (BHI) (Millipore) broth were prepared and 100 µL of bacteria were preincubated at room temperature for 1 hour with 100 µL of phage dilution. Then, top soft agar (0.5% BHI agar) was added on them and the bottom agar was spread rapidly on the plate and incubated at 37 °C overnight. After incubation, plates showing lysis were selected and the top agar was scraped with the help of a scalpel. The scraped agar was added to 3 ml of BHI broth and incubated for 4 hours at 37°C. The incubated high-titer phage solution was centrifuged at 8,000 xg for 10 minutes and the supernatant was passed through a sterile filter with a pore diameter of 0.22 µm. After the part to be used for DNA isolation was separated, 50% (v/v) sterile glycerol was added to the remaining phage solution and stored at -80°C.

### 2.2 Phage DNA Isolation

Genomic DNA isolation of the related phage developed by the double agar method was performed according to the Norgen Phage DNA Isolation Kit protocol (Cat. No.: 46800)[20].

### 2.3 Determination of the Base Sequence of the Lytic Protein Gene and Primer Design of the Gene Region

The ORF region of the lytic protein gene is as follows and this sequence was retrieved from the National Center for Biotechnology Information (NCBI).

Primer design was done for cloning the gene of TMD region of lytic protein. Since the aLICator pLATE51 (Cat. No.: K1251) is used as the vector, the forward and reverse primers were designed for this vector.

### 2.4 Polymerase Chain Reaction (PCR)

PCR reaction (Table 1) was carried out in 35 cycles using Phusion High-Fidelity DNA Polymerase and reagents in the enzyme kit (Cat. No.: F530S)[21].

**Table 1.** PCR stages

| Stage | Temperature | Time |
|---|---|---|
| Initial Denaturation | 98°C | 2 min |
| Denaturation | 98 °C | 10 sec |
| Annealing | 61 °C | 30 sec |
| Extension | 72 °C | 1 min |
| Last Denaturation | 72 °C | 10 min |
| Cooling | 4°C | ∞ |

ISBN: 978-605-73552-2-5

### 2.5 Agarose Gel Electrophoresis

The desired length of the amplicon product and in the form of a single band was checked by running it in a 1% agarose gel electrophoresis system (Biorad Powerpac Basic).

### 2.6 Purification of PCR Product

After visualizing the DNA bands under UV light, purification of the PCR product from the tube was performed. Purification was done according to the QIAquick® Gel Extraction Kit protocol (Cat. No.:28704)[22].

### 2.7 Ultra Competent Cell Preparation

In order for the vector to enter the cell, the *E. coli Bl21 (DE3)* strain was made ultra-competent based on the protocol of Green and Sambrook [23].

### 2.8 Cloning and Transformation with aLICator Kit

The amount of purified gene was calculated as specified in the aLICator Kit to be used in cloning and cloning was performed according to the kit protocol [24].

The products formed in the cloning reaction were added to the tubes containing 50 µl of competent cells as 4 µl and 6 µl. It was incubated on ice for 30 minutes. After incubation, heat shock was applied at 42 °C for 1.5 minutes. It was then left on ice for another 2 minutes. It was taken into a 15 ml falcon and 950 µl of SOC medium was added. grown for 1 hour at 37 °C. After 1 hour, it was centrifuged at 3000 xg for 2 minutes at room temperature and 800 µl of the supernatant was discarded. The pellet was resuspended with the remaining 150 µl supernatant. 100 µl was taken and cultivated with the help of drigalski in a petri dish containing LB agar with ampicillin. Petri dishes were incubated at 37 °C for 16 hours.

### 2.9 Colony PCR

A total of 3 colonies were selected from two separate petri dishes, and 10 µl of sterile water was added to the PCR tubes with the help of loop, so that half of the colonies were filled. After blasting the cells for 5 minutes at 95 °C, 25 cycles of colony PCR were established according to the aLICator Kit protocol [24] (Table 2).

**Table 2.** Stages of Colony PCR

| Stage | Temperature | Time |
|---|---|---|
| Initial Denaturation | 95°C | 3 min |
| Denaturation | 94 °C | 30 sec |
| Annealing | 58 °C | 30 sec |
| Extension | 72 °C | 1 min |
| Cooling | 4°C | ∞ |

### 2.10 Plasmid Isolation

In order to isolate the vectors containing the TMD region from *E. coli Bl21(DE3)* cells, 100 µg/ml ampicillin was added in 5 ml LB medium and the colony was inoculated into the medium with the aid of loop from the colonies with positive results in PCR. Bacteria were incubated overnight at 37°C in a shaker oven. Bacterial plasmids were isolated according to the QIAprep Spin Miniprep Kit protocol (Cat. No.:27104)[25].

### 2.11 Plasmid DNA Sequence Analysis

It was sent to a sequencing analysis firm to determine the sequence of the isolated plasmid DNA. Then BLASTn was made and aligned with the original sequence.

### 3.1 Reproduction of Staphylococcus aureus Phage in Culture Media

Petries are incubated at 37°C for 1 night (at least 18 hours). It is given in Figure 1.

ISBN: 978-605-73552-2-5

**Figure 1.** Formed phages by using double agar method

### 3.2 Isolation of Staphylococcus aureus Phage Genomic DNA

The amount of DNA in elution 1 and 2 obtained as a result of genomic DNA isolation of *S. aureus* phage according to the Phage DNA Isolation Kit (Norgen) protocol was measured in the NanoDrop device. Elution 1 and 2 in the NanoDrop device (Table 3) were determined as 13.1 and 13.2 ng/µl, respectively.

**Table 3.** Measurement results of *S. aureus* phage genomic DNA in NanoDrop device

| **Samples** | **ng/µl** |
|---|---|
| **Elution 1** | 13.1 |
| **Elution 2** | 13.2 |

### 3.3 Amplification of *S. aureus* Phage of Relevant Region of Lytic Protein Gene by Polymerase Chain Reaction (PCR), Agarose Gel Electrophoresis, and Tube Purification

#### 3.3.1 Agarose Gel Electrophoresis

The desired size and single band form of approximately 267 bp amplicon product obtained as a result of amplification of the relevant region of the Staphylococcus aureus phage lytic protein gene with PCR device was checked by running it in a 1% agarose gel electrophoresis system. In the obtained gel image (Figure 2), it was seen that the amplicon product was in the form of a single band and approximately 267 bp long. At the same time, because it gives a single band-shaped image in the gel; The relevant gene region was purified from the tube by purification method.

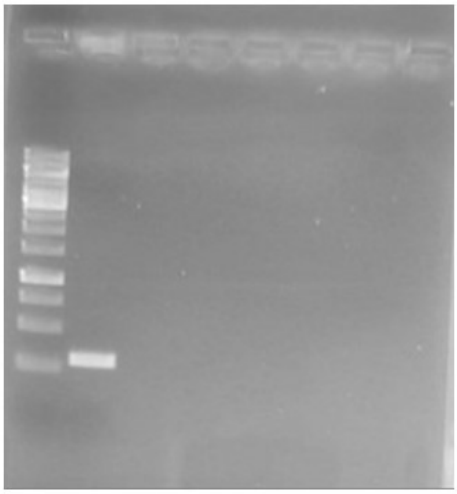

**Figure 2.** Agarose gel electrophoresis image of the relevant region of the *S. aureus* phage lytic protein gene

ISBN: 978-605-73552-2-5

### 3.3.2 Purification

The relevant gene region amplified by the PCR reaction was purified from the tube according to the Zymoclean™ Gel DNA Recovery Kit protocol. The amount of DNA in elution 1 and 2 obtained because of purification was measured with the NanoDrop device. Elution 1 and 2 were determined as 22.4 and 11.6 ng/µl, respectively, in the NanoDrop device (Table 4).

**Table 4.** The measurement results of the elutions obtained by the purification of the relevant region of the lytic protein gene of the *S. aureus* phage from the tube in the NanoDrop device

| Samples | ng/µl |
|---|---|
| **Elution 1** | 22.4 |
| **Elution 2** | 11.6 |

### 3.3.3 Verification of Transformation by Colony PCR and Isolation of Recombinant Plasmid

After the cloning of the relevant region of the lytic protein gene of *S. aureus* phage into pLATE51 LIC vector, 5 colonies in petri dishes were observed as a result of the transformation of the recombinant plasmid into competent cells (Figure 3).

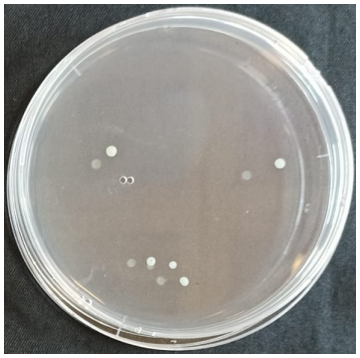

**Figure 3.** Colonies formed after transformation into *E. coli (Bl21 DE3)*

Colony PCR was first performed to confirm the transformation. The size of the recombinant plasmid product obtained because of colony PCR was controlled by running on a 1% agarose gel electrophoresis system. In the obtained gel image (Figure 4), it was seen that the recombinant plasmid product obtained was approximately 472 bp long.

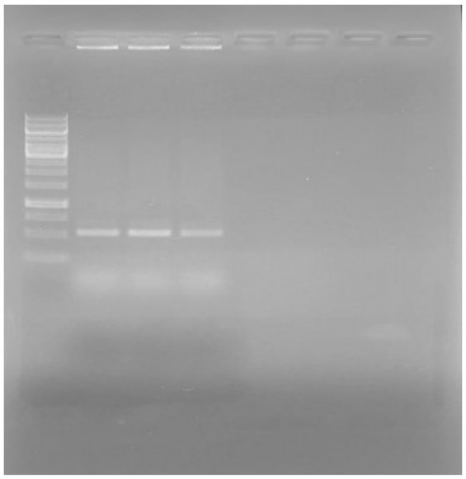

**Figure 4.** Agarose gel electrophoresis image of the recombinant plasmid product obtained because of colony PCR

To verify the transformation process; After colony PCR, isolation of recombinant plasmid was performed. The amount of recombinant plasmid isolated as a result of the isolation of the recombinant plasmid (elution 1 and 2) was measured

ISBN: 978-605-73552-2-5

with the NanoDrop device. Elution 1 and 2 were determined as 104.7 and 42.0 ng/µl, respectively, in the NanoDrop device (Table 5).

**Table 5.** Result of plasmid isolation in the NanoDrop device

| **Samples** | **ng/µl** |
|---|---|
| **Elution 1** | 104.7 |
| **Elution 2** | 42.0 |

Finally, recombinant plasmids isolated as a result of recombinant plasmid isolation were sent to sequencing with LIC Forward Sequencing primer. The sequencing result is shown in Figure 5.

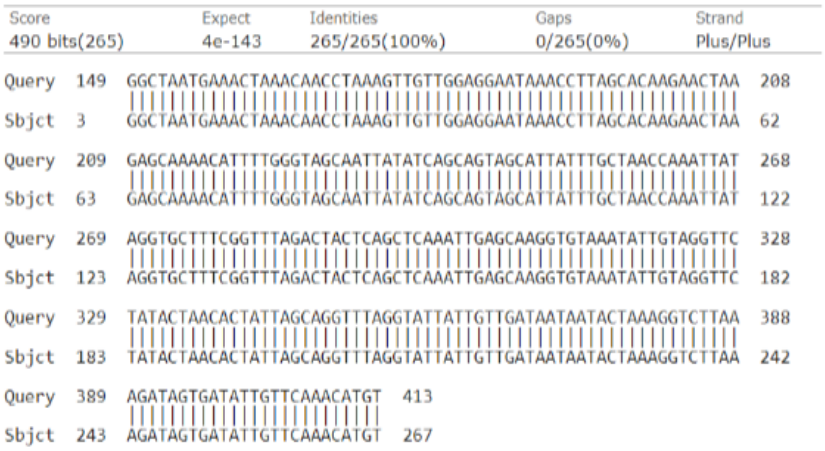


**Figure 5.** Alignment of the resulting sequence of the plasmid containing the TMD gene region with the TMD gene sequence using BLASTn. Sbjct: Original array, Query: Array as a result of sequencing.

## 4. DISSUCCION

In this thesis study, firstly, genomic DNA was isolated from commercially available *S. aureus* phage and PCR reaction was established using primers designed in accordance with the TMD gene region of the lytic protein and the vector to be cloned. TMD gene region was successfully amplified by PCR reaction. The obtained TMD amplicon was purified from other PCR products and cloned into the pLATE51 vector with the aLICator kit. The expression vector in which the gene for the TMD region of the lytic protein was cloned was transformed into a competent *E. coli Bl21(DE3)* strain. Colonies grown on LB agar with ampicillin were checked by colony PCR, and plasmid was isolated from the colonies. Sequencing analyzes of the isolated plasmids were performed by a company. As a result of the sequencing, the BLASTn program were aligned with the base and amino acid sequences of the original lytic gene, resulting in 100% similarity between the two sequences.

In the light of this information obtained, it is predicted that *S. aureus* phage lytic proteins can be used as safe, environmentally friendly, chemical-free alternative products in many areas. Especially in the health field, they are shown as promising drugs that can be used both alone and in combination with antibiotics or other lytic proteins in the treatment of resistant *S. aureus*-related nosocomial infections. nominated as candidates.

ISBN: 978-605-73552-2-5

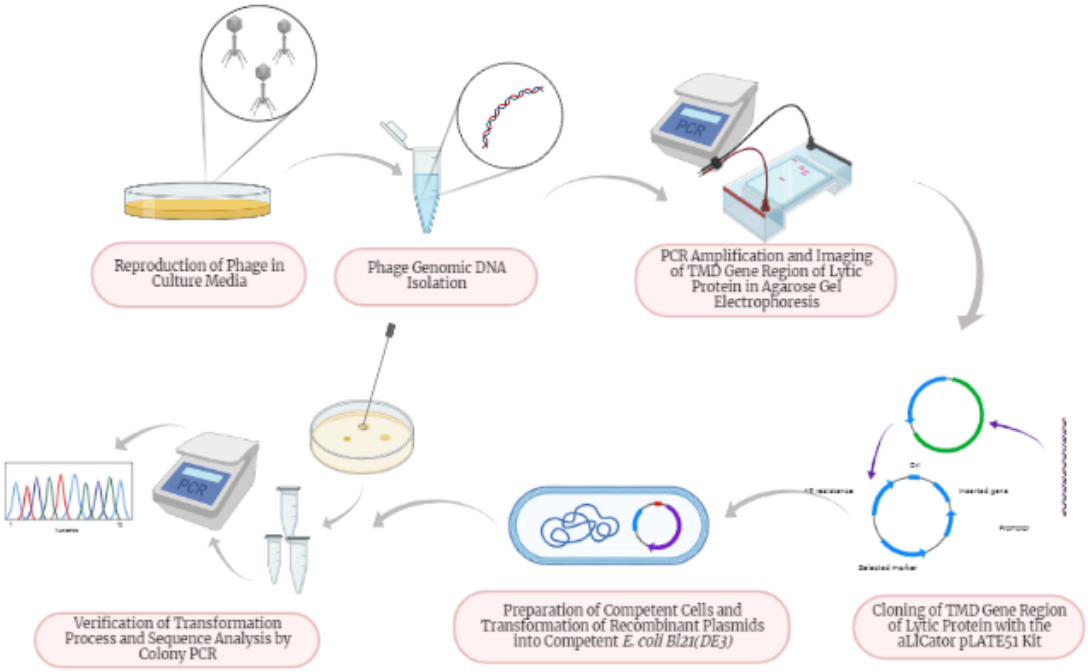


**Figure 6.** Flow chart of experimental methods applied in this study

**ACKNOWLEDGMENT**

I thank the TUBITAK 122Z026 project for supporting this project.

## 3. REFERANCE

[1] J. P. Rasigade and F. Vandenesch, "Staphylococcus aureus: A pathogen with still unresolved issues," *Infect. Genet. Evol.*, 2014, doi: 10.1016/j.meegid.2013.08.018.

[2] U. Nagaich, "Recombinant DNA technology: A revolutionizing outlook," *Journal of Advanced Pharmaceutical Technology and Research*. 2015, doi: 10.4103/2231-4040.166456.

[3] L. Pray, "Recombinant DNA Technology and Transgenic Animals," *Nature Education*. 2008.

[4] C. H. Hekimoğlu, E. Batır, E. Y. Gözel, and D. Altun, "Ulusal Sağlık Hizmet İlişkili Enfeksiyonlar Sürveyans Ağı (USHİESA) Özet Raporu 2021," 2022.

[5] S. A. Baltzer and M. H. Brown, "Antimicrobial peptides-promising alternatives to conventional antibiotics," *Journal of Molecular Microbiology and Biotechnology*. 2011, doi: 10.1159/000331009.

[6] L. Czaplewski *et al.*, "Alternatives to antibiotics-a pipeline portfolio review," *The Lancet Infectious Diseases*. 2016, doi: 10.1016/S1473-3099(15)00466-1.

[7] J. Song *et al.*, "The Phage Holin HolGH15 Exhibits Potential As an Antibacterial Agent to Control Listeria monocytogenes," *Foodborne Pathog. Dis.*, 2021, doi: 10.1089/fpd.2020.2833.

[8] A. Álvarez, L. Fernández, D. Gutiérrez, B. Iglesias, A. Rodríguez, and P. García, "Methicillin-resistant staphylococcus aureus in hospitals: Latest trends and treatments based on bacteriophages," *J. Clin. Microbiol.*, 2019, doi: 10.1128/JCM.01006-19.

[9] L. K. Harada *et al.*, "Biotechnological applications of bacteriophages: State of the art," *Microbiological Research*, vol. 212–213. 2018, doi: 10.1016/j.micres.2018.04.007.

[10] L. Fernández, D. Gutiérrez, P. García, and A. Rodríguez, "The perfect bacteriophage for therapeutic applications—A quick guide," *Antibiotics*, vol. 8, no. 3. 2019, doi: 10.3390/antibiotics8030126.

[11] Y. Shi *et al.*, "Characterization and determination of holin protein of Streptococcus suis bacteriophage SMP in heterologous host," *Virol. J.*, vol. 9, no. 1, p. 70, 2012, doi: 10.1186/1743-422X-9-70.

[12] S. Fernandes and C. São-José, "More than a hole: the holin lethal function may be required to fully sensitize bacteria to the lytic action of canonical endolysins," *Mol. Microbiol.*, 2016, doi: 10.1111/mmi.13448.

[13] H. Gerstmans, L. Rodríguez-Rubio, R. Lavigne, and Y. Briers, "From endolysins to Artilysin®s: Novel enzyme-based approaches to kill drug-resistant bacteria," *Biochem. Soc. Trans.*, 2016, doi: 10.1042/BST20150192.

[14] Y. Shi *et al.*, "Combined Antibacterial activity of phage lytic proteins holin and lysin from streptococcus suis

bacteriophage SMP," *Curr. Microbiol.*, vol. 65, no. 1, 2012, doi: 10.1007/s00284-012-0119-2.
[15] C. A. Agu *et al.*, "The cytotoxic activity of the bacteriophage λ-holin protein reduces tumour growth rates in mammary cancer cell xenograft models," *J. Gene Med.*, vol. 8, no. 2, 2006, doi: 10.1002/jgm.833.
[16] M. Fenton *et al.*, "The truncated phage lysin CHAPk eliminates staphylococcus aureus in the nares of mice," *Bioeng. Bugs*, 2010, doi: 10.4161/bbug.1.6.13422.
[17] M. Fenton, R. Keary, O. McAuliffe, R. P. Ross, J. O'Mahony, and A. Coffey, "Bacteriophage-derived peptidase CHAPK eliminates and prevents staphylococcal biofilms," *Int. J. Microbiol.*, 2013, doi: 10.1155/2013/625341.
[18] J. T. Hoopes, C. J. Stark, H. A. Kim, D. J. Sussman, D. M. Donovan, and D. C. Nelson, "Use of a bacteriophage lysin, PlyC, as an enzyme disinfectant against Streptococcus equi," *Appl. Environ. Microbiol.*, 2009, doi: 10.1128/AEM.02195-08.
[19] X. Li, C. Zhang, F. Wei, F. Yu, and Z. Zhao, "Bactericidal activity of a holin-endolysin system derived from Vibrio alginolyticus phage HH109," *Microb. Pathog.*, vol. 159, 2021, doi: 10.1016/j.micpath.2021.105135.
[20] Norgen, "Phage DNA Isolation Kit," no. 905, pp. 3–4, 2010.
[21] T. Fisher Scientific, "Thermo Scientific Phusion High–Fidelity DNA Polymerase Product Information Sheet (Pub. No. MAN0012393 E.0)."
[22] "QIAquick ® Spin Handbook," Jan. .
[23] M. R. Green and J. Sambrook, "The Inoue Method for Preparation and Transformation of Competent Escherichia coli: 'Ultracompetent' Cells," *Cold Spring Harb. Protoc.*, vol. 2020, no. 6, 2020, doi: 10.1101/pdb.prot101196.
[24] Thermo Fisher Scientific, "aLICator Ligation Independent Cloning and Expression System, #K1281," vol. 1, pp. 1–29, 2015.
[25] "Sample to Insight__ QIAprep ® Miniprep Handbook," 2020.

ISBN: 978-605-73552-2-5

# BIOSYNTHESIS OF SILVER NANOPARTICLES USING POTATO AND THEIR CYTOTOXIC EFFECTS

**Tunay KARAN[1*], Yasin Bedrettin KARAN,[2] Busra BOZER[3], Ramazan ERENLER[4]**

[1] Department of Genetics, Faculty of Veterinary, Yozgat Bozok University, Yozgat, Turkiye
[2] Department of Field Crops, Faculty of Agriculture, Tokat Gaziosmanpasa University, Tokat, Turkiye
[3] Scientific Technical Research and Application Center, Hitit University, Corum, Turkiye
[4] Department of Chemistry, Faculty of Arts and Sciences, Tokat Gaziosmanpasa University,Tokat, Turkiye

## ABSTRACT

Silve nanoparticles were synthesized using promising potato breeding line. TOGU 3/110 potato clone (*Solanum tuberosum*) was extracted with distilled water and then, they were filtered. The filtrate was treated with $AgNO_3$ to produce the AgNPs. The structure of green synthesized AgNPs was determined by Ultraviolet-visible (UV-Vis), and Fourier transform infrared (FTIR) spectroscopic methods. The cytotoxic effect of extract and AgNPs was carried out on L929 fibroblast, A-549 (Human lung carcinoma), and DLD-1 (Colon adenocarcinoma) cell lines using MTT [3- (4,5-dimethyl-thiazol-2-yl)-2,5-diphenyl tetrazolium bromide] assay. The solution of extract and AgNPs were prepared at the concentration of 1.0 mg/mL, 0.5 mg/mL, 0.25 mg/mL, 0.125 mg/mL and 0.0625 mg/mL and mixed with the medium. The absorbance values were read in the ELISA 96-well plate at 570 nm to determine cell viability. The viability of (%) A-549 cell lines for AgNPs was found as 30.21 ± 2.94 (1.0 mg/mL), 33.20 ± 1.72 (0,5 mg/mL), 80.98 ± 3.46 (0.25 mg/mL). However, the viability of A-549 cell lines for extract was determined as 10.24 ± 0.80 (1.0 mg/mL), 9.17 ± 0.67 (0.5 mg/mL), 14.29 ± 0.45 (0.25 mg/mL). The viability of DLD-1 cell lines for AgNPs was presented as 14.13 ± 0.930 (1.0 mg/mL), 31.38 ± 1.03 (0.5 mg/mL), 25.77 ± 1.56 (0.25 mg/mL). The viability of DLD-1 cells for extract was 53.37 ± 6.92 (1.0 mg/mL), 13.97 ± 1.56 (0.5 mg/mL), 13.48 ± 0.34 (0.25 mg/mL). The viability of L929 fibroblast for AgNPs was found as 49.26 ± 1.89 (1.0 mg/mL), 63.59 ± 3.12 (0.5 mg/mL), 71.27 ± 2.75 (0.25 mg/mL). Moreover, the viability of L929 fibroblast for extract was 68.95 ± 5.73 (1.0 mg/mL), 84.67 ± 2.20 (0.5 mg/mL), 100.15 ± 4.58 (0.25 mg/mL). Percentages of apoptotic and necrotic cells were obtained by the double staining method. Apoptotic effects for AgNPs on A549 and DLD-1 cell lines were higher than the extract sample. The apoptotic effects of the AgNPs and extract were lower in fibroblast cells compared to cancer cells. While AgNPs showed the toxic effect on A-549 and DLD-1 cancerous cell lines, they did not show a noticeable toxic effect on L929 cells. These results indicated that the AgNPs synthesized from *Solanum tuberosum* and extract have the potential to be used for anticancer agents and further study should be carried out to determine potential usage in the drug development process.

**Keywords:** Potato, *Solanum tuberosum*, cytotoxicity; silver nanoparticles

## 1. INTRODUCTION

Natural products exhibit a major position in drug discovery improving due to their broad spectrum of biological effects [1]. After the discovery of spectroscopy and chromatography in 19$^{th}$ century plants became the focus of science, many bioactive compounds were isolated and identified from plants [2-4]. In addition, Synthetic chemists have synthesized many natural compounds inspired by corresponding natural molecules [5]. Natural products were reported to reveal significant biological activities [6-11]. Nanotechnology is the multifaceted area of science that deals with particles in nanosized ranges from 10 to 100 nm [12]. There are numerous structures of nanomaterials used in fields of technology and science such as agriculture, food, medicine and energy production. Characterizations of nanoparticles (NPs) are based on their form, and among several NPs, metal NPs have attracted more attention in recent years due to their characteristic properties [13]. AgNPs have been used in environmental pollution clean-up, medical imaging methods, and also shows up more in the biomedical field due to its enormous surface field to volume ratio [14]. AgNPs are potent antiseptic and antibacterial agent and are used as an antibiotic in the therapy of burn wounds. In addition, AgNPs were reported to display strong biological activity such as anticancer, antibacterial, antifungal, antioxidant, anti-inflammatory, antiparasitic properties [15, 16].

Chemical and physical techniques have been developed to synthesize silver nanoparticles (AgNPs). However, these techniques include the harsh reaction condition, toxic chemicals. Therefore, there is a growing essential to develop environment friendly approaches for AgNPs synthesis. Lately, biosynthesis of AgNPs has received considerable interest, and proposals many advantages. The microorganisms and plant materials in AgNPs synthesis has been explored. The secondary metabolites such as flavonoids, terpenoids, alkaloids, etc act as a reducing, stabilizing and capping agent [17-19].

Potato (*Solanum tuberosum* L.) is the most valuable food crops in the world with vital nutrients. Potato is the good source of polyphenols and carotenoids that have a beneficial effect on health. Previous research presented the

agricultural and health benefits of potatoes and biological activity such as antibiotics, anticancer, and antioxidant properties [20].
Herein, silver nanoparticles were synthesized using the *Solanum tuberosum*. The cytotoxic impact of extract and AgNPs was executed on L929 fibroblast, A-549 (Human lung carcinoma), and DLD-1 (Colon adenocarcinoma) cell lines utilising MTT [3- (4,5-dimethyl-thiazol-2-yl)-2,5-diphenyl tetrazolium bromide] analyse.

## 2. MATERIAL and METHODS

### 2.1. Material
In the experiment, promising potato breeding line was used as plant material. TOGU 3/110 potato clone used in experiment and its pedigree was Serrana × TS-9.

### 2.2 Chemicals and cell lines
The solvents, silver nitrate, trypsin-EDTA, FBS, L-glutamine were supplied from Merck (Darmstadt, Germany). DLD-1 colorectal cancer cells, A-549 lung cancer cells, and L929 fibroblast cells, were provided from Kirikkale University, Turkey.

### 2.3 Synthesis of nanoparticles
Potato tubers (10.0 g) were heated in deionized water (100 mL) for 2 h at 55 °C. After the filtration, the filtrate was treated with the silver nitrate solution in deionized water (5.0 mM, 100 mL) for 2.5 h at 50 °C. After the completion of the reaction, the mixture was centrifuged at 10000 rpm for 10 min, then the formed nanoparticles were washed with deionized water, dried entirely by lyophilisation [15].

### 2.4. Identification of silver nanoparticles
The structure of AgNPs was identified by spectroscopic methods. UV-Vis spectra were recorded on Hitachi U-2900 spectrophotometer. X-ray diffraction (XRD) pattern was recorded on an Empyrean, Malvern Panalytical diffractometer. Scanning electron microscope (SEM) analysis was executed by Quanta Feg450. Fourier transform infrared spectroscopy (FTIR 4700) was used to present the functional group of the compounds acting as reducing agent.

### 2.5. MTT assay for cytotoxicity
L929 fibroblast cells, A-549 lung cancer cells, and DLD-1 colorectal cancer cells were used for cytotoxicity by MTT assay. The cells ($10 \times 10^3$ cells/mL) were seeded in 96-well plates and incubated for 24 hours then the extract and AgNPs at various concentration were added to the cells and incubated for 24 h. After discharged of the medium in the well plates, MTT (50 mL, 1 mg/mL) was added to the wells, incubated (2.5 h) at 37°C. Later, MTT solution in the wells was removed, then MTT solvent (isopropanol) was added. ELISA plate reader was used at 570 nm to calculate the percentage of viable cells. The control cell viability was accepted as 100% and the cell viability of each group was determined by the given formula (1)
Cell viability % = [Ax/Ay] × 100 (1)
Ax is the sample of optical density. Ay is the control [21-23].

### 2.6. Apoptotic and necrotic cells analysis
After the inoculation of the cells into 48 well plates with $15\times10^3$ cells per well, the mixture was incubated for 24 h (5% $CO_2$, 37°C) then, media on the plates were discharged and samples (200 µL) at various concentration were added, incubated for 24 h. Afterward, media was removed and added to 70 µL double staining solution (500 µL of Hoechst 33342, 100 µL of propidium iodide, 100 µL of Ribonuclease A were added to 10 mL of PBS) and incubated for 15 minutes. Later, apoptosis cells and necrotic cells were evaluated by a Fluorescence Inverted Microscopy (Leica DMI 6000 B, Germany) with DAPI and FITC filters respectively [15].

### 2.7. Statistical analysis
The statistical analysis was achieved by GraphPad Prism (8.0.1) with one-way ANOVA. The multiple comparison test was executed by Tukey's test. The results were presented as mean values ± SDs of three independent analyses ($P < 0.05$).

ISBN: 978-605-73552-2-5

## 3. RESULTS

### 3.1. Synthesis and characterisation of AgNPs

Silver nanoparticles were synthesized using *Solanum tuberosum.* The maximum absorption was observed at 438 nm in UV-Vis spectroscopy (Figure 1).

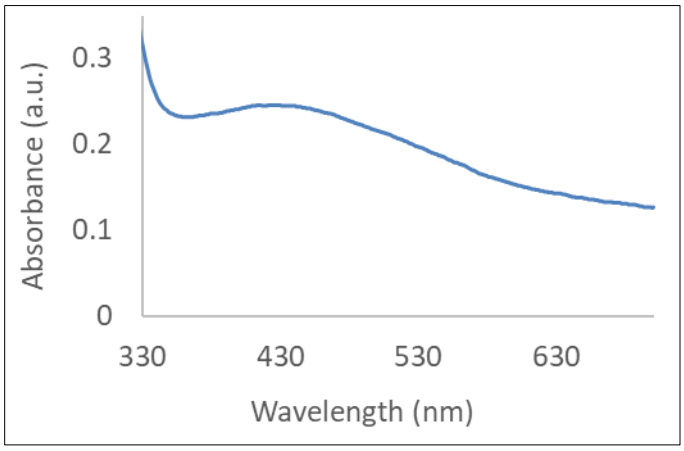


**Figure 1.** UV-Vis spectrum of AgNPs

FTIR analysis displayed the functional groups of natural compounds responsible for reducing and stabilizing agents. (Figure 2).

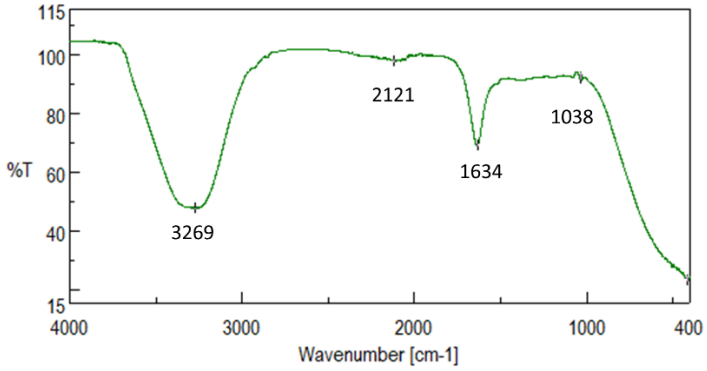


**Figure 2.** FTIR spectrum of AgNPs

X-ray diffraction (XRD) analysis presented the structure of silver nanoparticles. The peaks (2θ) at 38.25°, 44.47°, 64.67°, 77.69° corresponded to 111, 200, 220 and 311 planes respectively that confirmed face-centered cubic structure of metallic silver (JCPDS No. 04–0783) (Figure 3).

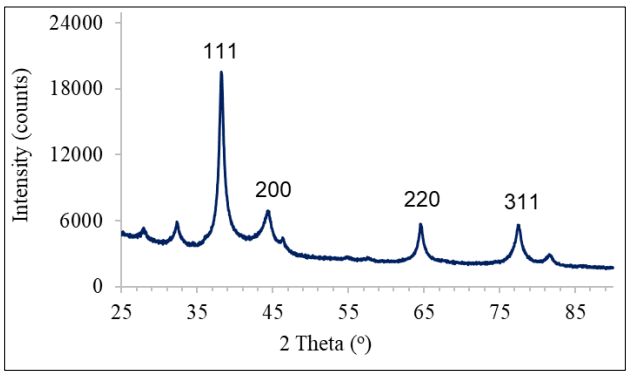

ISBN: 978-605-73552-2-5

**Figure 3.** XRD model of AgNPs

The size, shape, and surface morphology of the synthesized AgNPs were presented by Scanning Electron Microscope (SEM). The AgNPs had spherical shapes and monodisperse distribution. The average dimension of nanoparticles was calculated as 73.2 nm (Figure 4).

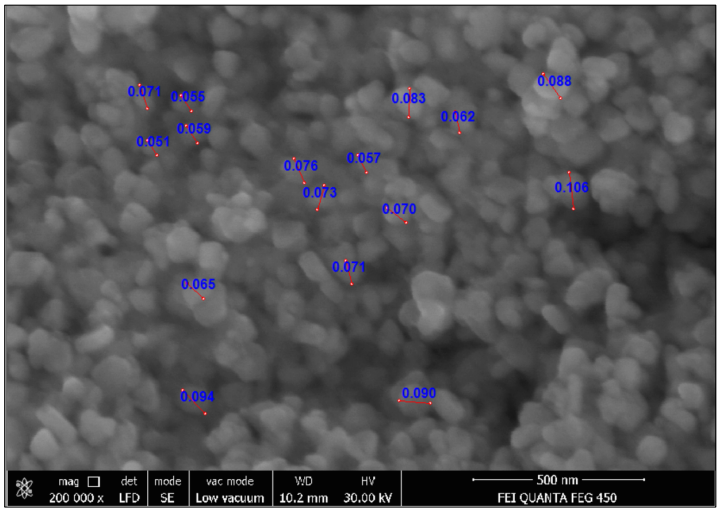


**Figure 4.** SEM picture of AgNPs

## 3.2. Cytotoxic effect

Cytotoxic effect of extract and AgNPs was executed using the A549, DLD-1, and L929 cell lines.

**Table 1.** Cytotoxic effect of extract and AgNPs from potato clone tubers (%Viability)

| Concentration (mg/mL) | A549 | | DLD-1 | | L929 | |
|---|---|---|---|---|---|---|
| | Extract | AgNPs | Extract | AgNPs | Extract | AgNPs |
| 1.0 | 10.2 ± 0.8$^{b}$ | 30.2 ± 2.9$^{a}$ | 5.4 ± 1.4$^{a}$ | 14.1 ± 0.9$^{a}$ | 68.9 ± 2.4$^{a}$ | 49.3 ± 1.9$^{a}$ |
| 0.5 | 9.2 ± 0.7$^{a}$ | 33.2 ± 1.7$^{b}$ | 13.9 ± 0.5$^{b}$ | 31.4 ± 1.1$^{c}$ | 84.7± 2.2$^{b}$ | 63.6 ± 1.9$^{b}$ |
| 0.25 | 14.3 ± 0.5$^{c}$ | 80.9 ± 3.4$^{c}$ | 13.8 ± 0.3$^{b}$ | 25.8 ± 1.6$^{b}$ | 100.1 ± 4.5$^{c}$ | 71.3 ± 2.8$^{c}$ |
| 0.125 | 15.2 ± 1.1$^{d}$ | 87.2 ± 2.7$^{d}$ | 21.1 ± 0.3$^{c}$ | 67.1± 1.7$^{d}$ | 105.0 ± 3.3$^{d}$ | 93.4 ± 4.5$^{e}$ |
| 0.0625 | 20.8 ± 4.0$^{e}$ | 118.6 ± 3.8$^{e}$ | 51.0 ± 1.2$^{d}$ | 124.7 ± 0.7$^{e}$ | 143.9 ± 1.5$^{e}$ | 87.5 ± 4.5$^{d}$ |

Cytotoxic effects were reported as mean values ± SDs of three independent assays ($P < 0.05$). Values followed by the same letter are not significantly different.

## 3.3. Apoptotic and necrotic cells investigation

Apoptotic and necrotic index of of extract and AgNPs on on A549, DLD-1 and L929 cell lines were presented in Table 2. The apoptotic indexes of AgNPs on A549, DLD-1 and L929 were calculated as 38.6±0.7, 30.2±1.3, 23.5±0.5 respectively (Table 2).

**Table 2.** Apoptotic index and necrotic index of extract and AgNPs on A549, DLD-1 and L929 cell lines at 1.0 mg/mL

| **Samples** | **A549** | | **DLD-1** | | **L929** | |
|---|---|---|---|---|---|---|
| | A | N | A | N | A | N |
| **Extract** | 2.5±0.2$^{a}$ | 6.5±0.5$^{a}$ | 6.5±1.5$^{a}$ | 10±1$^{a}$ | 18±0.7$^{a}$ | 6.6±1.3$^{b}$ |
| **AgNPs** | 38.6±0.7$^{b}$ | 8.0±1.5$^{b}$ | 30.2±1.3$^{b}$ | 12.1±2.1$^{b}$ | 23.5±0.5$^{b}$ | 4.4±0.2$^{a}$ |

A: Apoptotic index (%), N: Necrotic index (%). Statistical analysis was carried out for each column as multiple comparison test. Different letters in each column indicated the statistically different ($p<0.05$).

## 4. DISCUSSION

Due to the side effect of synthetic drugs, tendency in natural product in drug development process has increased recently. Natural products especially natural compounds display the biological activities [24-27]. Hence, they could ack a crucial position in drug development stages. In this study, silver nanoparticles were synthesized using potato and their cytotoxic effect was examined. The fully spectroscopic techniques were used for identification of synthesized nanoparticles. The colour change from light yellow to dark brown proved the nanoparticles formation. In UV-Vis spectrum, the maximum absorption was appeared at 438 nm indicating the formation of desired product. The absorbance in the range of 350-550 nm proves the silver nanoparticles formation [28]. FTIR analysis showed the functional groups of the compounds. The signal observed at 3269 $cm^{-1}$ was due to the hydroxyl group. The peak at 2121 $cm^{-1}$ might be attributed to monosubstituted alkyne and the strong peak at 1634 $cm^{-1}$ could belong to the monosubstituted alkene. The weak signal at 1038 $cm^{-1}$ may belong to C-O stretching. XRD analysis proved the nanoparticles to be face centered cubic structure. The morphology of the particles was defined by SEM analysis. The viability of A549 cell lines for extract and AgNPs at 1.0 mg/mL was observed as 10.2%, 30.2% respectively. Moreover, the viability of DLD-1 cells lines for extract and AgNPs at 0.5 mg/mL was determined as 13.9% and 31.4% respectively. The significant cytotoxic effect of extract and AgNPs was not detected on the L929 cell lines which was the normal cells. Hence, extract and AgNPs generated from *Solanum tuberosum* could be a favorable material for drug development procedure, including cancer drugs. The apoptotic and necrotic index indicated that the AgNPs have a likely impact on given cancerous cell lines.

## 5. CONCLUSION

An easy, fast, low-cost, eco-friendly technique was used for the synthesis of silver nanoparticles from *Solanum tuberosum.* The extract and AgNPs revealed the outstanding activity against cancerous cell lines. However, they did not damage the normal cell lines L929. Hence, extract and AgNPs have a potential to be anticancer agents for cancer drugs.

## REFERENCES


[1] Newman DJ, Cragg GM. Natural products as sources of new drugs over the last 25 years. J Nat Prod 2007; 70(3):461-477. doi:https://doi.org/10.1021/np068054v

[2] Topçu G, Erenler R, Çakmak O, Johansson CB, Çelik C, Chai H-B, Pezzuto JM. Diterpenes from the berries of *Juniperus excelsa*. Phytochemistry 1999; 50(7):1195-1199. doi:https://doi.org/10.1016/S0031-9422(98)00675-X

[3] Elmastas M, Ozturk L, Gokce I, Erenler R, Aboul-Enein HY. Determination of antioxidant activity of marshmallow flower (*Althaea officinalis* L.). Anal Lett 2004; 37(9):1859-1869. doi:https://doi.org/10.1081/AL-120039431

[4] Demirtas I, Erenler R, Elmastas M, Goktasoglu A. Studies on the antioxidant potential of flavones of *Allium vineale* isolated from its water-soluble fraction. Food Chem 2013; 136(1):34-40. doi:https://doi.org/10.1016/j.foodchem.2012.07.086

[5] Chen F-E, Huang J. Reserpine: a challenge for total synthesis of natural products. Chemical reviews 2005; 105(12):4671-4706. doi:https://doi.org/10.1021/cr050521a

[6] Karan T, Simsek S, Yildiz I, Erenler R. Chemical composition and insecticidal activity of *Origanum syriacum* L. essential oil against *Sitophilus oryzae* and *Rhyzopertha dominica*. Int J Sec Metabol 2018; 5(2):87-93. doi:https://doi.org/10.21448/ijsm.404114

[7] Karan T, Yildiz I, Aydin A, Erenler R. Inhibition of various cancer cells proliferation of bornyl acetate and essential oil from *Inula graveolens* (Linnaeus) Desf. Rec Nat Prod 2018; 12(3):273-283.

[8] Koysu P, Genc N, Elmastas M, Aksit H, Erenler R. Isolation, identification of secondary metabolites from *Salvia absconditiflora* and evaluation of their antioxidative properties. Nat Prod Res 2019; 33(24):3592-3595. doi:https://doi.org/10.1080/14786419.2018.1488700

[9] Nusret G, Elmastas M, Telci I, Erenler R. Quantitative analysis of phenolic compounds of commercial basil cultivars (Ocimum basilicum L.) by LC-TOF-MS and their antioxidant effects. Int. J. Chem. Technol. 2020; 4(2):179-184. doi:https://doi.org/10.32571/ijct.795629

[10] Karan T, Erenler R. Effect of Salt and pH Stress of Bioactive Metabolite Production in *Geitlerinema carotinosum*. International Journal of Secondary Metabolite (IJSM) 2017; 4(3):16-19.

[11] Karan T, Erenler R. Fatty acid constituents and anticancer activity of *Cladophora fracta* (OF Müller ex Vahl) Kützing. Trop J Pharm Res 2018; 17(10):1977-1982.

[12] Zhang D, Ma X-l, Gu Y, Huang H, Zhang G-w. Green Synthesis of Metallic Nanoparticles and Their Potential Applications to Treat Cancer. Front. Chem. 2020; 8:Article ID: 799. doi:https://doi.org/10.3389/fchem.2020.00799

[13] Geçer EN, Erenler R. Biosynthesis of silver nanoparticles using *Dittrichia graveolens* (Asteraceae) leaves extract: characterisation and assessment of their antioxidant activity. Turk J Biodiv 2022; 5(1):50-56. doi:https://doi.org/10.38059/biodiversity.1090549

[14] Burlacu E, Tanase C, Coman N-A, Berta L. A review of bark-extract-mediated green synthesis of metallic nanoparticles and their applications. Molecules 2019; 24(23):4354. doi:https://doi.org/10.3390/molecules24234354

[15] Karan T, Erenler R, Bozer BM. Synthesis and characterization of silver nanoparticles using curcumin: cytotoxic, apoptotic, and necrotic effects on various cell lines. Z. Naturforsch. C 2022. doi:https://doi.org/10.1515/znc-2021-0298

[16] Erenler R, Dag B. Biosynthesis of silver nanoparticles using *Origanum majorana* L. and evaluation of their antioxidant activity. Inorg Nano-Met Chem 2022; 52(4):485-492. doi:https://doi.org/10.1080/24701556.2021.1952263

[17] Genc N, Yildiz I, Chaoui R, Erenler R, Temiz C, Elmastas M. Biosynthesis, characterization and antioxidant activity of oleuropein-mediated silver nanoparticles. Inorg Nano-Met Chem 2021; 51(3):411-419. doi:https://doi.org/10.1080/24701556.2020.1792495

[18] Gecer EN, Erenler R, Temiz C, Genc N, Yildiz I. Green synthesis of silver nanoparticles from *Echinacea purpurea* (L.) Moench with antioxidant profile. Particul Sci Technol 2021; 40(1):50-57. doi:https://doi.org/10.1080/02726351.2021.1904309

[19] Kumari S, Tehri N, Gahlaut A, Hooda V. Actinomycetes mediated synthesis, characterization, and applications of metallic nanoparticles. Inorg Nano-Met Chem 2020; 51(10):1386-1395. doi:https://doi.org/10.1080/24701556.2020.1835978

[20] Kim J, Soh SY, Bae H, Nam S-Y. Antioxidant and phenolic contents in potatoes (*Solanum tuberosum* L.) and micropropagated potatoes. Appl Biol Chem 2019; 62:Art No 17. doi:https://doi.org/10.1186/s13765-019-0422-8

[21] Ökten S, Çakmak O, Erenler R, Yüce Ö, Tekin S. Simple and convenient preparation of novel 6,8-disubstituted quinoline derivatives and their promising anticancer activities. Turk J Chem 2013; 37(6):896-908. doi:https://doi.org/10.3906/kim-1301-30

[22] Sahin Yaglioglu A, Akdulum B, Erenler R, Demirtas I, Telci I, Tekin S. Antiproliferative activity of pentadeca-(8E, 13Z) dien-11-yn-2-one and (E)-1,8-pentadecadiene from *Echinacea pallida* (Nutt.) Nutt. roots. Med Chem Res 2013; 22(6):2946-2953. doi:https://doi.org/10.1007/s00044-012-0297-2

[23] Aydin A, Erenler R, Yılmaz B, Tekin Ş. Antiproliferative effect of *Cherry laurel*. J Turk Chem Soc, Sec A: Chem 2016; 3(3):217-228. doi:https://doi.org/10.18596/jotcsa.21204

[24] Saidi A, Hambaba L, Kucuk B, Cacan E, Erenler R. Phenolic Profile, Acute Toxicity, and Hepatoprotective and Antiproliferative Activities of Algerian *Ruta tuberculata* Forssk. Current Bioactive Compounds 2022; 18(3):72-83. doi:https://doi.org/10.2174/1573407217666211119092552

[25] Heyem Z, Nassima B, Ahmed M, Erenler R, Lahcene Z, Fadila B, Ameddah S. Phytochemical Profile, Anti-lipid peroxidation and Anti-diabetic activities of *Thymus algeriensis* Boiss. & Reut. Egyptian Journal of Chemistry 2022. doi:https://doi.org/10.21608/EJCHEM.2022.126336.5600

[26] Boulechfar S, Zellagui A, Asan-Ozusaglam M, Bensouici C, Erenler R, Yildiz İ, Tacer S, Boural H, Demirtas I. Chemical composition, antioxidant, and antimicrobial activities of two essential oils from Algerian propolis. Z. Naturforsch. C 2022; 77(3-4):105-112. doi:https://doi.org/10.1515/znc-2021-0028

[27] Bayram M, Topuz S, Karabıyıklı S, Elmastas M, Kaya C, Erenler R, Onaran A. Isolation of oleuropein from olive leaf by effective method and investigation of its antimicrobial properties. Indian J Tradit Know 2022; 21(1):215-223.

[28] Zuas O, Hamim N, Sampora Y. Bio-synthesis of silver nanoparticles using water extract of *Myrmecodia pendan* (Sarang Semut plant). Mater Lett 2014; 123:156-159. doi:https://doi.org/10.1016/j.matlet.2014.03.026

ISBN: 978-605-73552-2-5

# STABLE ISOTOPE RATIO OF BASAL SOURCES AND CONSUMERS IN KARACAÖREN RESERVOIR

**Nehir KAYMAK[1*], Nesrin EMRE[1], F. Banu YALIM[2], Cihan TOSLAK[2], Yılmaz EMRE[1], Şenol AKIN[3]**

[1] Biology, Faculty of Science, Akdeniz Üniversity, Antalya, Turkey
[2] Mediterranean Fisheries Research, Production and Training Institute Antalya, Turkey
[3] Biology, Faculty of Science, Bozok Üniversity, Yozgat, Turkey
**Corresponding author:* nehirkaymak@akdeniz.edu.tr

## ABSTRACT

Stable isotope analysis has become a key technique in determining anthropogenic pressures and land use effects on aquatic systems. Both carbon and nitrogen stable isotopes are sensitive to nutrient enrichment and increased primary productivity, especially $\delta^{15}N$ values. In this study, the isotope ratios of both consumer and basal sources in the Karacaören reservoir were evaluated, and seasonal variation in C and N isotope ratios of organisms was investigated.

We sampled fishes, benthic and pelagic invertebrates, and basal production sources in summer and winter from the reservoir during 2019-2020. We used one-way analysis of variance to test the significance of seasonal differences in $\delta^{13}C$ and $\delta^{15}N$ of basal resources and consumers. Pairwise differences were tested using Tukey's post hoc test. All analyses were conducted using SPSS.

Both $\delta^{13}C$ and $\delta^{15}N$ of macrophyte and detritus were significantly lower in winter than in summer. Seston, invertebrates, and fish samples had similar $\delta^{13}C$ values in both seasons. However, it has been determined that all consumers and seston were much more $^{15}N$-enriched. The Aksu Stream flowing into the reservoir carries a very high risk of pollution because of the discharge of sewage into streams. These findings might explain the high $\delta^{15}N$ values of both seston and consumer tissues.

**Keywords:** stable isotope, nitrogen isotope, nutrient load; bioindicators, Karacaören reservoir

## 1. INTRODUCTION

Changing streams by human action causes permanent and significant changes in their productivity and properties [1]. The most important of these is the construction of dams and the regulation of rivers [2], [3]. Dams can adversely affect river ecosystems by drastically changing the waterway from lotic to lentic systems [4]. Controlling stream flow due to dams causes major changes in nutrient and organism movements, water temperature, sediment transport from dam outlet to habitats, downstream food web, productivity through habitat, and nutrient loss [5]. In addition to these, they cause biological, chemical, and physical changes in the entire river basin. Therefore, ecosystem assessments are important after dam construction for water quality management and biodiversity conservation.

Stable isotopes, especially those of carbon and nitrogen, are now commonly used to study food webs and energy flow within freshwater ecosystems [6]. Carbon and nitrogen stable isotopes can be used to determine the origin of organic matter and energy sources in food webs [7], [8]. For example, the difference in carbon isotope signatures between zooplankton and POM reflected the relative contribution of allochthonous and autochthonous organic matter to bulk POM and varied with trophic status. In lakes, the seasonal variation of $\delta^{13}C$-zooplankton may be related to the seasonal succession of phytoplankton and is directly related to $\delta^{13}C$-phytoplankton [9], [10], [6]. Additionally, stable isotopes can be used as a tool to study relationships between surface waters and the surrounding watershed. Recent studies have used $\delta^{15}N$ measurements in lakes to attribute increases in nitrogen loading from anthropogenic sources to eutrophication

ISBN: 978-605-73552-2-5

[11], [12]. $\delta^{15}N$ has proven useful as a tracer of the main source of nitrogen entering freshwaters and coastal waters. The joint use of $\delta^{15}N$ and $\delta^{13}C$ has shown promise as a tool to help explain how external sources of N as well as C sources have been introduced into aquatic food webs. Knowledge of seasonal variation in stable isotope ratios is important as a reflection of biogeochemical and ecological processes, as well as expected variability for sampling programs and applied for monitoring programs.

In this context, the aims of this study were to describe the temporal variations of stable carbon and nitrogen isotopes in primary production sources, to describe temporal variations of stable carbon and nitrogen isotopes of the macroinvertebrates, and fish species inhabiting the reservoir, and to discuss the possible mechanisms underlying these variations.

## 2. MATERIALS AND METHODS

### 2.1. Study sites

Karacaören I Dam Lake is located within the borders of Isparta and Burdur provinces (Figure 1). The height of the dam lake on Aksu Stream is 270 m above sea level, and its deepest point is 85 m. At the normal water level, the lake area is 45.5 km2 and the lake volume is 1.234*106 m3 [13].

The construction of the dam was started in 1977 for irrigation of 9500 ha area downstream, flood protection, and electricity generation, and was put into operation in 1989. The water income consists of snow and rainwater coming from the Göksu spring and Aksu Stream, as well as Köy Çay, Kızıllı Stream, and Ballıktaş Streams. While the surface waters of the lake decrease to 10°C in winter, it rises to 27-28°C in summer. Karacaoren I Dam Lake (Fig. 1) is connected with Lake Kovada and Egirdir via the Aksu and Kovada Rivers and is 50 km away from Lake Kovada and 75 km away from Lake Egirdir [14].

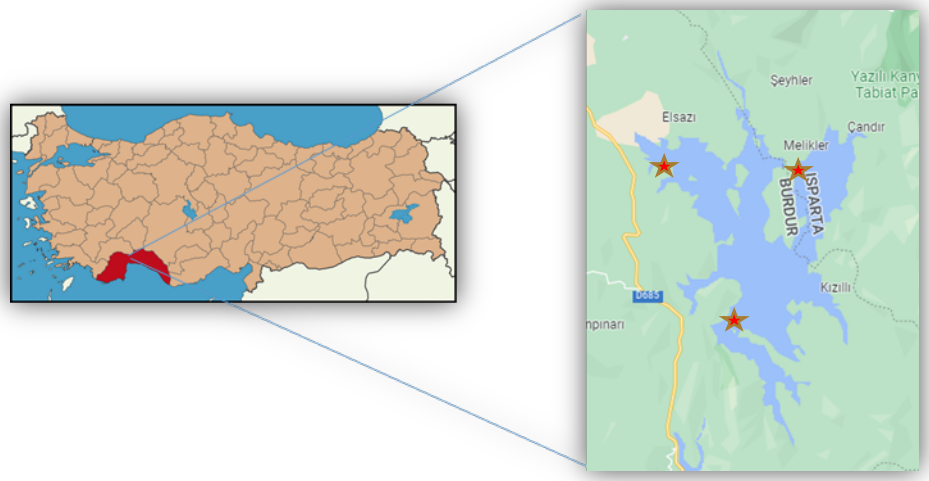


Figure 1. Study location and sites, Karacaören I reservoir [15].

### 2.2. Sample collection and preparation

In this study, samples were collected at three sites in this Reservoir (Fig. 1). Common primary production sources and consumers were sampled at each site during two seasons: wet season (winter) and dry season (summer) between 2019-2020. At a given location, tissue samples of basal production sources and consumer taxa were collected on the same day.

We measured stable-isotopic values in particulate organic matter (POM), macroalgae, macrobenthos, zooplankton, and fish in each of the three sites. To evaluate the seasonal variation in the isotopic values, we repeated the sampling in November (2005), and in February, May, and July (2006) at the two sites in the south arm of the estuary. Submerged

ISBN: 978-605-73552-2-5

and floating-leaved macrophytes, seston, and detritüs. Floating-leaved plants (*Potamageton* spp., etc) were collected by hand, and submerged plants (*Nitella* sp., etc.) were collected by using a rake. Water samples were collected in 5-L opaque bottles and filtered through a 63-mm sieve to remove zooplankton; the remaining particles that settled onto the bottom were collected as seston samples. All samples were placed in plastic bags and stored on ice in the field and then in a freezer in the laboratory. Detritus originating from dead or recently fallen leaves, branches, and seeds from terrestrial vegetation was collected from the water surface.

Zooplankton was collected from an offshore area of the lake using a standard plankton net (60 µm). Benthic invertebrates were collected with an Ekman grab on the lake bottom, and *Chironomus* sp. (Blood-red Chironomidae larvae) made up the overwhelming majority of invertebrates samples. Fish were collected during the evening between 11:00 pm and 09:00 am using experimental gill nets with panels of 25-, 30-, 40-, 50-, 60-, 70- and 80-mm mesh. Fishes also were collected with a bag seine net alongshore. Fish specimens were killed in an ice bath and stored on ice for transport to the laboratory, where they were identified to species level, weighed, and measured for standard length (SL).

### 2.3. Stable-Isotope Analysis

In the laboratory, aquatic plant leaves and detritus were rinsed with distilled water, and then any debris or invertebrates were removed during examination under a stereomicroscope. Zooplankton samples were filtered through precombusted (450°C, 4 h) GF/F filters. Invertebrate samples were rinsed with distilled water. Boneless and skinless samples of muscle tissue were extracted from the flanks of fish specimens below the dorsal fin and then rinsed with distilled water. For larger consumers (fish, benthic macroinvertebrates), each sample consisted of a single individual; however, for smaller consumers, a sample was a composite of 10 individuals to generate minimal weights (2 mg) for stable isotope analyses. Samples were dried at 608C for 48 h. Dried samples were ground into a fine powder and stored in glass vials. Approximately 3 mg of each sample was subsequently weighed to 0.001 mg and sealed inside ultrapure tin capsules (Elemental Microanalysis Ltd, Okehampton, UK). Samples were analyzed for carbon and nitrogen isotope ratios using mass spectrometry at the Akdeniz University, Food Safety and Agricultural Research Center. Ratios (R) of the heavy to light isotopes (i.e. $^{13}C/^{12}C$, $^{15}N/^{14}N$) are expressed in parts per thousand, relative to the standards in delta notation according to the following formula:

$$\delta X=[(R_{sample}/R_{standard}-1)] \times 10^3$$

in which the standards are Pee Dee Belemnite limestone and atmospheric molecular nitrogen for C and N respectively. Atmospheric nitrogen (for $\delta^{15}N$) and Peedee belemnite (PDB) (for $\delta^{13}C$) were used as the standards. The analytical precision was within 0.1‰ and 0.2‰ for carbon and nitrogen isotope measurements, respectively.

The data were analyzed using ANOVA to test the null hypothesis that there were no significant differences in either the $\delta^{15}N$ or $\delta^{13}C$ composition of each group/species among seasons (winter and summer). Pairwise differences were tested using Tukey's post hoc test. All analyses were conducted using SPSS.

## 3. RESULTS

### 3.1. Stable isotope ratios of primary production sources

We analyzed stable carbon and nitrogen isotopic compositions of four primary producers groups. The primary production sources were in general isotopically differentiated for $\delta^{13}C$ ($F=54.59$, $p=0.000$, ANOVA) and $\delta^{15}N$ ($F=9.06$, $p= 0.001$, ANOVA). $\delta^{13}C$ values of floating macrophytes were more 13C enriched than other primary producers, while detritüs was more $^{13}C$ depleted (Fig. 2). Carbon isotope ratios of seston and submerged macrophytes overlapped to varying degrees. Although, detritüs, floatining and submerged macrophytes had similar δ15N values ($p>0.05$), seston had heavier $\delta^{15}N$ values ($p<0.05$) (Fig. 2).

There were no differences between the carbon and nitrogen isotope signatures of samples of seston ($\delta^{13}C$ $F=0.366$, $p>0.05$, and $\delta^{15}N$ $F=0.07$, $p>0.05$) collected from winter and summer seasons (Fig. 3). There was significant seasonal variation in $\delta^{13}C$ ($F=14.61$, $p<0.05$) and $\delta^{15}N$ values of submerged macrophytes ($F= 26.9$, $P<0.05$). Submerged macrophytes were more $^{13}C$ and $^{15}N$ enriched in summer compared to winter. $\delta^{13}C$ of detritus was generally higher in

ISBN: 978-605-73552-2-5

summer than winter (F=22.79, p<0.05), while there was a consistent lack of seasonal pattern in the $\delta^{15}N$ values of detritus (F=0.329, p>0.05). Although there were no significant differences in $\delta^{13}C$ values of floating-leave macrophytes among seasons (F=0.501, p>0.05), $\delta^{15}N$ was approximately 4‰ higher during winter (F=25.61, p<0.05) (Fig. 3).

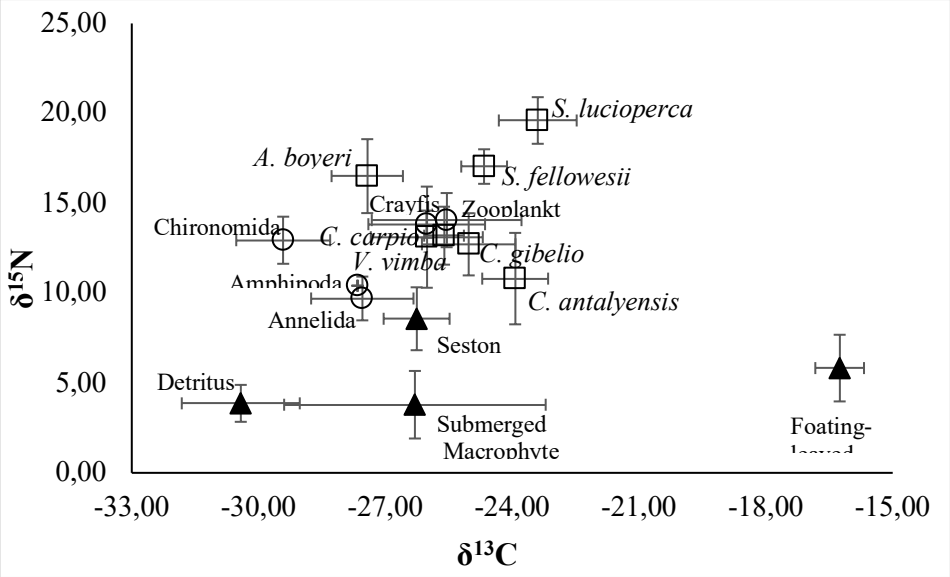


Figure 2. Mean (± 1 SD) values of $\delta^{13}C$ and $\delta^{15}N$ of the primary production sources and consumers.

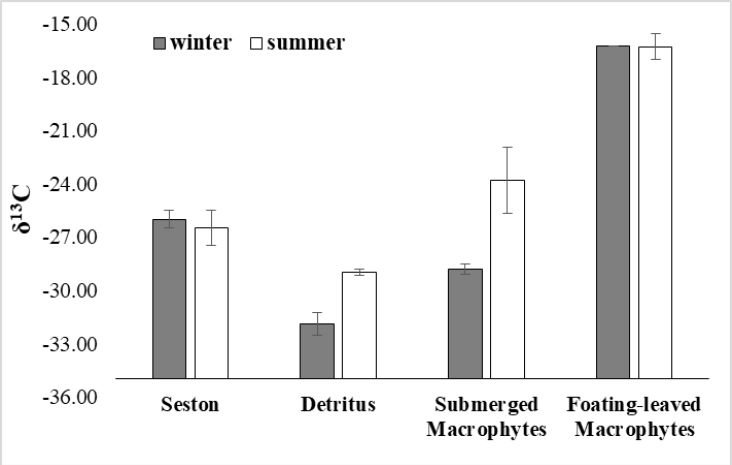

ISBN: 978-605-73552-2-5


Figure 3. Seasonal variation in mean stable nitrogen and carbon isotope ratios of primary production sources during winter and summer seasons.

### 3.2. Stable isotope ratios of consumers

Five macroinvertebrate groups such as zooplankton, chironomid larvae, annelida, amphipoda and crayfish, and seven fish species, including *Atherina boyeri, Cyprinus carpio, Carassius gibelio, Sander lucioperca, Capoeta antalyensis, Squalius fellowesii,* and *Vimba vimba* were sampled for stable isotope analysis.

The stable nitrogen and carbon isotope ratios of fish species differed significantly ($F=19.54$, $p<0.05$, and $F=19.44$, $p<0.05$, respectively) (Fig. 2). The most depleted $\delta^{13}C$ values (-27.43‰) were for *A. boyeri,* while *S. lucioperca* exhibited the most enriched values (-23.40‰). $\delta^{15}N$ values of *A. boyeri*, *S. fellowesii* and *S. lucioperca* were higher than those of *C. antalyensis, C. carpio* and *C. gibelio.* The macroinvertebrate groups were in general isotopically differentiated for $\delta^{13}C$ ($F= 7.736$, $p<0.05$), such as chironomid larva was more $^{13}C$-depleted than crayfish and zooplankton. $\delta^{15}N$ of Annelida was lower than those of all other taxa ($F=9.74$, $p<0.05$) (Fig. 2).

There were no significant differences in $\delta^{13}C$ of *C. antalyensis, S. fellowesii* and *C. gibelio* between seasons ($F=0.490$, $F=0.141$, and $F=0.05$, $p>0.05$), while $\delta^{15}N$ of these species varied seasonally ($F=40.03$, $F=9.39$, and $F=7.32$, $p<0.05$) (Fig. 4). $\delta^{15}N$ of *C. antalyensis* and *S. fellowesii* was generally higher in the summer season, whereas higher in the winter season for *C. gibelio.* Both $\delta^{13}C$ and $\delta^{15}N$ of *A. boyeri* and *C. carpio* showed significant seasonal variation ($F=6.01$, and $F=8.38$, $p<0.05$). *C. carpio* was more $^{15}N$-enriched, but $^{13}C$-depleted in winter, while the opposite is true for *A. boyeri* (Fig. 4).

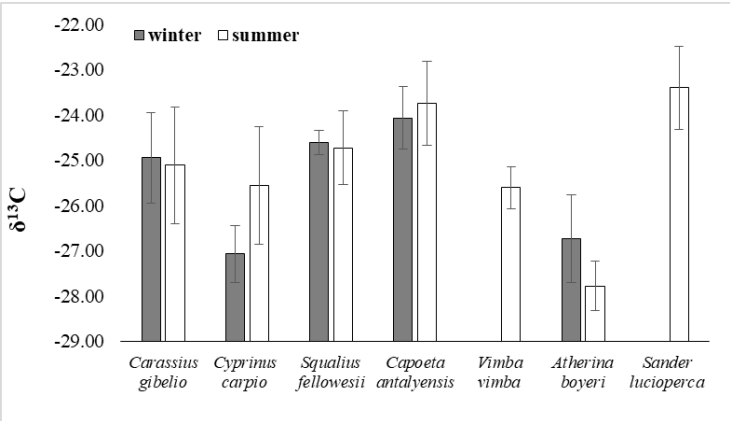

ISBN: 978-605-73552-2-5

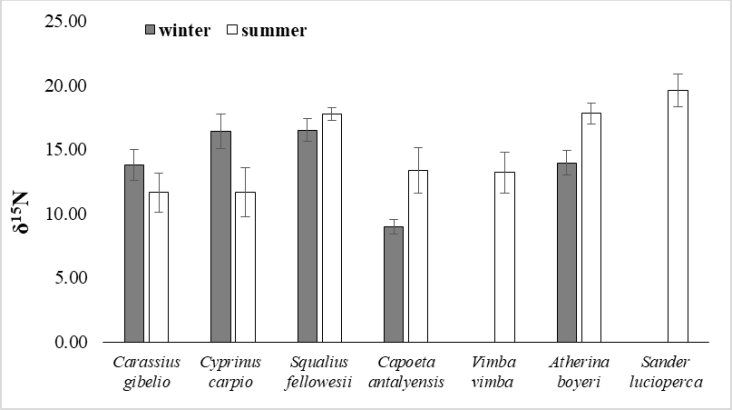


Figure 4. Seasonal variation in mean stable nitrogen and carbon isotope ratios of fish species during winter and summer seasons.

There were no significant seasonal differences in $\delta^{13}C$ and $\delta^{15}N$ of zooplankton samples ($F=0.184$, and $F=1.167$, $p>0.05$). $\delta^{13}C$ of crayfish ($F=14.57$, $p<0.05$) and $\delta^{15}N$ of chironomid larvae ($F=69.09$, $p<0.05$) showed consistent seasonal changes between seasons (Fig. 5).

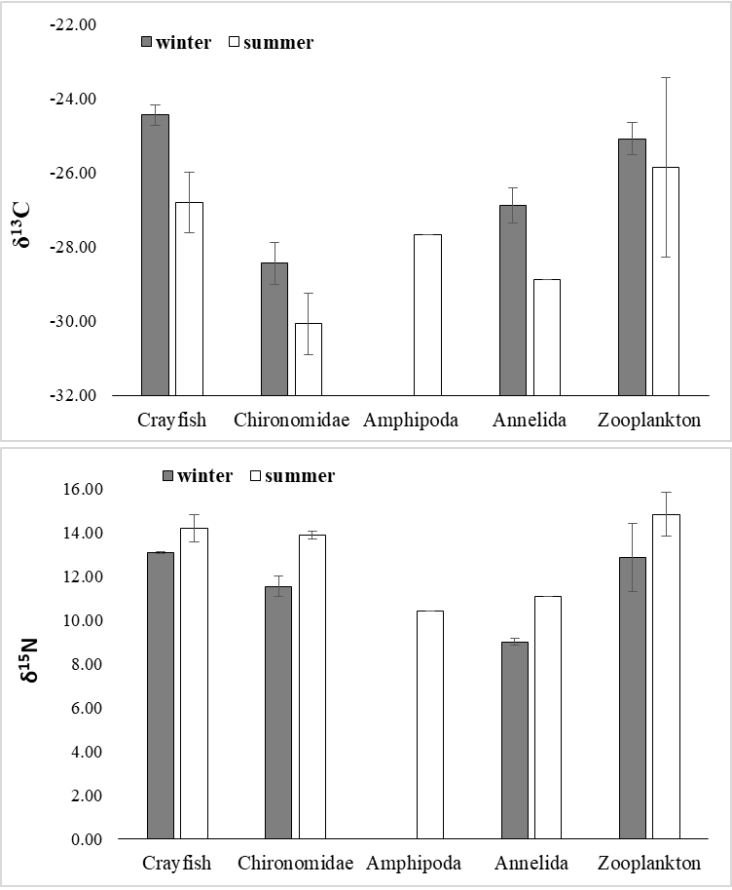


Figure 5. Seasonal variation in mean stable nitrogen and carbon isotope ratios of macroinvertebrates during winter and summer seasons.

ISBN: 978-605-73552-2-5

## 4. DISCUSSION

In the Karacaören I reservoir, floating leave macrophytes tended to be more $^{13}C$ enriched than all other basal sources. Potamageton species constituted the majority of floating-leaved plants in this reservoir, especially in the summer season. Bulk $\delta^{15}C$ values for Potamogeton leaves showed considerable variation, with -5.8‰ and -18.1‰ values [16], [17]. Our data from floating leaf macrophytes were consistent with this finding. In addition, the $\delta^{15}N$ value of macrophyte leaves had higher than other basal sources except for seston. Our results indicated that the mean content of leaf $\delta^{15}N$ was 8.51‰, which is significantly enriched than that of submerged macrophytes leaves (2.22‰) in winter. Seasonal differences are probably related to environmental factors. Freshwater run-off, irradiance levels, temperature, carbon and nitrogen sources, and water movements are the main factors known to affect carbon and nitrogen isotopic composition in basal sources [18]. Besides environmental factors, land use can significantly affect plant leaf $\delta^{15}N$ characteristics [19]. Seston samples were a proxy for pelagic phytoplankton, and were more $^{13}C$ and $^{15}N$ enriched in this study. The $\delta^{15}C$ values of seston are within the range of (-42‰ and -24‰) freshwater plankton reported in the literature [20]. Less depleted $\delta^{15}C$ values in winter may be explained by the greater contribution of $^{13}C$-enriched organic matter within seston. Because flood pulses had a strong influence on the entrance of terrestrial organic matter into the reservoir in the rainy winter season [21]. The relatively high $\delta^{15}N$ of seston (8.88-8.37‰) in the reservoir might be due to high levels of anthropogenically derived N introduced from the surrounding landscape since anthropogenically derived waste usually have high $\delta^{15}N$ [22]. The nitrogen metabolism concomitant with eutrophication in lake sediment including biochemical and physicochemical processes also cause the enrichment of $^{15}N$ [22].

There was a consistent lack of seasonal pattern in the isotopic values of seston and zooplankton, but zooplankton and other invertebrate taxa followed changes in seston which they ingest. The $\delta^{15}N$ signatures of the consumers (fish and invertebrates) ranged from 9.00 to 19.60‰. All consumer taxa would reflect these higher $\delta^{15}N$ values if basal sources are being assimilated, either directly or indirectly. It has been reported that the Aksu stream flowing into the reservoir carries a very high risk of pollution because of the discharge of sewage into streams [23]. These findings might explain the high $\delta^{15}N$ values of both seston and consumers.

*Cyprinus carpio* and *Atherina boyeri* mean $\delta^{15}C$ changed seasonally in the reservoir. However, other fish species' mean $\delta^{15}N$ changed seasonally, and there were no differences for mean $\delta^{15}C$. These results can be explained by two hypotheses. The first one is that the isotopic composition of fish muscle tissue might have reflected seasonal variation in the isotopic composition of primary producers supporting fish biomass. The second one is that fish diets might have changed in response to seasonally abundant food resources. For example, the $\delta^{15}N$ values of nonnative fish, *C. carpio,* and *C. gibelio* were higher in winter. This probably indicated that these fish assimilated more material derived from terrestrial production sources which receive by precipitation runoff to the reservoir. On the contrary, $\delta^{15}N$ values of these fishes decreased in summer as it may contribute to fish biomass in seston and macrophytes as well as terrestrial sources. Other native fish species (*C. antalyensis* and *S. fellowesii*) in the reservoir exhibited higher nitrogen values in the summer season, suggesting that these fish might assimilate energy from a single food source (seston or zooplankton) in a high proportion. In addition, another non-native fish, *S. lucioperca*, was sampled only in the summer season, and the $\delta^{15}C$ and $\delta^{15}N$ values of this fish reflected that they can be fed especially on native fish (Fig. 2).

## 5. CONCLUSION

This study showed that this reservoir is under very high pollution pressure, which is supported by the high nitrogen values of all the organisms. Because nitrogen isotope ratios of organisms are also used as a bioindicator in aquatic ecosystem studies. We can say that the food preferences of non-native fish are wide, and they are generalists. However, it has been observed that native fish may have narrower food preferences.

ISBN: 978-605-73552-2-5

## ACKNOWLEDGEMENTS

This study was supported by the Akdeniz University Research Fund (Project Number: FBA-2018-4161).

## REFERENCES

[1] Naiman, RJ. Turner MG. A future perspective on North America's freshwater ecosystems. Ecological Applications 2000; 10, 958-970.

[2] Petts GE, Gurnell AM. Dams and Geomorphology: Research progress and future directions. Geomorphology 2005; 71, 27– 47.

[3] Naliato DA, Nogueıra MG, Perbıche-Neves G. Discharge Pulses Of Hydroelectric Dams And Their Effects İn The Downstream Limnological Conditions: A Case Study İn A Large Tropical River (SE Brazil). Lakes and Reservoirs: Research and Management 2009; 14, 301–314.

[4] McAllister DE, Craig JF, Davidson N, Delany S, Seddon M. Biodiversity Impacts of Large Dams. vol Background Paper Nr. 1. 2001. IUCN/UNEP/WCD, 68.

[5] Wootton JT, Parker MS, Power ME. Effects of Disturbance on River Food webs. Science 1996; 273, 5281, 1558-1561.

[6] Syväranta J, Hämäläinen H, Jones R. Within-lake variability in carbon and nitrogen stable isotope signatures. Freshwater Biology 200; 51: 1090–1102.

[7] Minagawa M, Wada E. Stepwise enrichment of 15N along food chains: further evidence and the relation between δ15N and animal age. Geochimica et Cosmochimica Acta 1984; 48: 1135–1140.

[8] Vander Zanden MJ, Rasmussen JB. Variation in $\delta^{15}N$ and $\delta^{13}C$ trophic fractionation: implications for aquatic food web studies. Limnology and Oceanography 2001; 46, 8, 2061–206.

[9] Zohary T, Erez J, Gophen M, Berman-Frank I, Stiller M. Seasonality of stable carbon isotopes within the pelagic food web of Lake Kinneret. Limnology and Oceanography 1994; 39: 1030–1043.

[10] Gu B, Alexander V, Schell DM. Seasonal and interannual variability of plankton carbon isotope ratios in a subarctic lake. Freshwater Biology1999; 42: 417–426.

[11] Anderson C, Cabana G. Does δ15N in river food webs reflect the intensity and origin of N loads from the watershed?. Science of the Total Environment 2006;367: 968–978.

[12] Risk MJ, Lapointe BE, Sherwood OA, Bedford BJ. The use of δ15N in assessing sewage stress on coral reefs. Marine Pollution Bulletin2009; 58: 793–802.

[13] Becer Özvarol ZA, İkiz, R. KARACAÖREN I BARAJ GÖLÜ'NDEKİ SUDAK, Sander lucioperca (Lin., 1758) POPULASYONUNUN BÜYÜME ve ÖLÜM ORANLARI İLE STOK ANALİZİ. Journal of Fisheries Sciences 2008; 2(2): 134-145.

[14] Becer Özvarol ZA, Kılıç Z. EFFECT ON LAKE FISHERY AND SOME BIOLOGICAL CHARACTERS OF THE SAND SMELT, (ATHERINA BOYERI RISSO, 1810) INTRODUCED TO KARACAOREN I DAM LAKE (TURKEY). Fresenius Environmental Bulletin 2018; 27(12A): 9392-9398.

ISBN: 978-605-73552-2-5

[15] Anonymus. https://tr.m.wikipedia.org/wiki/Dosya:Latrans-Turkey_location_Antalya.svg. 29.08.2022.

[16] Aichner B, Herzschuh U, Wilkes H. Influence of aquatic macrophytes on the stable carbon isotopic signatures of sedimentary organic matter in lakes on the Tibetan Plateau. Organic Geochemistry 2010; 41 (7): 706-718.

[17] Chappuis E, Seriñá V, Martí E, Ballesteros E, Gacia E. Decrypting stable-isotope (δ13C and δ15N) variability in aquatic plants. Freshwater Biol. 2017; 62: 1807– 1818

[18] Vizzini S, Mazzola A. Seasonal variations in the stable carbon and nitrogen isotope ratios (13C/12C and 15N/14N) of primary producers and consumers in a western Mediterranean coastal lagoon. Marine Biology 2003; 142: 1009–1018.

[19] Gong X, Xu Z, Peng Q, et al. Spatial patterns of leaf δ13C and δ15N of aquatic macrophytes in the arid zone of northwestern China. Ecol Evol. 2021; 11: 3110– 3119.

[20] Kendall C, Silva SR, Kelly VJ. Carbon and nitrogen isotopic compositions of particulate organic matter in four large river systems across the United States. Hydrological Processes 2001; 15, 1301-1346.

[21] Zeug SC, Winemiller KO. Evidence supporting the importance of terrestrial carbon in a large-river food web. Ecology 2008; 89: 1733–1743.

[22] Xu J, Xie P, Zhang M. et al. Variation in stable isotope signatures of seston and a zooplanktivorous fish in a eutrophic Chinese lake. Hydrobiologia 2005; 541, 215–220.

[23] Kalyoncu L, Kalyoncu H, Arslan G. Determination of heavy metals and metals levels in five fish species from I¸sıklı Dam Lake and Karacaören Dam Lake (Turkey). Environ Monit Assess 2012; 184:2231–2235.

ISBN: 978-605-73552-2-5

# EXPERIMENTAL STUDY OF ELECTRICAL HEATER WORKING FUNCTION FOR IMPROVING ENERGY CONSUMPTION IN A DOMESTIC OVEN

**Ayberk Salim MAYIL[1,*], Can UGURELLİ[1], Ayben CENGİZ[2], Burak GÜZELTEPE[2]**

[1] Haier Europe, Candy- Hoover Group, Research and Development Center, Eskişehir, Türkiye-amayil@hoover.com.tr
[1] Haier Europe, Candy- Hoover Group, Research and Development Center, Eskişehir, Türkiye- cugurelli@hoover.com.tr
[2] Haier Europe, Candy- Hoover Group, Research and Development Center, Eskişehir, Türkiye-acengiz@hoover.com.tr
[2]Haier Europe, Candy- Hoover Group, Research and Development Center, Eskişehir, Türkiye- bguzeltepe@hoover.com.tr

## ABSTRACT

There is a big demand from the customer and regulatory side for higher efficiency products to save electricity consumption and decrease the carbon footprint. Manufacturers and designers must check new improvements to afford such an important request. New improvements related with the energy efficiency cause the new competitive between manufacturers about fast cooking, multi cooking, well designed esthetics etc. During the studies, it needs to high number test to ensure the international regulatory standards. In this study, different heater functions are examined to decrease energy consumption of the oven during standard energy test as an experimentally. 3 versions of the heater working cycles are studied and it shows what is the effect of these function on energy consumption.

**Keywords:** Household Oven, Energy improvements, Experimental methods.

## 1. INTRODUCTION

Due to the obligations and competition conditions brought by international standards and the efficient use of energy resources in the world, efforts to reduce energy consumption and increase cooking quality in household electric ovens are increasing rapidly. In the design of domestic ovens, there are different important parameters for low energy consumption. To provide optimized energy consumption; insulation, cavity, fan properties, baffle, software flexibility, low faulty production etc. are particularly important parameters.

Literature includes different attempts to decrease energy consumption. Burlon applied experimental studies for creating different technical solutions to decrease energy consumption of the ovens. In the results of that studied, between %4-%25 energy saving was observed by applying different solutions [1]. Bozgeyik et al. examined different insulation materials to check what the effect on energy consumption [2]. They compared needle glass wool, rock wool, yellow glass wool, ceramics wool and dynaguard. Results showed that density of insulation material is effective on thermal inertia of oven the cavity. Despite heat conduction coefficient is lower, if density is extremely high, total energy consumption of the oven is increased. There are different methods other than insulation improvement to optimized domestic ovens. Scarisbrick et al. applied experimental analysis related to thermal performance of ovens [3]. Different heating element configurations, low-emissivity internal oven-lining, well-designed control system for internal air temperature of oven and various thermal insulation systems are tried. Overall, studies showed %17 – %20 thermal efficiency increment. B.M. Shaughnessy et al. studied low emissivity ovens and compared them with the conventional ovens [4]. Low-emissivity components (oven compartment, removable panels, and door-inner) emissivity were 0,07. Results showed, %35 energy-savings by comparison with the conventional ovens. Özge et al. studied experimental examination of oven doors impact on energy consumption for household ovens [5]**.** Interior glass covered with Al foil during energy consumption test.

Results showed that covering the interior glass of oven with Al foil is 12% better than conventional oven as a means of energy consumption.

## 2. METHODOLOGY

A research and development activity or each development that is considered to be implemented cannot be directly implemented most of the time due to cost and budget. Before a designed product is put into serial production, it should be tested in order to examine its performance and determine its capabilities. In addition, any mistakes in the test processes can directly cause damage of life and property. For this reason, the necessary tests are performed before the

ISBN: 978-605-73552-2-5

project is applied. Although it is a time-consuming and difficult process to set up for the tests to be made, it directly contributes to the production, development and testing costs.

**Energy Test,** Energy consumption test is applied in accordance with EN-60350-1 standard. The energy test consists of 2 stages and is done at 230 volts. First, the preheating process takes place. In the last part, the load heating and performance measurement process takes place.
Energy performance measurement in accordance with EN 60350-1 standard; It is done in conventional (classical) and forced convection functions.

In this part of the investigation, versions 1,2 and 3 were applied in the existing built-in oven. The review in this study includes the experimental studies of the oven in different versions, with the features of the oven produced in the current production. Experimental studies in versions 1,2 and 3 were applied in accordance with the energy consumption test EN-60350-1 standard.

In this direction, the versions mentioned are examined one by one in order to examine the performance of a built-in oven. Tests are the process of conceptive, graphical or mathematical of physical processes. The purpose of tests is to predict the results of a process by defining certain conditions to the system. The tests carried out over time made it possible to realize it in a short time and in a practical way.

## 2.1 Oven Descriptions and Materials

The tests performed on the oven were carried out within the scope of a certain standard. In order to apply these tests, the temperature information of the bulb temperature, the central temperature of the built-in oven, the ambient temperature and the temperature of the bricks used were obtained with the help of thermocouples. This information was obtained thanks to the power measurement system used. Figure 1 and 2 display the schematic of the investigated built-in oven electrical oven upper and bottom resistance which is one in the present models of the Haier Europe for household. Some major technical specifications of the oven in the present study are as below:

- Electronic control panel
- 2500 (W) of total heating capacity and voltage of 220-240 (V)
- Circular (ring) heater power of 2200 (W)
- Insulation class of Rockwool (100 kg/m^3)
- 70 litters of declared volume
- Measured dimensions of the inside of the cavity (cooking room):
    - Cavity depth 396 (mm)
    - Cavity width 476 (mm)
    - Cavity height 365 (mm)

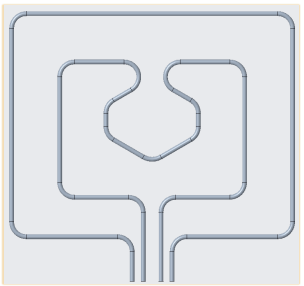

Figure 1:Schematic of investigated Haier Europe’s domestic built-in electrical oven upper rezistance

ISBN: 978-605-73552-2-5

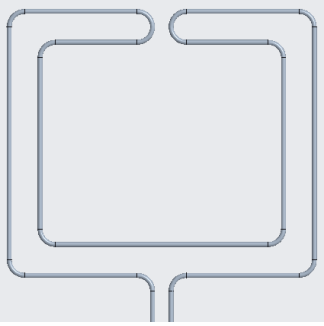

Figure 2:Schematic of investigated Haier Europe's domestic built-in electrical oven bottom rezistance

**The power measurement device (Yokogawa),** the instantaneous processing of the test results output data and the saving and making available at the same time allows the data to be processed in Excel.

**Thermocouple,** is a kind of temperature sensor which is K type.

**Offset** is the difference in temperature between the set point and the actual process temperature. When the offset has increased in this experiment, the overshooting of temperature getting higher degree. It was replaced the difference between the set temperature value and real temperature with adjust the offset.

**Working cycle,** the selected oven completes the cooking by working in three different phases. The first part is preheating phase which the oven works non-stop to reach the set temperature value in this phase. The second part is working cycle. The working cycle contributes to the energy saving side of the furnace with its constant on-off cycle. This cycle, which consists of on-off, repeats this at certain periods, for example 60 seconds, 120 seconds, and continues to work in this way until a certain time. As long as the oven is desired to work from the temperature it cuts off during preheating, the oven is operated with the working cycle during that time for example 60 minute.
The last part cycle starts with end of working cycle. It is the phase that tries to bring the oven back to the set temperature value after the oven door is opened and the cooked food is taken from the oven.

## 2.3 Modifications

In this study aim was the obtain optimised heater working function. As shown in the Table 1, three different heater versions were created to apply experimental test.

Table 1: Three different heater versions used in experimental tests

| VERSION/HEATERS | V1 | | V2 | | V3 | |
|---|---|---|---|---|---|---|
| | Pre-heating | Cycle | Pre-heating | Cycle | Pre-heating | Cycle |
| Upper outer resistance | X | X | | X | X | X |
| Upper inner resistance | | X | X | X | X | X |
| Bottom resistance | X | | | | X | |
| Cavity resistance | | | | | | |
| Fan | | X | X | X | | X |

### 2.3.1. Outer resistance+bottom resistance working cycle (Version-1)

In the preheat phase of Version 1, the upper external resistor and lower resistor were operated. It was set out with the idea that the brick would heat up faster with the operation of both the upper outer and lower resistance. It works until the oven stops working and goes into the working cycle.

### 2.3.2. Inner resistance+fan working cycle (Version-2)

Version 2 was tried for seeing how working of single resistance affect the oven cooking behaviour. The upper inner resistance which has lowest resistance value in oven has used for tests. The reasons for trying this version can be

ISBN: 978-605-73552-2-5

explained as follows. When the brick has placed in the oven center, that resistance affect directly the cooking of the brick because of the inner position. It is aimed to extend the preheating time and to heat the brick in the oven for a longer time with less power by operating only the upper inner resistance in the preheating.

### 2.3.3. Inner resistance+outer resistance+bottom resistance working cycle (Version-3)

The idea was for this version to observe what the effect of shock-cooking on preheating period during energy consumption test. It was used both upper inner resistance, upper outer resistance, bottom resistance and fan in preheating phase for this version. An attempt was made to create a shock effect on brick by working together with all the resistors. In this version, the offset was updated to value of 56 for 175K.

## 3. RESULTS

For this study, 5 different heater-working cycle versions was applied on domestic oven. All steps were analyzed and compared each other's. As shown in the table below, every trial is examined for the total energy consumption, total cooking time, pre-heating energy consumption and pre-heating time. For this experimental research, pre-heating cycle was the main target to create optimized energy cycle.
For the second phase of the energy test, there was not created any change to compare each version for one change.

Table 2: The measured data from experimental test for each heater versions

| CHECK POINTS | V1 | | | V2 | | | V3 | | |
|---|---|---|---|---|---|---|---|---|---|
| Temperature | 135K | 155K | 175K | 135K | 155K | 175K | 135K | 155K | 175K |
| EC (kwh) | 0.596 | 0.625 | 0.693 | 0.616 | 0.652 | 0.753 | 0.59 | 0.617 | 0.820 |
| Total Cooking Time | 64 | 56 | 52 | 72.3 | 58 | 50.9 | 62.9 | 57 | 47.6 |
| Preheating EC (kwh) | 0.331 | 0.372 | 0.419 | 0.363 | 0.473 | 0.655 | 0.320 | 0.340 | 0.450 |
| End of preheating(min) | 8.5 | 9.5 | 10.9 | 19 | 24.7 | 34.3 | 5.8 | 6.2 | 8.1 |

### 3.1 V1 Results

V1 was the first attempt to see effect of electrical heater working cycle on energy consumption test. Energy tests were done at the 135K, 155K and 175K for rack temperature differences. During V1 test, upper outer resistance and bottom resistance was on, fan was off as shown in the Table X. Energy consumption results were 0.596, 0,625, 0,693 [kWh] respectively for 135K, 155K and 175K. Total cooking times were, 64, 56, 52 [min] respectively. Preheating times were 8.5, 9.5 and 10.9 [min] respectively. Main observation was during preheating period, temperature change of the rack was 1C as an average. That means, for all preheating time, energy was consumed by rack-drying process. Thus, second step was created to try lower time cooking period to see temperature change of rack.

### 3.2 V2 Results

V2 was the second attempt to see what the effect of lower heater power during preheating period on energy consumption test was. During V2 test, upper inner resistance, and fan on. Energy consumption values were increased for each setting when they compared to V1. Reason of that, preheating time is increased between two-three times than V1 so that this increment had negative effect on energy consumption test. Contrary to this, V3 is created to check what the effect of higher heater power during preheating period on energy consumption test was.

### 3.3 V3 Results

V3 was the third trial to examine of the shock cooking process during preheating cycle. During V3 test upper inner resistance, upper outer resistance and bottom resistance were on, fan was off. For the 135K and 155K settings, energy consumption is decreased 1% - 2%. But for 175K result was 4.5% worse than V1. Main observation of 175K was, under the high electrical resistance power and high temperature setting, cavity probe reached off value without complete the preheating period. To prove this idea, under the V3 condition, offset increment was applied on oven. With this way, it was possible to check what the longer pre-heating time was under the V3 condition at 175K setting temperature.

ISBN: 978-605-73552-2-5

### 3.4 V3 Offset Results

During V3 test results, 175K setting point results showed worse behavior than V1 as a different from 135K and 155K setting points.

Because of high temperature and power conditions at V3 175K, cavity probe could reach off point fast so that this could be effective on rack-drying and rack-cooking process during preheating cycle. To observe if this idea corrects, offset study was implemented. In the Table 3 below, offset study results are shown. When offset was increased, preheating time was also increased.

As seen in the table, best energy consumption results were at the "56" offset test. Original offset was 18, that means when preheating time is increased, energy saving was gained.

When cooking time was increased more than 8min, results were getting worse than optimized point. Although 175K result was improved, V1 results were the best results.

Table 3: Offset experimental results at 175K in version 3

| 175K | | | | | |
|---|---|---|---|---|---|
| **V3 REZ** | **Offset** | **EC [Wh]** | **Pre-Heat [min]** | **Total Cook [min]** | **Pre-Heat EC [Wh]** |
| **T1** | 120 | 818 | 10.5 | 43 | 585 |
| **T2** | 106 | 802 | 10 | 44.6 | 556 |
| **T3** | 96 | 795 | 9.5 | 46 | 533 |
| **T4** | 86 | 790 | 9.25 | 47.3 | 513 |
| **T5** | 76 | 766 | 9 | 47.5 | 490 |
| **T6** | 66 | 735 | 8.25 | 47.1 | 459 |
| **T7** | 56 | 726 | 8 | 47.67 | 450 |
| **T8** | 46 | 786 | 7.8 | 57.5 | 427.11 |
| **T9** | 36 | 812 | 7.58 | 61.5 | 415 |

## 4. DISCUSSION

In this study, aim was creating to optimized electrical heater function during energy consumption test on domestic ovens for compensate the new energy demands on international standards. For this reason, 3 different heater operating cycle were tried. Working logic was shown in table x. Results showed the best working function is V1. When initial power is decreased, in the end of the preheating cycle, rack temperature was increased but preheating time was increased a lot so that on V2, negative effect was seen. For the V3, on 135K and 155K setting, better results were seen particularly. But on 175K, because of the probe was closed in a short time without finishing preheating properly. To solve this problem, different offset options were tried, and it was found optimized working condition. As a result of this study medium heater power, lower heater power and higher heater power were tried so.

- Most optimized configuration was V1.
- For all versions, optimized offset versions could be studied
- On V3, lowest energy consumption values were obtained. Upper inner resistance could be worked %40 - %60 percentage during preheating cycle for the V3.
- The best area was chosen between medium heater power and higher heater power.

Thanks to **Nurhan VATANSEVER** to support us fully for this project.

## REFERENCES

[1] F. Burlon, "Energy Efficiency of Combined Ovens", *Energy Procedia*, c. 82, ss. 986-993, Ara. 2015, doi: 10.1016/j.egypro.2015.11.856.

ISBN: 978-605-73552-2-5

[2] F. Enerj, A. Yönel, K. Yöntemler ve N. Deneysel, “İSTANBUL TEKNİK ÜNİVERSİTESİ  FEN BİLİMLERİ ENSTİTÜSÜ”, s. 63, 2006.

[3] C. Scarisbrick, M. Newborough ve S. D. Probert, “Improving the thermal performances of domestic electric ovens”, *Applied Energy*, c. 39, sy 4, ss. 263-300, Oca. 1991, doi: 10.1016/0306-2619(91)90001-E.

[4] B. M. Shaughnessy ve M. Newborough, “Energy performance of a low-emissivity electrically heated oven”, *Applied Thermal Engineering*, c. 20, sy 9, ss. 813-830, Haz. 2000, doi: 10.1016/S1359-4311(99)00072-1.

[5] Ö. Altun, Ş. Yıldız ve T. Anık, “Experimental Investigation of The Effect of Front Cover on Energy Consumption and Energy Level in Built-In House Oven”, *Pamukkale J Eng Sci*, c. 25, sy 4, ss. 403-409, 2019, doi: 10.5505/pajes.2018.23922.

ISBN: 978-605-73552-2-5

# ANTIPROLIFERATIVE AND APOPTOTIC EFFECTS OF *TRACHYSTEMON ORIENTALIS(L.) G. DON* ON HCT116, AGS AND HEPG2 CELLS

**Serkan SOYMAZ[1], Görkem DULGER[1*]**

[1] Department of Medical Biology, Faculty of Medicine, Duzce University, Duzce, Turkey

## ABSTRACT

In this study, the effectiveness of *Trachystemon orientalis (L.) G. Don* on gastrointestinal system cancer cells was investigated. Our results showed that increasing doses of the extract of this plant significantly reduced cell viability in HCT116 colon cancer, AGS gastric cancer and HepG2 hepatocellular carcinoma cell lines. While cell viability decreased in a dose-dependent manner in 24 h dose , cell proliferation inhibition increased in 48 h dose application in a time and dose-dependent manner. It was observed that the plant extract increased caspase activation at varying rates in all three cell lines. Caspase-3, 8 and 9 activation was observed in AGS cell line as a result of extract application, while Caspase-3 and 9 activation was significantly increased in HCT116 and HepG2 cell lines. Our study is important in that it contains important results for the transition to further in vivo studies with this plant extract.

**Keywords:** Anticancer, Apoptosis, *Trachystemon orienta/is(L.) G. Don*.

## 1. INTRODUCTION

T. orientalis is a plant of Eastern Bulgarian origin. In Turkey, it is popularly known as Galdirek, Kaldirik, Hodan, Kalduruk (Bolu). The plant, which is mainly found in the Western Caucasus and Black Sea regions, is consumed as a vegetable in Istanbul and other regions of the Black Sea [1,2]. A mixture of its fresh roots is used as a tonic on the skin against rheumatism and/or for the healing of flaming wounds [3]. It also has diuretic effects and can be used as a blood purifier. It has been reported that T.orientalis contains nitrate salts, tannins, mucilage, essential oils, resin and saponins [4. 5].

Gastrointestinal tract (GiS) cancers are one of the important health problems associated with high mortality rates worldwide [6]. GIS cancers; It is defined as cancer of the organs of the digestive system, including the esophagus, gallbladder, liver, pancreas, stomach, small intestine, large intestine, rectum, and anus. Current treatments include surgery, radiation, and chemotherapy with various ingredients, including cisplatin, mitomycin, and docetaxel. However, some limitations of these therapeutic agents lead to the development of new therapeutic platforms [7]. There are many studies on natural products as important sources for complementary therapy for cancer. Well-known examples of the therapeutic potential of plant-derived natural products are the microtubule inhibitors Vinca alkaloids. DNA topoisomerase I inhibitors are camptothecin, terpene paclitaxel, or podophyllotoxin-derived lignans, etoposide, and teniposide [8]. Research by the American National Cancer Institute has shown that a significant proportion of drugs approved as anticancer are either natural products or have been developed based on information obtained from natural products. Also today, about three-quarters of plant-derived drugs in clinical use have their origins in traditional herbal medicines.

A thorough understanding of the apoptotic mechanisms is important for the selective inhibition of cancer cells. Apoptosis is programmed cell death to eliminate functionally impaired cells. Apoptosis is regulated by opposing interactions of pro-apoptotic and anti-apoptotic molecules. Apoptotic signaling pathways are frequently disrupted in cancer cells. While this provides a vital advantage to malignant cells, it also causes resistance to chemotherapeutic agents. Apoptosis is initiated by cell surface death receptors (extrinsic pathway) or signals generated within the cell (mitochondrial pathway, intrinsic pathway). The internal pathway is controlled by pro-apoptotic (Bax, Bak) and anti-apoptotic (BcI-2 and BcI-XL) molecules that regulate the permeability of mitochondria. BcI-2 family members function in mitochondria and play a central role in apoptosis. Caspases are cytoplasmic proteases specific for apoptosis. These enzymes are responsible for the initiation and intracellular digestion of apoptosis. It is very important to selectively activate the apoptotic pathway in targeted therapies for cancer [9,10].

In this study, the antiproliferative effect level of *Trachystemon orientalis (L.) G. Don* plant extract was investigated by applying varying doses and times on HCT116 colon cancer, AGS gastric cancer and HepG2 hepatocellular carcinoma

ISBN: 978-605-73552-2-5

cell lines. In addition, the activation of Caspase-3, 8 and 9, which are important activation markers of apoptosis, was also investigated on these cells.

## 2. METHODS

### 2.1. Cell Culture

HCT116 colon cancer, AGS gastric cancer and HepG2 hepatocellular carcinoma cell lines were used in the study. Cells were grown in RPMI-1640 and DMEM media supplemented with 10% inactivated fetal bovine serum (Fetal Bovine Serum, FBS), 200 mM L-glutamine, 100 U/ml penicillin, 100 pg/ml streptomycin at 95% humidity and 5% They were reproduced by culturing in an incubator at 37 C in $CO_2$ environment.

### 2.2. Cell Proliferation Assay (WST-1 method)

The media were removed when the HCT116, AGS, and HepG2 cell lines covered approximately 70% of the T-75 cell flasks. Cells were separated from the base and each other using a trypsin-EDTA mixture, and after centrifugation at 1200 rpm for 10 minutes, RPMI-1640/DMEM medium containing 1% FBS was added to the pellet. Then, cells were homogeneously suspended in RPMI-1640/DMEM medium containing 1% FBS, and then seeded into 96-well cell culture dishes by drawing approximately 5000 cells/100µL into each well. After the cells were incubated overnight in an incubator at 37°C and 5% CO2, the media were removed. The extracts at the specified doses were added to the cells and incubated in a medium containing 1% FBS for 24 and 48 hours at 37°C with 5% $CO_2$. At the end of the specified times, the medium in each well was removed and replaced with 100 µL of phenol-rejection-free RPMI-1640/DMEM medium and 10 µL of WST-1 kit. The color change caused by the formazan product was determined at the wavelength range of 450 nm with a microplate reader after 4 hours. Each experiment was performed in triplicate. Cell viability calculations were made on the Excel program.

### 2.3. Protein isolation and ELISA assay

Protein isolation was performed 24 h after the plant extract was applied to cells at doses of 400 µg/mL and 600 µg/mL with RIPA buffer (A.B.T, Turkey) following the appropriate protocol steps. BCA protein assay kit (ABP Biosciences, LLC) was used to determine the amount and concentration after protein isolation. Colorimetric human Caspase-3, 8 and 9 ELISA kits (BT LAB, Shanghai, China) were used to determine protein expression levels of Caspase-3, 8 and 9 in cell supernatant samples treated with plant extract according to manufacturer's instructions. After the procedures, the results were obtained by reading the ELISA reader (Epoch Microplate Spectrophotometer, Agilent Technologies, Inc., USA) at Optical Density (OD) of 450 nm.

### 2.4. Statistical analysis

Each experiment was performed in triplicate independently of each other. The data of the experiments were statistically analyzed using Student's t-test. Values with $p<0.05$ were considered significant.

## 3. RESULTS

### 3.1. Antiproliferative effects of *Trachystemon orientalis (L.) G. Don* plant extract on HCT116, AGS and HepG2 cells.

*Trachystemon orientalis* plant extract was applied to all three cell lines at doses of 25-600 µg/ml for 24 and 48 hours. HCT116 cells did not show a significant reduction in proliferation at the 24-hour administration doses. At the highest application dose of 600µg/ml, 35% inhibition of proliferation was observed in the cells (Figure-1A). On the contrary, inhibition of proliferation was observed quite clearly in AGS cells. Cell proliferation rate was 48% at 600µg/ml application dose for 24 hours. Inhibition results were more remarkable at 48 hour doses. While the rate of cell proliferation inhibition was 50% at 150µg/ml application dose, this rate increased to 79% at 600µg/ml dose (Figure-1B). HepG2 cells exhibited an inhibition profile that was average of the other two cell lines. While there was no significant change in proliferation inhibition up to 600µg/ml application dose, the inhibition rate observed at this dose was 34%. A decrease in proliferation was observed starting from 100µg/ml dose in 48 hours application. While the inhibition rate was 42% at 400µg/ml dose, this rate increased to 59% at 600µg/ml application dose (Figure-1C).

ISBN: 978-605-73552-2-5

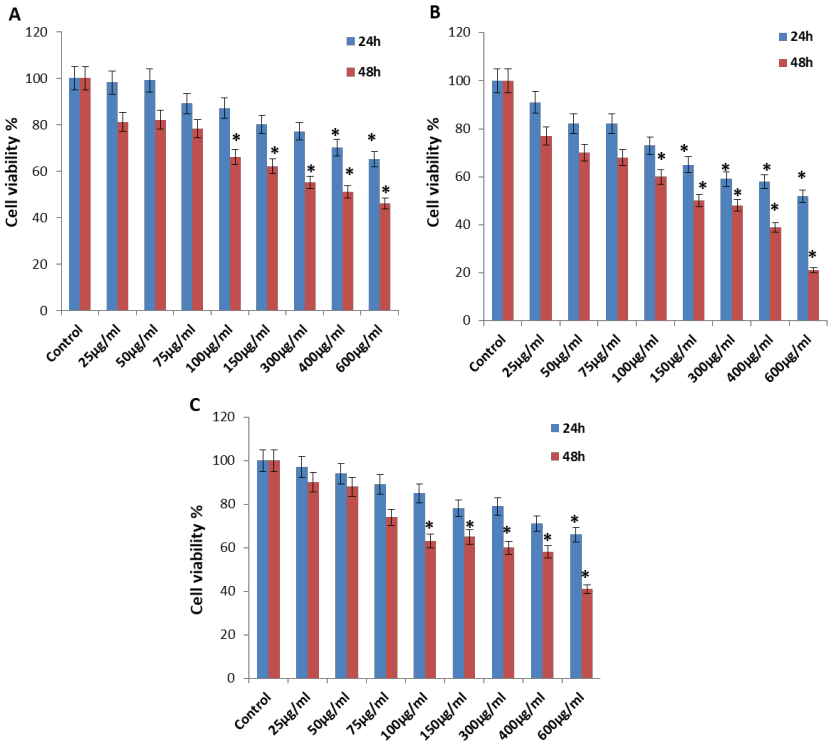


**Figure 1:** The effect of *Trachystemon orientalis (L.) G. Don* plant extract on proliferation of HCT116 (A), AGS (B) and HepG2 (C) cells (*;p<0.05).

### 3.2. Effect of Trachystemon orientalis (L.) G. Don plant extract on caspase-3, 8 and 9 expression levels in HCT116, AGS and HepG2 cell lines.

Caspase-3 activation showed a two-fold increase in HCT116 cells at a dose of 400µg/ml for 24 hours compared to the control. In 600µg/ml application, this increase was approximately 4-fold compared to the control ($p<0.05$). There were increases in caspase-8 activation at both doses compared to the control, but these increases were not significant ($p>0.05$) (Figure 2A). On the other hand, significant activation of all three caspase levels was observed in AGS cells, confirming the high level of proliferation inhibition observed. At the 600µg/ml application dose, an approximately 3.5-fold increase in Caspase-3 activation was observed compared to the control, while significant increases were observed in Caspase-8 and Caspase-9 activation at an approximate 3-fold level (Figure 2B). Caspase-3 and 9 activation was significantly observed in HepG2 cells, just as in HCT116 cells. Caspase -8 expression was also increased, but not at a significant level ($p>0.05$) (Figure 2C).

ISBN: 978-605-73552-2-5

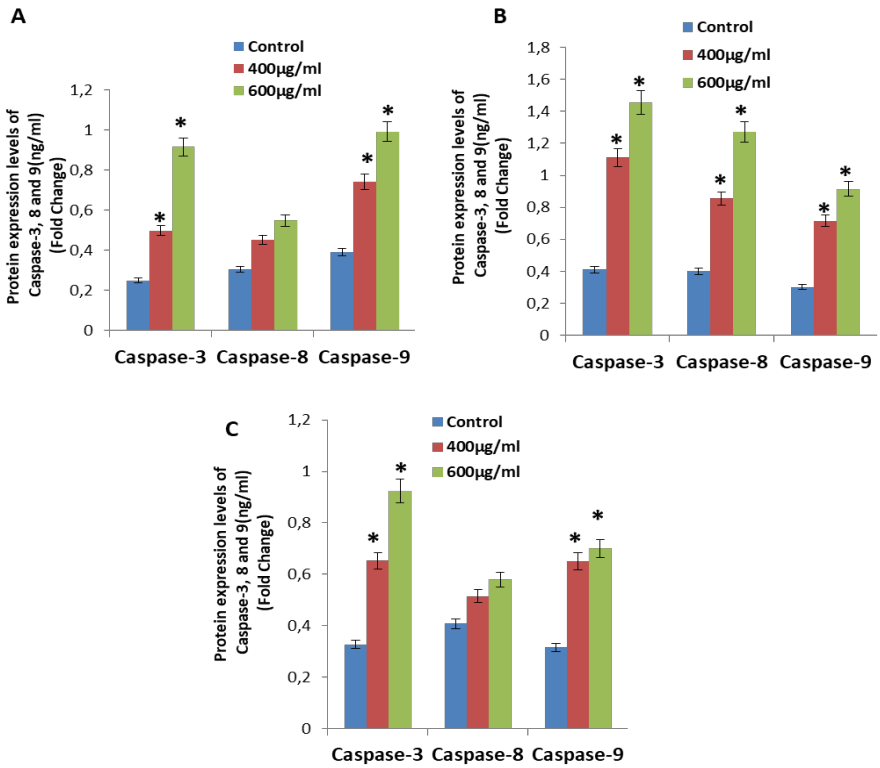


**Figure 2**: Effect of Trachystemon orientalis (L.) G. Don plant extract on Caspase-3, 8 and 9 expression levels on HCT116 (A), AGS (B) and HepG2 (C) cells (*;$p<0.05$).

Although the cell lines used in our study belong to GIS cancers as a whole, it is natural that there are differences between them in terms of their responses. As seen in our results, the AGS gastric cancer cell line has a distinct antiproliferation response compared to the other two. In addition, the increase in the activation of all three caspases is important in confirming this result.From this point of view, it would be reasonable for further studies to be conducted with this herb on gastric cancer. There is no study in the literature to understand the anticancer activity of *Trachystemon orientalis (L.) G. Don* plant. In this respect, our study is a first in this field. In a study, it was shown that T. orientalis (L.) is a good source of antioxidants due to its high content of flavonoids [11]. Since flavonoids are compounds with high anticancer activity, the high proliferation inhibition and increased caspase expression levels we obtained can be attributed to the high flavonoid source of this plant. In order to show the anticancer activity of this plant more clearly, this rich flavonoid content can be revealed with further studies and structural analyzes.

## CONCLUSION

As a result of our study, it has been shown that *Trachystemon orientalis (L.) G. Don* plant extract inhibits cell proliferation in GIS cancer cell lines and activates caspases, which are an important indicator of apoptosis. Determination of the effect of Trachystemon orientalis (L.) G. Don plant with further in vivo studies on apoptotic pathways will be illuminating in studies trying to understand the molecular biology of GIS cancers. In addition, the evaluation of this plant, which is common in our region, and the investigation of its effects in the gastrointestinal tract will provide useful information to the literature.

## CONFLICT OF INTEREST

The authors stated that there are no conflicts of interest regarding the publication of this article.

## ACKNOWLEDGEMENTS

We would like to thank Düzce University Scientific Research Projects Unit (Project code: DUBAP ....) for supporting this study as a master thesis.

ISBN: 978-605-73552-2-5

## REFERENCES

[1] Onaran, A, Melih Y. Antifungal activity of Trachystemon orientalis L. aqueous extracts against plant pathogens. Journal of Food, Agriculture & Environment Vol.10 (3&4): 287-291. 2012.

[2] Alici EH, Arabaci G. Purification of polyphenol oxidase from borage (Trachystem onorientalis L.) by using three-phase partitioning and investigation of kinetic properties." Int J Biol Macromol 2016 Dec;93(Pt A):1051-1056.

[3] Uzun E, Sariyar G. Adsersen A, Karakoc B, Ötük G, Oktayoglu E, Pirildar S. Traditional medicine in Sakarya province (Turkey) and antimicrobial activities of selected species. J Ethnopharmacol. 2004 Dec;95(2-3):287-96.

[4] Onaran A, Yilar M. Antifungal and herbicidal activity of Trachystemon orientalis (L.) G. Don against some plant pathogenic fungi and Cuscuta campestris Yunck. Iğdır Univ. J. Inst. Sci. & Tech. 8(1): 37-43, 2018

[5] Kaynak, B., Kolören, Z., & Karaman, Ü. Investigation of In Vitro Amoebicidal Activities of Trachystemon orientalis on Acanthamoeba castellanii Cysts and Trophozoites. Van Medical Journal, Van Tıp Derg 26(4): 483-490, 2019.

[6] Ferlay, 1., Soerjomataram, I., Dikshit, R., Eser, S., Plathers, C., Rebelo, M., Parkin, D.M., Forman, D., Bray, F. "Cancer incidence and mortality worldwide: sources, methods and major patterns in GLOBOCAN 2012". InIernational journal of cancer 136(5): E359- E386, 2015.

[7] Zali, H., Rezaei, T.M., Kariminia, A., Yousefi, R. Shokrgozar, M. A. Evaluation of growth inhibitory and apoptosis inducing activity of human calprotectin on the human gastric cell line AGS. Iran Biomed Journal 12 (1): 7-14, 2008.

[8] Efferth, T., Saeed, M.E., Mirghani, E., Alim, A., Yassin, Z., Saeed, E., Khalid. H.E and Daak, S. Integration of phytochemicals and phytotherapy into cancer precision medicine. Oncotarget 8(30) :50284, 2017.

[9] Demarchi F, Brancolini C. Altering protein turnover in tumor cells: new opportunities for anti- cancer therapies. Drug Resist Updat 8(6):359-68, 2005.

[10]Yang Y, Yu X. Regulation of apoptosis: the ubiquitous way." FASEB Journal 17(8):790- 9, 2003.

[11] Sacan O. Antioxidant Activity, Total Phenol and Total Flavonoid Contents of Trachystemon orientalis (L.) G. Don. Eur J Biol. 77(2): 70-75, 2018.

ISBN: 978-605-73552-2-5

# SYNTHESIS OF N-ACYLBENZOTRIAZOLYLPYRIDINE-RUTHENIUM COMPLEX AND INVESTIGATION HETEREGENOUS CATALYTIC HYDROGENATION ACTIVITY IN CONTINIOUS FLOW SYSTEM

**Pınar KAPÇI[1], Halenur ÖZER[1], Filiz YILMAZ[1*], Deniz HÜR[1]**

[1] Chemistry Department, Faculty of Science, Eskişehir Technical University, Eskişehir, Türkiye

## ABSTRACT

It is known that synthetic organic chemistry reactions have great application area in industry. Especially, since the flow chemistry provides safer conditions, great advantages can be obtained by applying it to green chemistry. Compared to batch chemistry, it is very advantageous in that it provides the opportunity to work at lower concentrations, allows quick and easy adjustment of such as temperature and pressure parameters. At the same time, flow chemistry gains importance with the reusability of catalysts and the possibility of working with hazardous chemicals quite safely. In this study, a ruthenium catalyst was obtained after synthesis and characterization of (1H-benzo[d][1,2,3]triazole-1-yl)(pyridine-2-yl)methanone, PyrCOBt, ligand designed for use in continuous flow systems. In order to examine the effect of the synthesized catalyst on heterogeneous catalytic hydrogenation, its catalytic activity on hydrogenation of cyclohexene, 1-octene, and styrene were investigated by continuous flow heterogeneous hydrogenations.

**Keywords:** Continuous flow systems, Heterogeneous catalytic hydrogenation, Ruthenium catalyst

## 1. INTRODUCTION

Heterogeneous catalytic hydrogenation (HCH) is described as the reduction or saturation of unsaturated systems in the presence of a catalyst. HCH, which is important on an industrial scale, has found many application areas in various disciplines such as pharmacy, agriculture, and the food industry [1-3]. The biggest advantage of heterogeneous catalysts is being more easily removed from the reaction media and this property increases the importance of heterogeneous catalysts. Investigation of the effectiveness of these heterogeneous catalysts on reactions with organic molecules by continuous flow chemistry with faster, cheaper, safer, and effective methods making flow chemistry among the interesting topics. Organic conversion reactions performed under continuous flow conditions have become increasingly notable in synthetic organic chemistry [4-6]. Continuous flow chemistry excels in changing parameters such as temperature, pressure, and stoichiometry very easily and quickly. At the same time, the possibility of fine-tuning in flow systems gives superiority to syntheses in terms of efficiency, and safety. In particular, the in-situ generations of hydrogen gas in the hydrogenation reactions of flow chemistry demonstrate the advantages of the system preventing problems that may arise with the inattentive use of hydrogen gas cylinders. The advantages of continuous flow systems are simply that they provide an almost perfect control mechanism that cannot be achieved on basic parameters in classical batch methods [4,7].

The most commonly used metals in heterogeneous catalytic hydrogenation are palladium, platinum, rhodium, nickel, cobalt and ruthenium. Ruthenium catalysts are known to play an important role in hydrogenation reactions. There are many studies on ruthenium catalysts such as heterogeneous hydrogenation reactions, selective hydrogenation reactions around isolated double bonds of a carbonyl group, selective reduction of chiral molecules that are difficult to apply to homogeneous systems, and $CO_2$ hydrogenation [4,8-10].

## 2. EXPERIMENTAL

### 2.1. Materials

All chemicals used were obtained from Merck. KBr was used to prepare the pellets to be used in FT-IR and between 400 and 4000 $cm^{-1}$ were recorded using the Perkin Elmer Spectrum 100 Spectrometer. Agilent DDR2 400-MHz spectrometer was used for $^{1}H$ and $^{13}C$ NMR spectra. Hydrogenation reactions for alkenes were carried out with ThalesNano H-Cube®. Thermo Finnigan Trace GC with FID detector and Permabond column (SE-54-DF-0.25, 25 m x 0.32 mm i.d.) was used to determine product distributions in catalytic experiments.

Hydrogenation reactions were carried out with ThalesNano H-Cube® device. The column was filled with 125 mg of silica and 3 mg of catalyst. Silica and catalyst are grounded to ensure uniformity inside the column. Ethanol was used to dissolve the alkenes to be used in the hydrogenation. Then, the prepared solution was given to the system by HPLC

ISBN: 978-605-73552-2-5

pump and it was ensured that it interacted with the catalyst over the cartridge. The parameters which is desired to examined in the system and given in Table 1(temperature, pressure, flow rate) were also controlled simultaneously via the device.

The system cleaning processes were carried out in order to wash the system and ready for the next experiments. Studies were also carried out for the optimization of cleaning processes and controlled with GC. After GC analysis, it has been observed that the most appropriate time for the cleaning is 40 minutes. Ethanol, which is used as a solvent in the reaction, was also chosen in the cleaning process. Washing the column has been carried out by continuously washing the system with ethanol.

## 2.2. Synthesis

### 2.2.1. Synthesis of (1H-benzo[d][1,2,3]triazole-1-yl)(pyridin-2-yl)methanone, PyrCOBt

A solution of 2-picolinic acid (1 eq), mesitylbenzotriazole (1 eq), and triethyl amine (2 eq) in 20 ml of dry THF dissolve in an 80 ml pressure-proof tube under a nitrogen atmosphere. The reaction mixture is stirred under 80 W MW irradiation for an hour. After the reaction is completed, the solvent is evaporated under vacuum. The reaction mixture is dissolved in ethyl acetate and extracted with 20% $Na_2CO_3$(aq) solution (5x20 mL). The organic phase is dried with sodium sulfate. The organic solvent is evaporated under a vacuum to obtain **PyrCOBt** ligand [11]. Yield: 92%; $^1$H NMR (400 MHz, $CDCl_3$, TMS). δ: 8.81 (d, J= 4.64 Hz, 1H), 8.33 (d, J= 8.83 Hz, 1H), 8.11 (d, J= 7.68 Hz, 1H), 8.07 (d, J= 7.86 Hz, 1H), 7.91 (t, J= 7.78 Hz, 1H), 7.66 (t, J= 7.69 Hz, 1H), 7.56-7.48 (m, 2H) ppm; $^{13}$C NMR (100 MHz, $CDCl_3$, TMS). δ: 114.5, 120.2, 125.7, 126.3, 126.5, 126.9, 130.5, 131.8, 136.7, 145.6, 149.8, 165.0 ppm (Figure 1 and 2).

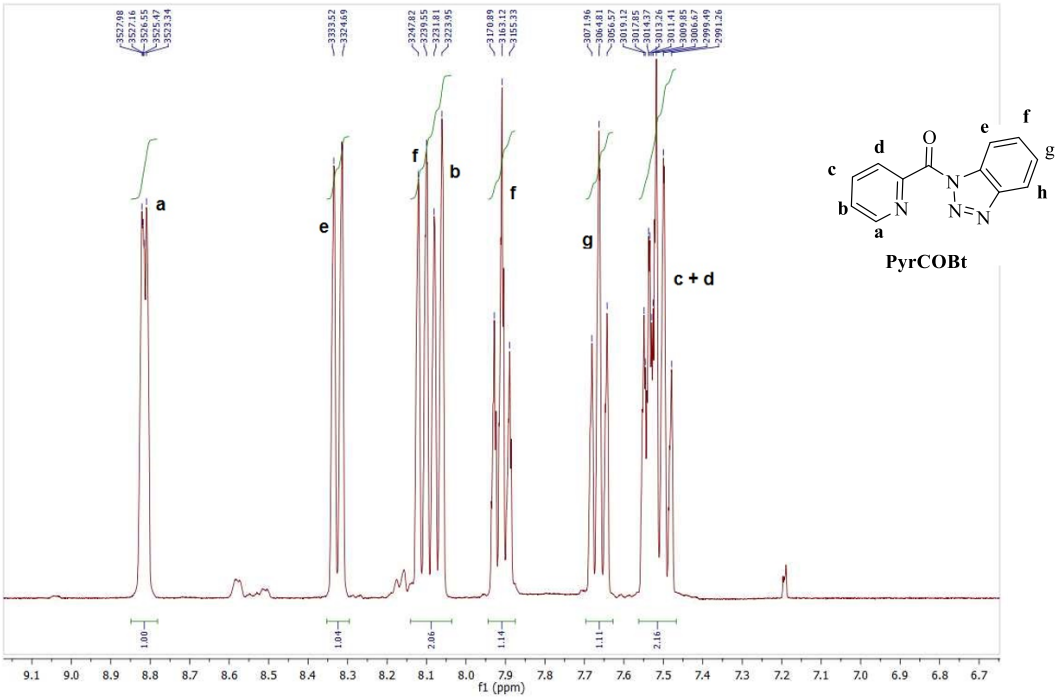


**Figure 1.** $^1$H NMR spectrum of PyrCOBt compound

ISBN: 978-605-73552-2-5

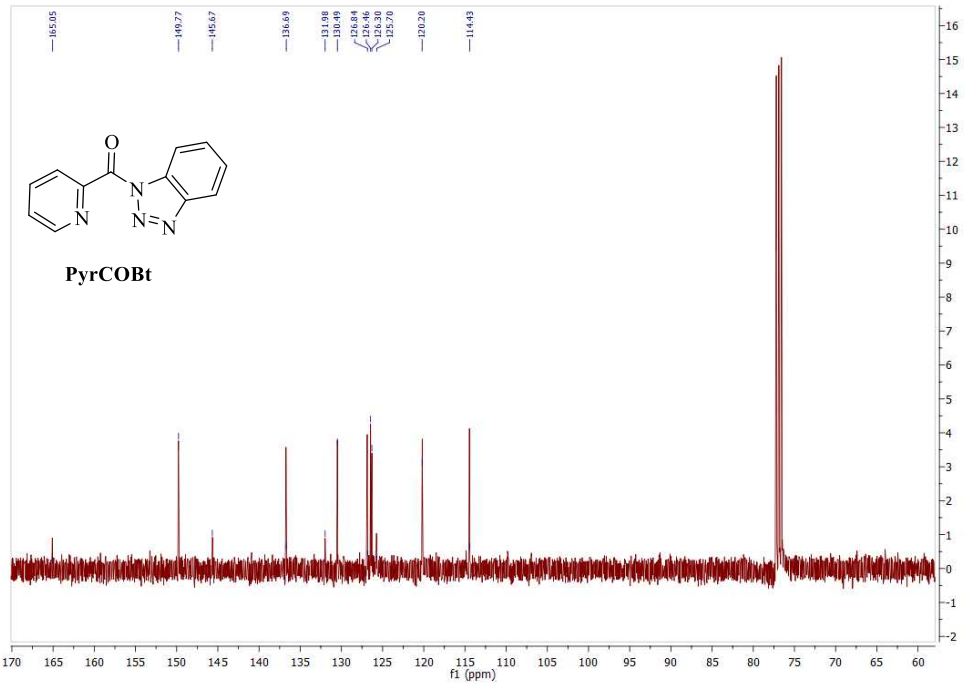


**Figure 2.** $^{13}$C NMR spectrum of PyrCOBt compound

### 2.2.2. Synthesis of a PyrCOBt-Ru Catalyst

Ruthenium chloride hydrate (1 eq) solution in 5 mL water was added dropwise to the solution of PyrCOBt ligand (1 eq) in 10 mL of ethanol and the mixture stirred for 24 hours. The green-black precipitate formed during the reaction was filtered off and washed with ether. The compound was dried in a vacuum oven to obtain the product. Yield: 68% (decomposition point >250ºC).

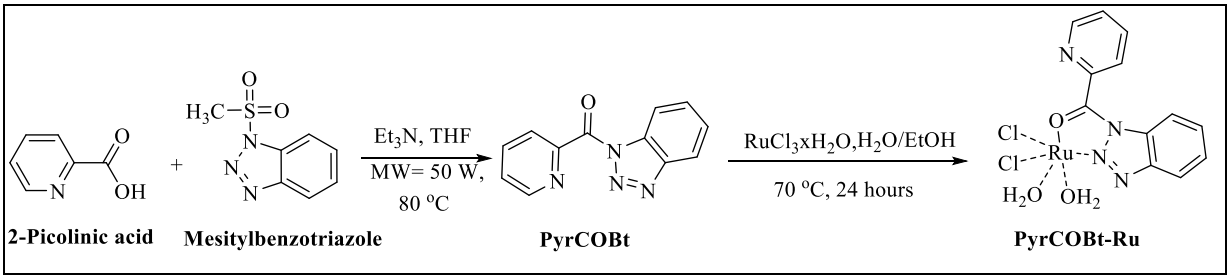


**Figure 3.** Preparation of PyrCOBt ligand and PyrCOBt-Ru catalyst

Although NMR spectroscopy was desired to characterize the complex, NMR characterization could not be performed because the PyrCOBt-Ru was insoluble in solvents, and for the same reason, it was not possible to crystallize the complex. Thus, FT-IR spectroscopy was used to elucidate the structure of the PyrCOBt-Ru complex.

In the FT-IR spectrum of the ligand (Figure 5), C-H stretching vibrations of the benzotriazole ring are observed at 3059 $cm^{-1}$, C=O stretching vibrations at 1709 $cm^{-1}$, and combination bands of C=N and N=N stretches at 1583-1484 $cm^{-1}$ values. C-H vibrations in the pyridine ring of the ligand are observed at 3084 $cm^{-1}$ values, C-N single bond stretching vibrations at 1289 $cm^{-1}$ values. After the ligand coordinates to the metal, there is no significant shift in C-N vibrations in the pyridine ring. The decrease in the C=O vibrations observed at 1709 $cm^{-1}$ to 1634 $cm^{-1}$ and the shift of the N-N vibrations in the benzotriazole ring to 1443 $cm^{-1}$ give the idea that the ligand is coordinated to the metal through the carbonyl group and the nitrogen donor atom in the benzotriazole ring (Figure 4). The broad peaks observed in the 3400

ISBN: 978-605-73552-2-5

$cm^{-1}$ region indicate that the $H_2O$ ligand is coordinated to the metal. It is thought that the complex obtained with this information is as in Figure 3.

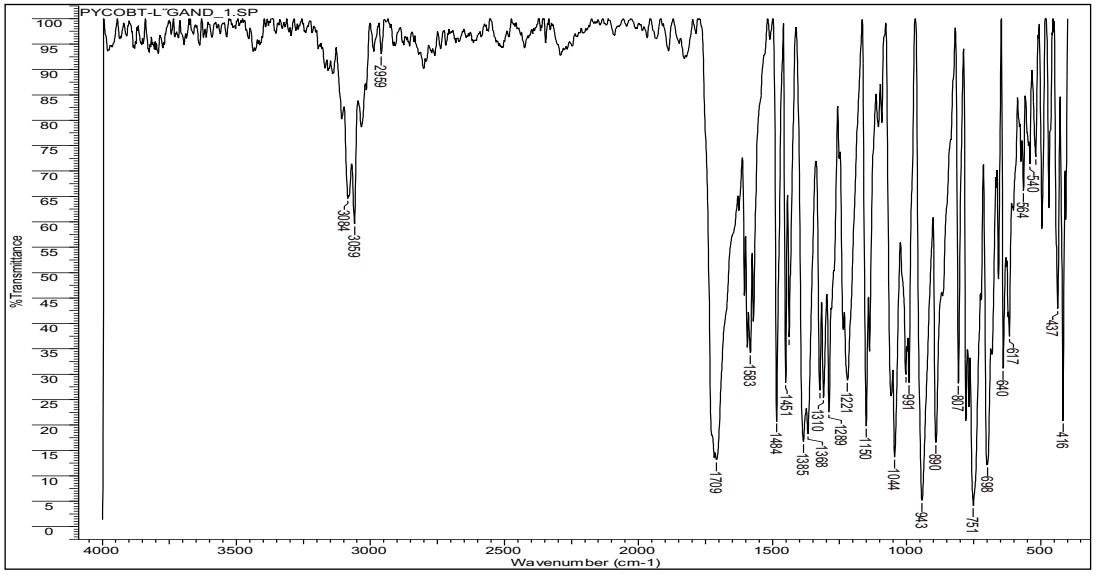


**Figure 4.** FT-IR spectrum of the PyrCOBt-Ru complex

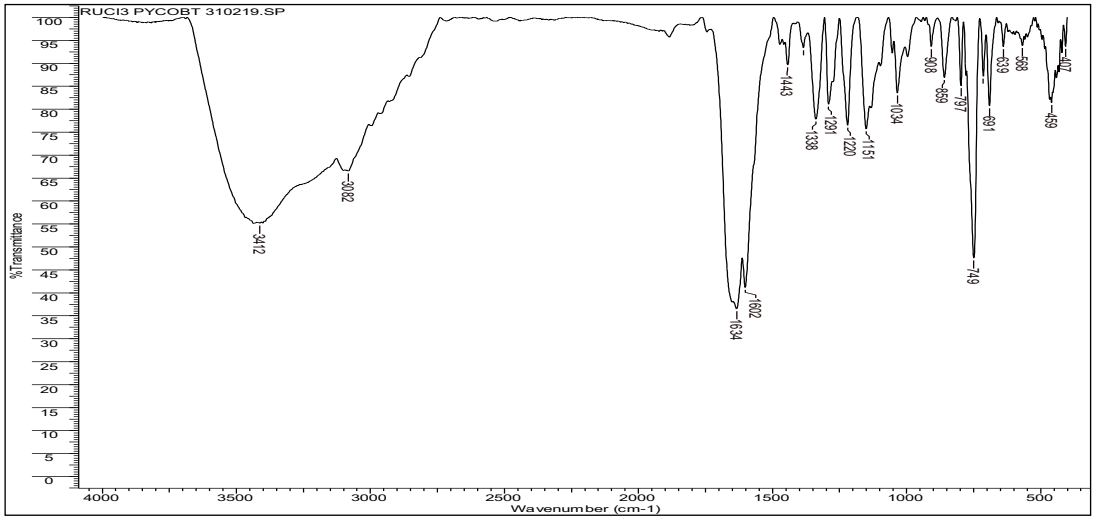


**Figure 5.** FT-IR spectrum of the PyrCOBt ligand

## 3. RESULTS AND DISCUSSION

### 3.1. Catalytic Activity of PyrCOBt-Ru

The catalytic activity of PyrCOBt-Ru complex was investigated in the hydrogenation reactions of styrene, 1-octene, and cyclohexene. In the experiments, the effects of parameters such as temperature, $H_2$ gas pressure, substrate concentration and flow rate on the efficiency of the catalyst were investigated. The ideal column washing time was determined as 40 minutes and all experiments were started after this period of time.

ISBN: 978-605-73552-2-5

### 3.1.1. Styren Hydrogenation

The product of hydrogenation of styrene is ethyl benzene. In styrene hydrogenation at 25 ºC, ethyl benzene conversion was determined as 59.68% ($M_{styrene}$: 0.1 M, flow rate: 1 $mLmin^{-1}$; $H_2$ pressure: 10 bar) (Entry 1). The conversion increased to 73.25% when the temperature was increased to 50 ºC while keeping other parameters constant, indicating that the catalyst activity increased with temperature (Entry 2). In order to examine the effect of the flow rate selected as another parameter, only the flow rate was changed at low temperature. It was determined that the conversion increased (73,18%) when the temperature was kept constant at 25 ºC and the flow rate was reduced to 0.5 $mLmin^{-1}$ (thereby providing more interaction between the catalyst in the cartridge and the substrate). This shows that the reaction efficiency is increased with low flow rate at low temperatures (Entry 3). It was determined that there was an increase of approximately 10% in conversion when the flow rate was kept constant at 1 mL and the $H_2$ pressure was increased from 10 bar to 30 bar. This shows that pressure has a positive effect on the catalytic reaction. For this reason, styrene hydrogenation reaction carried out at low temperature, the flow rate was reduced and the $H_2$ pressure was increased to 50 bar. Under these conditions, 99.14% ethylbenzene conversion was achieved (Entry 5). As a result, it was concluded that low flow rate and high $H_2$ gas pressure gave the best results for styrene hydrogenation. Finally, substrate concentration was investigated after optimum pressure and flow rate conditions. The efficiency of the catalyst in high concentration styrene solution was also investigated. When the substrate concentration was increased from 0.1M to 0.5M at 25 ºC temperature, 50 bar $H_2$ gas pressure and 0.5 $mLmin^{-1}$ flow rate, 97.71% ethyl benzene conversion was detected. When the amount of catalyst is constant, the high conversion rate against the increasing amount of substrates indicates that the catalyst has high activity (Entry 7).

### 3.1.2. 1-Octene Hydrogenation

1-octene is hydrogenated to n-octane, but isomerization products such as *trans*-2-octene and *trans*-3-octene can also be formed in the hydrogenation reaction. In the 1-octene hydrogenation reaction we carried out at 25ºC at 10 bar $H_2$ pressure and 1 $mLmin^{-1}$ flow rate, it was observed that Ru complex provided 10.52 % n-octane conversion (Entry 8). When the temperature was increased to 50 ºC, a 20% increase in n-octane conversion was detected (Entry 9). It was concluded that the catalyst's selectivity to n-octane was low at both temperature values. Since the reaction efficiency was low at both temperatures, the effects on the reaction efficiency were investigated by changing other parameters. When the $H_2$ gas pressure was increased to 30 bar by keeping the temperature, flow rate and concentration constant, no significant effect was observed on the total conversion and selectivity. (Entry 10). When the flow rate was reduced to 0.5 $mLmin^{-1}$, the n-octane conversion reached 100% and no isomerization products were observed (Entry 11). These reaction conditions are optimum conditions for the hydrogenation of 1-octene. When the 1-octene concentration was increased to 0.5 M under optimum reaction conditions, it was observed that there was 94% n-octane selectivity and small amounts of isomerization products were formed. This shows that the catalyst maintains its effectiveness with high selectivity even at higher substrate concentration (Entry 12).

### 3.1.3. Cyclohexene Hydrogenation

In the hydrogenation of cyclohexene, the conversion to cyclohexane is 55.85% at 25ºC temperature, 10 bar $H_2$ gas pressure, and 1$mLmin^{-1}$ flow rate (Entry 13). By increasing the temperature to 50 ºC, the yield increases to 62.52% (Entry 14). Due to the positive effect of temperature, the temperature was kept constant at 50 ºC and other parameters were examined. It was observed that the cyclohexane ratio increased to 85.34% when the $H_2$ pressure was increased to 30 bar (Entry 15). This high increase highlights the need for further investigation of the effect of pressure. For this reason, the $H_2$ pressure was increased to 50 bar. The highest efficiency (99.91%) was determined at 50 bar $H_2$ pressure. (Entry 16). When the system flow was reduced to 0.5 $mLmin^{-1}$ in order to examine the effect of flow rate on cyclohexene hydrogenation, no great effect was observed on the efficiency. (Entry 17). It was observed that the yield decreased to 71.64% when the substrate concentration was increased to 0.5 M (Entry 18). Compared to other substrates, the highest decrease in activity was observed in the high concentration cyclohexene medium.

**Table 1.** Catalytic activity of PyrCOBt-Ru

| Substrate | Entry | *T* (ºC) | $C_{subst.}$ (M) | Flow rate (mL $min^{-1}$) | $H_2$ pres. (bar) | Total conv. (%) | Main product (Distrib. %) |
|---|---|---|---|---|---|---|---|
| Styrene | 1 | 25 | 0,1 | 1 | 10 | 59.68 | Ethyl benzene |
| | 2 | 50 | 0,1 | 1 | 10 | 73.25 | Ethyl benzene |

ISBN: 978-605-73552-2-5

| | | | | | | | |
|---|---|---|---|---|---|---|---|
| | 3 | 25 | 0,1 | 0,5 | 10 | 73.18 | Ethyl benzene |
| | 4 | 25 | 0,1 | 1 | 30 | 71.08 | Ethyl benzene |
| | 5 | 25 | 0,1 | 0,5 | 30 | 95.41 | Ethyl benzene |
| | 6 | 25 | 0,1 | 0,5 | 50 | 99.14 | Ethyl benzene |
| | 7 | 25 | 0,5 | 0,5 | 50 | 97.71 | Ethyl benzene |
| 1-octene | 8 | 25 | 0,1 | 1 | 10 | 19.03 | n-octane (10.52%)<br>*t*-2-octene (4.09%)<br>*t*-3-octene (4.42%) |
| | 9 | 50 | 0,1 | 1 | 10 | 38.72 | n-octane (30.56%)<br>*t*-2-octene (5.82%)<br>*t*-3-octene (2.34%) |
| | 10 | 25 | 0,1 | 1 | 30 | 33.97 | n-octane (25.56%)<br>*t*-2-octene (5.25%)<br>*t*-3-octene (3.16%) |
| | 11 | 25 | 0,1 | 0,5 | 30 | 100 | n-octane |
| | 12 | 25 | 0,5 | 0,5 | 30 | 96.16 | n-octane (94.13%)<br>*t*-2-octene (1.35%)<br>*t*-3-octene (0.68%) |
| cyclohexene | 13 | 25 | 0,1 | 1 | 10 | 55.85 | cyclohexane |
| | 14 | 50 | 0,1 | 1 | 10 | 62.52 | cyclohexane |
| | 15 | 50 | 0,1 | 1 | 30 | 85.34 | cyclohexane |
| | 16 | 50 | 0,1 | 1 | 50 | 99.91 | cyclohexane |
| | 17 | 50 | 0,1 | 0,5 | 30 | 89.11 | cyclohexane |
| | 18 | 50 | 0,5 | 1 | 50 | 71.64 | cyclohexane |

### 3.2. Recycling Experiments

In the cycle studies carried out to examine the reusability of the catalyst, after the first reaction, the system was washed with a solvent and the system was cleaned of product and substrate residues. In order to determine the ideal washing time, samples were taken from the system at certain times and analyzed with the GC device. Washing was continued until the pure solvent peak was observed. According to the studies, the ideal column washing time was determined as 40 minutes in all experiments. The post-reaction wash was repeated in each of the cycle experiments**.** Recycling experiments were performed for 10 cycles under optimal reaction conditions where the efficiency of the catalysts was the highest for each substrate in hydrogenation reactions.

Reusability experiments for styrene were performed for 10 cycles at $PH_2$=50 Bar, 25 $^oC$, and a flow rate of 0.5 $mLmin^{-1}$ (where the highest conversion was achieved). The post-reaction wash was repeated in each of the cycle experiments. It was determined that the catalyst increased its efficiency in the first cycle after the first use and 100% ethylbenzene conversion was achieved. This high conversion rate continued for 7 cycles with only a slight decrease compared to the $8^{th}$ cycle. In the reusability experiments for 1-octene, 100% efficiency and 100% n-octane selectivity were observed even in the $10^{th}$ cycle (Table 2). In the recycle studies for cyclohexene, the catalyst maintained its efficiency over 98% in the first 5 cycles at a flow rate of 1 $mLmin^{-1}$ and started to lose its effectiveness from the $6^{th}$ cycle. Therefore, it was concluded that the catalyst is suitable for use for 5 cycles in cyclohexene hydrogenation.

ISBN: 978-605-73552-2-5

**Table 2.** Reusability experiments of PyrCOBt-Ru

| | **Styrene** | **1-Octene** | **Cyclohexene** |
|---|---|---|---|
| | $PH_2$=50 Bar, T=25°C, 0,5 $mLmin^{-1}$ | $PH_2$=30 bar, T=25°C, 0,5 $mLmin^{-1}$ | $PH_2$=50 bar, T=50°C, 1,0 $mLmin^{-1}$ |
| | Total conv. (%) | Total conv. (%) | Total conv. (%) |
| 1th Exp. | 99.14 | 100 | 99.91 |
| Cycle | | | |
| 1 | 100 | 100 | 99.23 |
| 2 | 100 | 100 | 97.58 |
| 3 | 100 | 100 | 98.07 |
| 4 | 100 | 100 | 98.71 |
| 5 | 100 | 100 | 98.72 |
| 6 | 100 | 100 | 77.75 |
| 7 | 100 | 100 | 62.56 |
| 8 | 99.72 | 100 | 52.46 |
| 9 | 99.67 | 100 | 43.80 |
| 10 | 99.38 | 100 | 22.81 |

## 4. CONCLUSION

In this study, a new PyrCOBt-Ru catalyst was synthesized for the first time. The catalytic activities of the synthesized PyrCOBt-Ru catalyst on various alkenes were investigated and the effects of temperature, $H_2$ pressure and flow rate on the reaction efficiency were investigated. Optimum hydrogenation conditions were determined for each substrate in catalytic studies.

The best reaction parameters for each substrate are shown in Table 1. It is seen that while PyrCOBt-Ru catalyst requires high pressure for hydrogenation of styrene (Entry 6) and cyclohexene (Entry 16), it can perform hydrogenation at lower pressure for 1-octene (Entry 11). As seen in Entry 11, hydrogenation of 1-octene with Ru complex was obtained with 100% selectivity. Although very few isomerization products are formed with the increase in concentration (Entry 12), it is seen that the selectivity is still preserved. When the reusability of the PyrCOBt-Ru catalyst was examined, it was observed that it remained active for styrene and 1-octene for 10 cycles, but the efficiency started to decrease slightly in the 5th cycle of cyclohexene hydrogenation. As a result, the new PyrCOBt-Ru complex synthesized in this study was found to be a catalyst with high efficiency and selectivity for olefin hydrogenation carried out in the continuous flow system.

## ACKNOWLEDGEMENTS

This work financially supported by Eskişehir Technical University. (Project No: 1701F025)

## REFERENCES

[1] Ahmed M J, Hameed B H. Hydrogenation of Glucose and Fructose into Hexitols Over Heterogeneous Catalysts: A Review. J Taiwan Inst Chem Eng; 2019; 96: 341-352.

[2] Saudan L A. Hydrogenation Processes in the Synthesis of Perfumery Ingredients. Acc Chem Res; 2007; **40**, 12, 1309–1319.

[3] Unglaube F, Schlapp J, Quade A, Schäferb J, Mejía E. Highly Active Heterogeneous Hydrogenation Catalysts Prepared from Cobalt Complexes and Rice Husk Waste. Catal Sci Technol; 2022; 12: 3123-3136.

[4] Plutschack M B, Pieber B, Gilmore K, Seeberger P H. The Hitchhiker's Guide to Flow Chemistry. Chem Rev; 2017; 117: 11796−11893.

[5] Cantillo D, Kappe CO. Halogenation of Organic Compounds Using Continuous Flow and Microreactor Technology. React Chem Eng; 2017; 2: 7-19.

[6] Jas G, Kirschning A. Continuous Flow Techniques in Organic Synthesis. Chem Eur J; 2003; 9: 5708-5723.

[7] Holtze C, Boehling R. Batch or Flow Chemistry? A Current Industrial Opinion on Process Selection. Curr Opin Chem Eng; 2022; 36: 100798.

[8] Mihalcik D J, Lin W. Mesoporous Silica Nanosphere Supported Ruthenium Catalysts for Asymmetric Hydrogenation. Angew Chem; 2008; **120**; **33**: 6325-6328.

[9] Gunasekar G H, Padmanaban S, Park K, Jung K-D, Yoon S. An Efficient and Practical System for the Synthesis of N,N-Dimethylformamide by $CO_2$ Hydrogenation using a Heterogeneous Ru Catalyst: From Batch to Continuous Flow. Chem Sus Chem; 2020; 13: 1735-1739.

[10] Kluson P, Cerveny L. Selective Hydrogenation Over Ruthenium Catalysts. Appl. Catal; 1995; 128: 13-31.

[11] Katritzky A R, Suzuki K, Singh S K, He H. Regiospecific C-Acylation of Pyrroles and Indoles Using N-Acylbenzotriazoles. J Org Chem; 2003; **68**; 14: 5720–5723.

ISBN: 978-605-73552-2-5

# NH FUSE WITH NEW POLYMER THERMOSET BODY

**Oğuz Kaan ATAR[1,*], Mutlu BEKTAŞ[2], Tuba BUĞDAYCI AVŞAR[3]**

[1] Research and Development,Yeşilırmak Electricity Distribution Co.,Samsun,Türkiye
[2] Research and Development,Yeşilırmak Electricity Distribution Co.,Samsun,Türkiye
[3] Research and Development,Yeşilırmak Electricity Distribution Co.,Samsun,Türkiye

## ABSTRACT

Blade type fuses are in the family of fusible wire fuses, like plug fuses. The main principle of operation of these fuses is the heat effect of electric current. It consists of a short circuit for a short period of time. In this paper, a comparison of the new generation NH blade fuse with polymer thermoset body produced by BMC (Bulk Molding Compound) injection and the currently used porcelain blade fuse is compared.

**Keywords:** Blade type fuses; BMC(Bulk Molding Compound); steatite porcelain fuses; short circuit current; NH Fuses; Polymer thermoset.

## 1. INTRODUCTION

Blade fuses are in the family of fusible wire fuses, like plug fuses. The basic working principle of these fuses is the heat effect of electric current. The high heat generated during the short circuit causes the copper conductor in the body to break off from the weakened points, and thus the circuit is cut off before the short circuit current grows. Quartz sand that in blade type fuses :

a) The high heat generated during the short circuit is evenly distributed in the plug body, preventing the plug porcelain from breaking down due to heat imbalance.

b) It prevents the arc from extinguishing faster by entering between the broken wires and prevents the wire parts remaining inside from contacting each other again.

c) It fills the inside of the plug and reduces the amount of air inside, so that the air expands in the short-circuit heat and the explosion of the plug is prevented, and the oxidation of the copper inside is less.

The fuse-plug contacts got this name because they fit between the tulip contacts on the base. NH is the German abbreviation. (Niederspannungs - Hochleistungssicherung) Blade fuses come in a wide variety of current ratings. For this reason, the plugs and the bases on which they are attached are produced in different sizes.

## 2. STEATITE MATERIALS AND STEATITE NH FUSES

Steatite material, which is in the C-221 subgroup, with a density of 2.7 g/m3, is used in the body of the existing NH Fuses. The best commercial steatite reserves are found in Australia, Austria, Brazil, China, Finland, India, Italy, Japan, North Korea, Russia and the USA. Since NH fuses trip according to the heating principle, the body must be made of durable material, and its resistance to dynamic forces and heating must be high. In existing fuses, the steatite body is processed as glazed ceramic. In this case, steatite is converted into ceramics by heat treatment and glazing is required to protect the surfaces of ceramic products. NH Plugs with steatite material, which are currently used, have a higher impact resistance, light weight, non-corrosion, due to their low impact resistance, their density being 1.57 times heavier than BMC material, their raw material being supplied from abroad, their fragile structure and the fact that the existing product cannot be reused in case the fuse blows. A new product has been created from BMC material, which is recyclable, insulating, resistant to high temperature and fire.

## 3. NEW GENERATION NH FUSES

The invention mentioned in the study is an NH blade fuse with a polymer thermoset body. The body of the invention is produced by BMC injection method from insulating thermoset material suitable for V-0 class resistant to extraordinary heat and fire. Thus, the material with polymer thermoset body (7) has a higher impact resistance, more resistance to corrosion and UV radiation, and a lighter density. Figure 1 shows the components of the new generation NH plug-in fuses.

ISBN: 978-605-73552-2-5

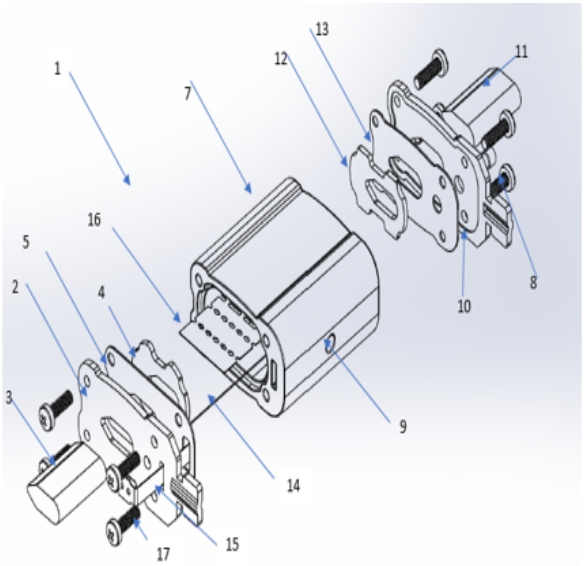


Figure 3 New Generation NH Plug Fuse Components

The feature of the combi signal indicator assembly in NH fuse links with blades; Thanks to the signal indicator spring (6 and 15), when the signal indicator wire (14) on the indicator (9) is broken, the red color disappears from the circular indicator showing that the plug (7), which consists of the thermoset body, is deactivated.

## 4. COMPOSITE MATERIALS, TECHNICAL PROPERTIES AND EXPLANATIONS

### 4.1. COMPOSITE MATERIALS

Composite materials are structures formed by combining two or more components that are practically insoluble in each other and are brought together to produce new and desired materials. As a system, the composite material is formed by bringing together the reinforcement element (fibers, particles, layers) and the matrix holding the reinforcement element together under appropriate conditions, under certain physical and chemical conditions. It can be ensured that the component materials that make up the composite materials have the intended and desired new properties apart from their own properties. These features can be listed as; corrosion resistance, high strength, rigidity, lightness, ease of design, dimensional stability, chemical resistance and other properties required according to the place of use (UV resistance, heat and sound insulation). It is preferred because it is light when compared to metals and alloys. Composite material of equal weight may have higher strength value against metal materials. They are structures produced by reinforcing with fibers for purposes such as improving the weak technological properties of brittle matrix materials with low tensile, bending and impact strengths, and increasing the toughness and ductility of the material. Fibers are defined as materials that have a cross-section-to-length ratio of at least 1:100 and are rigid yet flexible enough to be molded. The main unit that meets the external loads and forces is the fiber. Especially when preparing polymer composites, some important points determine the character of the material. The most important of these basic points are the mechanical properties of the fiber, the ratio of the fiber to the matrix material, the thickness of the fiber, the orientation of the fiber according to the applied load and forces. Figure 2 shows the filling types of composite materials.

ISBN: 978-605-73552-2-5

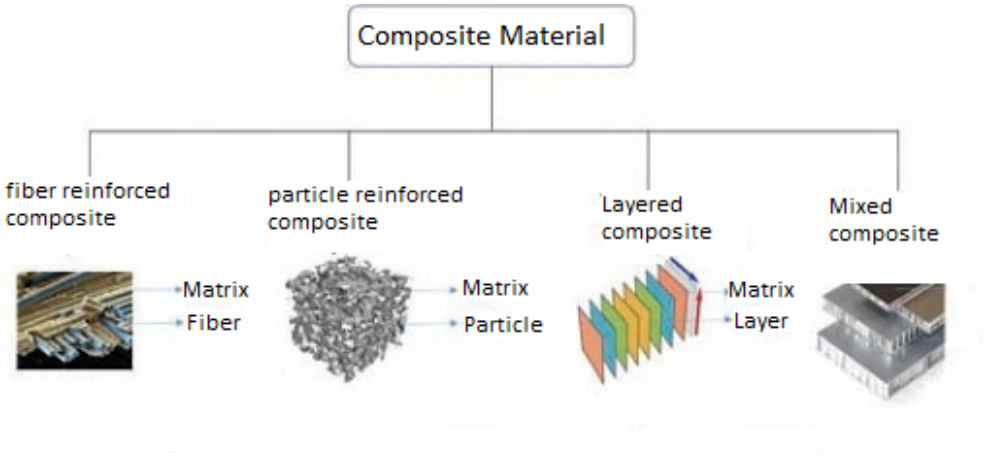


Figure 4 Composite materials by filling types

## 4.2 FIBER LAYOUT CONFIGURATIONS

The distribution of fibers determines the strength of the composite material. As the diameter and length of the fibers increase, the amount of load transmitted by the matrix to the fiber fibers increases. Increasing the fiber bending surface of the polymer causes an increase in fiber-matrix interaction. In this way, a healthier distribution of load and force in the composite structure is ensured. The bundles formed by bringing the fibers together have a stronger structure than the block form of the polymer from which the fibers are produced. The settlement forms where the strength values are maximum and the directions where the mechanical strength is high are shown in Figure 3.

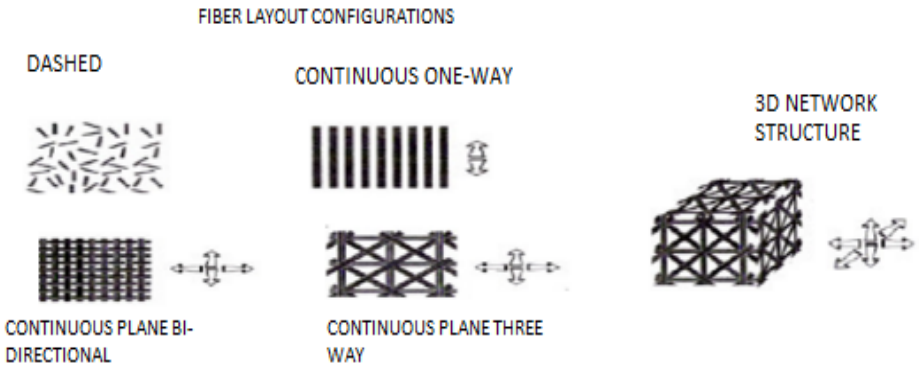


Figure 5 Placement of fibers in composite material

## 4.3 BMC (BULK MOULDING COMPAUND)

BMC are hot pressing productions. Hot press molding, on the other hand, is the method of molding a pulped polyester mixture under high pressure with heated metal molds. Although it is possible to make mass production with these methods, it is difficult to produce large parts due to mold costs. In BMC production, the composition is in the form of a pulp containing polyester, chopped fiber, filler and shrinkage reducing additives, and a thickening period is not required before it is put into production. Thus, the prepared dough can be placed directly into the mold or injected in closed molds. Electrical parts and automotive parts can be counted among the products produced by the BMC method. The parts produced by the BMC method can be more intricate and complex parts. With the SMC method, parts in the form of a wider layer are suitable for production.

## 4.4 PRODUCTION

BMC injection or hydraulic pressing methods are production methods using previously prepared BMC dough. Although the same raw material is used in these two methods, the production techniques are different from each other. In injection production, BMC raw material is filled into the hopper of the machine. The raw material taken into the chamber is

ISBN: 978-605-73552-2-5

brought to the tip of the nozzle where it will be transferred into the hot mold with the help of Archimedes screw. The raw material coming to this end is sprayed into the mold with the desired pressure and speed values. BMC injection technique has its own main parameters. The most important of these parameters are; injection chamber setting, injection speed, injection pressure, ironing settings, degassing settings and back suction settings. All these parameters are brought to optimum points according to the design, the raw material and the operation of the process.

## 5. APPLICATION AREAS OF COMPOSITES

Composite materials have potential for many engineering applications due to their useful and interesting properties. Scientific studies on composites, which are used significantly in the aircraft industry and many other sectors, continue intensively today. BMCs primarily compete with metal castings and engineering thermoplastics. It is estimated that the usage rate will increase even more due to the low manufacturing costs.

### 5.1 APPLICATION IN THE FIELD OF ELECTRICAL AND ELECTRONICS

In terms of lightness, rigidity, high mechanical properties, high chemical resistance, high heat resistance and electrical properties, composite materials affect every field as well as affect technology in the field of electronics and electricity, that is, in terms of industrial and energy, and are frequently used. Wind turbine, circuit breakers, fuse panels, lighting housings, electrical distribution panels, solar panels, cable carriers, insulating platforms etc. In terms of electrical-electronic components in materials of structures such as these, these features are especially important because they are essential

### 5.2 APPLICATION IN THE FIELD OF ELECTRICAL AND ELECTRONICS

By using advanced polymer matrix composite materials in the aircraft aerospace industry, a weight reduction of 25-40% is achieved compared to aluminum structures. This saves $50 to $500 per kg. Since weight is very important in spacecraft, composites are used in every possible part. For example, propellant tanks are made of carbon fiber reinforced PEEK matrix composites, while gas outlet nozzles are made of carbon fiber reinforced phenolic resins or carbon-carbon composites

### 5.3 APPLICATIONS IN THE FIELD OF AUTOMOTIVE AND TRANSPORTATION

Automobile companies produce light cars in order to meet the needs of their customers and increase their competitiveness. Light cars are very important mechanically (acceleration and braking) as well as energy saving.

## 6.TECHNICAL DESCRIPTIONS AND FORMULAS ABOUT COMPOSITE MATERIALS

### 6.1 GENERAL PROPERTIES OF COMPOSITES

The properties of composite materials depend on the properties of the composite components and their relative composition, size, shape, distribution and orientation. In Figure 4, an example of the distribution of the components of composite materials is given.

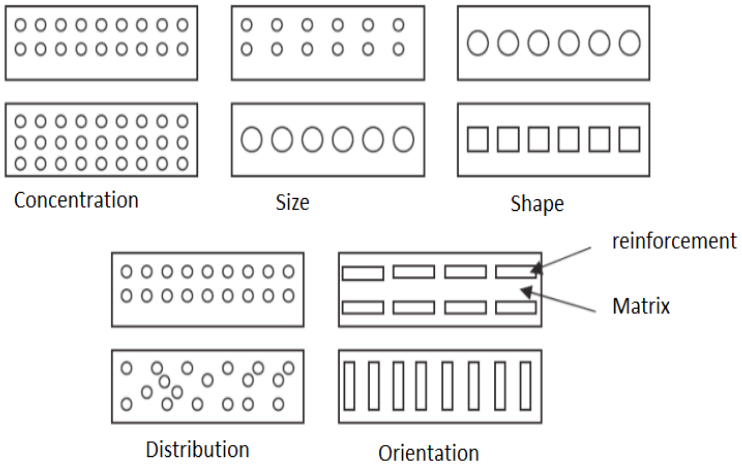


Figure 6 Distribution of components of Composite Materials

ISBN: 978-605-73552-2-5

Although composite actually means a mixture, it does not consist of soluble and dissolving components. There is no exchange of atoms between the components. Composite components do not affect each other chemically. Composites are generally composed of a base material called matrix and a reinforcing element fiber, a more durable material called fiber. Of these two material groups, the reinforcement material plays a role in the strength and load-bearing properties of the composite material, and the matrix material prevents the crack propagation that may occur during the transition to plastic deformation and delays the rupture of the composite material.

### 6.2 TECHNICAL PROPERTIES

The relative composition of the composite material components is given as a ratio by weight or ratio by volume. While the ratio by weight is generally used in the production phase, the ratio by volume is used to determine the properties of composite materials. These two values are associated with each other by considering the density value.

For reinforcement element:

$$Wf = Wf/Wc = Pf/Pc * Vf \quad (1)$$

For matrix:

$$Wm = Wm/Wc = Pm/Pc\ Vf \quad (2)$$

W: Weight,
V: density,
f : reinforcement element
c: composite
m: matrix

The density of composite materials can be calculated when the ratio by volume or ratio by weight is known.

$$\rho c = \rho f Vf + \rho m Vf \quad (3)$$

$$1/\rho c = Wf/\rho f + Wm/\rho m \quad (4)$$

The density equation, based on the ratio by volume, can be written for all properties of composite materials (hardness, modulus of elasticity, etc.) in certain cases.

$$Xc = XfVf + XmVm \quad (5)$$

## 7.NEW GENERATION NH PLUG FUSE PRODUCTION PROCESSES

### 7.1 CREATING THE POLYMER THERMOSET BODY MOLD

First of all, it is necessary to prepare molds that will form the polymer thermoset body in order to design the new generation NH fuse. The molds were prepared with the SolidWorks drawing program, and 16 polymer bodies are produced in each printing process. Figure 5 shows the NH Plug Drawing prepared for the mold.

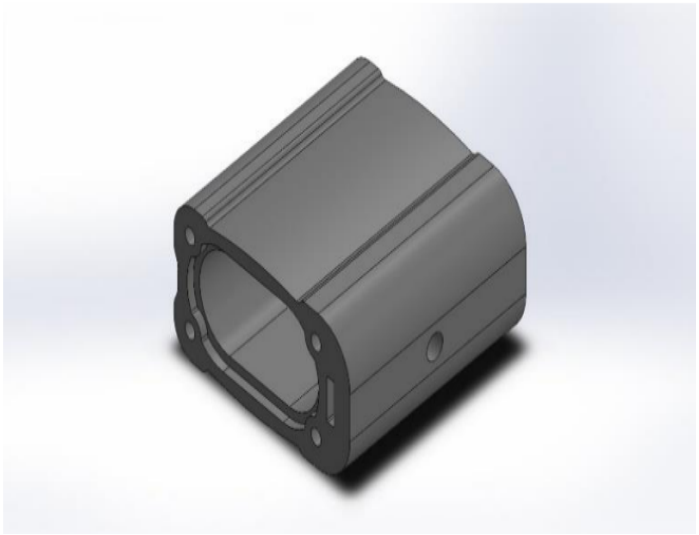

Figure 7 NH Plug Drawing prepared for the mold

The following processes were followed in the mold creation process:

ISBN: 978-605-73552-2-5

### 7.1.1 DETERMINATION OF HOT WORK STEEL PATTERNS

The type of mold steels has been determined. In the mold manufacturing phase, it was decided to produce the back plates, pusher plate, wedges from CK45 steel, which is suitable for heat and long-term use, and the core parts from 2344 steel.

### 7.1.2 DETERMINATION OF MOLDING EXIT ANGLES

By making use of the drawings of the New Generation NH Plug-in Fuse and the prototypes produced, the molding process was started by giving the exit angles of the molds.

### 7.1.3 NITRIDING OF MOLD STEELS

The parts coming from the hardening process started to be processed by chipping the steel part in accordance with the drawings made in the CNC machining center and mold shapes were formed.

### 7.1.4 BEGINNING OF MOLD MAKING IN CNC MACHINING UNIT

The parts coming from the hardening process started to be processed by chipping the steel part in accordance with the drawings made in the CNC machining center and mold shapes were formed.

### 7.1.5 ASSEMBLING POWER RESISTANCES FOR HEATING BY COLLECTING MOLD PARTS AND GETTING READY FOR THE PRODUCT PRINTING

After the production of the mold parts in the CNC machining center, the mold parts were subjected to nitration again. The parts from the nitration process were processed in the CNC machining center to make final corrections and the mold parts were collected. Figure 6 shows the assembly of mold parts in a computer aided environment and Figure 7 shows the first samples.

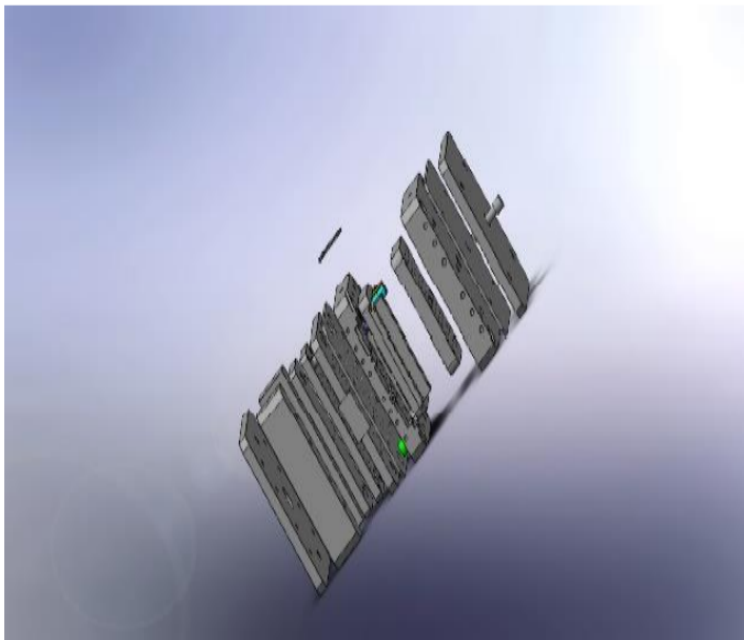

Figure 8 Assembly of Mold Parts

ISBN: 978-605-73552-2-5

Figure 9 Figure 7 First Sample Product

## 7.2 PRODUCTION AND ASSEMBLY OF FUSE INTERNAL EQUIPMENT

The main fuse is formed by the process of combining the body part of NH Plug Fuse with the other internal equipment that makes up the fuse. The main function of the fuse is the melting wire, which is used to cut short circuits and high currents. The copper used as the melting wire; With the thickness, size and attenuation holes opened on the melting wire, their resistance to current can be increased or decreased. Inner copper forming the melting wire of the NH plug is entered into the first mold as a raw material in roll strip. Figure 8 shows the strip punch cutting machine.

Figure 10 Strip Punching Cutting Machine

ISBN: 978-605-73552-2-5

Machine steps are given in order:
a) Punching and periphery crushing process
b) Applying the soldering process to the determined dimensions and points at certain intervals
c) Length cutting process
Drilling, soldering and dimensions are determined according to the current carrying capacity of the melting wire. With the strip drilling and cutting machine, 1 melting wire can be formed every 2 seconds.
In Figure 6, the width dimensions of the 0.2 mm thick melting wire for the NH 00 length are given according to the current carrying capacity. The width of the melting wire increases according to the current carrying capacity. Current carrying capacities of NH 00 fuse melting wire are given in Table 1.

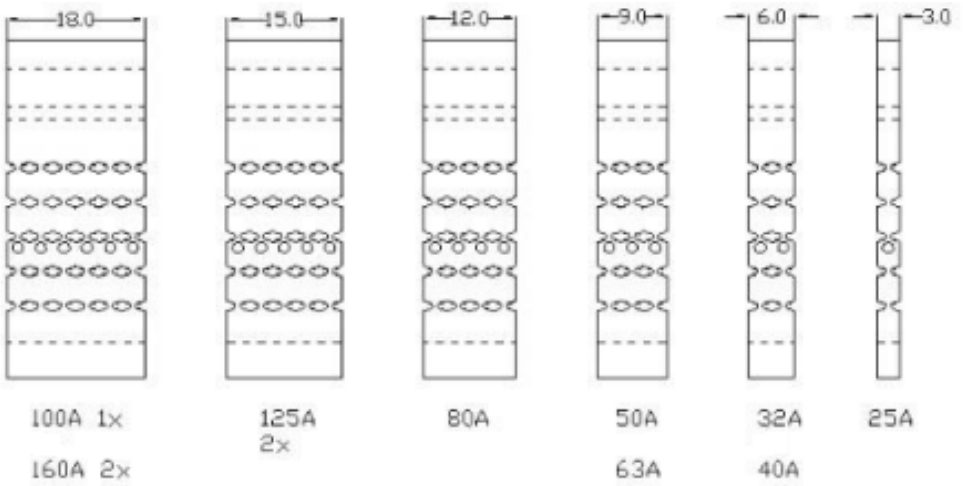


Figure 11 NH 00 Fuse Melting Wire Figures

| NH 00 Fuse | NH 00 Fuse Melting Wire Current Capacities | | | | | | |
|---|---|---|---|---|---|---|---|
| | ***25A*** | ***32A / 40 A*** | ***50A/ 63A*** | ***80A*** | ***100A*** | ***125A*** | ***163A*** |
| Melt Wire Width (mm) | 3.0 | 6.0 | 9.0 | 12.0 | 18.0 | 2x (15.0) | 2x (18.0) |

Table 4 NH 00 Fuse Melting Wire Current Capacities

The formed melting wire is welded to the blades of the NH plug fuse by pointing method. Figure 10 shows the punto machine. Since the blade and the melting wire are made of copper material, a punto machine with tips made of tungsten with high heat resistance is used in order to make boiling healthier. In this way, both the welding quality increases, and it offers the possibility of mass production for a longer time. Figure 11 shows the punctuated product.

ISBN: 978-605-73552-2-5

Figure 12 Punto Machine

Figure 13 Punctuated Product

The melt wire, which is combined with the blades, is combined with the upper and lower covers and placed inside the main polymer thermoset body. For sand filling process, quartz sand filling process is performed by arranging the fuse as four on the fully automatic vibration machine. Since the sand filling is done with vibration, there is no gap in it. This process takes 30 seconds for 4 NH plugs. in progress. Figure 12 shows the vibration machine and the filling tips.

Figure 14 Vibrating Machine and Filling Tips

ISBN: 978-605-73552-2-5

The filling openings of NH plugs filled with quartz sand are closed with an aluminum capsule piece. Capsule fixing machine is used to provide sealing and to perform the process in series. 1 NH plug closure can be done in a single press. In this process, the operation time is 7 seconds. Capsule fixing machine is shown in Figure 13.

Figure 15 Capsule Fixing Machine

The front surface of the NH plugs is marked after the capsule is fixed and the assembly process is completed. Hard-to-clean ink is used for the marking process in black. Product features, current resistance and manufacturer's names are written on the NH plug fuse. After this process, NH insurance is packaged and made suitable for shipment. Figure 14 shows the final product obtained.


Figure 16Final Product

The difference of the new generation NH Plug fuse from normal porcelain blade fuses is that it consists of a polymer thermoset body. The production and assembly of other internal equipment includes similar processes as porcelain blade fuses. Thanks to the production of fuses with blades from polymer thermoset body;

### 7.2.1 Many products can be taken at the same time with the mold system

ISBN: 978-605-73552-2-5

Thanks to the mold systems, 16 products can be produced at once at the same time, and thanks to its rapid cooling, it becomes ready for use. Since porcelain fuses are produced by casting, a single product emerges and requires time to cool.

### 7.2.2 Lighter products can be produced

The fact that the composite material is light and has high strength enables lighter products to emerge compared to porcelain fuses. This will facilitate assembly and transportation. Figure 15 shows the comparison of the polymer thermoset body and the porcelain body.

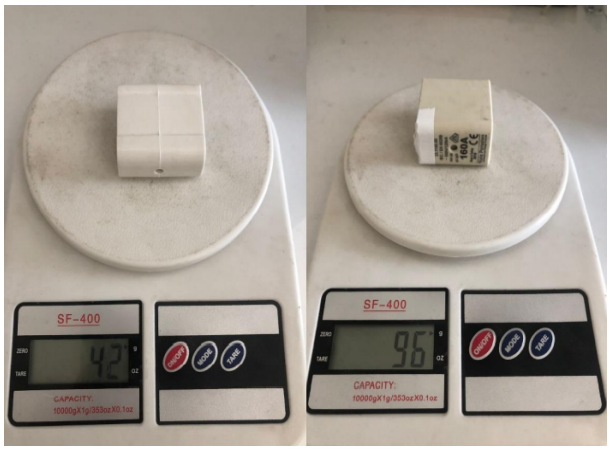


Figure 17 Comparison of Polymer Thermoset Body and Porcelain Body

### 7.2.3 It can be produced in different colors and designs.

Special productions can be made with the revisions to be made in the mold system and the change of the raw material content used. In Figure 16, products produced in different colors are shown.

Figure 18 Products Produced in Different Colors

ISBN: 978-605-73552-2-5

### 7.2.4 More cost-effective fuses are produced

The fact that the composite material is light and has high strength enables lighter products to emerge compared to porcelain fuses. In this way, ease of assembly and transportation has been created. For the same type of fuse-links, the porcelain fuse-body is approximately twice as heavy.

## 8.ASSESSMENT

The process of preparing the production line was completed with the creation of the assembly line with the necessary machines for the production of NH fuse polymer thermoset outer body molds, the production of other equipment and their assembly in the main body. After the necessary test processes are completed and the conformity is obtained, mass production can be started.

Production line; It has all the necessary equipment and equipment starting from the production of the polymer outer body to the latest marking and packaging processes.

With the start of mass production, it is anticipated that 4,000-4,500 units of NH Plug fuses will be produced for each shift, initially. Considering the supply-demand balances, it will be possible to increase the production to 2 or 3 shifts and increase the production equipment in the following processes.

The New Generation NH Plug Fuse samples, which were subjected to test processes according to TS EN 60269-1 and TS HD 60269-2 standards, passed the test processes successfully.

## 9.CONCLUSION

This study aims to evaluate the advantages and differences of new generation polymer thermoset NH Plugs compared to steatite body NH Plugs used in the energy sector and industry. Existing NH Fuses with steatite body;

• Steatite material in the C-221 subgroup with a density of 2.7 g/m3 is used in its body.

• Steatite body is processed as glazed ceramic.

• Glaze is applied to protect the surface of ceramic products. Spraying and dipping technologies are used for the glaze process.

• The glaze process prevents mass production and causes excessive labor.

• In the manufacture of only one NH fuse, the spraying and dipping process used in glazing causes extra time and overtime.

• The density of steatites is 1.57 times heavier than the density of BMC raw material. This increases the cost.

• Due to the fact that steatite material is not much in our country, import dependency is increasing. In the production of New Generation NH Plug-in Fuses, it is produced from an insulating thermoset material suitable for V-0 class, with BMC injection, which is made of extraordinary heat and fire resistant material as the body material. The general properties of BMC material and its superiority over steatites highlight the feasibility of the study.

Some of these features are;

- Its density is 1.72 g/m3.
- The most important point in BMC is to adjust the features that can provide the best performance at the most affordable cost to suit the demands of the CTP application.
- Superior hardness and flame resistance are provided with the addition of a high amount of filler.
- It is halogen free.
- The combination of very high filling material and low reinforcing material provides low cost and high material performance both in the preparation of BMC composition and in the molded product.
- In injection molding, when transferring material to a closed mold, it is possible to use secondary reinforcement materials, which is not usually possible in compression molding. NH New Generation NH, which is formed by producing the body from thermoset material rather than steatite material in blade fuses.

With Plug Fuses;

- 1.72 g/cm3 density glass fiber reinforced thermoset NH Fuses are 1.57 times lighter than Steatite Body NH Fuses. With its lightness, it reduces the transportation and assembly costs and the cost by 45%.
- Due to the fact that steatite material is not very common in our country, it reduces the dependence on imports and brings in the localization policy.
- Thermoset NH Fuses are not affected by corrosion. It is completely resistant to humid, foggy, salty atmospheric conditions and UV radiation.
- Its bending modulus is high, it is suitable for versatile use.
- High impact resistance: Composite (GRP) NH Fuses have high impact resistance thanks to the glass fiber they contain.
- Because they are insulators, they are products that provide work safety against electricity leakage.

ISBN: 978-605-73552-2-5

In this direction, a total of 40 samples, including one 63 A, nine 80 A, ten 100 A, ten 125 A and ten 160 A samples, were produced, quality control tests were carried out and sent to the field for use in YEDAS DSO pilot regions. Field installations of 40 samples were completed by YEDAS DSO operating units and they were included in the low voltage monitoring system (LVMS) and remotely monitored.
A total of 40 new generation Thermoset body NH Plug fuses, whose assembly has been completed in the YEDAS DSO Service region, have a cost efficiency of approximately 45% in body cost and 12% in total product cost compared to steatite material, their ability to be produced in our country and depending on the size of the molds from printed molds 16-32-64 Being able to go into mass production as a result; It is considered that it will provide more efficiency in high margin productions compared to the commonly used steatite body fuses.
Evaluated in line with production efficiency and financial efficiency, NH Plug fuses with thermoset body will become widespread in the energy sector and contribute positively to the country's economy.
With the widespread use of thermoset fuses;
• Instead of semi-finished products, semi-finished products will be produced in our country with the supply of raw materials,
• Imports will be prevented and there will be no delays regarding delivery,
• More qualified products will be produced,
• Foreign dependency will decrease,
• It will contribute to occupational safety thanks to its insulator and dielectric properties.

## ACKNOWLEDGEMENTS

The authors would like to thank the Turkish Energy Market Regulatory Agency and the Yesilirmak Distribution System Operator for their support.

## REFERENCES

Szulborski, Michał & Łapczyński, Sebastian & Kolimas, Lukasz & Kozarek, Łukasz & Rasolomampionona, Desire Dauphin & Żelaziński, Tomasz & Smolarczyk, Adam. (2021). Transient Thermal Analysis of NH000 gG 100A Fuse Link Employing Finite Element Method. Energies. 14. 1421. 10.3390/en14051421.

T. Tanaka and M. Yamasaki, "Modeling of fuses for melting time and fusing current analysis," INTELEC 2004. 26th Annual International Telecommunications Energy Conference, 2004, pp. 671-675, doi: 10.1109/INTLEC.2004.1401542.
Kolimas, Lukasz & Daszczyński, Tadeusz. (2020). Uncertainty of the Characteristics of Electrical Devices Based on the Measurements of the Time-current Characteristics of MV Fuses. Bulletin of the Polish Academy of Sciences. 10.24425/bpasts.2020.XXXXX.

Kuhnel, Christian & Schlegel, Stephan & Großmann, Steffen. (2017). Investigations on the long-term behavior and switching function of fuse-elements for NH-fuse-links (gG) at higher thermal stress. 1-8. 10.1109/IYCE.2017.8003691.

Demir, Murat & Kahramanoglu, Gurmen & Yildiz, Ali. (2016). Calculating of fuse melting point for power electronics circuits by inrush energy and determination of the eligibility. 1-6. 10.1109/EPE.2016.7695322.

Li, Dan & Qi, Li. (2013). Energy based fuse modeling and simulation. 487-492. 10.1109/ESTS.2013.6523781.
IEEE. C37.42-2009-IEEE Standard Specifications for High-Voltage (>1000 V) Expulsion-Type Distribution-Class Fuses, Fuse and Disconnecting Cutouts, Fuse Disconnecting Switches, and Fuse Links, and Accessories Used with These Devices; IEEE: New York, NY, USA, 2010; doi:10.1109/IEEESTD.2010.5410745

Gräf, T.; Kunze, A. Damage avoidance due to the use of high voltage fuses and temperature monitoring. In Proceedings of the 10th International Conference on Electric Fuses and their Applications, Frankfurt am Main, Germany, 14-16 September 2015; Dresden University of Technology: Dresden, Germany, 2015; pp. 1-7

Psomopoulos, Constantinos & Karras, Y. & Karagiannopoulos, Panagiotis & Karras, Christos & Diamadopoulos, D.. (2009). Recycling potential for the low voltage high breaking capacity fuse links used by P.P.C. of Greece.
Bessei H., 2007. Fuse Manual. NH-HH-Recycling e.V., Frankfurt

ISBN: 978-605-73552-2-5

Psomopoulos, C. S., Ioannidis, G. C., & Karras, Y. (2014). Role of low-voltage/NH fuselinks rated voltage in distribution network losses. An evaluation based on the Hellenic low-voltage distribution network. *IET Generation, Transmission & Distribution*, *8*(5), 803-810.

Schoenau, J., & Noack, F. (2004). Lightning pulse current response of low-voltage fuses; Blitzstromverhalten von Niederspannungs-Hochleistun

ISBN: 978-605-73552-2-5

# ESTIMATION OF MULTI-RESPONSE SEMIPARAMETRIC REGRESSION MODEL BASED ON KERNEL SMOOTHER: AN APPLICATION WITH AGRICULTURAL DATA

**Dursun Aydın**[1] duaydin@mu.edu.tr

**Ersin Yılmaz**[1*] ersinyilmaz@mu.edu.tr

[1] : Mugla Sitki Kocman University, Faculty of Science, Department of Statistics, Mugla, Turkey

## Abstract

A multi-response semiparametric regression model differs from the classical semiparametric model by involving the multiple response variables. Accordingly, parametric, and nonparametric components affect the responses individually. Another difference of multi-response model is an existence of a correlation between the response variables. This case brings a need of a symmetric weight matrix. To estimate the introduced model, this paper considers a kernel smoothing method which works based on Nadaraya-Watson estimator. Accordingly, estimators of multi-response semiparametric model are obtained based on weighted least squares technique. Finite-sample properties of the estimators are provided. To show the behaviors of the mentioned estimators, agricultural data obtained from Turkey is analyzed and results are presented.

**Keywords:** Multi-response semiparametric model, symmetric weight matrix, kernel smoothing,

## 1. Introduction and Purpose of Study

In the literature although, multivariate regression is a well-known phenomenon (i.e., Miller and Wegman, 1987; Yee and Wild, 1996; You et al. 2007), There is very few studies on estimation of multivariate semiparametric regression models. Some related studies about multivariate semiparametric regression can be ordered as: Li et al. (2018) studied multivariate semiparametric mixed model based on adaptive-group Lasso to make proper variable selection for the model. Therefore, they consider the nonparametric component of the model as random effects. In a similar manner, Papageorgiou and Hinde (2012) considered the same subject for the generalized linear mixed models. Wibowo et al. (2012) estimated multi-response semiparametric model for completely observed data and they considered univariate nonparametric component and used polynomial natural splines as a smoother. Chamidah et al. (2022) inspected the asymptotic properties and consistency of the estimators of multivariate semiparametric additive model based on B-spline smoothing. In addition, Bonat (2018) developed an R package for multivariate regression model.

The main difference of this study from the previous study is that it focuses on the modified kernel smoother to estimate the multi-response semiparametric regression model. Then, applying the obtained estimators to the agricultural data and improving the estimation risk on this field. As known, in agricultural data set, multiple responses may be affected by the same covariates such as fertility, prices of the product, amount of import are affected jointly by the agricultural production variables. Modelling the multiple-response variables simultaneously might has an important contribution to the literature.

## 2. Methodology

### 2.1 Multi – response Semiparametric regression

We consider the problem of modelling the relationship between "$m$" response variables $\{Z_{k,}k = 1, \dots, m\}$ based on "$n$" observations. A set of parametric explanatory variables $\{x_{j,}\, j = 1, \dots, p\}$. A univariate nonparametric covariate $\{T_{i,}\, i = 1, \dots, n\}$. Such a relationship can be stated with the following standard multivariate (Multi-response) partially linear regression model:

$$Z_{ik} = \sum_{j=1}^{p} \beta_{jk}\, x_{ij} + \sum_{k=1}^{m} g(T_i) + \varepsilon_{ik} \qquad (1)$$

Model (1) can be written as the following matrix and vector form:

$$Z_{ik} = \mathbf{X}_i \boldsymbol{\beta}_k + g(\mathbf{T}_i) + \varepsilon_{ik} \qquad (2)$$

$Z_{ik} = z_{i1}, \dots, z_{im}$ is the $n \times m$ response matrix with $z_{ik} = (z_{1k}, \dots, z_{nk})'$ denoting the $k^{th}$ column vector of the response matrix, $\mathbf{X}_i = (\mathbf{x}_1, \dots, \mathbf{x}_p)$ is a $n \times p$ dimensional parametric design matrix with $\mathbf{x}_j = (x_{1j}, \dots, x_{nj})'$ showing

ISBN: 978-605-73552-2-5

the $j^{th}$ column vector of $\mathbf{X}$, $\boldsymbol{\beta}_k=(\boldsymbol{\beta}_{1k,}\dots,\boldsymbol{\beta}_{pk})'$ is a $p \times m$ regression coefficient matrix with $\boldsymbol{\beta}_j = (\beta_{j1}, \dots, \beta_{jm})'$ denoting the $k^{th}$ coefficient vector $(p \times 1)$, $\mathbf{T}_i = (T_1, \dots, T_n)'$ is a $n \times 1$ nonparametric design vector, g is a one – dimensional smooth function with $g(T_i) = [g(T_1), \dots, g(T_n)]' \in \mathbb{R}^{n\times 1}$, $\varepsilon_{ik} = (\varepsilon_{i1} \dots, \varepsilon_{im})'$ is a n × $m$ random error matrix with $\boldsymbol{\varepsilon}_{ik} = (\varepsilon_{1k}, \dots, \varepsilon_{nk})'$ representing the $k^{th}$ column vector of the matrix ε, which has $E(\boldsymbol{\varepsilon}) = 0$ and $Cov(\varepsilon) = \sum$ as defined above.

### 2.2. Modified Kernel Smoothing

To obtain modified kernel smoother, the penalized least squares criterion is used:

$$\min_{\boldsymbol{\beta}} \sum_{i=1}^{n}\left[\sum_{k=1}^{m} \boldsymbol{W_k}\{(\boldsymbol{Z_{ik}} - \boldsymbol{X'}_i\boldsymbol{\beta_k}) - \boldsymbol{g}\}\right]^2 \quad (3)$$

Where $\boldsymbol{W_k}$ is the $(n \times n)$ matrix of Nadaraya-Watson weights obtained by using well-known kernel function $K(.)$ for $k^{th}$ response.,

$$\mathbf{W_{kt}} = diag\left(K\left(\tfrac{T_1 - t}{h}\right), \dots, K\left(\tfrac{T_n - t}{h}\right)\right) = W_{n,h}(t, T_i) \quad (4)$$

Where $t$'s are the ordered distinct values for obtaining kernel intervals and it changes between $\min(T) < t_1 < \cdots t_n < \max(T)$. Accordingly, estimation of $\mathbf{g}$ is written as:

$$\hat{\mathbf{g}}_{\boldsymbol{k}} = W_k(t_0)(\mathbf{Z_k} - \mathbf{X}\boldsymbol{\beta}_k) \quad (5)$$

Where $\hat{\mathbf{g}}_{\boldsymbol{k}}$ means estimated function for $k^{th}$ response. To obtain this estimation, $\widehat{\boldsymbol{\beta}}_{\boldsymbol{k}}$ must be found at the first place. To obtain $\boldsymbol{\beta}_k$ partial residuals are used used that are:

$$\tilde{\mathbf{Z}}_{\mathbf{k}} = (\mathbf{I_n} - \mathbf{W_k})\mathbf{Z_k}$$
$$\tilde{\mathbf{X}} = (\mathbf{I_n} - \mathbf{W_k})\mathbf{X}$$
$$\tilde{\boldsymbol{\varepsilon}}_{\mathbf{k}} = (\mathbf{I_n} - \mathbf{W_k})\boldsymbol{\varepsilon_k}$$

where $\mathbf{I}_n$ is an $(n \times n)$ identity matrix. Accordingly multivariate semiparametric model can be written as a linear model and estimate of $\boldsymbol{\beta}_k$ can be obtained easily;

$$\widehat{\boldsymbol{\beta}}_{\mathbf{k}}^{\mathbf{KS}} = (\widehat{\boldsymbol{\beta}}_{\mathbf{1}}^{\mathbf{KS}}, \dots, \widehat{\boldsymbol{\beta}}_{\mathbf{m}}^{\mathbf{KS}})' = (\tilde{\mathbf{X}}'\tilde{\mathbf{X}})^{-1}\tilde{\mathbf{X}}'\tilde{\mathbf{Z}} \quad (6)$$

Correspondingly, a "*modified local polynomial estimator*" $\hat{\mathbf{g}}_{\mathbf{K}}^{\mathbf{KS}}(.)$ of the function $\mathbf{g}_{\boldsymbol{k}}(.)$ for the nonparametric part in the semiparametric model is defined as

$$\hat{\mathbf{g}}_{\mathbf{K}}^{\mathbf{KS}}(t) = \left(\hat{\mathbf{g}}_{\mathbf{1}}^{\mathbf{KS}}(t), \dots, \hat{\mathbf{g}}_{\mathbf{m}}^{\mathbf{KS}}(t)\right)' = \mathbf{W_k}\left(\mathbf{Z_k} - \mathbf{X}\widehat{\boldsymbol{\beta}}_{\mathbf{k}}^{\mathbf{KS}}\right) \quad (7)$$

Prove of the estimators by using partial residuals quite similar to the linear regression estimators

## 3. Evaluation Metrics

To evaluate model performance RMSE and estimated model variances are used for each model based on different response

$$\text{RMSE}(\hat{Z}_k) = \sqrt{n^{-1}\sum_{k=1}^{n}\left(Z_k - \hat{Z}_k\right)^2}$$

$$\hat{\sigma}_k^2 = var(\boldsymbol{\varepsilon}) = \frac{(\mathbf{Z_k} - \hat{\mathbf{Z}}_{\mathbf{k}})^{\mathbf{T}}(\mathbf{Z_k} - \hat{\mathbf{Z}}_{\mathbf{k}})}{\mathbf{tr}[(\mathbf{I_n} - \mathbf{H_k})^{\mathbf{T}}\ \mathbf{I_n} - \mathbf{H_k})]}$$

where $\mathbf{H}_k = \tilde{\mathbf{X}}(\tilde{\mathbf{X}}^T\tilde{\mathbf{X}})^{-1}\tilde{\mathbf{X}}^T$ and $tr[(\mathbf{I}_n - \mathbf{H}_k)^T\ \mathbf{I}_n - \mathbf{H}_k)]$ is the degrees of freedom of residuals. To evaluate performance of $\hat{\mathbf{g}}_{\boldsymbol{k}}$ Accordingly, the performance scores can be computed as follows:

$$MSE(\hat{\mathbf{g}}_{\boldsymbol{k}}) = n^{-1}(\mathbf{g_k} - \hat{\mathbf{g}}_{\mathbf{k}})^{\boldsymbol{T}}(\mathbf{g_k} - \hat{\mathbf{g}}_{\mathbf{k}}),\ k = 1, \dots m$$
$$TMSE(\hat{\mathbf{g}}_{\boldsymbol{k}}) = m^{-1}\sum_{k=1}^{m} n^{-1}(\mathbf{g_k} - \hat{\mathbf{g}}_{\mathbf{k}})$$

## 4. Real data example: Agricultural data

In this part, Australian soybean dataset are examined which is a publicly accessed dataset in "Agridat" package of R software. Dataset involves 464 data points and totally 10 variables. However, this study takes account for seven variables in multivariate semiparametric regression model. We considered three response variables, three covariates and one nonparametric variable.

ISBN: 978-605-73552-2-5

**Table 1**. Variable information of the model for soybean dataset

| Predictors | | Responses |
|---|---|---|
| **Parametric component** | **Nonparametric component** | |
| Env: 8 levels of environment<br>Height: Meters<br>Lodging: Settlement of Prod. | Size: Seed size, (mm) | Yield: Metric tons/hectare<br>Protein (%)<br>Oil (%) |

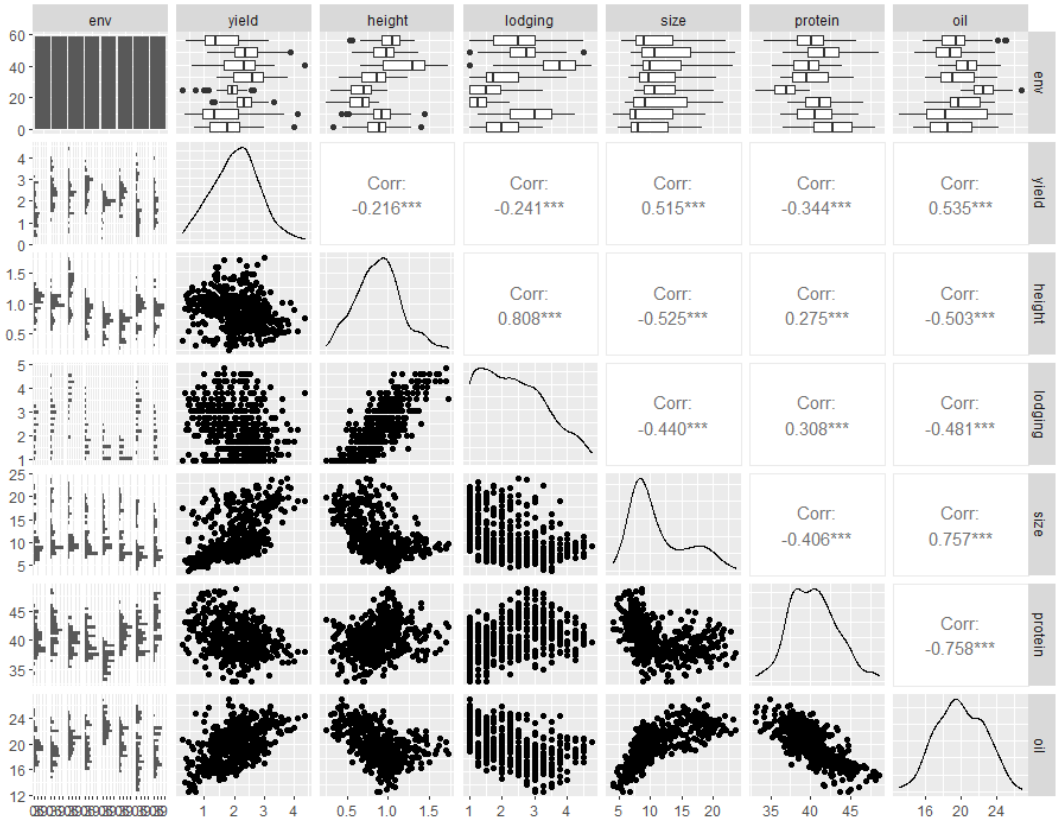


**Figure 1**. Pairs of data to observe the relationship between responses and predictors.

### 4.1. Defining Models

Accordingly obtained model can be written as follows:

$$\begin{cases} yield_i & = \beta_1 env_i + \beta_2 height_i + \beta_3 lodge_i + g(size_i) + \varepsilon_{1i}, i = 1, \dots, n \\ oil_i & = \beta_1 env_i + \beta_2 height_i + \beta_3 lodge_i + g(size_i) + \varepsilon_{2i}, j = 1, \dots, n \\ protein_i & = \beta_1 env_i + \beta_2 height_i + \beta_3 lodge_i + g(size_i) + \varepsilon_{3i}, j = 1, \dots, n \end{cases}$$

where $n = 464$ for all cases and it is assumed that the error terms are different for each model and they have normal distribution with zero mean and a constant variance such as $\varepsilon_j \sim N\ (0, \sigma_\varepsilon^2)$. As mentioned before, our main purpose is estimating the given three models simultaneously with realizing the multivariate regression analysis based on the kernel smoothing technique.

### 4.2. Selection of Bandwidth

To select optimal bandwidth, we used generalized cross-validation. Figure 2 given below shows the process for each function related to the three responses: $Z_1$*: Yield,* $Z_2$*: Protein,* $Z_3$*: Oil*

ISBN: 978-605-73552-2-5

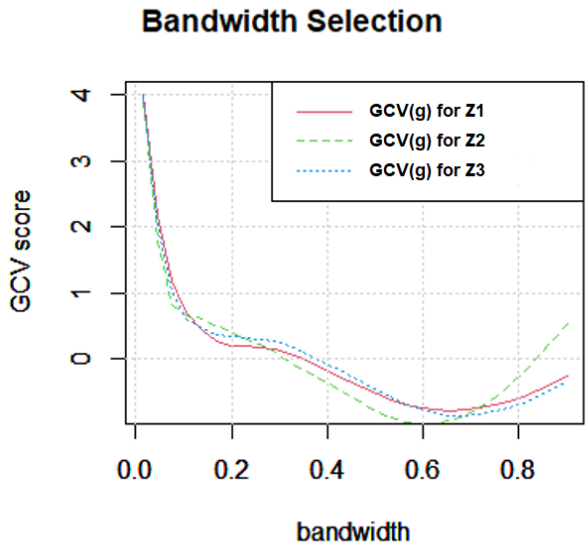


**Figure 2.** GCV process for bandwidth selection

### 4.3. General Performances

The Table 1 involves the performance measures that defined before for the models of different response variables. Thusly, their effects on the different response can be observed easily.

**Table 2**. General performance of the estimated models

| | $\hat{\beta}_{env}$ | $\hat{\beta}_{height}$ | $\hat{\beta}_{lodging}$ | $RMSE(\hat{Z})$ | $\hat{\sigma}^2$ |
|---|---|---|---|---|---|
| Yield | 0.023 | 2.702 | -0.36 | 0.96 | 0.924 |
| Protein | 2.021 | 34.807 | -1.895 | 0.993 | 0.989 |
| Oil | 1.043 | 17.452 | -1.933 | 0.834 | 0.698 |

Figure 3 and Table 3 show the performances of the nonparametric component estimation for each model. It is clearly seen that which response variable is affected by the nonparametric "seed size" covariate. Table 2 involves the performances of the fitted curves. MSE and TMSE scores are provided. Effects of the nonparametric covariate to the responses can be observed clearly.

**Table 3**. Performance of the fitted curves

| | **Yield** $(Z_1)$ | **Protein** $(Z_2)$ | **Oil** $(Z_3)$ |
|---|---|---|---|
| $MSE$ | 1.757 | 1.685 | 2.339 |
| $TMSE$ | 1.927 | | |

ISBN: 978-605-73552-2-5

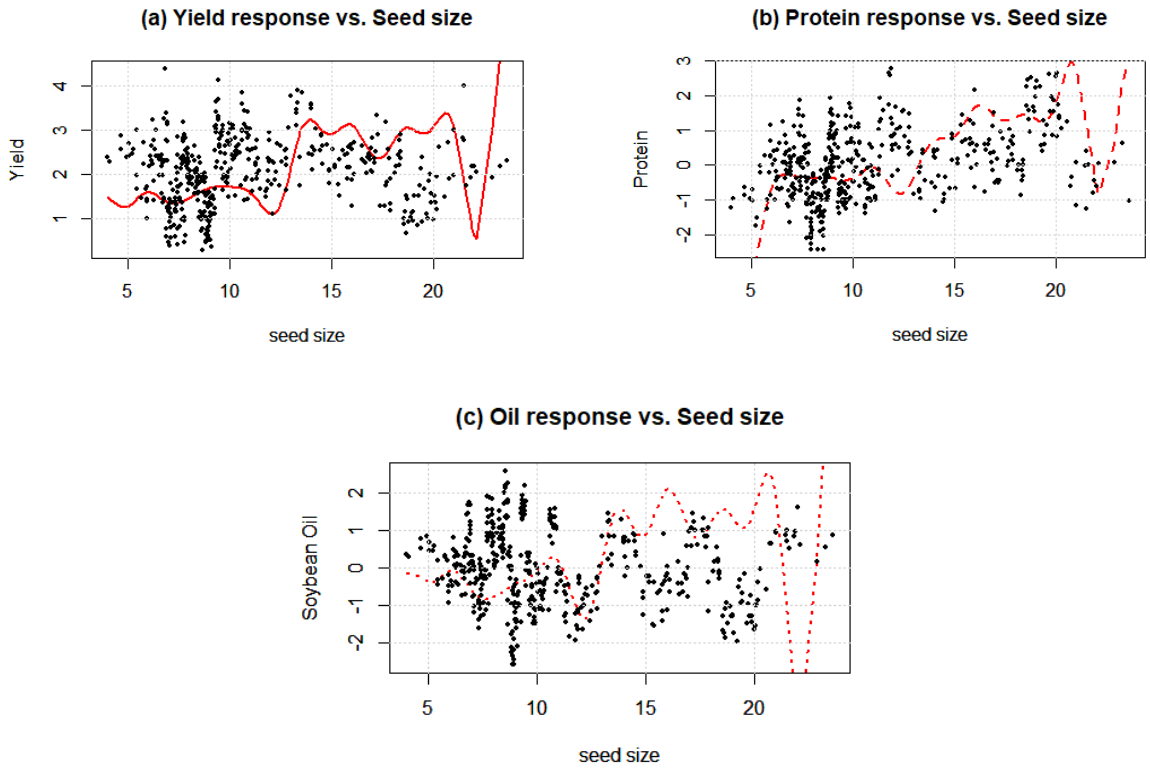


**Figure 3**. Fitted curves for the three estimated models based on the three responses: Yield, Protein and Oil.

## 5. Conclusion

- This paper showed that the proposed modified kernel estimator for multivariate semiparametric regression provides satisfying results.
- Contributions of the predictors to the three different response variables Yield, Protein and Oil, are modelled simultaneously.
- RMSE and variances of the models are obtained relatively small and close to each other which proves the stability of the estimator.
- If fitted curves are examined carefully, except for Oil response, the effect of the seed size on Yield and Protein responses modelled successfully.
- From the claim of this study, our expectation is that the proposed estimator may provide important contributions to the agricultural data analysis in terms of making predictions.

## References

Aydin, D., & Yilmaz, E. (2018). Modified spline regression based on randomly right-censored data: A comparative study. *Communications in Statistics-Simulation and Computation*, 47(9), 2587-2611.

Bonat, W. H. (2018). Multiple response variables regression models in R: The mcglm package. *Journal of Statistical Software*, 84, 1-30.

Delecroix, M., Lopez, O., & Patilea, V. (2008). Nonlinear censored regression using synthetic data. *Scandinavian journal of statistics*, 35(2), 248-265.

Fan, J., Gijbels, I., Hu, T. C., & Huang, L. S. (1996). A study of variable bandwidth selection for local polynomial regression. *Statistica Sinica*, 113-127.

Kaplan, E. L., & Meier, P. (1958). Nonparametric estimation from incomplete observations. *Journal of the American statistical association*, 53(282), 457-481.

ISBN: 978-605-73552-2-5

Khardani, S., Lemdani, M., & Ould Saïd, E. (2012). On the strong uniform consistency of the mode estimator for censored time series. *Metrika*, 75(2), 229-241.

Koul, H., Susarla, V., & Van Ryzin, J. (1981). Regression analysis with randomly right-censored data. *The Annals of statistics*, 1276-1288.

Johnson, R. A., & Wichern, D. W. (2002). *Applied multivariate statistical analysis* (Vol. 5, No. 8). Upper Saddle River, NJ: Prentice hall.

Miller, J. J., & Wegman, E. J. (1987). Vector function estimation using splines. *Journal of statistical planning and inference*, 17, 173-180.

Nadaraya, E. A. (1964). On estimating regression. *Theory of Probability & Its Applications*, 9(1), 141-142.

Yee, T. W., & Wild, C. J. (1996). Vector generalized additive models. *Journal of the Royal Statistical Society: Series B (Methodological)*, 58(3), 481-493.

You, J., & Chen, G. (2007). Semiparametric generalized least squares estimation in partially linear regression models with correlated errors. *Journal of Statistical Planning and Inference*, 137(1), 117-132.

Li, Z., Liu, H., & Tu, W. (2018). Model selection in multivariate semiparametric regression. *Statistical Methods in Medical Research*, 27(10), 3026-3038.

Chamidah, N., Lestari, B., Budiantara, I. N., Saifudin, T., Rulaningtyas, R., Aryati, A., ... & Aydin, D. (2022). Consistency and asymptotic normality of estimator for parameters in multiresponse multipredictor semiparametric regression model. *Symmetry*, 14(2), 336.

Pateiro-López, B., & González-Manteiga, W. (2006). Multivariate partially linear models. *Statistics & probability letters*, 76(14), 1543-1549.

Papageorgiou, G., & Hinde, J. (2012). Multivariate generalized linear mixed models with semi-nonparametric and smooth nonparametric random effects densities. *Statistics and Computing*, 22(1), 79-92.

Speckman, P. (1988). Kernel smoothing in partial linear models. *Journal of the Royal Statistical Society: Series B (Methodological),* 50(3), 413-436.

Watson, G. S. (1964). Smooth regression analysis. *Sankhyā: The Indian Journal of Statistics*, *Series A*, 359-372.

Wibowo, W., Haryatmi, S. and Budiantara, I.N. (2012). On multiresponse semiparametric regression model, *Journal of Mathematics and Statistics*, 8(4), 489-499.

You, J., Zhou, Y., & Chen, G. (2013). Statistical inference for multivariate partially linear regression models. *Canadian Journal of Statistics*, 41(1), 1-22.

ISBN: 978-605-73552-2-5

# ON THE CLASSICAL IDEAL GAS IN TWO DIMENSIONS

**Ibrahim A. SADIQ[1*], Wisam MOHAMMED [2], Noor M. YASEEN [3]**

[1,2,3] Department of Physics, College of Science, Al-Nahrain University, Baghdad, Iraq.

ibrahim.sadiq@nahrainuniv.edu.iq

## ABSTRACT

The kinetic theory of gases is revisited for an ideal classical gas geometrically confined in two dimensions, i.e. two-dimensional gas (2D gas). In this revision, the equation of state for the 2D gas is determined as well as some of its thermodynamic quantities. The thermodynamic quantities are like the internal energy, the heat capacities, and distribution functions of molecular speeds and molecular velocities as well as some of the characteristic velocities and the speed of sound. The work shows that the distribution functions of the molecular velocities are unchanged due to the reduction in the size of the spatial dimension but all other revisited quantities are changed. The most remarkable results in the 2D gas are those concern the gas temperature and the speed of sound (compressional waves). The same mean square velocity of the molecules gives a higher temperature in the 2D gas than it gives in the same gas enclosed by a surface, i.e. three-dimensional gas (3D gas). The other remark is that sound waves in the 2D gas are faster than sound waves in the 3D gas and these sound waves can travel further and last longer than sound waves for the same gas enclosed by a surface (3D gas) at the same temperature.

**Keywords:** ideal gas in two dimensions, equation of state, distribution molecular velocities, speed of sound, temperature,

## 1. INTRODUCTION

Thermodynamics of classical gases taught in high schools and colleges is that of a three-dimensional (3D) gas for it concerns to gases occupy a 3D space. This is completely right because in our daily life we deal with gases contained in vessels or containers (tubes, beakers, cylinders, etc.) which have geometrical shapes surround a 3D space. This 3D space is the volume ($V$). Despite, all these containers differ in sizes and shapes, all these containers possess a volume ($V$) which represents one of the thermodynamic coordinates that specifies the state of the gas.

Thermodynamic laws (relations) and quantities of these 3D gases were experimentally determined and theoretically justified by the kinetic theory of gases and statistical mechanics. In this work, we aim to evaluate the equation of state and some thermodynamic quantities of an ideal classical gas in two dimensions using the kinetic theory of gases in a manner similar to the approach of [1].

## 2. THE GAS INTERNAL ENERGY

In a 3D gas, the molecules possess three degrees of freedom for the kinetic energy. Each degree of freedom is associated with equal share of thermal agitation energy $\left(\frac{mv_x^2}{2}+\frac{mv_y^2}{2}+\frac{mv_z^2}{2}=\frac{kT}{2}+\frac{kT}{2}+\frac{kT}{2}\right)$, where $k$ is Boltzmann constant and $T$ is the gas temperature. So, the mean kinetic energy of one molecule is $\bar{\epsilon}=3kT/2$ . Then, the internal energy $U$ of the gas of $N$ number of molecules is $U=N\bar{\epsilon}=3NkT/2$. When the total number of molecules $N$ is equal to Avogadro's number $N_A$, the product $(N_A\,k)=R$, where $R$ is the gas constant and the internal energy becomes $U=3RT/2$ [1,2].

ISBN: 978-605-73552-2-5

If the ideal gas molecules are geometrically confined in two dimensions, each molecule of such a gas possesses only two degrees of freedom for the kinetic energy. Each degree of freedom is associated with equal share of thermal agitation energy $\left(\frac{mv_x^2}{2}+\frac{mv_y^2}{2}=\frac{kT}{2}+\frac{kT}{2}\right)$. So, the mean kinetic energy of one molecule is

$$\bar{\epsilon} = kT \tag{1}$$

Then, the internal energy $U$ of the 2D gas of $N$ number of molecules is

$$U = N\bar{\epsilon} = NkT \tag{2}$$

When the total number of molecules $N$ is equal to Avogadro's number $N_A$, the product $(N_A\, k) = R$, where $R$ is the gas constant and equation (2) becomes

$$U = RT \tag{3}$$

## 3. THE EQUATION OF STATE

When a gas is enclosed by a surface, the state of the 3D gas is defined by the thermodynamic coordinates $p$ (pressure), $V$ (containing volume) and $T$ via the equation $pV = NkT$. When $N = N_A$, $pV = RT$. Thus, the relation between the internal energy of the 3D gas ($U = 3RT/2$) and the equation of state and the is $pV = 2U/3$, which correct not only for classical ideal gases but to quantum gases as well [1,2].

The product of the coordinates $p$ (the perpendicular force per unit area) and $V$ (the size of the confining space) yields a physical quantity whose unit is that of energy. If the ideal gas molecules are geometrically confined in two dimensions and enclosed by a single curve, we can assume the case of a 2D gas. To evaluate the equation of state of such a gas, it is notable that the thermodynamic coordinates $V$ and consequently $p$ (used for the case of 3D gas) are not proper coordinates for the 2D gas. In 2D, the space confining the gas molecules is an area $A$ enclosed by the curve rather than a volume $V$ enclosed by a surface. Therefore, the area $A$ would replace the volume $V$ as a thermodynamic coordinate that specifies the state of the gas in two dimensions. The physical quantity that is conjugate to the area $A$ and their product yields the physical quantity whose unit is that of energy is the perpendicular force per unit length $f = F/l$. Mathematically, this can be proved by assuming an ideal gas of total number of molecules $N$ enclosed by a square of side-length $l$. The sides of this square are parallel to the axes of the Cartesian system $x$ and $y$. A molecule of mass $m$ moving along the x-axis with velocity $v_x$ released from one side towards the opposite side. Then, it collide the opposite side elastically and rebounded with velocity $-v_x$. The change in momentum of this molecule is $\Delta p_x = 2mv_x$ and the total distance travelled by the molecule is $2l$ and the time interval of this trip is $\Delta t = 2l/v_x$. The force due to the impact of this molecule is

$$F = \frac{\Delta p}{\Delta t} = \frac{mv_x^2}{l} \tag{4}$$

The mean value of the square of velocities for the $N$ molecules along the x-axis is $(v_{x1}^2+v_{x2}^2+\ldots+x_{xN}^2/N)$. The force imposed on this side of the square is due to the impacts of the molecules that possess velocities along the x-axis

$$F = \frac{Nm}{l}\left(\frac{v_{x1}^2+v_{x2}^2+\ldots+x_{xN}^2}{N}\right) = \frac{Nm}{l}\overline{v_x^2} \tag{5}$$

ISBN: 978-605-73552-2-5

Since, there are only two degrees of freedom in the two dimensional space, so $\overline{v^2} = \overline{(v_x^2 + v_y^2)}$, and we can write $\overline{v_x^2} = \overline{(v^2/2)}$ and express (5) as

$$F = \frac{1}{l}\left(\frac{Nm\overline{v^2}}{2}\right) \tag{6}$$

where $(m\overline{v^2}/2)$ is the mean kinetic energy of one molecule. The pressure in a 3D gas is obtained by dividing the force $F$ imposed on a surface by its area $(p = F/A)$. But in this 2D gas the, pressure is not a proper thermodynamic coordinate because the molecules only move in the confining plane and hence only impose a force on the curve surrounding the molecules. So, the force per unit length $(f = F/l)$ is the thermodynamic coordinate of the 2D gas, which is analogue to the pressure $p$ in the 3D gas. Dividing both sides of (6) by the length of the side of the square yields

$$F/l = \frac{1}{l^2}\left(\frac{Nm\overline{v^2}}{2}\right) = f = \frac{1}{A}\left(\frac{Nm\overline{v^2}}{2}\right) \tag{7}$$

where $l^2$ is the area of the square $A$. Equation (7) shows that the product of $(f\,A)$ gives the mean kinetic energy of the gas. Replacing the mean kinetic energy of one molecule $(m\overline{v^2}/2)$ by its total agitation thermal energy ($kT$), equation (7) reads

$$f\,A = NkT \tag{8}$$

The variables $f$ and $A$ are conjugate variables because their product gives the unit of energy exactly as the product of $pV$ in the 3D gas. Thus, Equation (8) is the equation that specifies the state of an ideal 2D gas via its coordinates $f$, $A$ and $T$. If $N = N_A$, then (9) becomes

$$f\,A = RT \tag{9}$$

Comparing (9) with (3) and (8) with (2), one obtains the relation between the equation of state of the 2D gas with its internal energy given by

$$f\,A = U \tag{10}$$

Equations (8) and (7) define the root mean-square velocity $v_{rms}$, the mean- square velocity $\overline{v^2}$, and the 2D gas temperature, given respectively by (11) and (12).

$$v_{rms} = \sqrt{\overline{v^2}} = \sqrt{2kT/m} \tag{11}$$

$$T = m\overline{v^2}/2k \tag{12}$$

Equation (12) infers that when the mean square velocity of the molecules of a 2D gas is the same as for the molecules of the same gas in 3D, the temperature of the 2D gas is higher than the temperature of the same gas in three dimensions which is given by the expression [1] $T = m\overline{v^2}/3k$.

## 4. THE HEAT CAPACITIES AND THE SPEED OF SOUND

Thermodynamics of a 3D gas involves two types of heat capacities, one is the heat capacity at constant volume ($C_V$) and the other is the heat capacity at constant pressure ($C_p$). The heat capacity at constant volume is defined by $C_v = dU/dT$ [1,2]. The heat capacity at constant pressure can be evaluated mathematically through the definition $C_p - C_v = T(dp/dT)(dV/dT)$. The ratio of these heat capacities[1] $(c_p/c_V) = \gamma$ is one of the characteristics of gases. One of the utilities of this ratio is in

ISBN: 978-605-73552-2-5

determining the speed of sound of ideal gases at given temperature [1] $v_{sound} = \sqrt{\gamma kT/m}$ . In ideal gases the value of $\gamma = 5/3$ [1] and, hence, the speed of sound is $v_{sound} = \sqrt{5kT/3m}$ .

In the case of 2D gas, the physical quantity that is analogous to $C_V$ is $C_A$ by differentiating (3) with respect to temperature $T$

$$C_A = \frac{dU}{dT} = \frac{d(RT)}{dT} = R \tag{13}$$

The physical quantity that is analogous to $C_p$ is $C_f$. Determining $C_f$ can be obtained in a manner similar to that for determining $C_p$ using the analogous quantities for $p$ and $V$ in the 2D gas.

$$C_f - C_A = T(df/dT)(dA/dT) \tag{14}$$

From (9) $\quad f = (RT/A) \rightarrow (df/dT) = (R/A)$ and

$$A = (RT/f) \rightarrow (dA/dT) = (R/f)$$

Using the latter expression in (13), we get

$$C_f - C_A = (RT/A)(R/f) \tag{15}$$

But $(RT/A) = f$, then (15) becomes

$$C_f - C_A = R \tag{16}$$

Using (13) in (16)

$$C_f = 2R \tag{17}$$

From (17) and (13), the ratio $(C_f/C_A) = 2$. Hence, the speed of sound in the 2D gases is $v_{sound} = \sqrt{2kT/m}$ . This means that speed of sound at any temperature in the 2D gas is equal to the root-mean square velocity given by equation (11).

## 5. THE DISTRIBUTION OF MOLECULAR VELOCITIES

The study of molecular velocities of gases in 3D is necessary for determining many thermodynamic quantities for those gases. The frequently used molecular velocities (speeds indeed) are the root mean-square velocity $v_{rms} = \sqrt{3kT/m}$ , the mean velocity $\bar{v} = \sqrt{8kT/\pi m}$ and the most probable velocity $v_{mp} = \sqrt{2kT/m}$ [1,2]. Comparing these characteristic velocities with the speed of sound in the 3D gas shows that the speed of sound is the lowest in its value and that's why the sound waves dissipate and die out into the thermal noise.

$$v_{sound} = \sqrt{\frac{5kT}{3m}} < v_{mp} = \sqrt{\frac{2kT}{m}} < \bar{v} = \sqrt{\frac{8kT}{\pi m}} < v_{rms} = \sqrt{\frac{3kT}{m}}$$

In this section, we derive the distribution functions of molecular velocities to evaluate the root mean-square velocity ($v_{rms}$), the average velocity $\bar{v}$ and the most probable velocity $v_{mp}$ for ideal gases in 2D. Our approach is the same of kinetic theory proceeded in [1].The molecules of a 3D gas can

ISBN: 978-605-73552-2-5

possess the velocity components $v_x, v_y$ and $v_z$ but in 2D gases molecules can possess only two of these velocity components, say $v_x$ and $v_y$. The derivation follows the approach of determining the distribution of molecular velocities of a 3D gas illustrated by [1]. The distribution functions of molecular velocities, $f(v_x)$ $and$ $f(v_y)$, of the 2D gas are defined along the Cartesian coordinate system (x and y axes) as:

$$\frac{dNv_x}{N} = f(v_x)\,dv_x \tag{18}$$

$$\frac{dNv_y}{N} = f(v_y)\,dv_y \tag{19}$$

where $dNv_x$ and $dNv_y$ are the portions of molecules that possess velocity components along the x and y axes and $dv_x$ and $dv_y$ are the differentials of the velocity components. Multiplying the functions in (18) and (19) yields

$$\frac{d^2Nv_xv_y}{N} = f(v_x)f(v_y)\,dv_x\,dv_y \tag{20}$$

The product of $dv_x$ and $dv_y$represents differential element of area in the Cartesian system of the molecules velocities $d(A_v)$. Dividing $d^2Nv_xv_y$ by $dv_xdv_y$ gives a constant quantity per unit area defined by

$$\rho = \frac{d^2Nv_xNv_y}{dv_x\,dv_y} = Nf(v_x)f(v_y) \tag{21}$$

Differentiating (21) gives $0 = d\rho = \frac{d\rho}{dv_x}dv_x + \frac{d\rho}{dv_y}dv_y$ (22)

$$\frac{d\rho}{dv_x} = Nf'(v_x)f(v_y) \tag{23}$$

Similarity

$$\frac{d\rho}{dv_y} = Nf(v_x)f'(v_y) \tag{24}$$

Substituting (24) and (23) in (22) and dividing by $Nf(v_x)f(v_y)$, we get

$$0 = \frac{f'(v_x)}{f(v_x)}dv_x + \frac{f'(v_y)}{f(v_y)}dv_y \tag{25}$$

The latter equation can be solved by Legendre's undetermined multipliers:

$$0 = \left(\frac{f'(v_x)}{f(v_x)} + \lambda v_x\right)dv_x + \left(\frac{f'(v_y)}{f(v_y)} + \lambda v_y\right)dv_y \tag{26}$$

Equation (26) doesn't hold unless each term is equal to zero. Integrating each term gives the corresponding velocity distribution function and defining $\beta^2 = \frac{\lambda}{2}$, we get

$$f(v_x) = \alpha e^{-\beta^2 v_x^2} \tag{27}$$

$$f(v_y) = \alpha e^{-\beta^2 v_y^2} \tag{28}$$

To determine these functions completely, it requires to evaluate $\alpha$ and $\beta$. Substituting (27) and (28) in (20), we get

ISBN: 978-605-73552-2-5

$$d^2N v_x v_y = N\,\alpha^2\, e^{-\beta^2(v_x^2+v_y^2)}\;\; dv_x\, dv_y \tag{29}$$

Noting that $v_x^2 + v_y^2$ represents the square of the speed $v^2$ and $dv_x dv_y$ stands for $d(A_v)$ , then equation (29) can be written as

$$\rho = \frac{d^2N v_x v_y}{dv_x\, dv_y} = N\alpha^2 e^{-\beta^2 v^2} \tag{30}$$

The simplest method to calculate the number of molecules with speeds between $(v)$ and $(v + dv)$ is to recall the surface density which is uniform in a thin circular ring of radius $(v)$. It is important to stress here that the speed $v$ is a scalar quantity whose values are $(0 < v < \infty)$. The area of the ring is $d(A_v) = d(\pi v)^2 = 2\pi v dv$. Now, the number of molecules in the ring is $dN_v = \rho dA_v$. Using (30), the number of molecules in the ring is

$$dN_v = N\alpha^2 e^{-\beta^2 v^2}(2\pi v dv) = 2\pi N\alpha^2 v e^{-\beta^2 v^2} dv \tag{31}$$

The next step is to integrate (31) over the speed $v$ from 0 to $\infty$ and dividing both sides by the total number of molecules $N$ we get

$$1 = \int_0^\infty 2\pi\alpha^2 v e^{-\beta^2 v^2} dv \tag{32}$$

The integrand of (32) represents the normalized distribution function of molecular speeds of the 2D gas.

$$f(v) = 2\pi\alpha^2 v e^{-\beta^2 v^2} \tag{33}$$

Integrating (33) using the definition $\int_0^\infty x^m e^{-r x^2} dv = \left( \frac{\Gamma((m+1)/2)}{2r^{(m+1)/2}} \right)$

(34) leads to evaluate $\alpha$, where $\Gamma$ is the gamma function.

$$\alpha = \beta/\sqrt{\pi} \tag{35}$$

Using (35) in (33) yields

$$f(v) = 2\beta^2 v e^{-\beta^2 v^2} \tag{36}$$

Evaluating $\beta$ can be determined using the mean square velocity $(\overline{v^2})$. The mean square velocity can be evaluated using the distribution function of the molecular speeds

$$\overline{v^2} = \int_0^\infty v^2 f(v) dv = 2\beta^2 \int_0^\infty v^3 e^{-\beta^2 v^2} dv \tag{37}$$

Using the definition (34) in the latter equation, leads that $\beta^2 = \frac{1}{\overline{v^2}}$. Using (11) in the latter expression, we get

$$\beta^2 = (m/2kT) \rightarrow \beta = \sqrt{m/2kT} \tag{38}$$

ISBN: 978-605-73552-2-5

Equations (38, 35, 28 and 27) show that the definitions of $\beta$, $\alpha$, $f(v_y)$ and $f(v_x)$ are the same Substituting $\beta$ in (36), leads to express the distribution function of molecular speeds of the 2D gas in terms of the gas temperature and the mass of the molecule of the gas.

$$f(v) = \frac{m}{kT} v\, e^{-(mv^2/2kT)} \tag{38}$$

Substituting $\beta$ and $\alpha$ in (27) and (28), leads to express the distribution function of molecular velocities of the 2D gas in terms of the gas temperature and the mass of the molecule of the gas.

$$f(v_x) = \sqrt{m/2\pi kT}\; e^{-(mv_x^2/2kT)} \tag{39}$$

$$f(v_y) = \sqrt{m/2\pi kT}\; e^{-(mv_y^2/2kT)} \tag{40}$$

It is important to stress here that both $v_x$ and $v_y$ are vector quantities, and thus $(-\infty < v_x < \infty)$ and $(-\infty < v_y < \infty)$.

## 6. THE MEAN AND THE MOST PROBABLE VELOCITIES (SPEEDS)

The mean or average velocity $\bar{v}$ can be evaluated using the distribution function of molecular speeds using the definition $\bar{v} = \int_0^\infty v f(v) dv$ to get $\bar{v} = 2\beta^2 \int_0^\infty v^2 \bar{e}^{\beta^2 v^2} dv$. This integral is solved by the definition (34) to obtain

$$\bar{v} = \sqrt{\pi kT/2m} \tag{41}$$

The most probable velocity $v_{mp}$ can be determined via maximizing (36) by differentiation to obtain

$$v_{mp} = \sqrt{kT/m} \tag{42}$$

Comparing the results (42, 41 and 11), shows that the speed of sound in the 2D gas is the highest in its value.

$$v_{mp} = \sqrt{\frac{kT}{m}} < \bar{v} = \sqrt{\frac{\pi kT}{2m}} < v_{rms} = \sqrt{\frac{2kT}{m}} = v_{sound}$$

This result shows that sound waves in the 2D gas can overcome thermal noise better than sound waves do in the 3D gas and emphasizes that sound waves in the 2D gas can travel further and last longer than sound waves can do in the 3D gas. This result also declares that for the same type of molecules and at any temperature, sound waves in the 2D gas are faster than the sound waves in the 3D gas.

## 7. CONCLUSIONS

The equation of state of an ideal 2D is determined as well as and the distribution functions of molecular speed, the distribution functions of molecular velocities, its internal energy, heat capacities, and the speed of sound. The table summarizes the results of the 2D gas and compares its results with corresponding quantities in the 3D gas. The results exhibit that the definitions of $\beta$, $\alpha$ and the

ISBN: 978-605-73552-2-5

distribution functions of molecular velocities $f(v_x)$ and $f(v_y)$ in the 3D gas are unchanged in the 2D gas. This observation infers that these quantities are independent of the size of the spatial dimension confining the classical gas.

Thermodynamic quantities of the 2D gas versus those of the 3D gas

| | 3D Gas [1,2] | 2D Gas |
|---|---|---|
| The definition of $\beta$ and $\alpha$ | $\beta = \sqrt{m/2kT},\ \alpha = \beta/\sqrt{\pi}$ | $\beta = \sqrt{m/2kT},\ \alpha = \beta/\sqrt{\pi}$ |
| The distribution functions of molecular velocities | $f(v_x) = \alpha \exp(-\beta^2 v_x^2)$<br>$f(v_y) = \alpha \exp(-\beta^2 v_y^2)$<br>$f(v_z) = \alpha \exp(-\beta^2 v_z^2)$ | $f(v_x) = \alpha \exp(-\beta^2 v_x^2)$<br>$f(v_y) = \alpha \exp(-\beta^2 v_y^2)$ |
| The distribution function of molecular speeds | $f(v) = 4\pi\alpha^3 v^2 e^{-\beta^2 v^2}$ | $f(v) = 2\pi\alpha^2 v e^{-\beta^2 v^2}$ |
| The mean kinetic energy | $\bar{\epsilon} = 3kT/2$ | $\bar{\epsilon} = kT$ |
| internal energy | $U = 3NkT/2$ | $U = NkT$ |
| Equation of state | $pV = NkT = 2U/3$ | $fA = NkT = U$ |
| Temperature | $T = m\overline{v^2}/3k$ | $T = m\overline{v^2}/2k$ |
| The ratio of the heat capacities | $\gamma = 5/3$ | $\gamma = 2$ |
| The speed of sound | $v_{sound} = \sqrt{5kT/3m}$ | $v_{sound} = \sqrt{2kT/m}$ |
| The root-mean square velocity (speed) | $v_{rms} = \sqrt{3kT/m}$ | $v_{rms} = \sqrt{2kT/m}$ |
| The mean velocity (speed) | $\bar{v} = \sqrt{8kT/\pi m}$ | $\bar{v} = \sqrt{\pi kT/2m}$ |
| The most probable velocity (speed) | $v_{mp} = \sqrt{2kT/m}$ | $v_{mp} = \sqrt{kT/m}$ |

All other quantities show a direct dependence on the spatial dimension. The internal energy of a gas confined in in two dimensions is lower than that of the same gas when enclosed in three dimensions. This, in turn, led to the reduction in the heat capacities of the 2D gas in comparison with the heat capacities of the 3D gas. This result is a direct consequence of the reduction in the number of degrees of freedom due to the reduction in the size of the geometrical dimension confining the gas.

This justification is also true for the reduction in values of the most probable, the mean and the root mean-square velocities in the a gas confined in two dimensions in comparison to the corresponding values in the same gas enclosed by a surface.

The most remarkable results are the temperature and the speed of sound in the 2D gas. Concerning the temperature, in the 2D gas, it is higher in comparison with the temperature in the gas 3D when both gases possess the same mean square velocity. The molecules in the 2D gas with the same mean square velocity of the molecules of the 3D give higher temperature than the same molecules give in the 3D gas. The other remark is that sound waves in the 2D are faster than sound waves in the 3D gas and these waves can travel further and last longer and sound waves in the same gas enclosed by a surface (3D gas) at the same temperature.

**References**

[1] Introduction to Thermodynamics, The Kinetic Theory of Gases and Statistical Mechanics 2nd.ed., Sears Watson Francis, John-Wiley and Sons Inc. , NY. 1972.
[2] An Introduction to Statistical Physics for Students, A. J. Pointon, Longman, London, 1967.

ISBN: 978-605-73552-2-5

# HOW THE PRE-SERVICE TEACHERS ARE ADAPTED FOR AN UNEXPECTED SITUATION: EVALUATING THE ACTIVITIES DESIGNED FOR ONLINE LEARNING ENVIRONMENTS

Emine Nur UNVEREN-BILGIC, Emre CAM, Nazire Burcin HAMUTOGLU*

[1] Mathematics Education, Education Faculty, Düzce University, Düzce, Turkey
[2] Niksar Vocational School, Tokat Gaziosmanpasa University, Tokat, Turkey
[3] The Centre for Teaching and Learning Excellence, Eskisehir Technical University, Eskisehir, Turkey

## ABSTRACT

This study was carried out in order to reveal the current situation of teacher candidates regarding the teaching process in case of a possible emergency teaching environment. The study deals with the instructional design processes of teacher candidates within the scope of the course conducted within the scope of "Material Design" in a state university. In this course, the design of 123 pre-service teachers was subjected to content analysis according to the ICCEE Model. Among the findings of the research carried out with the qualitative paradigm, the following can be listed: Pre-service teachers did not determine the course format, and there was no expression in the designs regarding the level of use of the technology included in the design. While pre-service teachers write explanatory statements that may attract students' academic interest, they present insufficient designs in the context of social and emotional interaction and belonging.
**Keywords:** emergency remote teaching, mathematics education, instructional design

## INTRODUCTION

Considered as an important component in the development of technology, mathematics has placed it in an advantageous position for sustainable development in the 21st century (Odumosu and Eguntola, 2010). Maths; It is an excellent tool for the development of a person's intellectual competence in logical reasoning, spatial visualization, analysis and abstract thinking, for the qualities required by the 21st century. Individuals develop arithmetic, reasoning, thinking skills and problem solving skills through the learning and application of Mathematics. They are highly valuable not only in science and technology, but also in everyday life. Developing a scientific and technologically based highly skilled manpower requires a strong foundation in Mathematics (Ministry of Education, Singapore, 2006). Most of the people consider specializing in mathematics or becoming able to use mathematics in life as a very difficult goal for them to reach. But math is a tool and language used to solve problems big and small. Mathematical reasoning is required for everyday problems such as budgeting and saving, financing a house or car, calculating tips at a restaurant, and estimating distances and gas mileage (Leonard, Steve & Art, 2004). Mathematical knowledge and skills provide a key to enter the rapidly changing technological world (Leonard, et al, 2004). Lawrence and Kolawale (2007), while accepting the importance and contribution of mathematics to the culture of modern science and technology, said that "there is no science without mathematics, there is no modern technology without science, and there is no modern society without modern technology". These changes have always been necessary with the understanding of the role that mathematics should play in the scientific and technological development of the country, as well as the responses to societal needs and demands (Lawrence & Kolawole, 2007). They also said that today's world is considered a global village characterized by computers and information technology. This age has brought many developments in mathematics in order to sustain these developments.

### THE AIM AND SIGNIFICANCE OF THE STUDY

We may need to ask broader questions regarding the transformed math classrooms with the pandemic: Is it possible that the use of digital technology creates a crisis of ignorance of how to use it in math education? Conversely, if the crisis lasts long, can digital technologies provide alternative ways to apply mathematics education? There isn't a lot of research on online math education for young children, but if something similar happens in the future, will we apply our experience without doing enough research? Shouldn't it be necessary to develop research on mathematics education for a possible "COVID-2X" crisis? Based on all these questions, it has been considered very important how to transfer mathematics learning environments to online environments with the pandemic and to reveal the current situation in this regard.

### RESEARCH QUESTION

In this context, the aim of the research is to investigate how the pre-service teachers are ready for an unexpected situation with the basis of online learning environments dynamics.

ISBN: 978-605-73552-2-5

Accordingly, the question sought to be answered in the study is given below.
**RQ:** "How are the learning environments designed by pre-service teachers in the context of online teaching?"

## METHOD

The designed teaching and learning activities by pre-service teachers will be assessed via a rubric developed by researchers. The process will be assessed formatively and the pre-service teachers will be informed about the feedback on their designed materials to develop their adaptability skills for an unexpected situation. Activities designed by pre-service teachers were examined in detail in order to increase the awareness and adaptability skills of pre-service teachers about emergency online applications in the learning environments. For the purpose of the research, it was designed as an internal case study by following the qualitative paradigm. Internal case studies are frequently used by educational researchers to describe a program and to show how effective it is. For this purpose, activities designed by 123 pre-service teachers were used as data.

### Collection of Data

The data used in the research process were collected face to face in a material design course for teaching mathematics. Feedback was provided during the data collection process. However, the feedback was limited to only mathematics teaching methods.

### Analyzing of Data

The data were analysed by using the ICCEE ( Identify, Choose, Create, Engage, and Evaluate), developed by Chen (2016) online instructional design model for theoretical framework.

According to this theory of Chen (2018), the steps of ICCEE are explained as follows:Identification step: Identifying a course format is essential in the initial process when designing an online course, as the nature of an online course is so different from a traditional face-to-face course and a blended course. Course formats range from a fully face-to-face course, to blended courses with a small amount of online component, to a class with a high online component or fully online. Choose step: After identifying the necessary formats and elements suitable for an online teaching, an online instructor can begin to choose. At this stage, online instructors choose the content editing layout, which is a way of organizing online course content and materials, linear or non-linear. Choosing the content organization format is important at this step as it affects students' first impressions of online courses, as well as how they access and navigate the course content. Creation step: The third step is to create or develop. In this step, online instructors begin to create and create intuitive course path or flow, create teaching methods and materials for content delivery, assignment and assessment, create interactive communication methods, and create supporting materials for students. Engage step: According to a research report, online learning tends to have a high dropout rate, how to retain and engage online students becomes indispensable. Therefore, during the implementation phase of an online course, online instructors should focus on the process of how to perform online learning. Evaluation step: The last step in this model is evaluation. Student assessment should be holistic and formative. Online instructors monitor students' performance in projects, presentations, assignments, tests, communication posts, etc. can be evaluated with multiple strategies such as Students' performance in the online classroom should also be evaluated progressively and periodically. Online instructors should also evaluate the effectiveness of their teaching methods and materials by checking with their online students through questionnaires, surveys, interviews, online observations, or others.

*Reliability and validity:*

In order to ensure the internal validity of the research, an expert in the field was provided to evaluate the research process and the methods used in detail. The following percentage of agreement suggested by Miles and Huberman (1994) was used to calculate the reliability of the study.

Reliability=(Agreement)/(Agreement + Disagreement)

While using this formula, the evaluations of the first author and a researcher who is an expert in the field were used. As a result of the calculations, the percentage of agreement in the study was calculated as 87.65%.

### Findings

The findings obtained as a result of the analysis of the data obtained in the research are presented in Table 1.

| | | | |
|---|---|---|---|
| Identify | • Course format | Partly Online<br>Entirely Online<br>Not explained | K2, K5, K9K1,K3, K4, K6, K7, K8, K10, K11, K12, K13, K14, K15, K16, K17, K18, K19, …, K123 |

ISBN: 978-605-73552-2-5

| | | | |
|---|---|---|---|
| | • Instructional objectives Terminal objectives related to learning outcomes | Instructional objectives | K1, K2, K3, K4, K5, K6, K7, K8, K9, K10, K11, K12, K13, K14, K15, K16, K17, K18, K19, |
| | | Terminal objectives | K1, K2, K3, K6, K7, K8, K9, K10, K11, K12, K13, K14, K15, K16, K17, K18, K19, |
| | | Not explained | K20, …, K123 |
| | • Learners' needs and characteristics | Existent | K2, K3, K4, K5, K6, K7, K8, K9, K10, K11, K12, K13, K14, K15, K16, K17, K18, K19 |
| | | Not existent | K1, K20,...,K123 |
| | • Technology usage | Take into considiration | |
| | | let alone | K1, K2, K3, K4, K5, K6, K7, K8, K9, K10, K11, K12, K13, K14, K15, K16, K17, K18, K19,...,K123 |
| | • Learning context | Clear | K1, K2, K3, K4, K5, K6, K7, K8, K9, K10, K11, K12, K13, K14, K15, K16, K17, K18, K19,...,K123 |
| | | Not clear | |
| | • Appropriate pedagogy | Explained | |
| | | Not explained | K1, K2, K3, K4, K5, K6, K7, K8, K9, K10, K11, K12, K13, K14, K15, K16, K17, K18, K19, …, K123 |
| Choose | • Effective technology tool | Explained | K1, K3, K4, K2, K6, K7, K8, K10, K11, K12, K13, K14, K15, K16, K17, K18, K19,...,K123 |
| | | Not explained | K5, K9 |
| Create | • Course pat hor flow | Explained | K1, K2, K3, K4, K5, K6, K7, K8, K9, K10, K11, K12, K13, K14, K15, K16, K17, K18, K19,...,K123 |
| | | Not explained | |
| | • Instructional methods and materials for content presentation | Existent | K9 |
| | | Not existent | K1, K2, K3, K4, K5, K6, K7, K8, K10, K11, K12, K13, K14, K15, K16, K17, K18, K19,...,K123 |
| | • Assignment | Existent | K1, K2, K3, K4, K5, K6, K7, K8, K9, K10, K11, K12, K13, K14*, K15, K16, K17, K18, K19,...,K123 |
| | | Notexistent | |
| | • Interactive communication methods | Existent | K1, K6, K7, K8, K10*, K12, K13*, K14, K15*, K16, K17, K18, K19 |
| | | Notexistent | K2, K3, K4, K5, K9, K11,...,K123 |
| | • Supporting materials | | K1, K2, K3, K4, K5, K6, K7, K8, K10, K11, K12, K13, K14, K15, K16, K17, K18, K19,...,K123 |
| | | Notexistent | K9 |
| Engage | • academic | Existent | K1, K2, K3, K4, K5, K6, K7, K8, K9, K10, K11, K12, K13, K14, K15, K16, K17, K18, K19,...,K123 |

ISBN: 978-605-73552-2-5

| | | | |
|---|---|---|---|
| | | Notexistent | |
| | • social | Existent | |
| | | Notexistent | K1, K2, K3, K4, K5, K6, K7, K8, K9, K10, K11, K12, K13, K14, K15, K16, K17, K18, K19,...,K123 |
| | • emotional | Existent | |
| | | Notexistent | K1, K2, K3, K4, K5, K6, K7, K8, K9, K10, K11, K12, K13, K14, K15, K16, K17, K18, K19,...,K123 |
| Evaluate | • Holistic | | K12 |
| | • Formative | | K1, K2, K3, K4, K5, K6, K7, K8, K9, K13, K14, K15, K16, K17, K18, K19,...,K123 |
| | • None | | K10, K11 |
| | • Types (Survey, questionnarie, interview, online observations, etc… | Existent | K5 |
| | | Notexistent | K1, K2, K3, K4, K6, K7, K8, K9, K12, K13, K14, K15, K16, K17, K18, K19,...,K123 |
| | • Instructor evaluation | Existent | |
| | | Notexistent | K1, K2, K3, K4, K5, K6, K7, K8, K9, K10, K11, K12, K13, K14, K15, K16, K17, K18, K19,...,K123 |

It is seen that pre-service teachers do not define the course format. In addition, terminal outputs that enable the establishment of relations with learning objectives and learning needs and charachteristics are also defined in very few of them. At the same time, it is seen that the pre-service teachers did not include a statement about the level of use of the technology included in the design by the students.

It is seen that teacher candidates generally try to integrate digital technologies suitable for the content into the process. Although they clearly reveal the course flow for themselves, it is seen that few of them prepare presentations for the students. It is seen that pre-service teachers include interim evaluations in the teaching process. It is seen that pre-service teachers include interactive applications especially in the evaluation part. However, in designs with modeling problems, it is seen that the focus is on students using the software themselves, especially with a construction protocol. In these designs, pre-service teachers preferred to stay away from interaction.

It is seen that pre-service teachers put forward inadequate designs in the context of interaction and belonging in social and emotional sense, while clearly writing statements that can engage students in academic terms. In addition, it can be said that there are more formative evaluations in the designs and that the pre-service teachers are closed to self-evaluation.

## CONCLUSIONS

Based on the findings of the research; the necessity of adding a course that will deal with emergency distance education in teacher training programs has been revealed. In addition, the need for the Computer Education and Technologies Department has been underlined once again. There is a lack of awareness of pre-service teachers about the contexts that will reveal the relationship between learning outcomes and learning outcomes. Students need to develop an awareness of the level of technology they will use.they need to be supported in using interactive digital environments. Students need to gain an awareness that they need not only academic but also social and emotional support in online environments. It is necessary to underline the importance of holistic assessment and multidimensional assessment in online learning environments for teacher candidates.

## SUGGESTIONS

Based on the findings of the research; the necessity of adding a course that will deal with emergency distance education in teacher training programs has been revealed. In addition, the need for the Computer Education and Technologies Department has been underlined once again.

ISBN: 978-605-73552-2-5

**REFERENCES**

Odumosu, M. O., & Eguntola, E. G. (2010). Everyday mathematics for sustainable development in 21st century: Pre-service Teachers perception. In Conference proceedings of School of Science (pp. 185-190).

Ministry of Education, Singapore. (2006). Education statistics digest 2006. Moulding the Future of our Notion. Retrieved from http://www.moe.gov.sg/esd/ESD2006.pdf

Leonard, M. K., Steve, T., & Art, J. (2004). Guiding Children's Learning of Mathematics (10th eds.). USA: Thompson Learning, Inc

Lawrence, I. A. & Kolawole, O. U. (2007). Mathematics Education for Dynamic Economy in Nigeria in the 21st Century. Journal of Social Sciences, 15(3): 293-296.

Chen, L. L. (2016). A model for effective online instructional design. Literacy Information and Computer Education Journal, 6(2), 2303-2308.

ISBN: 978-605-73552-2-5

# A PRACTICE FOR QUALITY ASSURANCE IN THE DESIGN OF BLENDED LEARNING ENVIRONMENTS: EDUCATIONAL PROGRAM GOALS

**Emre CAM, Emine Nur UNVEREN-BILGIC, Nazire Burcin HAMUTOGLU***

[1] Niksar Vocational School, Tokat Gaziosmanpasa University, Tokat,
[2] Mathematics Education, Education Faculty, Düzce University, Düzce, Turkey
[3] The Centre for Teaching and Learning Excellence, Eskisehir Technical University, Eskisehir, Turkey

## ABSTRACT

This study provides an infrastructure regarding the necessity of designing activities to be carried out in blended learning environments. In the study, an example of instructional design related to the subject area titled " Mathematics Teacher Training" carried out within the scope of " Teaching Statistics and Probability" in a state university is presented. The educational program goals of mathematics teacher training departments (f=76) in Turkey were examined via qualitative research methods. Regarding the findings on educational program goals, the design of the Teaching Statistics and Probability course was carried out with the basis of blended learning dynamics. In this online activity, the design of instruction consists of the steps of plan, implement, control and take action to ensure quality assurance. It is thought that the related study will provide a framework for providing quality assurance in the effective, efficient and attractive design of activities to be carried out in blended learning environments. In addition, a lesson plan for "Probability and Statistics Teaching", which is an important subject area in the process of training mathematics teachers who are the instructors of the discipline of mathematics, which has a difficult, abstract and cumulative structure, will be brought to the literature in line with the quality assurance system.

**Keywords:** blended learning, mathematics education, probability and statistics teaching, educational program goals, quality assurance.

### INTRODUCTION

Educational Program Goals (EPGs) are clear and general statements that inform how a program will plan its educational mission and meet the needs of its stakeholders. The educational goals of the program are statements that describe what graduates are expected to achieve within 3-5 years of completing a program. Accordinly, it is possbile to say that EPG;
-determines what kind of career the program expects from its graduates,
-reveals the career differences between graduates of the program and graduates of similar programs,
-ensures that the career goals expected from the graduates of the program are learned by the stakeholders and the society,
-provides the evaluation of teaching methods, teaching processes and teaching to be used in the program and creates a starting point that improves the program over time.
According to this, while educational program goals are determining, it is important to determine and answer the question of “What kind of graduate do we want”? The answer of stated question needs to be taken into account the followings:

- **Stakeholder Engagement:** the process of involving people who may be affected by or influence the implementation of an organization's decisions.
- **Needs Analysis:** the formal process that accompanies the needs analysis and focuses on the human aspects of the requirements.

Before we can do a job, we must first have needs. It is the process of collecting information to determine the differences between the existing situation and the situation that should be, and developing solution proposals by analyzing the problem in the light of the collected information. The most basic definition of need is the difference between expected conditions and current conditions. Stages of determining an educational need;
1. Identifying the problem situation and what kind of information will be collected about this problem.
2. Identifying information collection sources.
3. Developing information collection tools.
   - ♦ Which method or methods will be used to collect data
     - ✓ The amount of information requested
     - ✓ The type of information requested
   - ➢ The characteristics of the sources to be collected and the results
   - ➢ Depends on how quickly it is needed.

   - ♦ The most used information collection tools are;
     - ✓ Interview (Interview)

- ✓ Questionnaire
- ✓ Observation
- ✓ Examination of Archives

4. To identify the source of the problem and possible solutions.
5. Setting priorities
6. Analyzing resources and limitations.
7. Summarizing the results.

After considering the needs and collecting data to meet the demand it is expected that EPGs should be

- aligned with the mission of the Institution, Unit, and Department.
- published.
- established an assessment and evaluation process in operation.
- proved that the educational goals of the program have been achieved.
- updated at appropriate intervals.
- should be monitored the graduates regularly.

**THE AIM AND SIGNIFICANCE OF THE STUDY**

In this study, it is aimed to examine the "Primary Education Mathematics Education" programs of higher education institutions in Turkey based on the design of blended learning environments of the "Statistics and Probability" course of the EPGs, with an approach based on raising awareness about providing quality assurance and spreading the quality culture to all units. Although the Covid-19 pandemic has disrupted learning and teaching activities in educational institutions (Ünveren-Bilgiç, Çam, & Hamutoğlu, 2021), based on the study, it is important that the EPGs are an important issue to ensure the quality assurance and the design of a blended learning environment. This study is providing a road map and conducted with the instructional methods, techniques and strategies that can be used in the design of a blended course in the programs of higher education institutions (i.e. Elementary Education Mathematics Teaching) to the design of an effective, efficient and attractive blended learning and teaching environments and ensure the quality assurance, and also including the collaborative tools

It is thought that the related study will provide a framework for providing quality assurance in the effective, efficient and attractive design of activities to be carried out in blended learning environments. There is a need for explanations in the context of the teaching staff working as practitioners to reveal the relationship between the learning outcomes of the courses and the country's qualifications framework, and based on this situation, the mission differentiation of the universities (Ünveren Bilgiç, 2021).In addition, a lesson plan for "Probability and Statistics Teaching", which is an important subject area in the process of training mathematics teachers who are the instructors of the discipline of mathematics, which has a difficult, abstract and cumulative structure, will be brought to the literature in line with the quality assurance system. In particular, it is very important that the applications carried out in the presented study include collaborative applications by considering the interaction element. The widespread use of the online environment and tools in our country's higher education institutions by raising awareness about quality assurance with a holistic approach and ensuring quality assurance constitute a strong infrastructure for the presented study (URL 1).

**RESEARCH QUESTION**

In this context, the aim of the research is to provide an infrastructure regarding the necessity of designing activities to be carried out in blended learning environments. In the study, the importance of EPGs are emphasized. An example of instructional design related to the subject area titled "Mathematics Teacher Training" carried out within the scope of the course named "Teaching Statistics and Probability" among the state universities is presented inline with the educational program goals.

Accordingly, the question sought to be answered in the study is given below.

**RQ:** "How the educational program goals could be related while designing a course in the blended learning environment?"

**METHOD**

The EPGs of mathematics teacher training departments (f=76) in Turkey were examined via qualitative research methods. Regarding the findings on EPGs, the design of the Teaching Statistics and Probability course was carried out with the basis of blended learning dynamics considering the importance of educational program goals. Accordingly, the design of instruction consists of the steps of plan, do, control and take action to ensure quality assurance. The abtaimed data was analyzed in two sections: The first section is used to see the big picture by using a wordle program.

ISBN: 978-605-73552-2-5

Accordingly, the EPGs in Turkey were collected and a web 2.0 tool was used with the basis of frequencies. The second section is used via qualitative research methods.

**Collection of Data**

Data collection process was managed by the official web site of the institutions in Turkey. Accordingly, the instutitons that have the department of mathematics teacher training and their EPGs were examined. The dataset was consisted.

**Analyzing of Data**

Data analyzing was completed in two sections. The deatiled fort he sections are as followings:

**The first section:** The first section of the data analyzing process was completed via a web 2.0 tool called as wordle. This action was done to Show the big picture in the determining the EPGs. The principle of the tool is working with the basis of frequncy analysis. Accordingly, the most used words are seen the biggest in the output.

**The second section:** The second section of the data analyszing process was completed with the basis of qualitative research methods. Accordingly it can be stated that the obtained data are handled with content analysis. Content analysis is summarizing and specifying the basic contents of the written information and the messages they contain (Cohen, Manion, & Morrison, 2000). ……

*Reliability and validity:*

In order to ensure the internal validity of the research, a researcher was provided with a detailed evaluation of the research process and the methods used. The following percentage of agreement suggested by Miles and Huberman (1994) was used to calculate the reliability of the study.

Reliability=(Agreement)/(Agreement + Disagreement)

While using this formula, the evaluations made by two researchers were used. As a result of the calculations, the percentage of agreement in the study was calculated as 89.71%. The fact that the percentage of agreement obtained as a result of this process is over 70% is considered reliable for the research (Miles & Huberman, 1994).

**Findings**

The results of the analysis have showed in this part and the interpretion of the findings have been given in two sections. Accordingly while the first section has been structured with the basis of frequency analysis, the second section has the principle of the qualitative research method.

**The first section**

In the first section, the results of the wordle output is placed in Figure 1.

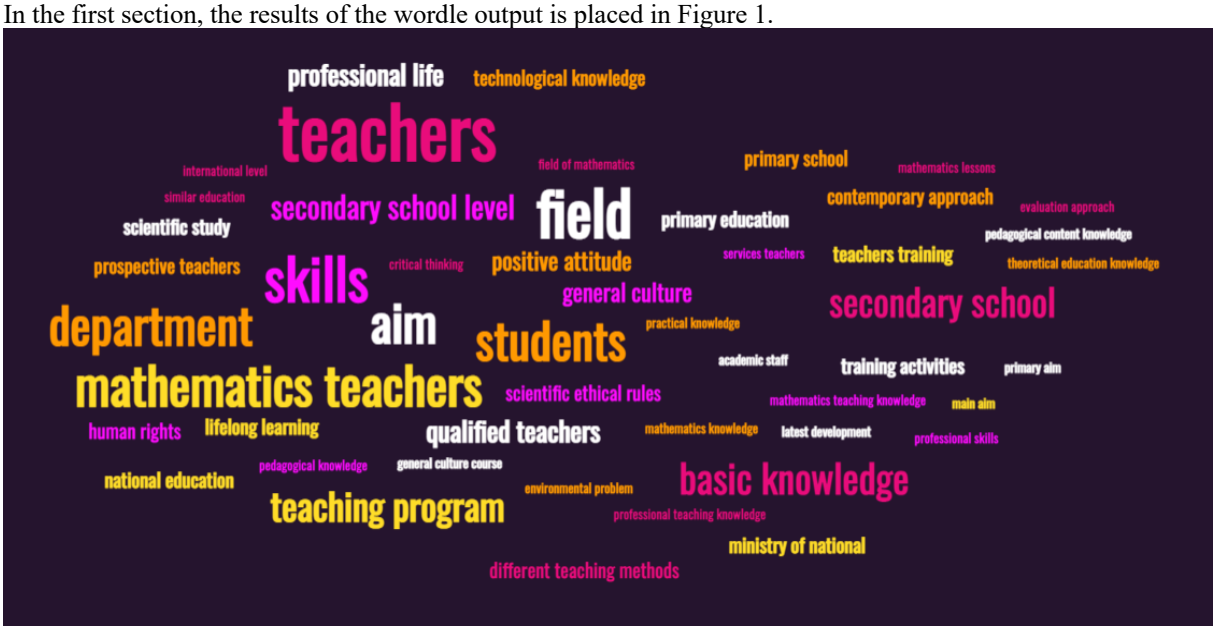


**Figure 1.** The result of Web 2.0 tool- Wordle: The most used word while determining the EPGs of mathematics teacher training departments in Turkey

Figure 1 shows that among the 76 programs of the departments of mathematics teacher training have used the words of skills, teachers, basic knowledge, technological knowledge, lifelong learning, pedagogical content, environmental problem, critical thinking, positive attitude, professional life, international level, different teaching methods mostly while determining EPGs. The used words are important in terms of providing quality assurance from top to bottom and bottom to top. At the buttom while a course is designing it is important to consider the EPGs. The goals are aligned with the mission, vision, learning outcomes etc. Accordingly, a well defined

ISBN: 978-605-73552-2-5

EPGs would be a road map for the instructor at the buttom while designing a blended learning environment for the course that s/he is responsible for teaching.

**The second section**

In the second section, the results of the qualitative research analysis is placed in Figure 2.

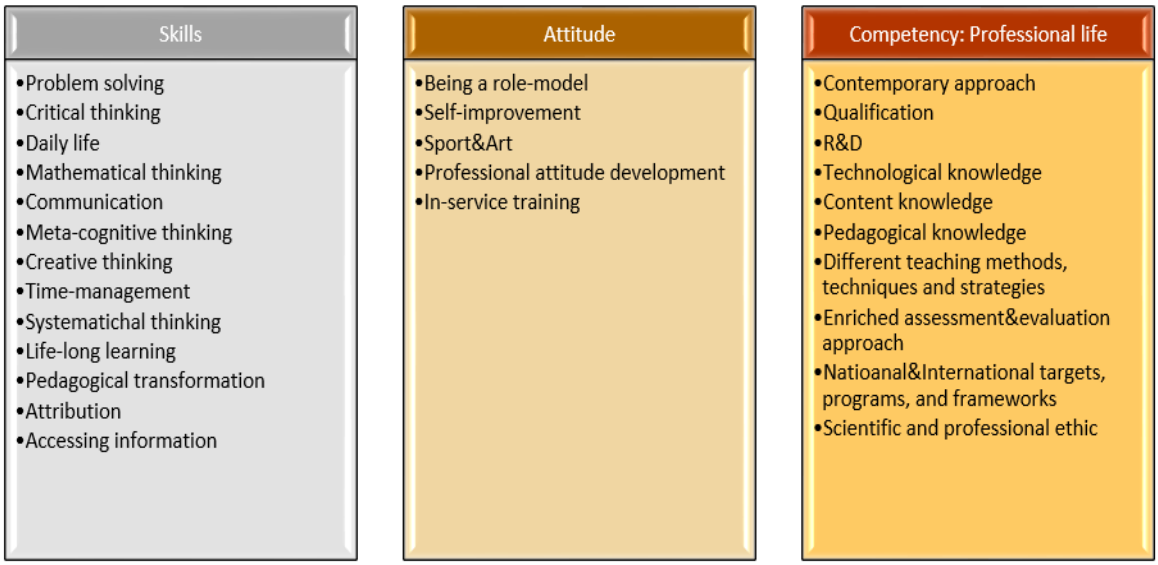


**Figure 2.** The result of qualitative research method while determining the EPGs of mathematics teacher training departments in Turkey

In Figure 2, it is possible to see the EPGs in three phases. Accordingly, while the first phase is related about the *skills,* the second phase is related about the *attitude.* Finally, the third phase is related about *competency: Professional life.*

*The first phase: Skills*

The sub-themes under this theme cover the skills that are thought to be gained by the mathematics undergraduate program. "Being mathematically literate with skills such as problem solving, estimation, communication, relationship building, reasoning is very important in terms of understanding the Universe and keeping up with the rapidly changing world." expression can be used as an example.

*The second phase: Attitude*

The sub-themes under this theme include the pre-service teachers' equipment to guide their students in the life process. In a university, "Our aim is to train teachers of today and the future who are committed to the decision process, who use resources effectively, who are sensitive to the environment, who have high self-confidence, who are happy, who are healthy, who are strong, who understands the teaching behaviors, can choose the appropriate teaching approach, motivates students to learn, is aware of learning theories and puts the student in the center in educational activities, seeks resources, can see the difficulties and problems, establishes interdisciplinary connections, provides counseling on professional practices and individual pursuits, for a strong future that helps students in preparation for the profession, can make comments in the future-oriented processes and benefit from the basic information at hand; reading, thinking, questioning, expressing themselves, turning sports, art and science into a lifestyle, open to developments, respectful to differences, innovative, ethical values." is an example for this theme.

*The third phase: Competency-Professional life*

The sub-themes under this theme include the professional equipment that teacher candidates should have throughout their professional lives. As an example of this, given on the page of a university, "With the 4-year undergraduate program that it carries out on the basis of contemporary approaches in teacher training; aware of contemporary measurement-evaluation approaches, able to organize teaching activities in line with current educational needs and technological developments, able to use different teaching methods and strategies in teaching processes, It aims to train qualified teachers who can follow the studies. Within the framework of this purpose, courses for both providing professional development of students and field knowledge and general culture are included in the program of the department." can be shared as an example.

ISBN: 978-605-73552-2-5

**CONCLUSIONS**

The findings show that while determining the EPGs, in general, there have been some mistakes in frequently. According to this the general trend mistakes are as followed:

1-The department and the program's mission are written in the same way.

2-The EPGs are not written.

*3- Mission statements should be written in an ambiguous way, but they are written in the form of purpose.*

*4-The basis of the written EPG SMART Approach was not taken into account.*

5-Only department's missions are written. Program missions are not included.

*6-The written goals are of the nature of introducing the general program (program profile).*

7-Only program outcomes are included. There is neither mission nor EPGs.

As a conclusion, the results showed that only 76 State Universities that have Primary Education Mathematics Education Program in Turkey. Addition to this, although 36 of them have included content under the Educational Program Goals (EPGs) heading, this content is limited to general trends/mistakes 4 and 6. Moreover, although 22 of them include content under the name Mission instead of EPGs, this content is limited to 3 general trends/mistakes.

**Suggestions**

According to the results, it is important to be aware of the importance of EPGs while ensuring quality assurance and designing a learning environment. Educational processes should be well aligned and activities should be well assessed. At that point, the qualification of the graduates from the department of Computer Education and Instructional Technologies should be taken into account while designing a blended learning environement at the buttom of the quality assurance cycle. The abilitites of the instructors gradutes from the department are well-qualified in that area. Addition to this, the employment of Computer Instructional Technologies Educators and Institutional Development and Planning Directorate should be collaborate together while a(n) administrative, policy-maker and practitioner are getting involved in depth.

**Practical Suggestions for Administratives and Policy-makers**

**How should an EPG be?**

- should focus on what to expect from graduates 3-5 years after graduation.
- should be written according to an average graduate.
- should be written in clear language that can be understood by all stakeholders.
- few general, important goals should be written instead of many.
- a measurement and evaluation process used to determined.
- should be short and general statements.
- the mission of the institution, faculty and department should be in harmony with the educational purpose, strategy and objectives.
- should be determined by taking into account the needs of the internal and external stakeholders of the program.
- should be updated at appropriate intervals (4-5 years) in line with the needs of the program's internal and external stakeholders.

**How should an EPG not be?**

- should not include the special knowledge, skills and behaviors that graduates of the relevant program should have.
- should not evoke program outcomes and should not be defined similarly to program outcomes.
- should not include course-specific acquisitions (knowledge, skills, behavior) in the curriculum of the relevant program.
- should not be defined using the overall mission of the department.

**Practical Suggestions for Practitioners**

**Get SMART approach for EPGs**

*Program Education Purpose Measurement Chart*

(Each program training purpose should be defined in accordance with the SMART rule.)

ISBN: 978-605-73552-2-5

| EPG | Measurement Method | Performance Indicators | The Target |
|---|---|---|---|
| **EPG 1:** The graduates rise to manager/decision maker positions in their workplaces. | focus group interviews, individual interviews, surveys, etc. | Number of graduates who rose to decision-making/management positions in their workplaces | At least 10% of graduates |

The way the EPGs are written:
*X Program Alumni,*
EPG1. … rises.
EPG2. … continues.
EPG3. … takes charge.
**Forbidden verbs** (Program outcomes verbs (knowledge/skills/awareness/familiarity etc.) and/or verbs that cannot be measured concretely (teach/train etc.)):
... is to train....
... is to graduate....
... is to teach....
... is to educate....
... is the acquisition of the skill....
... has knowledge....
... has the ability....
... gains knowledge/skills.
**Sample lesson plan for blended learning environments**

ISBN: 978-605-73552-2-5

## I. Section – General Information

| | | | | |
|---|---|---|---|---|
| **Department/US/Program Name** | Elementary Mathematics Teaching | | | |
| **Course name:** | Probability | | | |
| **Lesson code** | **Semester** | **T+P (Hour)** | **Credit** | **ECTS** |
| | 4 | 2+0 | 2 | 3 |
| **Subject:** | Conditional Probability and Bayes' Theorem | | | |
| **Goal** | Recognizing conditional probability in contexts that may be encountered in daily life or scientific research | | | |
| **Objective** | Exploring conditional probability with dynamic software programs | | | |
| **Category** | Required (Field Course) | | | |
| **Acquisition** | At the end of this course, students<br>1. Solves problems related to conditional probability, independent events, Bayes' Theorem | | | |
| **Program outcomes related to Course Learning Outcomes** | 1. Have sufficient knowledge of the field related to the field<br>2. Knows the relationship between Mathematics-Society-Environment-History and uses it in his professional and daily life. | | | |
| **Course Prerequisites** | 1. Having a PADLET account<br>2. Have the GeoGebra app | | | |
| **Duration:** | 50+50 minutes | | | |
| **Evaluation** | Self-assessment (15%), peer review (25%), instructor rating (60%)<br><br>Rubric (50%) and Checklist (50%) | | | |
| | **In-Class Activities (hours)** | **Extracurricular Activities (hours)** | **Evaluation (Monitoring) (hours)** | **Total reserved workload (hours)** | **Impact on total ECTS-Total workload hours/25 (1 ECTS=25 hours)** |
| | 2+1 hours | 2+1 hours | 2+1 hours | 2+1 hours | 2+1 hours |

ISBN: 978-605-73552-2-5

## II. Section – Method and Technique

| Methods and Techniques Used |
| --- |
| The implementation of this activity will be carried out in 3 stages.<br><br>1. In the first stage, the target audience will be informed about the content, purpose and achievements of the subject, and their attention and readiness level will be increased.<br><br>2. In the second stage, a presentation will be made to the target audience about the content of the subject presented to them beforehand (at this stage, narration, case study, discussion, question-answer method will be used).<br><br>3. In the third stage, "Buzz 66 Technique" from Cooperative Learning methods. The implementation of this technique will be carried out through the Zoom online learning platform. |
| **Event Implementation Environment** |
| **1. In this context, the class team/room creation feature of the Zoom application will be utilized.**<br>**2. Care will be taken to include heterogeneous groups in the formation of the class team/room.**<br>**3. Buzz 66 discussion groups will use the PADLET application to answer the questions expected from them in the directive.**<br>**4. The application of the acquisition will be carried out with the GeoGebra dynamic software program.**<br>**5. The instructor responsible for completing the training visited the classroom team rooms, will participate in the learning environment.**<br>**6. After the completion of the activity, it is expected that the students will evaluate themselves and the course will be evaluated by the instructor and their peers according to the determined rubric/checklist (taking into account the learning outcomes of the course (considering the polygon concept and applications and the construction protocol).** |

ISBN: 978-605-73552-2-5

## III. Section – Learning Teaching Activities

| | |
|---|---|
| 262 / 5.000<br>Çeviri sonuçları<br>Introduction<br>• Attracting Attention<br>• Informing about targets<br>• Reminder of preliminary information<br><br>Improvement<br>• Presenting new information using stimulating material<br>• Guiding learning<br>• Uncovering the performance<br>• Giving feedback<br><br>Conclusion<br>• Evaluation<br>• Ensuring permanence and transfer | Introduction: In this section, the students were asked, "How much should we trust the tests performed during the pandemic process?" It is aimed to introduce the course by asking a question in the form of a question. (Attention)<br>Then the students will be informed about the achievements of the subject. (Do not notify the target). Ask the students, "What will we gain from knowing the reliability of the tests?" and "What kind of interpretation would you develop if we wanted to evaluate a test for all possible situations?" It is planned to bring the students to the level of readiness related to the subject by asking questions such as: remembering prior knowledge.<br>Improvement: Students will be provided with a discussion on PADLET to become aware of conditional probability. Then, they will be asked to prepare a presentation on the subject and the presentation prepared by the lecturer will be shared. (Presenting new information using stimulating material)<br>After this presentation, students will try an application in which conditional probability and Bayes Theorem are modeled through the Geogebra application. Within the scope of PADLET and related directive (Appendix A), students will be expected to make a judgment about conditional probability. (Guiding learning).<br>Students will be asked to realize their learning outcomes with active learning methods based on the principles given in the directive. After the discussion, reinforcement of the subject related to conditional probability and Bayes Theorem applications will be made by using the GeoGebra dynamic software program (Uncovering the performance).<br>Students' work will be guided by the course instructor and constructive feedback will be given (Feedback).<br>Conclusion: The performances of the students will be evaluated by the rubric and checklist (Appendix B) both by themselves and by the other members of the group and the instructor of the course.<br>(Evaluation).<br>Regarding the "circle concept and its applications" in the next topic, it is necessary to determine the situation regarding the permanence and transfer of the activity in the applications carried out for the acquisition of "obtaining a circle based on the polygon concept". (Ensuring Permanence and Transfer) |

### IV. Section – Achievements Prepared According to Bloom's Taxonomy

| | Cognitive | | | Affective | | | Kinetic | | |
|---|---|---|---|---|---|---|---|---|---|
| | What are learners expected to know? | | | Öğrenenlerden neye değer vermeleri/özen göstermeleri isteniyor? | | | Öğrenenlerden neleri yapabilmesi bekleniyor? | | |
| | Information | Skill | Competence | Information | Skill | Competence | Information | Skill | Competence |
| | *Recall<br>*Understanding | *Application<br>*Analyzing<br>*Evaluation | *Creating | *Taking<br>*React | *Valuation | *Organization<br>*Qualification | *Perception<br>*Installation<br>*Do with guide | *Mechanization<br>*Making a skill | *Adaptation/fitting<br>*Creating |
| 1. Acquisition | x | x | | x | | | x | | |

*(Hamutoğlu, 2021; Hamutoğlu, Çukurbaşı, & Kıyıcı 2022)*

ISBN: 978-605-73552-2-5

**REFERENCES**

HAMUTOĞLU, N. B., ÇUKURBAŞI, Ö. Ü. B., & KIYICI, M. (2022). TYYÇ Kapsamında Lisans Düzeyinde Çevrimiçi Öğrenme Ortamlarının Tasarlanması. 5. ULUSLARARASI SINIRSIZ EĞİTİM VE ARAŞTIRMA SEMPOZYUMU (USEAS 2021), 2021.

HAMUTOĞLU, N. B. (2021). A road map for the COVID-19 pandemic process to ensure quality of assurance active learning strategies in online learning environments: How to plan, implement, evaluate, and improve learning activities. In Handbook of Research on Emerging Pedagogies for the Future of Education: Trauma-Informed, Care, and Pandemic Pedagogy (pp. 101-126). IGI Global.

ÜNVEREN-BİLGİÇ, E. N. (2021). Geometri ve ölçme öğretimi dersinin çevrimiçi ortamlara uyarlaması. *TYYÇ kapsamında lisans düzeyinde çevrimiçi öğrenme ortamlarının tasarlanması* (Editörler: N. Hamutoğlu, B. Çukurbaşı, M. Kıyıcı) içinde, 656-688, Pegem, Ankara.

ÜNVEREN-BİLGİÇ, E., ÇAM, E., & HAMUTOĞLU, N. B. (2021). DETERMINING THE CHALLENGES OF ACADEMICIANS DURING THE COVID-19 PROCESS: A CASE STUDY. 3. ULUSLARARASI DOĞA BİLİMLERİ VE TEKNOLOJİLERİ KONFERANSI (ICONAT 2021), 2021.

URL 1. Türkiye Yükseköğretim Yeterlilikler Çerçevesi: Çevrimiçi Öğrenmede Kalite Güvencesi Çalıştayı Sonuç Bildirgesi. http://tyyccalistayi.mcbu.edu.tr/wp-content/uploads/2021/09/Calistay-Sonuc-Bildirgesi.pdf Accessed 22.06.2022.